DEC 7 - 1936

UNITED STATES DEPARTMENT OF COMMERCE

+

Journal of Research

of the

National Bureau of Standards

Vol. 17, No. 5 November 1936

CONTENTS

+

RP	TITLE AND AUTHOR		Page
933.	Heat of hydrogenation of ethylene. Frederick D. Rossini.	[Price 5c]	629
934.	Accurate representation of refractive index of distilled water as a function of wave length. Leroy W. Tilton.....	[Price 5c]	639
935.	Inks for recording instruments. C. E. Waters.....	[Price 5c]	651
936.	Change of volume of rubber on stretching: Effects of time, elongation, and temperature. William L. Holt and Archibald T. McPherson.....	[Price 5c]	657
937.	Changes in color temperature of tungsten-filament lamps at constant voltage. Deane B. Judd.....	[Price 5c]	679
938.	Thermal expansion of lead-antimony alloys. Peter Hidnert.....	[Price 10c]	697
939.	Solubility of mercurous sulphate in sulphuric-acid solutions. D. Norman Craig, George W. Vinal, and Francis E. Vinal..	[Price 5c]	709
940.	Ebulliometric and tonometric study of normal aliphatic alcohols. Mieczysław Wojciechowski.....	[Price 5c]	721
941.	The system lime—boric oxide—silica. E. P. Flint and Lansing S. Wells.....	[Price 10c]	727
942.	Care of filmslides and motion-picture films in libraries. Charles G. Weber and John R. Hill.....	[Price 5c]	753
943.	Hydrocarbons in the fraction of a midcontinent petroleum distilling between 115 and 124° C. Robert T. Leslie.....	[Price 10c]	761
944.	Estimation of chromaticity differences and nearest color temperature on the standard 1931 ICI colorimetric coordinate system. Deane B. Judd.....	[Price 5c]	771
945.	Soil-corrosion studies, 1934. Rates of loss of weight and penetration of nonferrous materials. Kirk H. Logan.....	[Price 10c]	781

+

The articles listed above may be purchased separately (see cover page II) at the prices indicated in the table of contents.

A monthly periodical of pure and applied science published by our National Government

Journal of Research

of the

National Bureau of Standards

The July 1936 issue of the Journal of Research of the National Bureau of Standards began the seventeenth semiannual volume of this periodical. Fundamental researches in progress in the Bureau's laboratories are reported in this JOURNAL. If you are interested in new developments in science and technology, you should receive the JOURNAL. If you are not already a subscriber you are invited to send in your subscription.

Technical News Bulletin

This is a monthly publication containing short articles reporting progress of work in the Bureau laboratories, abstracts of papers which appear in the Journal of Research, accounts of scientific and technical meetings in which the Bureau has taken part, a list of all publications by members of the staff, and other items within the Bureau's fields. The BULLETIN is designed primarily to give a general and timely review of the activities of the Bureau in brief form. It is a prompt and reliable source of official information. If you have not already subscribed for the BULLETIN, you are invited to do so.

ANNUAL SUBSCRIPTION	Prices	
	United States Canada, Cuba, Mexico, Newfoundland, Republic of Panama	Other countries
Journal of Research of the National Bureau of Standards:		
12 monthly issues (2 volumes), paper covers	$2.50	$3.25
Bound volume (½ year, 1 volume), blue buckram . . .	3.00	3.50
Technical News Bulletin, 12 monthly issues	.50	.70

Research Papers, reprinted individual articles appearing in the Journal of Research, are available from the Superintendent of Documents shortly after appearance of monthly issue of the JOURNAL.

Address orders only to
Superintendent of Documents, U. S. Government Printing Office,
Washington, D. C.

UNITED STATES DEPARTMENT OF COMMERCE
DANIEL C. ROPER, Secretary
NATIONAL BUREAU OF STANDARDS
LYMAN J. BRIGGS, Director

✦

Journal of Research

of the

National Bureau of Standards

✦

Volume 17, Number 5
November 1936

UNITED STATES
GOVERNMENT PRINTING OFFICE
WASHINGTON : 1936

For sale by the Superintendent of Documents, Washington, D. C. - - - - Price 25 cents
$2.50 per year on subscription

The prices of the separate Research Papers appearing in this JOURNAL are given on the front cover page. If 100 or more copies of any separate are ordered, a discount of 25 percent is allowed. Those who desire copies of separate Research Papers should send their orders and remittances without delay to the Superintendent of Documents, U. S. Government Printing Office, Washington, D. C. This will aid him to determine the number of copies to be printed for sale. Research Papers are not printed from electrotypes, and usually no more reprints can be had when the first and only printing is exhausted.

U. S. DEPARTMENT OF COMMERCE NATIONAL BUREAU OF STANDARDS

RESEARCH PAPER RP933

Part of Journal of Research of the National Bureau of Standards, Volume 17, November 1936

HEAT OF HYDROGENATION OF ETHYLENE

By Frederick D. Rossini

ABSTRACT

Extremely discordant values have been reported in recent years for the scientifically and industrially important thermodynamic quantity, the heat of hydrogenation of ethylene to ethane. From the value for the heat of combustion of ethylene recently obtained at the National Bureau of Standards by Rossini and Knowlton, and the values previously obtained by Rossini for the heats of combustion of hydrogen and ethane, a new value is deduced for the heat of hydrogenation of ethylene. The four earlier sets of calorimetric data leading to this quantity have been reviewed, and the following values deduced for $-\Delta H°$ at 25° C for the reaction, C_2H_4 (g) + H_2 (g) = C_2H_6 (g), in kilocalories per mole: Thomsen (1873–86), 32.3 ±1.5; Berthelot and Matignon (1893), 37.6 ±1.9; Von Wartenberg and Krause (1930), 30.6 ±0.4; Kistiakowsky, Romeyn, Ruhoff, Smith, and Vaughan (1935), (*a*) 32.58 ±0.06, (*b*) 32.64 ±0.06; National Bureau of Standards (1931–36), 32.78 ±0.13. (In deducing the estimated uncertainties, no allowance has been made for possible "unknown" systematic errors). It is concluded that the true heat of hydrogenation at 25° C lies in the immediate neighborhood of the last two values. The value of $-\Delta H°$ obtained by Teller and Topley and others, by combination of entropies computed statistically with the free energy determined experimentally, is apparently low by from 1.6 to 1.7 kilocalories per mole. The explanations of this discrepancy are briefly reviewed.

CONTENTS

	Page
I. Introduction	629
II. Review of the calorimetric data	630
1. Data of Thomsen, 1873–86	631
2. Data of Berthelot and Matignon, 1893	631
3. Data of Von Wartenberg and Krause, 1930	632
4. Data of Kistiakowsky, Romeyn, Ruhoff, Smith, and Vaughan, 1935	632
5. Data from the National Bureau of Standards, 1931–36	635
III. Summary of the values from the calorimetric data	635
IV. Value of ΔH obtained from the combination of entropies from statistical calculations with the free energy from equilibrium data	636
V. References	638

I. INTRODUCTION

The heat of hydrogenation of ethylene to form ethane has become, in recent years, a thermal quantity of considerable interest and speculation, the latter arising from the extreme discord among the existing values for this property, for which two modern values differ by 7 percent. In addition to the practical importance of this quantity in thermodynamic calculations, it possesses importance in connection with the proper description of the molecules for the purpose of com-

puting, by statistical methods, values of their entropies and heat contents as functions of the temperature. In the case of ethane, for example, this latter consideration includes the question of how much restriction, if any, exists in the rotation of the methyl groups about the carbon-carbon linkage.

Because of the recent completion by Rossini and Knowlton [1] [1][2] of measurements on the heat of combustion of ethylene, the data on which can be combined with data previously reported by Rossini [2] on the heats of combustion of hydrogen and ethane to obtain a value for the heat of hydrogenation of ethylene, it seems desirable to review the data which may be utilized to obtain values for the heat of the reaction

$$C_2H_4\ (g)+H_2\ (g)=C_2H_6\ (g) \tag{1}$$

There are two ways in which the heat of the above reaction may be determined from calorimetric data: first, from data on the direct reaction of hydrogenation according to equation 1; and, second, from data on the heats of combustion of ethylene, hydrogen, and ethane:

$$C_2H_4\ (g)+3\ O_2\ (g)=2\ CO_2\ (g)+2\ H_2O\ (liq) \tag{2}$$

$$H_2\ (g)+1/2\ O_2\ (g)=H_2O\ (liq) \tag{3}$$

$$C_2H_6\ (g)+3\ 1/2\ O_2\ (g)=2\ CO_2\ (g)+3\ H_2O\ (liq) \tag{4}$$

Because the value of the heat of hydrogenation of ethylene is about 1/2, 1/10, and 1/11, respectively, of the heats of combustion of hydrogen, ethylene, and ethane, it is evident that, in point of the accuracy of the relatively small value of the heat of hydrogenation, the direct method has an advantage of about fifteenfold over the indirect method. This advantage of the direct method, however, is partly counterbalanced by the simpler, purer, and more complete nature of the reaction of combustion as compared with that of hydrogenation. In the case of molecules with four or more carbon atoms, however, the advantage in favor of the direct method for determining the difference in the heats of formation of analogous olefin and paraffin hydrocarbons becomes overwhelmingly large.

In the utilization of the calorimetric data on heats of combustion for the present purpose, one obvious limitation must be made, and that is that in the derivation of any one value for the heat of hydrogenation only the combustion data from one laboratory on all three reactions should be used. The main reason for this procedure is that it helps to eliminate systematic errors in the work of a given laboratory.[3]

II. REVIEW OF THE CALORIMETRIC DATA

There are now available five completely independent sets of calorimetric data yielding values for the heat of hydrogenation of ethylene:

[1] The report of this work of Rossini and Knowlton will be published, along with other data on the olefine hydrocarbons, in a subsequent number of the Journal of Research of the National Bureau of Standards.

[2] The figures in brackets here and throughout the text refer to the references at the end of the paper.

[3] For example, if only 2 investigators, A and B, determined all 3 heats of combustion, Q_1, Q_2, and Q_3 independently, there would be 8 possible combinations which could be used to evaluate the heat of hydrogenation; but, of these, the 2 combinations involving AQ_1, AQ_2, AQ_3, and BQ_1, BQ_2, BQ_3 would be expected to be by far the most reliable.

two "old" sets of data on heats of combustion obtained about 50 years ago by Thomsen [3] and by Berthelot and Matignon [4]; two sets of "modern" data on the direct reaction of hydrogenation by Von Wartenberg and Krause [5] and by Kistiakowsky, Romeyn, Ruhoff, Smith, and Vaughan [6]; and one set of "modern" data on heats of combustion obtained at the National Bureau of Standards by Rossini [2] and Rossini and Knowlton [1].

In addition to these five values there is one recently derived by Teller and Topley [7] by a combination of the statistical calculations of the thermodynamic properties of the molecules, hydrogen, ethylene, and ethane, with the experimental data of others on the equilibrium represented by reaction (1). Their procedure in evaluating the heat of hydrogenation is substantially that of utilizing the relation,

$$\Delta H = \Delta F + T\Delta S, \tag{5}$$

where ΔF is the change in free energy, evaluated from equilibrium data, and ΔS is the change in entropy, calculated by statistical methods.

1. DATA OF THOMSEN, 1873–86

Thomsen's [3] data on the combustion of hydrogen and ethane have already been evaluated (see Rossini [2]) and yield $\Delta H° = -68.32 \pm 0.17$ and -368.9 ± 1.3, kilocalories per mole, at 25° C, for reactions (3) and (4), respectively.

Thomsen performed six experiments, two series of three each, on the heat of combustion of ethylene in a flame calorimeter at constant pressure and about 18° C, the amount of reaction being determined from the mass of carbon dioxide formed. By excluding the second experiment of the first series, because its deviation is nearly seven times the average deviation of the remaining five, and converting the data to modern units of energy, there is obtained the value $\Delta H° = -332.9 \pm 0.8$ kilocalories per mole, at 25° C, for reaction (2), the "error" being computed according to Rossini [8]. By combining Thomsen's data for reactions (2), (3), and (4), there is obtained for reaction (1), $\Delta H° = -32.3 \pm 1.5$ kilocalories per mole at 25° C.

2. DATA OF BERTHELOT AND MATIGNON, 1893

The data of Berthelot and Matignon [4] (see also Berthelot [9]) on the combustion of hydrogen and ethane have already been evaluated (see Rossini [2]) and yield $\Delta H° = -68.7 \pm 0.6$ and 372.1 ± 0.8 kilocalories per mole, at 25° C, for reactions (3) and (4), respectively.

Berthelot and Matignon [4] (see also Berthelot [9]) performed three experiments on the combustion of ethylene in a bomb at constant volume and about 14° C. The amount of reaction was determined both from the volume of ethylene burned and the mass of carbon dioxide formed, but the two analytical methods yielded significantly different but random results, the difference being as much as 0.6 percent in one experiment. Corrected to the modern unit of energy, these data yield $\Delta H° = -341.0 \pm 1.6$ kilocalories per mole for reaction (2) at 25° C. By combining the data of Berthelot and Matignon for reactions (2), (3), and (4), there is obtained for reaction (1), $\Delta H° = -37.6 \pm 1.9$ kilocalories per mole at 25° C.

3. DATA OF VON WARTENBERG AND KRAUSE, 1930

The direct hydrogenation experiments of Von Wartenberg and Krause [5] were carried out with a simple calorimetric system consisting of a 0.5-liter rubber-stoppered cylindrical vacuum flask containing the catalyzing solution (400 ml of water with 3 g each of sodium carbonate, gum arabic, and palladium chloride, in colloidal suspension), a Beckmann thermometer, an electrical heating coil, a gas inlet tube terminating in a glass filter plate in the solution near the bottom of the flask, and a gas exit tube above the solution. The hydrogen and ethylene gases were first saturated with water at an unstated temperature, mixed, and then led into the catalyzing solution where the reaction (which was not complete) occurred, presumably at the prevailing room temperature. The effluent gas (hydrogen, ethylene, ethane, and nitrogen) passed out of the reaction vessel carrying an unstated amount of water vapor, through liquid bromine to remove ethylene, through potassium hydroxide to remove bromine vapor, through a cold trap at 0° C to remove ethylene bromide, through potassium hydroxide and calcium chloride, over heated copper oxide in order to oxidize the hydrocarbon to carbon dioxide and water, through calcium chloride to remove water, and then through weighed tubes of soda lime in order to absorb the carbon dioxide, the mass of which determined the amount of reaction. Von Wartenberg and Krause gave no details concerning the evaluation of the electrical-energy equivalent of the calorimeter, except to say that it was determined with electrical energy measured with a voltmeter, an ammeter, and a watch. (Any systematic error in this quantity is directly carried over to the value for the heat of hydrogenation).

These experiments of Von Wartenberg and Krauss were analyzed by Kistiakowsky, Romeyn, Ruhoff, Smith, and Vaughan [6], who pointed out two serious objections to their work, the first one concerning the failure of the experimenters to demonstrate the absence of side reactions, such as irreversible adsorption, and the second (and apparently more serious one) concerning their manner of determining the amount of reaction. The writer has analyzed in detail the latter criticism and finds that the procedure employed by Von Wartenberg and Krause for determining the amount of reaction does leave open the possibility of a systematic error, whose value might conceivably be as large as 10 percent. This calculation confirms the statement of Kistiakowsky and his collaborators that "the ethylene bromide which might remain in the gases (going into the combustion tube) can more than account for the low value for the heat of hydrogenation obtained by Von Wartenberg and Krause."

Von Wartenberg and Krause reported the results of 12 experiments, the average of the first six being 2-percent lower than that of the last six. Making no allowance for possible "unknown" systematic errors, one obtains from the values reported by Von Wartenberg and Krause, $\Delta H° = -30.6 \pm 0.4$ kilocalories per mole, at 25° C, for reaction (1).

4. DATA OF KISTIAKOWSKY, ROMEYN, RUHOFF, SMITH, AND VAUGHAN, 1935

The recent experiments of Kistiakowsky, Romeyn, Ruhoff, Smith, and Vaughan on the direct hydrogenation of ethylene were carried

out with a careful regard for the accuracy of both the calorimetric and the chemical procedures. These experiments were described in detail in the original paper [6], and substantiating experiments were reported in a subsequent paper [10]. The calorimetric method employed was substantially the substitution method [8] wherein the heat evolved by a measured amount of chemical reaction is compared with the heat evolved by a measured amount of electrical energy, using the calorimeter as the absorber and comparator of the two kinds of energy.

The completeness of the reaction of hydrogenation was demonstrated by examination of the reaction products, which showed the absence of ethylene. The possible side reactions were (1) decomposition to form methane, (2) irreversible adsorption on the catalyst, and (3) polymerization plus hydrogenation. Appropriate tests indicated that the effects of the first two reactions, if they occurred at all, were insignificant. A test for the polymerization reaction was deemed not feasible and its existence in any significant amount was considered to be doubtful. As stated by the authors, if this reaction should be shown to occur, the heat of hydrogenation would have to be increased by 0.1 percent for each 0.6 percent of ethylene polymerized, with subsequent hydrogenation, to yield butane.

A possible systematic error, not specifically mentioned by Kistiakowsky, Romeyn, Ruhoff, Smith, and Vaughan, would occur if the ethylene contained some ethane. The effect of the presence of ethane as an impurity in the ethylene would be to increase the apparent amount of reaction, as measured by the carbon dioxide from the products of combustion of the effluent gases, without changing the amount of heat evolved, and, consequently, the observed value of the heat of hydrogenation would be lower than the true value by an amount (in percent) equal to the molal percentage of ethane present as an impurity. As stated below, one of the two "good" samples of ethylene used in these experiments undoubtedly contained a significant amount of ethane.

Kistiakowsky, Romeyn, Ruhoff, Smith, and Vaughan reported the heats of hydrogenation of three different samples of ethylene as follows: (1) a commercial sample, "99.5 percent pure", made from ethyl alcohol; (2) a middle fraction from an extended fractional distillation of the foregoing commercial sample; and (3) a sample, "99.8 percent pure", prepared specially by the Linde Air Products Co., by the fractional distillation of petroleum products. As recommended by the investigators, the data on the commercial sample may be disregarded because of its large amount of impurity, part of which was found to be diethyl ether.

The second sample above was considered to be the purest and the data on it correspondingly best. On this sample there were performed 10 experiments, having an average deviation of 0.10 percent, at an average temperature of 82° C. From the discussion presented by these investigators [6, 10], it would appear that the determination of the electrical-energy equivalent of the calorimeter system had an uncertainty of about 0.10 percent. Assuming an absolute error of ±0.10 percent due to an impurity in the reaction and the determination of the amount of reaction, and computing the errors as before, one finds that the values of these investigators for their "best" sample of ethylene yield $\Delta H^\circ = -32.833 \pm 0.053$ kilocalories per mole for reaction (1) at 82° C.

On the sample of ethylene prepared by Linde from petroleum products, marked "99.8 percent pure", Kistiakowsky, Romeyn, Ruhoff, Smith, and Vaughan reported the results of four very concordant experiments, which had an average deviation of 0.03 percent. Computing the "error" as before, one obtains $\Delta H°=-32.806 \pm 0.049$ kilocalories per mole for reaction (1) at 82° C. However, in their investigation on the heat of combustion of ethylene, Rossini and Knowlton [1] determined with considerable accuracy the amount of impurity in a sample of ethylene, marked "99.85 percent pure", which had been specially prepared by the Linde laboratory. They found 0.015 ± 0.010 mole percent of methane and 0.246 ± 0.032 mole percent of ethane. A private communication from the Buffalo laboratory of the Linde Air Products Co. reported that the ethylene prepared for the National Bureau of Standards was from a separate purification and contained slightly less ethane (about 0.05 percent less) than the sample prepared for the Harvard laboratory, both samples having been prepared in 1933. Assuming that the Linde sample of ethylene used by Kistiakowsky and his coworkers contained the same amount of impurity as that given above, one obtains from their data on the Linde sample, when appropriately corrected, the value $\Delta H°=-32.889 \pm 0.050$ kilocalories per mole for reaction (1) at 82° C.

As pointed out by Kistiakowsky and his collaborators, the effect of a possible side reaction of polymerization plus hydrogenation, such as

$$2\ C_2H_4\ (g)+H_2\ (g)=C_4H_{10}\ (g), \qquad (6)$$

would be corrected for by increasing numerically the observed values of the heat of hydrogenation by 0.1 percent for each 0.6 percent of ethylene polymerized. That the foregoing is a possible side reaction is evidenced by the free energy calculations recently made by Kassel [12], which yield, for reaction (6) at 82° C, a decrease in free energy of about 4.4 kilocalories per mole of butane. However, in later experiments on the heats of hydrogenation of propylene, butene–1, and heptene–1, Kistiakowsky, Ruhoff, Smith, and Vaughan [10] performed tests to determine the presence of a side reaction of polymerization plus hydrogenation, and reported negative results in tests which would have readily detected 0.5 percent of the hydrogenated polymer in the products of reaction.[4]

The next point to be considered is the reduction from 82° to 25° C of the above two values for the heat of hydrogenation. According to the experimentally determined values of Eucken and Parts [24] on the heat capacities of ethylene and ethane, and the statistical calculations of Eucken and Parts [24] and Smith and Vaughan [11] based upon these data, together with the known accurate values for hydrogen [14, 15], the amount of the reduction from 82 to 25° C may be taken as 0.25 kilocalorie per mole with a possible uncertainty of about ± 0.02 kilocalorie per mole. The two values from the work of Kistiakowsky and his collaborators then become, respectively, $\Delta H°=-32.58 \pm 0.06$ and -32.64 ± 0.06 kilocalories per mole for reaction (1) at 25° C.

[4] An extremely sensitive method of testing for such impurities is the differential vapor-pressure method described by Shepherd [13].

5. DATA FROM THE NATIONAL BUREAU OF STANDARDS, 1931–36

The data obtained at the National Bureau of Standards on the heats of combustion of hydrogen, ethane, and ethylene give the following values of $\Delta H°$ for the respective reactions at 25° C, in kilocalories [5] per mole: reaction (3), Rossini [2], −68.313 ±0.010; reaction (4), Rossini [2], −372.81 ±0.11; and reaction (2), Rossini and Knowlton [1], −337.28 ±0.07. Combination of these values yields, for reaction (1), $\Delta H° = -32.78$ ±0.13 kilocalories per mole at 25° C.

III. SUMMARY OF THE VALUES FROM THE CALORIMETRIC DATA

In table 1 are given the values from the five sets of data which have just been reviewed. These are plotted in figure 1. With regard to the half-century-old data of Thomsen [3] and Berthelot and Matignon [4], it would appear safe to conclude that the possibility of systematic errors in their work on heats of combustion is such as to make their values even more uncertain than is indicated by the assigned errors, and that, therefore, the values deduced from their work should be considered as approximations only.

Of the three sets of modern data, the two direct measurements are in complete discord, while the value from the modern data on heats of combustion is in accord with the higher and more recent of the two direct determinations. Because of the care and precautions taken to insure the accuracy of their chemical and calorimetric procedures, and because of the completely different reactions measured, the substantial concordance of the values deduced from the work of Kistiakowsky, Romeyn, Ruhoff, Smith, and Vaughan [6] at Harvard University and of Rossini [2] and Rossini and Knowlton [1] at the National Bureau of Standards is very gratifying. It would appear that some systematic error, possibly of the nature of those discussed

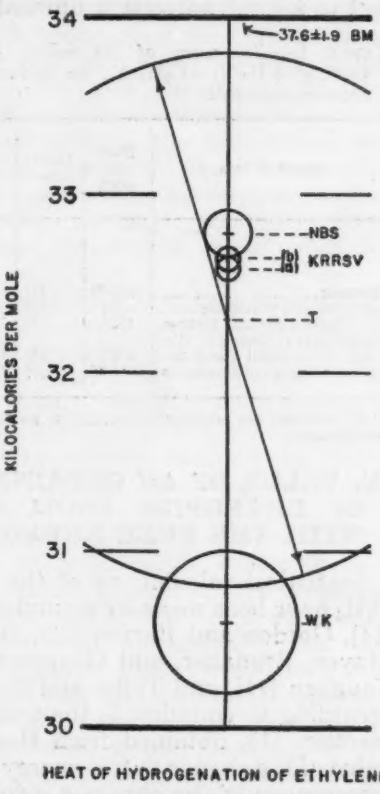

FIGURE 1.—*Plot of the values for the heat of hydrogenation of ethylene, as deduced from the calorimetric data.*

The scale of ordinates gives the value of $-\Delta H°$ at 25° C for the reaction, C_2H_4 (g)+H_2 (g)=C_2H_6 (g), in kilocalories per mole. The radii of the various circles indicate the estimated uncertainties (not including possible "unknown" systematic errors) of the values from the various sets of data: BM, Berthelot and Matignon [4]; NBS, National Bureau of Standards [1, 2]; KRRSV, Kistiakowsky, Romeyn, Ruhoff, Smith, and Vaughan [6]; T, Thomsen [3]; WK, Von Wartenberg and Krause [5].

[5] See Rossini [3] for a discussion of the unit of energy.

on page 632 existed in the work of Von Wartenberg and Krause [5], and it may be safely concluded, therefore, that the true value of the heat of hydrogenation lies in the immediate neighborhood of the two concordant values from the modern work. There is also a remote possibility, as discussed on page 633 that the values of Kistiakowsky, Romeyn, Ruhoff, Smith, and Vaughan may be subject to a small correction upward (numerically).

TABLE 1.—*Summary of the values for the heat of hydrogenation of ethylene,* $C_2H_4(g)+H_2(g)=C_2H_6(g)$, *as deduced by the present writer from the various calorimetric data*

Source of data	Date of work	Reference	Reactions measured	Value deduced for $-\Delta H°$ at 25° C	Estimated uncertainty[1]
				Kilocalories per mole	*Kilocalories per mole*
Thomsen	1873–86	[3]	Combustion of H_2, C_2H_4, C_2H_6	32.3	±1.5
Berthelot and Matignon	1893	[4]	Combustion of H_2, C_2H_4, C_2H_6	37.6	±1.9
Von Wartenberg and Krause	1930	[5]	Hydrogenation of C_2H_4	30.6	±0.4
Kistiakowsky, Romeyn, Ruhoff, Smith, and Vaughan	1935	[6]	Hydrogenation of C_2H_4	(a) 32.58 (b) 32.64	±0.06 ±0.06
National Bureau of Standards	1931–36	[1, 2]	Combustion of H_2, C_2H_4, C_2H_6	32.78	±0.13

[1] In deducing the estimated uncertainty, no allowance has been made for possible "unknown" systematic errors.

IV. VALUE OF ΔH OBTAINED FROM THE COMBINATION OF ENTROPIES FROM STATISTICAL CALCULATIONS WITH THE FREE ENERGY FROM EQUILIBRIUM DATA

Statistical calculations of the entropies of gaseous H_2, C_2H_4, and C_2H_6 have been made by a number of investigators, including Giauque [14], Gordon and Barnes [15], Davis and Johnston [16], Kassel [17], Mayer, Brunauer, and Goeppert-Mayer [18], Frost [19], Smith and Vaughan [11], and Teller and Topley [7]. It is possible to combine, according to equation 5, the value of the change in entropy, ΔS, for reaction (1), obtained from these statistical calculations, with the value of the change in free energy, ΔF, as determined from equilibrium measurements, to obtain a value for the change in heat content, ΔH, for reaction (1).

Teller and Topley [7] (see also Frost [19] and Smith and Vaughan [11]) reviewed the experimental data of Pease and Durgan [20], Travers and Pearce [21], Vvedenskii and Vinnikova [22], and Frey and Huppke [23] on the equilibrium conditions for reaction (1), and deduced a very concordant, and apparently quite reliable, value for the free-energy change for the reaction of hydrogenation at 863° K. Teller and Topley [7] (see also Frost [19], Kassel [17], and Smith and Vaughan [11]) made statistical calculations of values of the thermodynamic function, $(F°-E°_0)/T$, for gaseous C_2H_4 and C_2H_6, combined these with similar values computed for gaseous H_2 by Giauque [14], and obtained a value for the property $(\Delta F°-\Delta E°_0)/T$ for reaction (1). Combination with the "best" value of $\Delta F°$ for 863° K, as obtained from the equilibrium data, then yielded a value for $\Delta E°_0$. To this quantity was added the statistically computed value of $\int_0^{298}\Delta C_p dT$ for reaction (1) to obtain the value for $\Delta H°$ for the reaction of hydrogenation at 298° K or 25° C.

The value thus deduced by Teller and Topley [7] for the heat of reaction (1) was $\Delta H°=-31.05 \pm 0.30$ kilocalories per mole at 25° C. This uncertainty of ± 0.30 kilocalorie per mole was considered to be the limit of "probable" error, with the limit of "possible" error being ± 0.60 kilocalorie per mole. These limits of error were evaluated by Teller and Topley from a very critical analysis of the fallible factors entering into their calculations, namely: (1), the error in the value of the free energy from equilibrium data; (2), the error in the moments of inertia of ethylene and ethane; (3) the error in the vibrational frequencies of ethylene; (4), the uncertainty in the magnitude of the potential restricting the free rotation of the methyl groups in ethane; and (5), the uncertainty in the vibrational frequencies of ethane. Teller and Topley considered that the possible uncertainties in these quantities were such as to correspond, in the value of $\Delta H°$ at 25° C., in kilocalories per mole, to ± 0.10 from (1), to ± 0.17 from (2), to ± 0.10 from (3), and to ± 0.25 from (4) and (5) combined.

As a result of the concordant sets of calorimetric data from Harvard University and the National Bureau of Standards, it appears that the true value for the heat of hydrogenation of ethylene definitely lies from 1.6 to 1.7 kilocalories per mole numerically above the value deduced from the combination of entropies, computed statistically, with the free energy, determined experimentally. Therefore, it must be concluded that, for one or more of the sources analyzed by Teller and Topley [7], the error must greatly exceed what was considered to be the maximum possible.

Assuming that the heat of hydrogenation of ethylene according to reaction (1) is definitely limited to the range $-\Delta H°=32.6$ to 32.8 kilocalories per mole at 25° C., there remain several possible explanations for the discrepancy in the relation (see equation 5) between ΔH determined calorimetrically, ΔS computed statistically, and ΔF determined from equilibrium measurements. This discrepancy has been discussed by Kassel [12] and by Teller and Topley [7], and the possible explanations may be expressed as follows: (1), the experimentally determined equilibrium constants would need to e too large by a factor of about 3; (2), the assigned values for the vibrational frequencies in ethylene or ethane, or both, would need to be in considerable error; and (3), the present calculated difference between the rotational entropies of ethylene and ethane would need to be too large by about 2½ calories per degree per mole. From the many concordant equilibrium data obtained in diverse ways by different investigators, it seems rather improbable that the experimentally determined equilibrium constants can be in error by a significant mount. It appears then that an explanation for the discrepancy must come from the spectroscopic and other molecular data which are utilized in evaluating the rotational and vibrational energy levels of the ethylene and ethane molecules. For example, part or all of the discrepancy may be resolved by appropriately restricting, in the ethane molecule, the rotation of the two methyl groups about the carbon-carbon bond, or by reducing, in the ethylene molecule, the magnitude of the torsional frequency about the carbon-carbon double bond.

V. REFERENCES

[1] F. D. Rossini and J. W. Knowlton, Unpublished, see footnote 1, p. 630.
[2] F. D. Rossini, BS J. Research **6,** 1 (1931) RP259; **7,** 329 (1931) RP343; **12,** 735 (1934) RP686.
[3] J. Thomsen, Thermochemische Untersuchungen, II and IV (Barth, Leipzig; 1882, 1886).
[4] M. Berthelot and C. Matignon, Ann. chim. phys. **30,** 547 (1893).
[5] H. von Wartenberg and G. Krause, Z. physik. Chem. [A] **151,** 105 (1930).
[6] G. B. Kistiakowsky, H. Romeyn, Jr., J. R. Ruhoff, H. A. Smith, and W. E. Vaughan, J. Am. Chem. Soc. **57,** 65 (1935).
[7] E. Teller and B. Topley, J. Chem. Soc. 876 (1935).
[8] F. D. Rossini, Chem. Reviews **18,** 233 (1936).
[9] M. Berthelot, Ann. chim. phys. **23,** 176 (1881).
[10] G. B. Kistiakowsky, J. R. Ruhoff, H. A. Smith, and W. E. Vaughan, J. Am. Chem. Soc. **57,** 876 (1935); **58,** 137 (1936).
[11] H. A. Smith and W. E. Vaughan, J. Chem. Physics **3,** 341 (1935).
[12] L. S. Kassel, J. Chem. Physics **4,** 435 (1936).
[13] G. M. Shepherd, BS J. Research **12,** 185 (1934) RP643.
[14] W. F. Giauque, J. Am. Chem. Soc. **52,** 4816 (1930).
[15] A. R. Gordon and C. Barnes, J. Phys. Chem. **36,** 1143 (1932).
[16] C. O. Davis and H. L. Johnston, J. Am. Chem. Soc. **56,** 1045 (1934).
[17] L. S. Kassel, J. Am. Chem. Soc. **55,** 1351 (1933).
[18] J. E. Mayer, S. Brunauer, and M. Goeppert-Mayer, J. Am. Chem. Soc. **55,** 37 (1933).
[19] A. V. Frost, J. Gen. Chem. (Moscow) **4,** 124 (1934).
[20] R. N. Pease and E. S. Durgan, J. Am. Chem. Soc. **50,** 2715 (1928).
[21] M. W. Travers and T. J. P. Pearce, J. Soc. Chem. Ind. **53,** 322 (1934).
[22] A. A. Vvedenskii and S. G. Vinnikova, J. Gen. Chem. (Moscow) **4,** 120 (1934).
[23] F. E. Frey and W. F. Huppke, Ind. Eng. Chem. **25,** 54 (1933).
[24] A. Eucken and A. Parts, Z. physik. Chem. [B] **20,** 184 (1933).

WASHINGTON, August 12, 1936.

U. S. DEPARTMENT OF COMMERCE NATIONAL BUREAU OF STANDARDS

RESEARCH PAPER RP934

Part of Journal of Research of the National Bureau of Standards, Volume 17, November 1936

ACCURATE REPRESENTATION OF REFRACTIVE INDEX OF DISTILLED WATER AS A FUNCTION OF WAVE LENGTH

By Leroy W. Tilton

ABSTRACT

Technique in using the Ketteler-Helmholtz dispersion equation is discussed and validity in representing the dispersion of water over the visible range of wave lengths is tested by least-squares adjustments of sixth-decimal-place refractive indices. It is concluded that four parameters are sufficient for accuracy within the spectral range investigated.

CONTENTS

	Page
I. Introductory discussion of dispersion equations	639
II. Refractive-index data	642
III. Computational procedures	643
1. Equation 1, two Sellmeier terms, four (independent) parameters	644
2. Equation 4, infrared term expanded, five parameters	646
3. Equation 11, both Sellmeier terms expanded, six parameters	646
4. Equation 4, term in λ^4 omitted, four parameters	646
IV. Comparative merits of four, five, and six parameters	647
1. Relative goodness of fit and Chi-test	647
2. Concluding discussion	649

I. INTRODUCTORY DISCUSSION OF DISPERSION EQUATIONS

Many dispersion formulas in use for representing the refractive indices of transparent media are approximations to the form

$$n^2=a^2_\infty-\sum\frac{M}{L^2-\lambda^2}+\sum\frac{m}{\lambda^2-l^2}, \tag{1}$$

where

$$a^2_\infty=1+\sum\frac{M}{L^2}+\sum\frac{m}{l^2}$$

is the dielectric constant, L^2 and l^2 with appropriate subscripts are used to designate, respectively, the effective wave lengths of absorption bands in the infrared and the ultraviolet regions; and similarly M and m are corresponding parameters. This is the equation to which the complete Ketteler-Helmholtz equations reduce for regions exclusive of the absorption bands. Strictly speaking, vacuum values should be used for n, the index of refraction, and for λ, the wave

length, but the index of refraction of air is so near unity and its dispersion so small that dispersion equations are frequently used for the combined system air plus the medium in question. This practice has been followed in this paper and in evaluating parameters all wave lengths are expressed in microns.

In some cases it has been found that only one infrared term and one ultraviolet term are necessary for satisfactory approximations. With only these two Sellmeier terms there are in reality but four independent parameters to be determined and for a simultaneous solution the equation may be written as

$$n^2=-\frac{n^2-1}{\lambda^4}(l^2L^2)+\frac{n^2-1}{\lambda^2}(l^2+L^2)-\frac{1}{\lambda^2}\left(\frac{Ml^2}{L^2}+\frac{mL^2}{l^2}\right)+\left(1+\frac{M}{L^2}+\frac{m}{l^2}\right), \quad (2)$$

where, inclosed in parentheses, there is a linearly independent set of four groups of unknowns. If, then, equation 1 is limited to three terms, its five parameters may be computed from the four groups of parameters as formed in equation 2. Equation 2, however, is not necessarily suitable for direct adjustments by least squares because it is not solved [1] for n^2. Thus errors in the observed values of n^2 are involved in the coefficients to be used in the least-squares process and this may or may not be of importance in the adjustment that is obtained.

A thoroughly reliable adjustment of the parameters of equation 1 can be made after an approximate solution is obtained and the process of differentiation applied for obtaining the equation

$$\Delta n^2=\frac{\lambda^2}{\lambda^2-l^2}\left(\Delta\frac{m}{l^2}\right)-\frac{\lambda^2}{L^2-\lambda^2}\left(\Delta\frac{M}{L^2}\right)+\frac{m\lambda^2}{l^2[\lambda^2-l^2]^2}(\Delta l^2)+\frac{M\lambda^2}{L^2[L^2-\lambda^2]^2}(\Delta L^2), \quad (3)$$

which can then be used in adjusting by least squares the system of betterments inclosed in parentheses. These betterments in turn permit revision of the parameters which were used in the approximate solution. In applying a procedure of this kind it should be remembered that second and higher order derivatives are ignored. Consequently, it is important, perhaps especially so with this particular equation (see section III and fig. 1), that the approximate solution be so good that equation 3 can be used with validity.

It is evident that equation 1 is not desirably convenient for curve fitting and usually when two Sellmeier terms are to be used, at least one of them is expanded and a more convenient form such as

$$n^2=a^2-k\lambda^2-p\lambda^4-\text{----}+\frac{m}{\lambda^2-l^2} \quad (4)$$

is obtained. The remarkable success that has, in general, been attained in using this equation (even without the term in λ^4) is probably ascribable to the fact that not only one Sellmeier term but many are simultaneously approximated. That is,

[1] The fact that an equation is given for n^2 rather than for n is a relatively unimportant matter in its use for curve fitting. A least-squares adjustment of n^2 rather than of n is in effect an implicit weighting of the observations but the percentage variation in these weights over the total range of n is usually small and negligible. Throughout this paper it is assumed that errors in λ are small as compared with those otherwise involved in index measurement.

$$\left.\begin{aligned} a^2 &= a^2{}_\infty - \sum \frac{M}{L^2}, \\ k &= \sum \frac{M}{L^4}, \\ p &= \sum \frac{M}{L^6}, \text{ etc.}, \\ m, &\text{ and } l^2 \end{aligned}\right\} \quad (5)$$

are some of the potential values of the parameters in the expanded form. Incidentally this view shows, also, why it is unsafe to assume [2] that the ratio k/p equals L^2 and gives the location of an effective absorption band.

Equation 4 may, for convenience in simultaneous solutions, be written

$$n^2 = \frac{n^2}{\lambda^2}(l^2) + \frac{1}{\lambda^2}(m - a^2 l^2) - \lambda^2(k - pl^2) - \lambda^4(p) + (a^2 + kl^2), \quad (6)$$

but again, as for equation 2, a direct adjustment by least squares is, theoretically at least, inadvisable because the equation is not solved for n^2. One may, of course, use the differential process and the equation

$$\Delta n^2 = \Delta a^2 - \lambda^2 \Delta k - \lambda^4 \Delta p + \frac{1}{\lambda^2 - l^2}\Delta m + \frac{m}{(\lambda^2 - l^2)^2}\Delta l^2, \quad (7)$$

but there is a more direct procedure [3] which the writer has tried and found satisfactory. If for l^2 an approximate value $l^2{}_0$ can be found from previous experience, or in any way whatsoever, then after setting

$$\left.\begin{aligned} \mu^2 &= \lambda^2 - l_0{}^2, \\ \epsilon^2 &= l^2 - l_0{}^2, \\ b^2 &= (a^2 - l_0{}^2 k - l_0{}^4 p), \\ \text{and} \quad h &= (k + 2l_0{}^2 p), \end{aligned}\right\} \quad (8)$$

one may write

$$n^2 = b^2 - h\mu^2 - p\mu^4 + \frac{m}{\mu^2 - \epsilon^2} \quad (9)$$

to correspond to equation 4. Then the equation

$$n^2 = \frac{n^2}{\mu^2}\epsilon^2 + \frac{1}{\mu^2}(m - b^2\epsilon^2) - \mu^2(h - p\epsilon^2) - \mu^4 p + (b^2 + h\epsilon^2) \quad (10)$$

corresponds to equation 6 and can be used for a direct least-squares adjustment of the linearly independent set of unknowns ϵ^2, $(m - b^2\epsilon^2)$, $(h - p\epsilon^2)$, p, and $(b^2 + h\epsilon^2)$. If l_0^2 of equations 8 has been suitably chosen, then there will be no appreciable error introduced by neglecting in equation 10 the slight error in the coefficient, n^2/μ^2, of the first right-hand term.

[2] See, for example, p. 390 of Wood's Physical Optics, 1911 edition.
[3] Suggested to the writer by Dr. L. B. Tuckerman of this Bureau.

Referring again to equation 1, if both types of Sellmeier terms are expanded, there results

$$n^2=a^2-k\lambda^2-p\lambda^4-q\lambda^6-\text{----}+\frac{v}{\lambda^2}+\frac{w}{\lambda^4}+\text{----}, \quad (11)$$

where, in addition to the system expressed by equation 5, $v=\Sigma m$, $w=\Sigma ml^2$, etc. This equation 11 is linear in the parameters and comparatively convenient for a direct least-squares solution. If data with several significant figures must be adjusted and if, as is often the case with these dispersion equations, there is serious loss of significance in the process of solving the normal equations, then it may be necessary or advisable to adjust betterments by use of the equation

$$\Delta n^2=\Delta a^2-\lambda^2\Delta k-\lambda^4\Delta p-\lambda^6\Delta q-\text{----}+\frac{1}{\lambda^2}\Delta v+\frac{1}{\lambda^4}\Delta w+\text{----}, \quad (12)$$

which is obtained after differentiating equation 11.

II. REFRACTIVE-INDEX DATA

During a period of preparation for making definitive measurements on the index of refraction of distilled water, preliminary data were obtained by measurements on 24 samples, of approximately 9 ml each, taken successively from storage in a glass bottle of 5 gallons capacity on 24 working days between March 23 and May 4, 1931. The refractive indices of these samples were measured at 20.00° C for 25 different wave lengths from 3889 to 7679 angstroms. When measuring a single sample, only four or five spectral lines were used, but these were always so selected that each day's measurements were well distributed over the visible spectrum.

All index measurements were made by the method of minimum deviation using a water-jacketed hollow prism mounted in a stirred air bath on the table of a spectrometer. Temperatures were controlled within approximately ±0.01° C and were measured with a platinum-resistance thermometer. All index results were corrected to refer to dry air at 20.0° C and a pressure of 760 mm of mercury. The temperature-controlled prism housing and other auxiliary apparatus have been described in a previous paper,[4] and a description of the hollow prism will be given in a forth coming paper with Mr. John K. Taylor, who cooperated in taking the data that are used in these tests of dispersion equations.

Previously published tests of this kind have usually been made with four- and five-decimal-place data. In the present case it was estimated that errors in the observed indices were confined to the sixth decimal place and perhaps were less than ±5 parts per million.[5] Moreover, these indices were preliminary to experiments which were to be more carefully conducted. The latter, however, were to be based on fewer spectral lines and to be confined within a somewhat more restricted total range in the wave-length interval. Consequently, for subsequent use in adjusting the definitive data, it seemed desirable to use first the preliminary results in testing and selecting

[4] J. Research NBS 17, 389 (1936) RP919.

[5] Many precautionary details necessary for refractive-index determinations of this order of accuracy have been discussed by the writer in former papers. For a brief summary and references see J. Research NBS 14, 417 (1935) RP776.

a dispersion formula for which the added systematic errors of a computational nature should, if possible, be confined approximately to the seventh decimal place. Schönrock's[6] experience in accurately representing the refractive indices of fluorite with a five-parameter equation (4) indicated that success could probably be attained. Nevertheless, comparative tests were desired in order to select a convenient equation having a minimum number of parameters; also to permit an objective quantitative estimate of the systematic errors involved in its use for this particular medium, water.

For these reasons equations 1 (with three terms only), 4 (both with and without the λ^4 term), and 11 have been considered and tested in choosing a dispersion equation for use in adjusting, representing, and interpolating precise data on the refractive index of distilled water.

III. COMPUTATIONAL PROCEDURES

The numerical difficulties in making least-squares solutions for data having seven significant figures are formidable. Mere arithmetical accuracy in such computations on many data is difficult. In addition, during the process of solving normal equations,[7] there sometimes occurs a loss of significant figures that may be troublesome even when only two or three digits are required for expressing the parameters that are to be adjusted. Theoretically, of course, this can be avoided by some suitable change in the initial equation or in the manner in which the solution is attempted. Practically, however, it is usually quicker and easier to resolve the normal equations,[8] considering their coefficients as exact numbers and retaining throughout a second solution as many extra digits as were lost during the first attempt. When six or seven significant figures are required in some of the parameters it is evident, therefore, that the situation may become serious because the theoretically possible alternate procedure may be hopelessly involved and obscure, especially if one is concerned with as many as five or six unknowns.

It is, perhaps, partly for the reasons outlined above that dispersion parameters are seldom thoroughly and completely adjusted when four or more parameters are used. Usually a value based on entirely extraneous evidence is arbitrarily preassigned to one or more of the parameters. Empirically this course is usually justifiable and it is often advisable when the sole purpose is adjustment of the observations. It should be remembered, however, that this procedure may decidedly influence the values which will be obtained for some of

[6] Z. Instrk. **40**, 93–96 (1920); **41**, 103–105 (1921).

[7] Some of the numerical difficulties here discussed are, of course, not peculiar to normal equations but may occur in other computations. Dr. Tuckerman called the writer's attention to this simple illustrative example. Assume a current I flowing through a galvanometer of resistance R_g with a shunt R_s, where R_s is small in comparison with R_g, say approximately 1/10000 of R_g. Let each of these three quantities be observed to three or four significant figures. Then it appears at first impossible to get three or four significant figures when computing $I_g = I - I_s$ where $I_s = \frac{IR_g}{R_g + R_s}$. Nevertheless, by considering the observed values as exact and retaining throughout the computation a sufficient number of significant figures, perhaps seven or eight, one obtains the same result (to three or four figures) that is found by using the more appropriate formula $I_g = \frac{IR_s}{R_g + R_s}$ and retaining only three or four significant figures in the computation.

[8] There seems to be no necessity of revising the "observational equations" and the squares and cross products after they have once been correctly computed and written with a sufficient number of significant figures to yield, by the process of summation, normal-equation coefficients having as many significant figures as are found in the initial data, if the solution is direct, or in the residuals if the process be one of differential betterment.

the other parameters. Such arbitrary selection of one parameter may, therefore, vitiate or call in question the inferences which in some instances are drawn from adjusted values of the others.[9] This point is particularly pertinent for dispersion equations of the type here considered. Some of these parameters are especially sensitive to arbitrary changes in others and yet their "adjusted" values are often regarded as having informative value regarding the location of resonance frequencies, or absorption bands.

1. EQUATION 1, TWO SELLMEIER TERMS, FOUR (INDEPENDENT) PARAMETERS

In using equations 2 and 3 for adjusting four parameters in (three terms of) equation 1, the computational difficulties were somewhat aggravated by the unsuitable nature or form of this two-Sellmeier-term equation as a means of accurately representing the dispersion of water. That this equation, as thus limited, might be found relatively unsuitable could have been predicted from dispersion theory and the known large dielectric constant of water. However, it does not follow that this equation 1 must necessarily be inferior to equation 4 when the latter is limited to four terms.

A simultaneous solution with equation 2 gave obviously large residuals. Differential betterment by least squares with equation 3 effected such large changes in the parameters that the results were even worse than the initial computations. A second simultaneous solution with equation 2 (using a second set of observed indices) likewise resulted in computed indices that agreed poorly with the observations, so poorly that a continuation with betterments by equation 3 was not advisable. Thus it seemed imperative to obtain better approximate values before second derivatives could safely be ignored. For this purpose a direct least-squares solution with equation 2 was attempted, but a solution of the normal equations, using nine significant figures, failed to yield even one significant figure for the group $\left(\frac{Ml^2}{L^2}+\frac{mL^2}{l^2}\right)$ of unknowns.

In most instances of difficult solutions at least some significant figures are obtained in solving for one of the unknowns and one knows at once how many digits must be retained in a successful re-solution of the normal equations. In this case, however, there was no indication as to what computational precision would be sufficient. Consequently, using the normal equations, the three other groups of unknowns were then expressed in terms of $\left(\frac{Ml^2}{L^2}+\frac{mL^2}{l^2}\right)$ and this system was repeatedly solved for several even (exact) values of L^2 such as 1, 2, 4, 9, and 36, all of which correspond roughly with known absorbing frequencies in the infrared spectrum of water.

In every case within this wide range of L^2 these sets of parameters were computed with internal consistency to about nine significant figures and they satisfied the normal equations to about eight or nine significant figures. Of these various sets of parameters none seemed really satisfactory but the one with $L^2=2$ gave the lowest sum of the squared residuals, and $L^2=4$ was next best. Then after trying 2.1,

[9] See, for example, E. Flatow, Ann. Physik [4] **12**, 93 (1903).

2.25, 2.4, and 3.0 and plotting (see fig. 1) the corresponding values of Σr^2, a value of $L^2=2.25$ was selected as approximately an optimum. The corresponding set of parameters was then bettered by a least-squares solution with the aid of equation 3. Some significant figures were lost in this last process, but the betterments themselves were comparatively small. In the resulting dispersion formula,

$$n^2=1.7726479-\frac{0.0315734}{2.2535795-\lambda^2}+\frac{0.00701841}{\lambda^2-0.0092513}, \qquad (13)$$

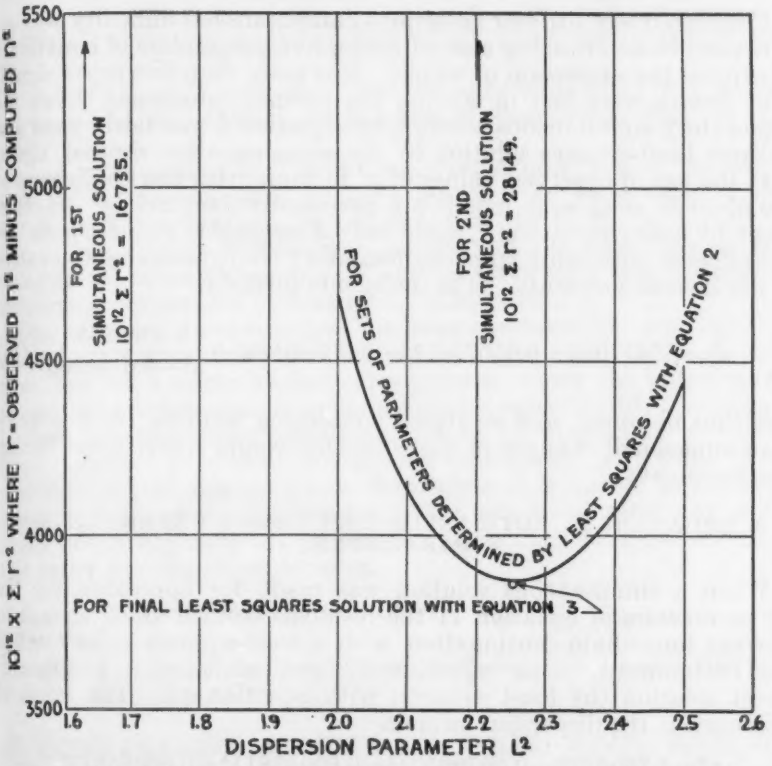

FIGURE 1.—*Determining by trial the first of four dispersion parameters of equation 1.*

In this difficult case of adjustment by least squares it was necessary to express three parameters in terms of a fourth and then plot Σr^2 for various arbitrarily selected values of the fourth. All sets of parameters having L^2 in the range 1 to 36 satisfied the normal equations to 8 or 9 significant figures.

the consistency of the full set of constants is adjusted with a precision fully as great as is warranted by the observations, but it is recognized that further least-squares adjustment by renewed application of equation 3 would introduce compensatory changes among these constants that in some instances might materially change the penultimate digits.

Incidentally, the final Σr^2, although slightly lower than the similar summation for $L^2=2.25$ is not noticeably off the curve which has been plotted in figure 1 for those various computations that are all in accord (to eight significant figures) with normal equations obtained by the aid of equation 2. This means that errors in the observed values of

n^2, which were allowed to enter in the right-hand of equation 2, were not in this instance of any importance. It also means that at least one of the constants of formula 13 can, with approximately the same validity in representing the observations, be rounded to three significant figures, provided it be considered as exact whenever used (including most particularly its use in the computation of the other constants in such manner that all of them form a consistent set that satisfies the normal equations).

2. EQUATION 4, INFRARED TERM EXPANDED, FIVE PARAMETERS

Comparatively little or no serious computational difficulty was experienced in determining and adjusting five parameters of equation 4 to express the dispersion of water. Not more than five or six significant figures were lost in solving the normal equations. Even the exploratory simultaneous solution by equation 6 was fairly good and a direct least-squares solution by the same equation showed, again, that the use of observed values of n^2 in computing the coefficients of the observational equations is not necessarily dangerous. A betterment by using equation 7 made only a negligible reduction in Σr^2 but effected noticeably large compensatory changes among the values of the several constants. The dispersion formula

$$n^2=1.7611069-0.0107941\lambda^2-0.0009048\lambda^4+\frac{0.00653385}{\lambda^2-0.0140700} \quad (14)$$

was thus obtained, and as stated concerning formula 13, it is likely that some small changes in the constants would result upon further readjustment.

3. EQUATION 11, BOTH SELLMEIER TERMS EXPANDED, SIX PARAMETERS

When a simultaneous solution was made for approximating the six parameters of equation 11 the residuals seemed small enough to warrant immediate continuation with a least-squares adjustment of the betterments, using equation 12 and omitting a preliminary direct solution (by least squares) with equation 11. The result of this work is the dispersion formula

$$n^2=1.7606279-0.0079050\lambda^2-0.0066381\lambda^4+0.0038681\lambda^6 +\frac{0.00649123}{\lambda^2}+\frac{0.000111406}{\lambda^4}, \quad (15)$$

for which Σr^2 is appreciably lower than for the initial (simultaneous) determination. Again, however, five or six significant figures were lost in solving the normal equations and some of the betterments were so large that the numerical coefficients in formula 15 are, perhaps, not in strictly optimum adjustment.

4. EQUATION 4, TERM IN λ^4 OMITTED, FOUR PARAMETERS

Equation 4, without the term in λ^4, is one of the most commonly used equations for expressing dispersion. For simultaneous solutions four parameters may be easily evaluated from the system of equations:

$$\left.\begin{aligned} l^2&=\frac{A\lambda_4^2-\lambda_1^2}{A-1},\\ m&=\delta_2\delta_3\delta_4\left(\frac{\Delta_{23}-\Delta_{34}}{\lambda_4^2-\lambda_2^2}\right),\\ k&=\Delta_{12}-\frac{m}{\delta_1\delta_2},\\ \text{and } a^2&=n_1^2+k\lambda_1^2-\frac{m}{\delta_1}, \end{aligned}\right\} \quad (16)$$

where $A=\dfrac{\lambda_3^2-\lambda_1^2}{(\Delta_{12}-\Delta_{23})}\left(\dfrac{\Delta_{23}-\Delta_{34}}{\lambda_4^2-\lambda_2^2}\right)$; $\Delta_{12}=\dfrac{n_1^2-n_2^2}{\lambda_2^2-\lambda_1^2}$, $\Delta_{23}=\dfrac{n_2^2-n_3^2}{\lambda_3^2-\lambda_2^2}$, etc.;

$\delta_1=(\lambda_1^2-l^2)$, $\delta_2=(\lambda^2{}_2-l^2)$, etc., and the subscripts refer successively to values of n^2 and λ^2 from the four sets of observations that are to be used.

In using equations 16 it is obviously important to have the sets of observed data separated by wide intervals in wave length. For water, with observations extending over the visible spectrum, no serious loss of significance need occur, and the constants as thus obtained are often sufficiently reliable to serve as a useful basis for differential betterment by four terms of equation 7.

Direct least-squares solutions for these constants by using equation 6 also have proved fairly satisfactory for adjustment of the observations, but for a single least-squares process, where the initial results are not to be bettered, it is preferable to use equation 10. In general, however, whether using equations 7, 6, or 10, about four significant figures are lost in solving the normal equations. Therefore, if one desires to adjust the constants themselves it is unsafe to neglect a betterment based on the residuals that are given after any initial least-squares adjustment. From the particular data considered in this paper the dispersion formula

$$n^2=1.7616034-0.0119397\lambda^2+\frac{0.00644940}{\lambda^2-0.0148669} \quad (17)$$

was finally obtained for comparison with formula 13 and the more elaborate formulas 14 and 15.

IV. COMPARATIVE MERITS OF FOUR, FIVE, AND SIX PARAMETERS

1. RELATIVE GOODNESS OF FIT AND CHI-TEST

When only one formula is used for representing a given set of data, some idea of its suitability for the purpose can be obtained by an examination of the residuals. Also, one may use the Chi-test[10] to measure quantitatively in terms of probability the goodness of fit which is obtained, provided a numerical estimate of the precision of the data is known a priori. When, however, for an identical set of data, and identical assumptions concerning the weighting, there are several different formulas fitted by least squares to the observations, then these formulas may be directly compared as to relative goodness of fit by forming in each case an estimate of some characteristic error for an observation of unit weight. Estimates of this sort may be

[10] For a recent discussion of this test, see W. Edwards Deming, J. Am. Statistical Assn. **29**, 372-382 (1934).

based on the assumption that the chances are about even for obtaining, purely by chance and exclusive of peculiarities or defects in the formula itself, a worse fit than has been found. Then, if probable error be the characteristic measure of precision selected for the basis of comparison it is estimated as $P.\ E.=0.6745\sqrt{\Sigma r^2/C}$, where C is the number of observations decreased by the number of adjustable parameters in the formula.

The results of tests and intercomparisons of formulas 17, 13, 14, and 15 are given in table 1 where many of the entries are self-explanatory. Excepting for the unsuitable formula 13, none of the estimated probable errors seems unreasonably large, especially when it is considered that these data were preliminary observations and not made with the approved technique which was later adopted for the definitive measurements. Moreover, it should be noticed that these estimated probable errors do not differ for the equations 17, 14, and 15 (with four, five, and six parameters, respectively) by as much as the probable error in these estimates, namely, $0.477\ P.\ E./\sqrt{C}$. Consequently, there is in this particular little or no definite indication that these three formulas would have the same relative standing if again compared by using them to represent another set of similar index data.

There should, of course, for this single set of data, be only one final estimate of the probable error of a single observation of weight unity. From the estimates in table 1 (and imperfection in a formula tends to make these values high) it appears that the probable error is not greater than $\pm 1.4\times 10^{-6}$ in index and from the details of the observations the probable error is directly computed as $\pm 1.26\times 10^{-6}$. Assuming, then, a probable error of $\pm 1.3\times 10^{-6}$ as an a priori estimate, there have been computed from the Chi-tables, and listed in table 1 the probabilities, P, that the actually observed degrees of failure to fit might be worse purely by chance even if the corresponding formulas were perfectly suitable for the purpose of expressing the dispersion of water. For formula 17, then, the tabulated probability 0.23 is not seriously below the optimum value which is 0.50 approximately. In other words, even a perfect formula would, in about 23 of 100 such tests, fail to appear as suitable as does formula 17 when judged by this one test.

TABLE 1.—*Statistical comparison of dispersion formulas*

Designation of formula	17	13	14	15
Number of independent parameters	4	4	5	6
Number of + residuals (observed minus computed index)	10	11	12	12
Number of − residuals	15	14	13	13
Number of changes in sign of adjacent residuals	12	6	11	14
Number of non-changes in sign of adjacent residuals	12	18	13	10
$10^6\Sigma r \equiv$algebraic sum of residuals	−0.03	+0.04	+0.18	0.00
$10^6\times$algebraic average residual	−0.001	+0.002	+0.007	0.000
$10^6\Sigma\lvert r\rvert \equiv$arithmetic sum of residuals	36.2	94.1	35.4	34.3
$10^6\times$arithmetic average residual	1.45	3.76	1.42	1.37
$10^6\times$median residual	1.24	3.9	1.12	1.19
$10^{12}\times\Sigma r^2$	94.6	541.4	84.0	72.9
$10^6\times$estimated *P. E.* (assuming that existing degree of fit can be worse by chance alone in 50 percent of such tests)	±1.43	±3.42	±1.38	±1.32
$10^6\times$estimated *P. E.* of estimated *P. E.*	±0.15	±0.36	±0.15	±0.14
Number of observations minus number of parameters	21	21	20	19
$\chi^2=\Sigma r^2/(1.483\ P.\ E.)^2$, where *P. E.* is estimated a priori as $\pm 1.3\times 10^{-6}$	25.5	146	22.6	19.6
Probability of worse fit by chance alone if *P. E.* is estimated a priori as $\pm 1.3\times 10^{-6}$ in index	0.23	Very small	0.31	0.42
Odds that formula is imperfect in form	3.4 to 1	Very great	2.2 to 1	1.4 to 1

2. CONCLUDING DISCUSSION

The manner in which the four dispersion formulas fit the refractive-index data is illustrated in figure 2, where everything is referred to a datum or reference line, $\Delta n=0$, that corresponds to values of the refractive index of distilled water as computed by the general interpolation formula which has been adjusted to fit all approved data [11] on water taken in the refractometric laboratory at this Bureau. The four-constant formula 13 is obviously unsuitable and necessarily inaccurate for representing the data, and it is thus indicated that there is no single effective location of an absorption band in the infrared region that will serve to replace the bands which actually exist for water.

Referring to the average location and trend of the other curves in figure 2, the general lack of parallelism to the line $\Delta n=0$ is probably attributable to the accidental distribution of errors in this sample of

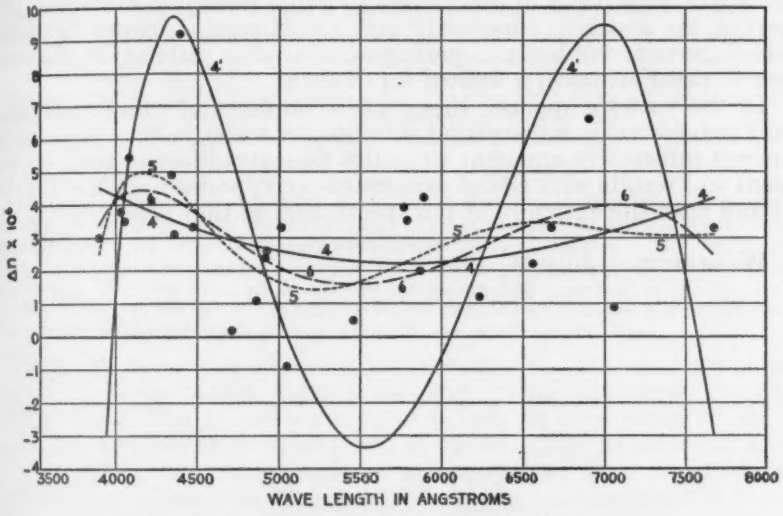

FIGURE 2.—*Comparison of dispersion formulas.*

Formulas 17, 13, 14, and 15, with 4, 4′, 5, and 6 parameters, respectively, were adjusted by least squares to fit preliminary refractive-index data taken at 20.0° C on distilled water. Circular dots represent observations and lines represent computed indices. The reference line $\Delta n=0$ corresponds to indices computed by a general interpolation formula (based on formula 17) to fit more numerous data on distilled water which were subsequently taken with improved technique and procedures.

only 25 observations. One notices, particularly, an especially high index for the faint helium line 4388 A; also the low value for the faint helium line 5048 A, and the high value for the faint mercury line 6907 A. The average increase of 3×10^{-6} in index which these samples show is attributed to slight contamination of the water which was not freshly distilled but had been stored in a dark-room where ammonia and other chemicals were kept. Moreover, during some of these initial experiments the hollow prism was almost entirely filled and a paper collar on the glass stem of the platinum-resistance thermometer was inadvertently allowed to touch the water. For these reasons,

[11] A total of 133 observations were used in adjusting by least squares a formula with 13 constants which represents the refractive index of distilled water in the visible region of the spectrum for the range 0 to 60° C. An account of this work by the writer, in collaboration with Mr. John K. Taylor, is being prepared for publication in this journal.

and also because complete tables of the refractive index and dispersion of water are to be included in a later account of work with more careful and approved procedures, no explicit values for these data are included in this paper.

It is evident from figure 2 that each of formulas 17, 14, and 15 agrees well with the average for all three of them. Aside from extremes of wave length, there is only one instance for which an individually computed index differs from this average by as much as 6×10^{-7}. Thus it seems that the Ketteler-Helmholtz dispersion formula 17 with four constants is probably adequate in representing the refractivity of water in the visible region to approximately $\pm5\times10^{-7}$ or better.

As shown by certain data in table 1, there is, from a purely statistical viewpoint, some indication of slight added superiority of the five- and six-constant formulas for fitting this particular sample of 25 indices. On the other hand, the slight advantage is not reliably indicated and, moreover, experience in using these formulas leads one to suspect that part of the apparent superiority may result from a greater flexibility which permits further and perhaps undesirable yielding to the accidental peculiarities of a limited set of data.

In the writer's opinion, then, the advantages of using more than four parameters in a dispersion equation for water in the visible range are not sufficiently apparent to justify the extra labor in their adjustment and results with added parameters may, perhaps, be less reliable at and near the extremes of the spectral range that is employed.

WASHINGTON, July 18, 1936.

U. S. Department of Commerce National Bureau of Standards

RESEARCH PAPER RP935

Part of Journal of Research of the National Bureau of Standards, Volume 17, November 1936

INKS FOR RECORDING INSTRUMENTS

By C. E. Waters

ABSTRACT

Inks for recording instruments are made by dissolving dyes in a mixture of glycerin and water. They dry chiefly by being absorbed by the paper, and for that reason lines drawn with them have a tendency to "feather", or have irregular edges. The paper and the nature of the dye determine whether or not there will be feathering. A series of 38 inks was made by dissolving each of 19 acid, or basic dyes in 2 mixtures (1:1 and 1:3) of glycerin and water. Another series of inks was made by dissolving each of 16 direct dyes in the 2 mixtures of glycerin and water; and a third series by dissolving the same 16 dyes in similarly diluted ethylene glycol. All the inks were tested by drawing lines on five kinds of paper, three of which were charts provided with recording instruments.

In the 190 tests of the 38 inks of the first series, on the 5 papers, only 10 lines were rated as nonfeathering, with 108 slightly, and 72 decidedly, feathering. The proportion of water made little difference in the results.

The inks of the second and third series, made with direct dyes, were in general greatly superior to those of the first series. The 16 direct dyes, each in 4 solvents, made 64 inks, with which 320 lines were drawn on the 5 papers. Of these lines, 227 were rated as nonfeathering, 48 as slightly feathering, and 45 as decidedly feathering. Further analysis of the results shows that glycerin is better than ethylene glycol at the same dilution, and that the inks with the larger proportion of water made sharper lines than those with less water.

There are numerous kinds of instruments for making continuous records of temperature, barometric and steam pressures, electric voltage, etc. The record consists of a line, or of a series of dots, on a circular card or on a long roll of paper. The instrument may have to run a long time without attention, so there must be an ample supply of ink of a kind that will not dry on the pen if it is indoors, nor freeze at outdoor temperatures in winter. For many years the United States Weather Bureau has used recording ink made by dissolving a dye in a mixture of equal volumes of glycerol and water. This mixture is a good "antifreeze", yet there are parts of the United States where it would be solid in winter. To overcome this difficulty, enough ethyl alcohol to keep the ink fluid at any winter temperature is added to the ink.

For use with instruments located indoors, a mixture of 1 volume of glycerol and 3 volumes of water has been found to make a satisfactory recording ink.

The properties of glycerol that make it so valuable in recording inks are disadvantages as soon as the ink is put upon paper. Because the ink must dry almost entirely by being absorbed, the marks are apt to be "feathered", or have uneven edges. The ink spreads in all directions from the actual marks made by the pen and does not simply sink into the paper.

Whether or not feathering occurs depends to a great extent upon the properties of the paper or card upon which the record is made,

but the results of tests to be described in this paper indicate that the nature of the dye is not to be overlooked. That this was the case had been suspected, and in order to get definite information on the subject, a number of experiments were made with inks prepared by dissolving selected dyes in glycerol and water of two dilutions. One set of inks was made with a mixture of equal volumes of glycerol and water, and another set with a mixture of 1 volume of glycerol and 3 of water. A series of 19 dyes, 17 of them acid and 7 basic, were chosen for the first series of experiments. Enough of each dye to give a satisfactory depth of color was dissolved. With the 36 inks made from these dyes, lines were drawn on 9 kinds of paper, including the thin cards provided by the manufacturers of some recording instruments. The lines were drawn with an ordinary gold writing pen, and after they had dried spontaneously, were inspected and rated. According to their appearance they were marked "*N*" (no feathering, "*SF*" (slight feathering), and "*F*" (decided feathering). Naturally there were no hard and fast boundaries between the three groups. Probably the majority of the "*SF*" lines would have passed muster as very satisfactory for nearly all uses.

Later, 2 series of tests were made with 16 other dyes, on 5 kinds of paper that were duplicate sheets of 5 of the kinds used in the first series of tests. A less confusing comparison can be made between the 2 sets of dyes if only the results obtained with these 5 kinds of paper are considered.

Table 1 summarizes the results on each of the 5 papers on which lines were drawn with 38 inks made with acid and basic dyes. Paper no. 3 was scratch-pad paper used at the National Bureau of Standards. This paper is usually satisfactory for writing with blue-black iron gallotannate ink, but at times red writing ink, made by dissolving a dye in water, shows a tendency to feather on it. Number 5 was a bond paper, used as a "heavy second" sheet for writing official letters at the Bureau. Numbers 7, 8, and 10 were circular charts, of different thicknesses, for use with 3 kinds of recording instruments.

TABLE 1.—*Tests with acid and basic dyes*

[Dissolved in the two mixtures of glycerol and water]

Paper number	3	5	7	8	10
Total *N*	6	0	0	0	4
Total *SF*	29	11	10	30	28
Total *F*	3	27	28	8	6

It is evident that 2 of the papers were distinctly inferior to the other 3, and that the 19 dyes did not make conspicuously good recording inks, unless the lines rated as "*SF*" would be acceptable. Only 10 of the total 190 lines were rated as "*N*".

An analysis of the results of the 190 tests made it clear that the nature of the dye had less to do with the feathering than the paper on which the lines were drawn. It seems unnecessary to give the detailed results, in view of what is to follow.

Direct dyes are those that are readily taken up by vegetable fibers and are firmly held, without the use of a mordant, to produce insoluble compounds with the dyes in and on the fibers. It seemed possible

[1] Acknowledgment is made of the courtesy of A. K. Gyzander, of the National Aniline & Chemical Co., New York, N. Y., for supplying without charge a 2-ounce sample of each of the dyes.

that inks made with direct dyes might show less feathering than those just discussed, because the fibers of the paper might adsorb the dyes at the marks made by the pen, or so close to the marks that their outlines would remain sharp. A few preliminary tests with direct dyes that happened to be at hand were sufficiently encouraging to make it desirable to carefully test a series of direct dyes obtained from a single manufacturer. Accordingly, 17 direct dyes were so obtained,[1] and were made into 34 inks by dissolving them in the 2 mixtures of glycerol and water, at the rate of 10 g of dye in a liter. This is the concentration of the recording inks used by the Weather Bureau.

One of the dyes, toluylene orange *R*, did not dissolve completely, and the turbid solution showed practically no sign of clearing by settling when left undisturbed for several days. Another dye, diamine green *B*, set to a sort of soft jelly on standing overnight. This became fluid when shaken, and there was no difficulty about drawing the lines with it. In all the tests with direct dyes, the lines were made with a ruling pen. There was one yellow dye, chloramine yellow, which is not included in the discussion of the inks made with direct dyes. Because of its pale color, and its brightness, there was little contrast between the lines and the white paper, so it was impossible to decide how the lines should be rated. Of the remaining 16 dyes, 2 were labeled differently by the manufactuer, though they had the same number in the Colour Index. They were considered as two distinct dyes, however. There were 32 inks in this set. Table 2 shows how much better results the direct dyes gave than were obtained with the acid and basic dyes.

TABLE 2.—*Tests with direct dyes*

[Dissolved in two mixtures of glycerol and water]

Paper number	3	5	7	8	10
Total *N*	26	21	27	25	32
Total *SF*	4	11	2	5	0
Total *F*	2	0	3	2	0

Of the 160 lines, 131 were rated as nonfeathering. If there had been the same proportion in the first series, 155 of the 190 lines would have been nonfeathering, instead of only 10.

Ethylene glycol is a liquid that is like glycerol in being hygroscopic and practically nonvolatile at ordinary temperatures, but differs from it in being somewhat more fluid. It was thought that it might make inks as good as those prepared with glycerol, so the 16 direct dyes were used for a series of 32 inks, half of which were made with a mixture of equal volumes of ethylene glycol and water, and the other half with 3 volumes of water to 1 of the glycol. They were tested on the same five papers as the other inks. The results of the 160 tests are in table 3.

TABLE 3.—*Tests with direct dyes*

[Dissolved in two mixtures of ethylene glycol and water]

Paper number	3	5	7	8	10
Total *N*	11	16	27	20	32
Total *SF*	8	4	2	7	0
Total *F*	13	12	3	5	0

A comparison of table 1 with tables 2 and 3 shows that the direct dyes are far superior to the acid and basic dyes that were tested. The direct dyes were selected for their range of colors, and not because of any definite knowledge that these particular ones would prove to be so superior. Indeed, the preliminary tests with direct dyes, referred to above, were made with nine dyes, only three of which were the same as those used in the more careful tests. It would strengthen the case for the direct dyes if the results of the preliminary tests were given, but this does not seem necessary.

Tables 2 and 3 show that mixtures of glycerol and water are better than mixtures of ethylene glycol and water as solvents for making recording inks. Table 4 presents the results in a different way, and shows that the inks with the larger proportion of water are much better than the others, so far as the direct dyes are concerned. There was no such clear-cut distinction in the case of the inks made with acid and basic dyes, so it is not worth while to give the detailed results of the tests made with them.

TABLE 4.—*Tests with direct dyes*

[Showing the effect of increasing the proportion of water]

Group	Glycerol-water		Glycol-water	
	1:1	1:3	1:1	1:3
Total *N*	52	79	27	69
Total *SF*	21	1	15	11
Total *F*	7	0	38	0

It should be said that the 2 sets of inks made with the 19 acid and basic dyes were prepared and tested 3 days apart, under somewhat different weather conditions on the 2 days. The 4 sets of inks containing the 16 direct dyes were prepared on different days, but the 160 lines were all drawn within about 3 hours, on a morning when there was no noticeable change in the weather. The temperature of the laboratory was 28° C (82° F), and the relative humidity about 65 percent.

TABLE 5.—*Direct dyes used in the tests*

Name of dye	Colour Index number	Name of dye	Colour Index number
Benzo fast scarlet	326	Benzo sky blue	520
Congo red	370	Diamine violet *N*	394
Toluylene orange *R*	446	Oxamine blue 4*R* (Erie violet 2*B*)	471
Toluylene orange *G*	478	Bismarck brown *R*	333
Pyrazol orange	653	Benzamine brown 3*GO*	396
Chloramine yellow	814	Columbia black *FF* extra	539
Chloramine green *B*	589	Direct deep black *RW* (Erie black *RXOO*)	562
Diamine green *B*	593	Direct deep black *RW* (Erie black *RW*)	562
Diamine sky blue *FF*	518		

For the information of those who may be interested, the names of the direct dyes are given in table 5. The yellow dye is included because it might be needed to modify the hue of an ink of another color. The corresponding numbers of the dyes in the Colour Index are given for the better identification of the dye types. The names

of the dyes are not those on the manufacturer's labels, because it seemed better to use the preferred names in the Year Book of the American Association of Textile Chemists and Colorists, but in three cases the manufacturer's names are added because there might otherwise be confusion.

A drawback to the use of a few of these dyes is the comparative dullness of their hues, in spite of the fact that they were selected because they were known to be brighter than the average direct dyes. The lines drawn with congo red were dark brownish red, and the solutions could have been less concentrated, to advantage. Chloramine green *B* and diamine green *B* made dull lines. If a brighter direct green dye cannot be had, a mixture of chloramine yellow and a blue dye might be tried. The three black inks should have contained more dye. This suggested the thought that if the solutions are made stronger so as to get a greater depth of color, the dye may not all be absorbed by the paper, and this may cause feathering, though the solution containing 10 g in a liter was satisfactory. To test this idea, eight inks were made with two concentrations of four of the dyes in the mixture of equal volumes of glycerol and water. Congo red and diamine sky blue *FF* showed feathering at a concentration of 10 g in a liter, so each of them was dissolved at concentrations of 5 and 7.5 g in a liter. Of the black dyes, Erie black *RXOO* was dissolved at the rate of 12.5 and 15 g, and Erie black *RW* at 11 and 12 g in a liter. These eight inks and the four originally tested were tried on the scratch-pad and bond papers. Changing the concentrations of the dyes had no definite effect upon the feathering of the inks.

It is believed that the results here given are sufficient to show that for making recording inks with a minimum of feathering, only the direct dyes should be used; that a mixture of 1 volume of glycerol, or of glycol, and 3 volumes of water is a much better solvent than a mixture of equal volumes of the two liquids; and that ethylene glycol is not as good as glycerol at either dilution.

The inks were prepared on July 9. On October 2 they were inspected, and it was found that some of the corks of the tubes in which the inks had been kept were moldy. When shaking the tubes to dissolve the dyes, all the corks had been wet with the inks. Of the inks made with equal volumes of glycerol and water, six contained dyes that permitted the growth of mold. Three, and possibly four, species of mold were growing and fruiting on the corks. With the mixture of 1 volume of glycerol and 3 volumes of water, there were 13 moldy corks, and in addition mold was growing on the surface of 3 of the inks. No mold could be detected on the corks that had been in contact with the inks made with ethylene glycol at either dilution.

WASHINGTON, August 17, 1936.

U. S. Department of Commerce National Bureau of Standards

RESEARCH PAPER RP936

Part of Journal of Research of the National Bureau of Standards, Volume 17, November 1936

CHANGE OF VOLUME OF RUBBER ON STRETCHING: EFFECTS OF TIME, ELONGATION, AND TEMPERATURE

By William L. Holt and Archibald T. McPherson

ABSTRACT

The change of volume on stretching was studied for four rubber compounds; two were pure gum, and one each contained 10 percent by volume of carbon black and whiting, respectively. Samples were made in the form of narrow molded rings. Measurements of the change with time up to about 20 minutes were made with a water-filled dilatometer; for longer periods a mercury-filled dilatometer was used. The whiting compound increased in volume on stretching, presumably on account of the formation of vacuoles around the coarse particles of filler. With the other compounds the volume remained constant up to an elongation of 200 or 300 percent, above which it decreased by an amount which was greater the higher the elongation, the lower the temperature, and the longer the time the rubber was kept stretched. The decrease was an approximately linear function of the logarithm of the time from a few minutes after stretching, to about 4 weeks, the duration of the experiment. The volume thermal expansivity of the stretched rubber was greater than that of the unstretched. Increased vulcanization of a given compound, in general, decreased the volume change on stretching. The results indicate that, in the absence of coarse fillers, Poisson's ratio for rubber is 0.5 or greater, the numerical value depending upon the composition, the temperature, the time after stretching, and other factors.

CONTENTS

	Page
I. Introduction	658
II. Preparation of samples	658
III. Methods of measuring volume change	660
1. Water-filled dilatometer for measurements at the shorter time intervals	660
2. Mercury-filled dilatometer for measurements at the longer time intervals	663
IV. Factors influencing change of volume	664
1. Composition	664
2. Elongation	666
3. Time	667
4. Temperature	671
5. State of vulcanization	674
6. Other factors	675
V. Poisson's ratio	676
VI. Interpretation of results	677
VII. Summary	678

I. INTRODUCTION

The present investigation was suggested by the work of Davey and his students,[1] who found that a time lag of a few seconds elapsed between the stretching of rubber and the development of the full intensity of the X-ray diffraction pattern. Feuchter [2] had previously shown that the volume of rubber decreased on stretching, and on the basis of these two observations one of the present authors predicted that a time lag would occur in the change of volume of rubber on stretching. When this time lag was looked for it was found without difficulty,[3] and seems to afford a simple, convenient means for studying the fibering or "crystallization" of stretched rubber. Incidental to studying this time lag observations were made as to the effect of composition, temperature, and elongation on the volume of stretched rubber.

The time lag has been recently observed in connection with the double refraction of stretched rubber, by Thiessen and Wittstadt,[4] and probably constitutes the effect which was dismissed by previous observers as "optical creep." [5]

The literature on rubber contains a wide range of values for the change of volume on stretching and for Poisson's ratio. Most of the data pertain to rubber-filler systems,[6] [7] which increase in volume on stretching because the formation of vacuoles around the coarse filler particles or aggregates increases the volume of the stretched rubber to a much greater extent than the fibering of the rubber phase decreases it.

Early investigators [8] who worked with rubber containing no fillers failed to observe any decrease in volume on stretching, probably for the reason that inhomogeneities such as sulphur crystals due to the relatively high percentage of sulphur used at that time led to the formation of vacuoles which masked the effect of fibering of the rubber phase.

II. PREPARATION OF SAMPLES

The samples used in the present investigation were molded rings which were made as thin as practical in the radial dimension so that when they were stretched the inside and the outside would have nearly the same elongation. The rings were approximately 1 mm in width, 4 mm in depth, and 100 mm in average circumference. The inside circumference was about 96.9 mm and the outside, 103.1 mm, hence when the rings were stretched by a relatively large amount the actual elongation of the rubber ranged from about 3 parts per 100 below to

[1] M. F. Acken, W. E. Singer, and W. P. Davey. *X-ray study of rubber structure*, Ind. Eng. Chem. **24**, 54–57 (1932).
John D. Long, William E. Singer, and W. P. Davey. *Fibering of rubber. Time lag and its relation to structure*, Ind. Eng. Chem. **26**, 543–547 (1934).
[2] H. Feuchter, *The volume contraction with the formation of anisotropic rubber systems by stretching*, Gummi-Ztg. **39**, 1167–1168 (1925).
[3] BS Tech. News Bul. 201, p. 6 (Jan. 1934).
[4] Peter A. Thiessen and Werner Wittstadt. *Crystals and fused substances in stretched rubber*, Z. phys. Chem. **29B**, 359–362 (1935). English translation, Rubber Chem. Tech. **9**, 52–54 (1936).
[5] Wilfred E. Thibodeau and Archibald T. McPherson. *Photoelastic properties of soft, vulcanized rubber*, J. Research NBS **13**, 887–896 (1934) RP751.
[6] H. F. Schippel, *Volume increase of compounded rubber under strain*, J. Ind. Eng. Chem. **12**, 33–37 (1920).
[7] W. W. Vogt and R. D. Evans, *Poisson's ratio and related properties for compounded rubber*, Ind. Eng. Chem. **15**, 1015–1018 (1923).
[8] A summary of the early work is given by Whitby in Plantation Rubber and the Testing of Rubber, p. 486–501 (Longmans, Green and Co., London, 1920).

3 parts per 100 above the average elongation, which is the figure reported in the present work.

The mold used for making the rings consisted of a heavy metal plate containing cylindrical cavities. In each cavity a removable disk, 1 mm smaller in radius than the cavity, was fitted in such a way as to leave an annular space in which the ring was molded. By taking out this central disk a sample which had been vulcanized in the cavity could be removed without damage. Details of the mold are shown in figure 1.

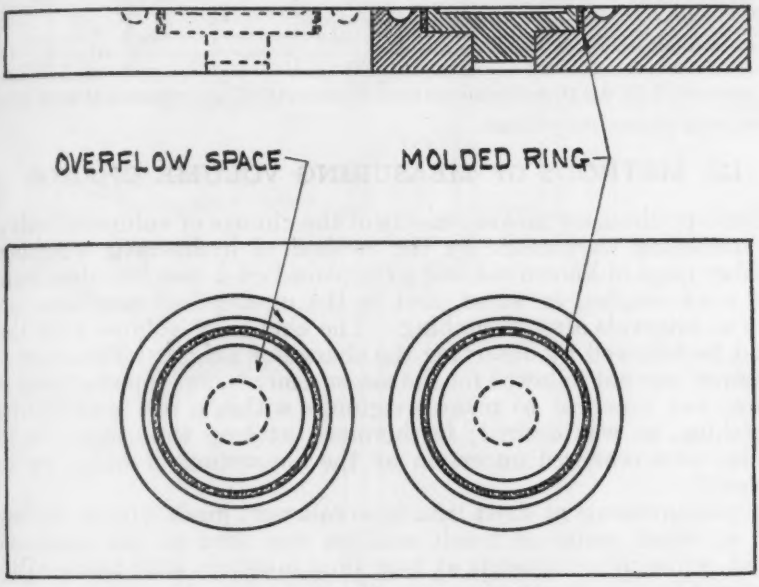

FIGURE 1.—*Mold for rubber test rings.*

The rings, after vulcanization, were carefully trimmed and inspected for flaws and inclusions before use. Those which were to be employed in the mercury-filled dilatometer were stored under mercury for some time to remove free sulphur and other constituents which might cause fouling.

Most of the work reported in this paper was done with two "pure gum" compounds which were vulcanized with mercaptobenzothiazole and tetramethylthiuram disulphide, respectively, as accelerators. These are compounds *I* and *II* in table 1. Compound *II* is identical with compound *B* which was used in photoelastic studies on rubber.[9] A few experiments were conducted with compounds *III* and *IV*, which contain 10 percent, by volume of whiting and carbon black, respectively.

[9] See footnote 5.

TABLE 1.—*Composition of rubber compounds*

Ingredients	Compounds [a] (parts by weight)			
	I	*II*	*III*	*IV*
Smoked sheet rubber	100		100	100
Pale crepe rubber		100		
Zinc oxide (Kadox)	1	1	5	5
Stearic acid	1	1	1	1
Mercaptobenzothiazole	1		0.8	0.8
Tetramethylthiuram disulphide		0.3		
Sulphur	2	2	3	3
Whiting			[b] 34	
Carbon black (Micronex)				[b] 22.6

[a] Compounds *I*, *III*, and *IV* were vulcanized for 30 minutes at 141° C, and compound *II*, for 30 minutes at 126° C.
[b] 10% of the volume of the compound.

III. METHODS OF MEASURING VOLUME CHANGE

Some preliminary measurements of the change of volume of rubber on stretching were made by the method of hydrostatic weighings. Rubber rings of known volume were placed on a stainless steel frame and were weighed in water, first in the unstretched condition, and then at intervals after stretching. The change of volume with time could be followed by observing the change of weight. This method, however, was not followed for the measurements here reported because it was not practical to make weighings within a few seconds after stretching, as was desired; furthermore, at long time intervals the results were rendered uncertain by the absorption of water by the rubber.[10]

The measurements at short time intervals were made with a dilatometer in which water or a salt solution was used as the containing liquid, while measurements at long time intervals were made with a mecury-filled dilatometer.

1. WATER-FILLED DILATOMETER FOR MEASUREMENTS AT THE SHORTER TIME INTERVALS

The apparatus which was used in measuring the change of volume at intervals from a few seconds to 20 or 30 minutes after stretching is illustrated in figure 2. It consisted essentially of a brass tube about ⅜ inch in diameter and 20 inches in length, connected by a side arm to a calibrated glass capillary tube. The brass tube was provided with stuffing boxes at each end, through which a 1-mm brass wire could be drawn back and forth. A ring-shaped sample could be stretched within the tube by means of a fixed hook attached at one end of the tube and a movable hook fastened to the brass wire.

In using the apparatus one or more rubber rings were mounted, unstretched, over the two hooks; the tube was then closed and filled with water or a salt solution to a convenient height on the glass capillary. The filling was facilitated by a second side tube which was provided with a stopcock. When the rubber rings were stretched by drawing the brass wire through the tube any change in the volume

[10] When water is taken up by unstretched rubber the swelled rubber occupies almost, if not precisely, the same volume as the rubber and the water taken separately, but in the case of stretched rubber there appears to be an appreciable net loss of volume on swelling. The authors do not wish to report numerical data regarding this effect until further experiments have been conducted.

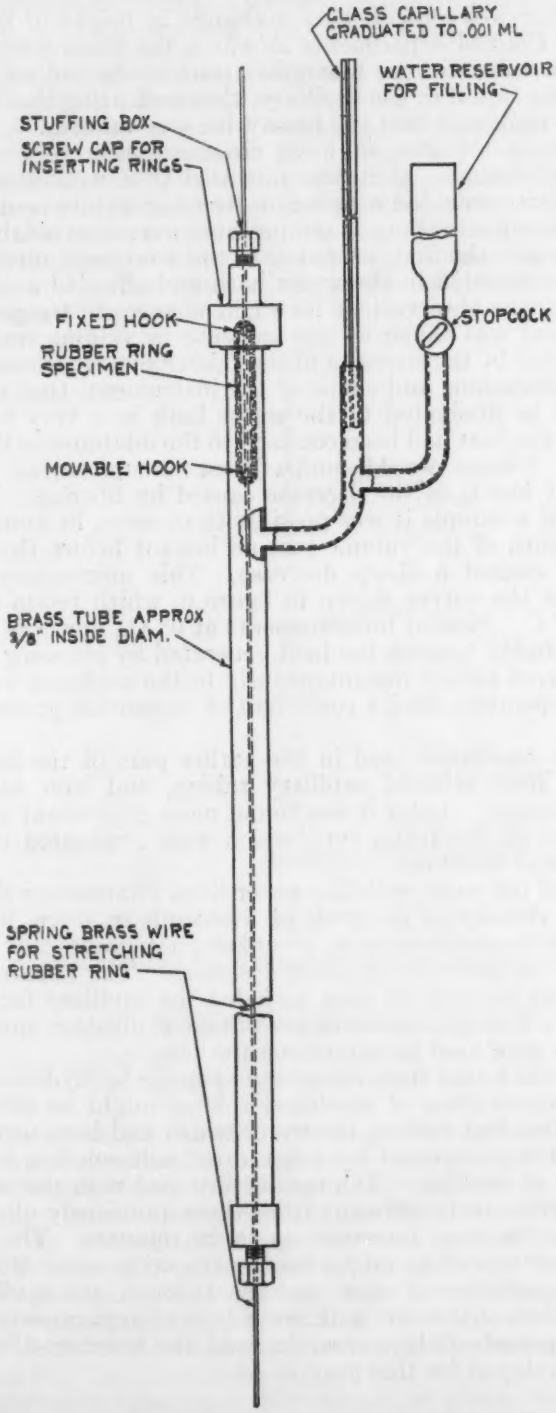

FIGURE 2.—*Water-filled dilatometer for measuring the change of volume of rubber on stretching.*

of the rubber was indicated by a change in height of liquid in the capillary. Control experiments in which the brass wire was drawn through the tube without a sample attached showed no appreciable motion of the liquid in the capillary, thus indicating that the stuffing boxes were tight and that the brass wire was uniform.

The dilatometer was, in most circumstances, very sensitive to temperature changes, so it was mounted in a well-insulated water bath which was provided with means for temperature control. Since, however, some fluctuations in temperature were unavoidable, a second dilatometer like the first, except that the stretching mechanism was absent, was mounted in the water bath and afforded a direct means of correcting the observations for slight changes in temperature.

No account was taken of any increase in volume resulting from heat generated by the stressing of the rubber since it seemed probable, from the dimensions and shape of the instrument, that most of this heat would be dissipated to the water bath in a very few seconds. But even if the heat had been confined to the dilatometer the resulting increase in volume would, under most circumstances, have been considerably less than the decrease caused by fibering. During the stretching of a sample it was possible to observe, in some instances, a slight upturn of the volume just an instant before the fibering of the rubber caused a sharp decrease. This momentary upturn is indicated on the curves shown in figure 6, which relate to observations at 25° C. Similar measurements at 0° C., however, showed no upturn, probably because the heat generated by stressing the sample was transferred almost instantaneously to the confining water which, at that temperature, had a coefficient of expansion practically equal to zero.

The glass capillaries used in the earlier part of the investigation were made from selected capillary tubing, and were calibrated in the usual manner. Later it was found more convenient to use capillary pipettes of the Kahn type which were graduated to 0.001 ml over a range of 0.200 ml.

In most of the work with the water-filled dilatometer the readings were made visually at intervals of 5 seconds or more, but in some experiments observations were recorded photographically on motion picture film at intervals of about 1 second. The apparatus was so arranged that the field of view included the capillary tubes, a stopwatch, and a tape graduated in percentage elongation and connected to the brass wire used for stretching the sample.

When it was found from observations made by hydrostatic weighings that the swelling of stretched rubber might be different from that of unstretched rubber, the water which had been used as a confining liquid was replaced by a saturated salt solution to minimize the amount of swelling. The results obtained with the salt solution were not significantly different from those previously obtained with water alone, for time intervals up to 20 minutes. The possibility that significant swelling might occur even with salt water, together with the possibility of slow leakage through the stuffing boxes, rendered it desirable to use a different type of apparatus for measurements over periods of days or weeks, and the mercury-filled dilatometer was developed for this purpose.

2. MERCURY-FILLED DILATOMETER FOR MEASUREMENTS AT THE LONGER TIME INTERVALS

The dilatometer in which mercury was used as a confining liquid is shown in figure 3. It consisted essentially of a heavy steel tube, closed at the ends by means of lapped steel disks, and connected through a steel capillary tube to a glass capillary. When the steel disks were lubricated lightly with stopcock grease and held securely in place by screw caps no leakage was observed under either vacuum or pressure. The steel capillary tube was provided with fins, as indicated in the figure, so that when the dilatometer was used at an elevated temperature the cemented glass-to-metal joint did not become hot enough to soften.

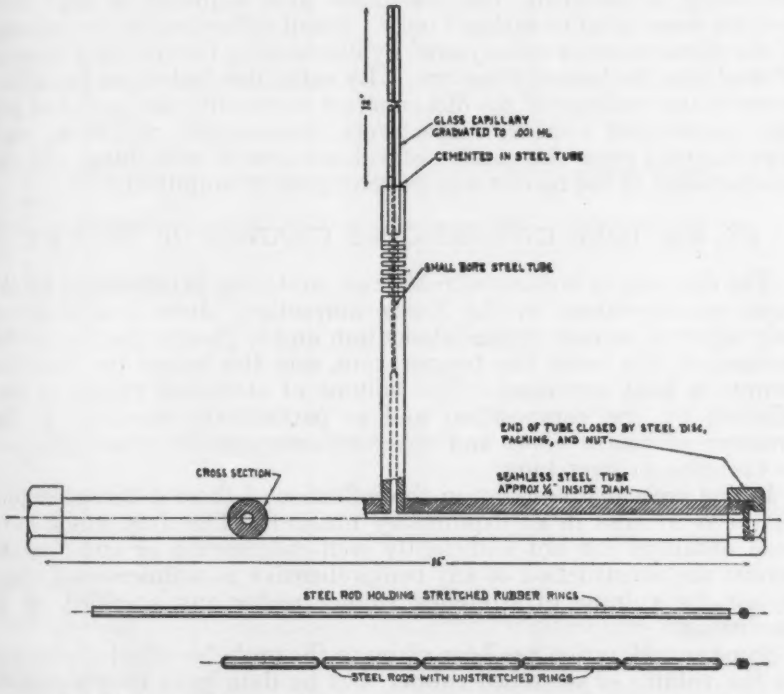
12"
GLASS CAPILLARY GRADUATED TO .001 ML
CEMENTED IN STEEL TUBE
SMALL BORE STEEL TUBE
END OF TUBE CLOSED BY STEEL DISC, PACKING, AND NUT
CROSS SECTION
SEAMLESS STEEL TUBE APPROX ¼" INSIDE DIAM.
25"
STEEL ROD HOLDING STRETCHED RUBBER RINGS
STEEL RODS WITH UNSTRETCHED RINGS

FIGURE 3.—*Mercury-filled dilatometer for measuring the change of volume of stretched rubber over long periods of time.*

Two methods were used for stretching the rubber rings. When the temperature at which the experiment was to be conducted differed appreciably from that of the room the rubber rings were slipped over hooks and placed, unstretched, in the steel tube. This was then brought to the desired temperature in an appropriate bath, after which it was removed quickly and wrapped in cloth to minimize temperature change. The rings were then stretched and the hooks fastened at the ends of the tube. When the temperature employed was that of the room the samples were stretched over a rod which was then slipped into the dilatometer tube.

The dilatometer tube, with the sample in place, was closed by means of the lapped steel disks, and was placed in a constant-

temperature bath. The air was then evacuated through the capillary and the whole filled with mercury by means of a two-way stopcock to an appropriate height in the capillary. This operation, from the time the sample was stretched, required about 20 minutes, so the experiments with the mercury-filled dilatometer served to indicate only that part of the volume change which occurred after the 20 minutes. In order to obtain the total volume change, the portion which occurred during the first 20 minutes was obtained by means of the water-filled dilatometer described in a preceding section.

Tests were always made with duplicate mercury-filled dilatometers, one containing unstretched, and the other, stretched rubber. The rubber samples, which weighed about 1.2 g, were selected so as to have the same weight to within 1 mg, and the hooks or rods used for stretching or mounting the specimens were adjusted so that their weights were equal to within 1 mg.[11] Small differences in the volumes of the dilatometers were adjusted by introducing the requisite amount of steel into the larger of the two. By using this technique the differences in the readings of the dilatometers containing the stretched and the unstretched rubber, respectively, represented within a small experimental error the change of volume due to stretching, and the computation of the results was thereby greatly simplified.

IV. FACTORS INFLUENCING CHANGE OF VOLUME

The decrease in volume of rubber on stretching is influenced by the same considerations as the X-ray diffraction, since it is observed only above a certain critical elongation and is greater the higher the elongation, the lower the temperature, and the longer the time the sample is kept stretched. The volume of stretched rubber is also affected by the composition and is particularly sensitive to the presence of coarse fillers and other inhomogeneities which give rise to vacuoles on stretching.

In the present investigation the influence of these different factors has been covered in an exploratory manner. The data which have been obtained are not sufficiently well-coordinated or complete to permit the construction of any comprehensive polydimensional chart giving the volume of stretched rubber under any specified set of conditions.

Some consideration has been given to the probable effect of pressure on the volume of stretched rubber, but no data have been obtained.

1. COMPOSITION

As indicated previously, most of the work here described was done with two "pure-gum" compounds, but some measurements were made on compounds containing 10 percent, by volume, of whiting and of carbon black, respectively, which illustrate two contrasting types of behavior. When the samples containing whiting were stretched there was an increase in volume which was greater the higher the elongation. But when these samples were held in the stretched condition the volume decreased with time, indicating that two effects were operating in different directions. During the stretching the

[11] This precise duplication was not necessary in the case of the two water-filled dilatometers because, with them, a very nearly constant temperature was maintained for each test, whereas in the present case the temperature was sometimes changed over a wide range in the course of a test.

rubber phase evidently pulled away from the filler particles and formed vacuoles of such magnitude as to cause a distinct increase in the volume of the sample as a whole, and to mask the decrease resulting from the fibering of the rubber phase. But when the sample was held in the stretched condition the fibering continued and caused a distinct decrease in the volume of the sample with time, as may be seen in figure 4. On releasing the sample the volume returned almost but not quite to the original volume, the slight increment, no doubt,

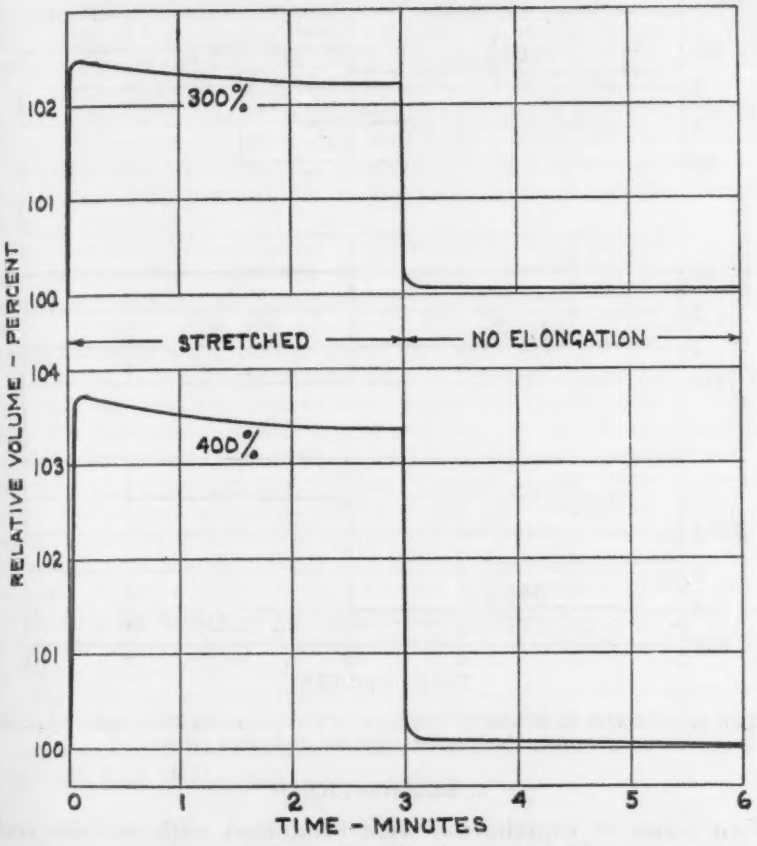

FIGURE 4.—*Changes in volume of compound III (containing 10 percent, by volume, of whiting) when stretched and when released.*

resulting from the presence of small amounts of gas which prevented the complete collapse of the vacuoles.

When the compound containing 10 percent of carbon black was stretched there was a decrease rather than an increase in volume, as is illustrated by the results shown in figure 5. This decrease became apparent at an elongation of 190 percent; this is somewhat lower than the elongation at which a decrease was observed with pure-gum rubber, a circumstance which is readily explained by the fact that the rubber phase in a compound containing filler is under greater actual elongation than that indicated by the stretch of the sample as a whole.

The fact that there was no increase in volume with the sample containing carbon black is an indication that the carbon black was present in such a state that no vacuoles were formed on stretching.

The relative behavior of the samples containing whiting and carbon black, respectively, suggests that the measurement of the change of volume on stretching may constitute a very simple and practical way of finding the nature and degree of dispersion of the filler in an unknown rubber compound.

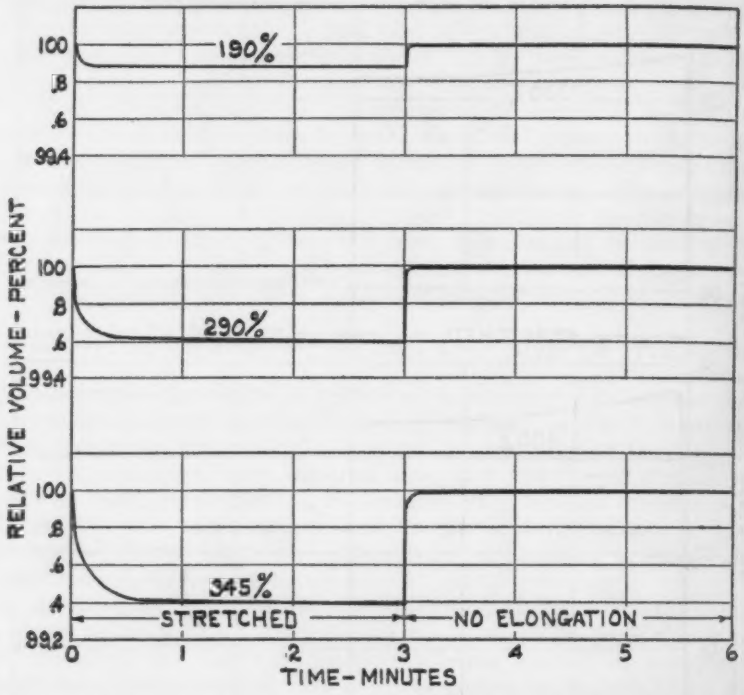

FIGURE 5.—*Changes in volume of compound IV (containing 10 percent, by volume, of carbon black) when stretched and when released.*

2. ELONGATION [11]

Two series of experiments were conducted with samples made from compound *II* to ascertain the effect of elongation on the change of volume during the first few minutes after stretching. In one series, the rubber was stretched to a given elongation and held at that elongation for 3 minutes, observations on the volume being made at frequent intervals. It was then released and observations again taken at intervals over a period of 3 minutes. The same procedure was repeated for successive different elongations.

In a second series of experiments the samples were stretched first to a relatively low elongation, 200 percent, and were held at this elongation for 3 minutes while observations were being made. Then, without release, the sample was stretched to successive higher elonga-

[11] The term "elongation" is used throughout this paper to mean the amount of stretch. A sample stretched to twice its original length, for example, has an elongation of 100 percent.

tions, each for 3 minutes, until the maximum elongation had been reached. The process was then reversed by the same stepwise procedure.

The results of the first series of experiments are shown graphically in figure 6. At an elongation of 450 percent the volume decreased by about 0.1 percent in 3 minutes. At higher elongations the decrease became progressively greater and amounted to nearly 2 percent at an elongation of 725 percent. After the observations had been made at elongations up to 600 percent a second set of readings was made on the same sample at elongations of 550 and 600 percent, respectively. The results, which are indicated by large circles on the graph, are in practical agreement with the first set of observations. This, and other experiments of a similar character, indicated that the change of volume on stretching was not significantly affected by the previous stress history of the sample, provided that it had been allowed to retract completely from the previous stretching. This is in contrast to the stress-strain behavior which is markedly altered by the first few cycles of stressing.[13]

The results of the second series of experiments in which the samples were stretched by a stepwise procedure are shown in figure 7. The changes of volume at the different elongations were, in general, slightly greater than the changes which were observed when the samples were released between each two elongations.

When the sample was released in a stepwise manner the volume showed a decided lag, and at any elongation except zero it was less than the volume attained on stretching to the same elongation. At zero elongation, however, the original volume was resumed. It might be thought that the volume attained at any given elongation in the release cycle would represent the equilibrium or final value which would be attained if rubber were stretched initially to that elongation and held for a very long time. Experiments reported in a subsequent part of this paper, however, indicate that when rubber is held for a long time in the stretched condition the volume may reach lower values than those shown in figure 7, and still give no indication of having become constant.

After the sample which had been put through the stepwise cycle was released it was stretched directly to 600-percent elongation, at which it assumed a volume practically identical with that observed on stepwise stretching to the same elongation.

3. TIME

The change of volume of stretched rubber with time is of such basic significance that it has, of necessity, been considered simultaneously with each of the other factors studied. Some observations, however, were made over relatively long periods in order to determine the nature of the relation between volume and time, and to ascertain whether a constant state would be reached. In these experiments mercury-filled dilatometers were employed in conjunction with dilatometers filled with water, and the curves obtained with the two instruments were joined at a point 20 minutes after stretching, as was indicated in a previous section. The results of two experiments are

[13] W. L. Holt, *Behavior of rubber under repeated stresses*, Ind. Eng. Chem. **23**, 1471-1475 (1931).

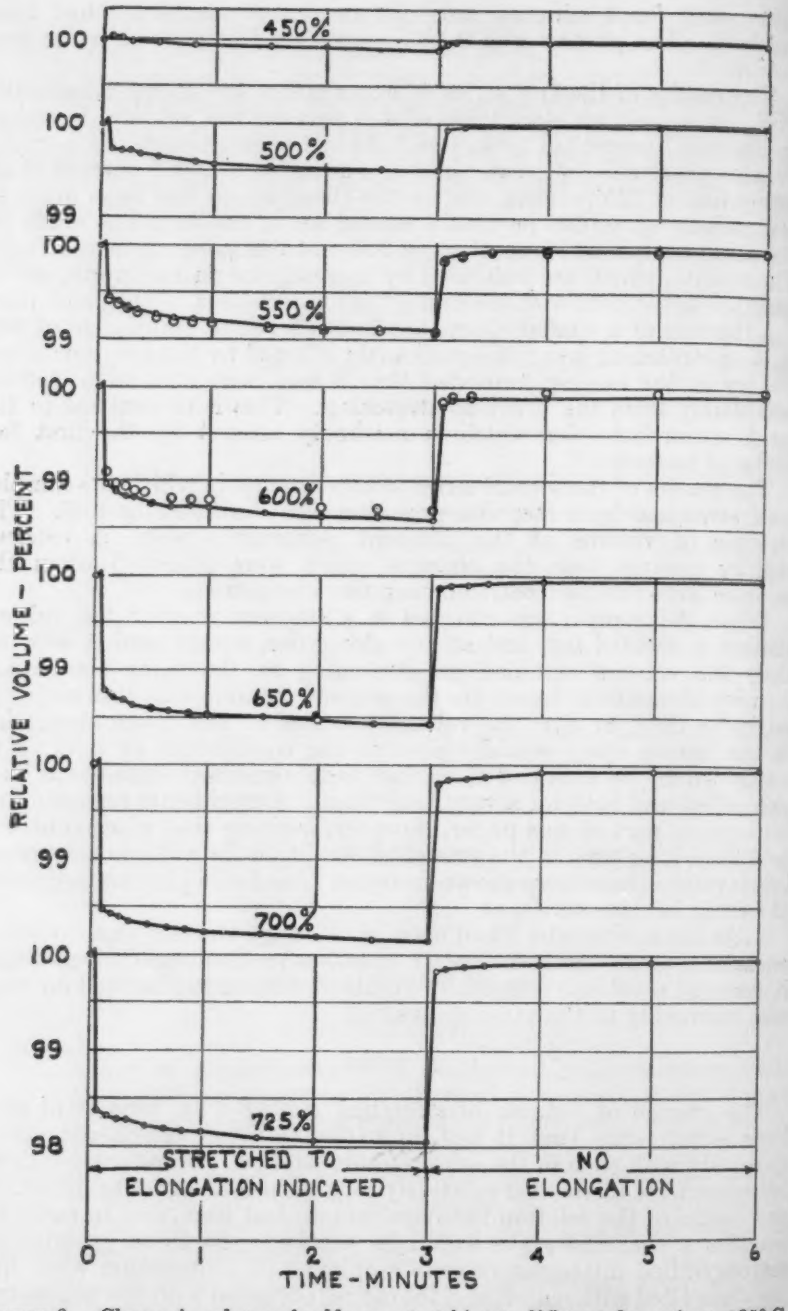

FIGURE 6.—*Change in volume of rubber on stretching to different elongations at* 25° C.

All tests were made on the same specimen which was stretched to the elongation indicated and held for 3 minutes, after which it was released and allowed to stand for 3 minutes before stretching to another elongation. The tests were made in the following order: —450-percent elongation, 500, 550, 600, 550 (second test), 600 (second test), 650, 700, and 725. The results of the second tests are indicated by the large circles.

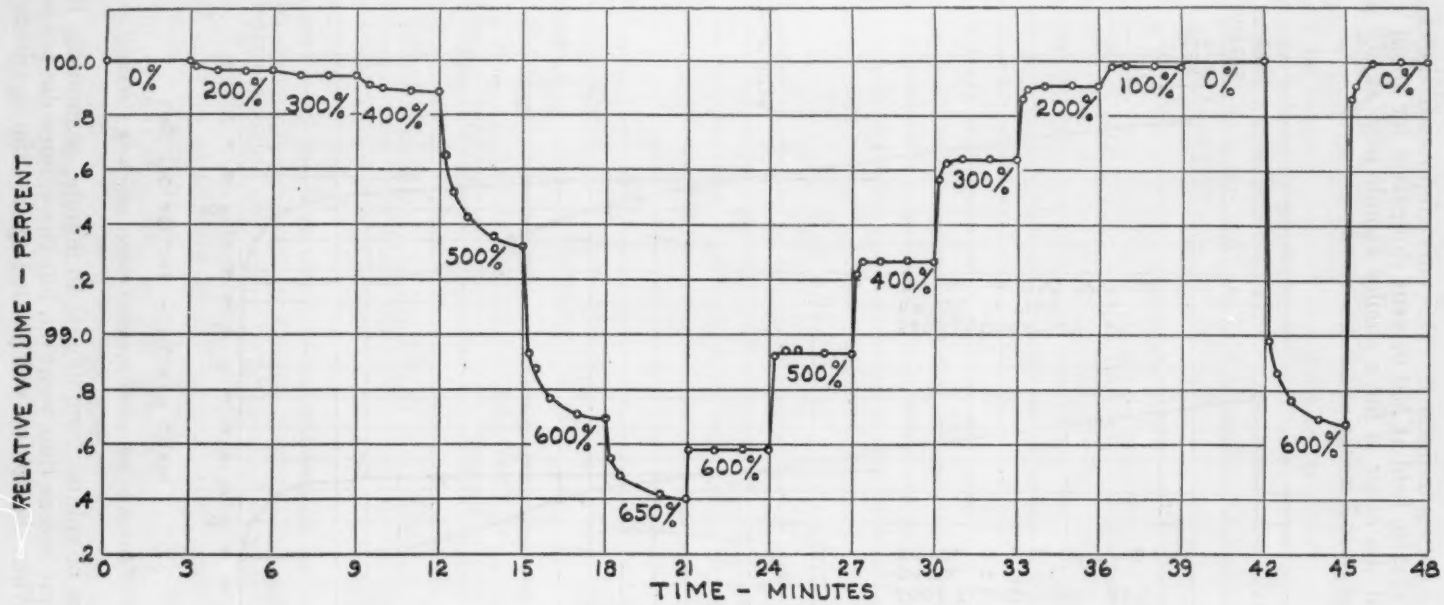

FIGURE 7.—*Change in volume of rubber when stretched and when released in a stepwise manner*

All tests were made on the same sample which was successively stretched (or released) and held at each of the elongations indicated for 3 minutes.

shown by the curves in figure 8. One curve represents the change of volume of a sample held at 550 percent elongation for about 2 weeks at 0° C., and the other is for a similar sample held at 600-percent elongation for over 3 weeks at 25° C.

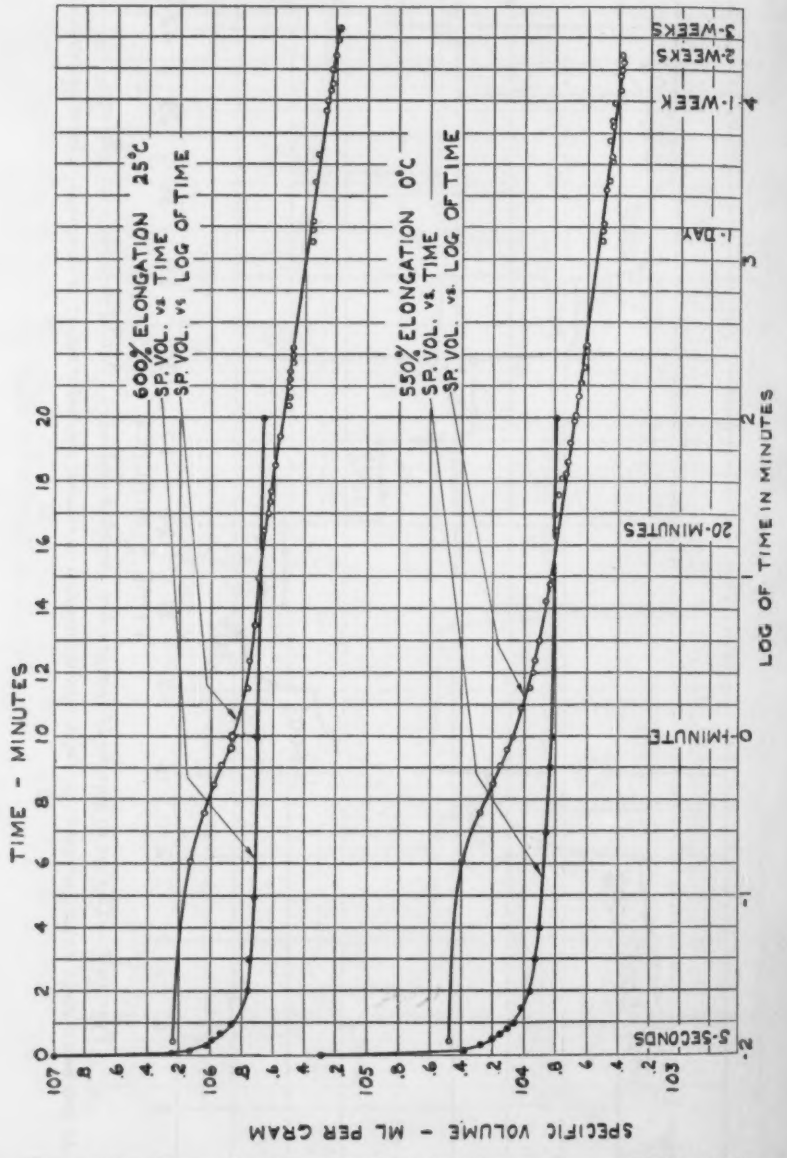

FIGURE 8.—*Change in volume of stretched rubber over long periods of time.*

The change of volume from minute to minute, or from day to day, rapidly became less as time went on, but the volume did not become constant. When the volume was plotted against the logarithm of the

time the curves so obtained were approximately linear after the first few minutes, indicating that the change in the rubber was proceeding at a constant rate with respect to the *logarithm of the time*. There was no indication that any limiting volume was being approached. It appears that observations over a considerably longer period of time will be required to give any definite indication of the final or equilibrium volume of stretched rubber. The inflection of the logarithmic curve at one minute is, of course, a natural characteristic of the curve and does not indicate any discontinuity in the behavior of the rubber at that point.

4. TEMPERATURE

The effect of temperature on the change of volume was investigated at two intervals of time after stretching—one minute and several days. The former measurements were made by stretching samples of rubber in a water-filled dilatometer at different temperatures and

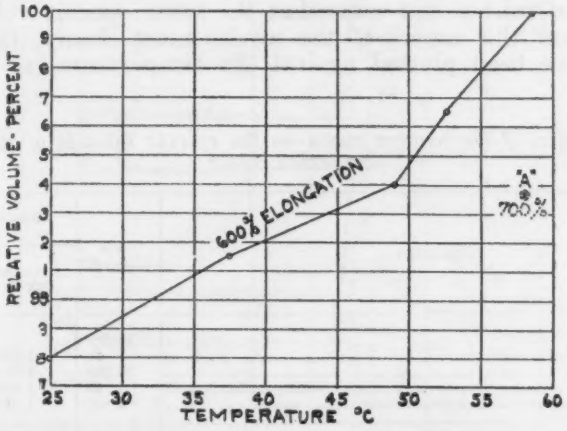

FIGURE 9.—*Change in volume of rubber when stretched to 600-percent elongation and held for 3 minutes at different temperatures.*

The same sample of compound *I* was used in all tests. After stretching to 600 percent at 58° C it was released and stretched to 700 percent with the result indicated by point *A*.

noting the volume change at the end of one minute. In the latter measurements a mercury-filled dilatometer containing a given sample was subjected to a series of temperatures, and the change of volume with temperature noted.

The results of the first series of experiments indicate that for a given elongation the change of volume becomes less the higher the temperature, a point ultimately being reached at which there is no change of volume on stretching. Typical results are shown in figure 9. At an elongation of 600 percent the change of volume ranges from 1.2 percent at 25° C to zero at 58° C. But when the same sample was stretched to 700 percent at 58° C there was a decrease in volume amounting to about 0.6 percent. The curve shown in figure 9 is simply a broken line connecting the observed points. The present data do not warrant any assumption as to the precise nature of the function.

In the second series of experiments a sample was stretched to 600-percent elongation at 25° C in a dilatometer with mercury as the confining liquid. A similar sample was mounted in another mercury-filled dilatometer of the same content as the first. After several days when the decrease in the volume of the stretched rubber from day to day had become very small the two dilatometers were carried through cycles of temperature between 25 and 0, −20, and 70° C, respectively. Duplicate samples of rubber were then taken and further observations were made, this time at temperatures of 25, 0, 100, and 25° C, respectively. The results computed in terms of specific volume are summarized in table 2, and are shown graphically in figure 10.

The specific volume of the stretched rubber was, at all temperatures, less than that of the unstretched rubber. It was anticipated that at 70° C the two samples would have the same specific volume, since the rubber underwent no change in volume when stretched to 600-percent elongation at temperatures above about 58° C. However, such was found not to be the case, and even at 100° C the stretched rubber had somewhat the lower specific volume. In order to show this aspect of the results more clearly, the specific volumes have been plotted against the temperature, as shown in figure 11.

TABLE 2.—*Effect of temperature cycles on the specific volumes of stretched and unstretched rubber*

Operation	Time interval	Specific volume	
		Stretched 600%	Unstretched
	Minutes		
Stretched at 25° C	20	1.0567	1.0700
Held at 25° C	30,000	1.0519	1.0700
Transferred to 0° C	20	1.0329	1.0530
Held at 0° C	2,800	1.0314	1.0530
Transferred to 25° C			
Held at 25° C	1,200	1.0519	1.0700
Transferred to −20° C	20	1.0179	1.0405
Held at −20° C	1,700	1.0158	1.0405
Transferred to 25° C	70	1.0519	1.0700
Transferred to 70° C	6	1.0949	1.1035
Transferred to 25° C	20	1.0536	1.0700
Held at 25° C	6,000	1.0526	1.0700
Transferred to 70° C after 8 cycles at 25 to 70° C	40	1.0935	1.1035
Transferred to 25° C	10	1.0542	1.0700
Held at 25° C	10,000	1.0521	1.0700

The curves for the stretched and the unstretched rubber, respectively, constitute two straight lines of different slopes which approach each other but lack somewhat of meeting at 100° C. The points indicating the specific volume of the stretched rubber at the different temperatures scatter somewhat because of changes with time and with the thermal history of the sample. The lower point at 25° C, for example, represents the volume after 30,000 minutes (about 3 weeks) at that temperature; the upper point represents the volume after a number of cycles, the last of which was from 70 to 25° C. The slopes of the curves indicate that the volume expansivity of the unstretched rubber is 0.00067, while that of the stretched rubber is approximately

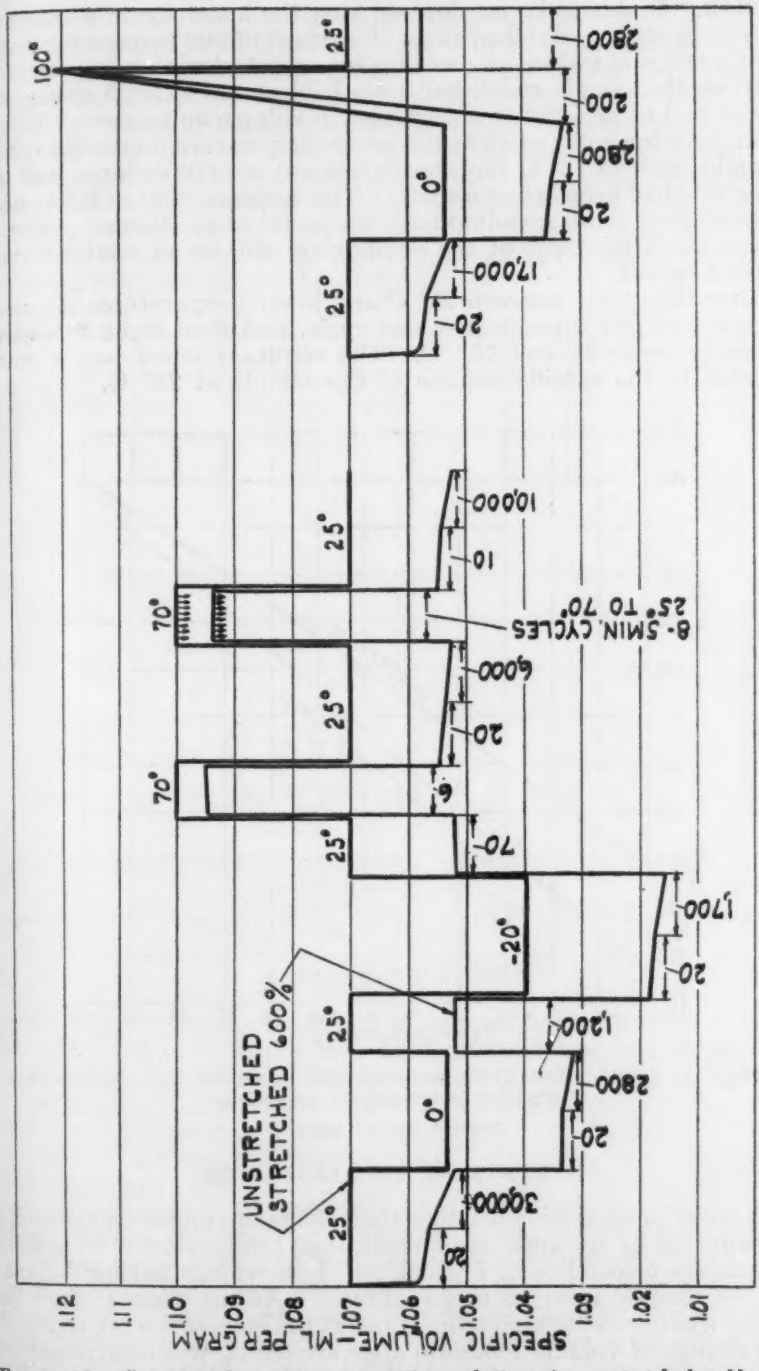

FIGURE 10.—*Specific volume-temperature-time relations for unstretched rubber and rubber stretched to 600-percent elongation.*

The two series of tests shown were conducted with two different samples of compound *I*.

0.00083. It should be emphasized that the latter figure pertains to pure-gum rubber stretched to an elongation of 600 percent for 2 to 4 weeks, and is in no sense a constant for stretched rubber in general.

When the sample which had been held at 25° C for 3 weeks was cooled to 0 or to −20° C it decreased in volume quite perceptibly on being kept for a day or so at the lower temperature, but when it was brought back to 25° C the specific volume in each instance was the same as it had been before cooling. This indicates that at least under some circumstances no advantage can be taken of thermal cycles to hasten the attainment of the equilibrium volume of stretched vulcanized rubber.

After the cycles between 25° C and lower temperatures the same sample was put through first one cycle, and then eight successive cycles between 25 and 70° C. The resultant effect was a small increase in the specific volume of the sample at 25° C.

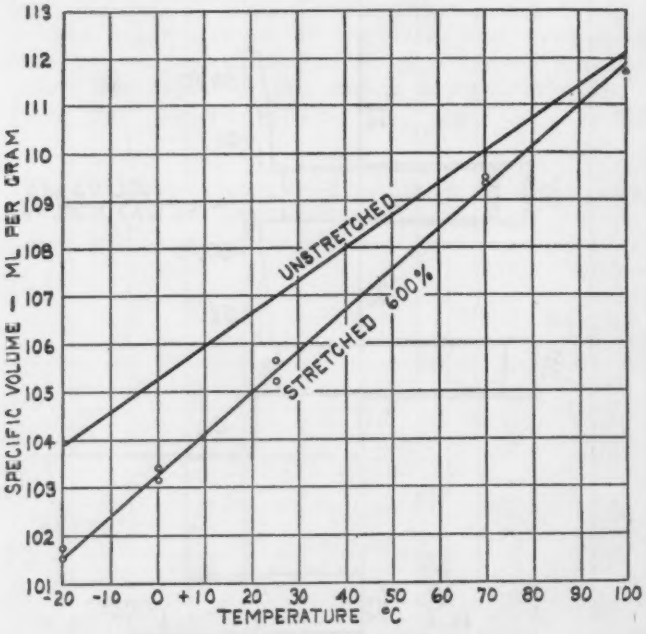

FIGURE 11.—*Specific volume-temperature relations for unstretched rubber and rubber stretched to 600-percent elongation.*

Based on data from figure 10.

5. STATE OF VULCANIZATION

In order to determine whether the change of volume on stretching was affected by the state of vulcanization, measurements were made on samples of compound *I* which had been vulcanized for different periods ranging from 15 to 60 minutes. At the shortest time the rubber was decidedly undercured, and at the longest it was overcured. The change of volume 1 minute after stretching was determined for each sample at a series of elongations, with results which are shown

in figure 12. For any given sample the volume, above a certain critical elongation, was found to decrease in an approximately linear manner with increasing elongation. The curves for the different samples lie rather close together, and are roughly parallel, except that the curve for the sample having the 15-minute cure crosses some of the others. In general an increase in the time of vulcanization results in a decrease in the volume change at a given elongation. Also an increase in the time of vulcanization results in an increase in the elongation at which the change of volume first becomes apparent. The relative effect of the degree of vulcanization is likely to be much greater at low elongations than at high.

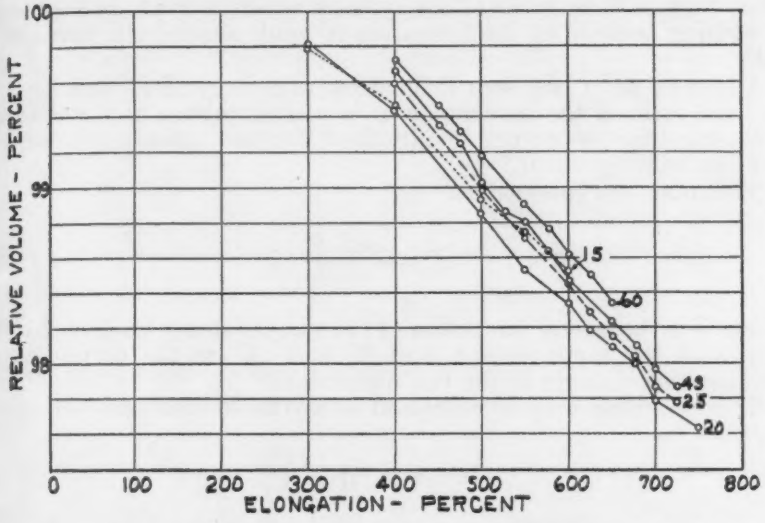

FIGURE 12.—*Effect of time of vulcanization on the change in volume of rubber when stretched to different elongations.*

Samples of compound *I* were vulcanized at 141° C for periods of from 15 to 60 minutes, as indicated on the curves. The change in volume was measured one minute after stretching.

6. OTHER FACTORS

The results which were obtained in the course of this work did not show as high an order of precision as the methods and apparatus were capable of giving. Variations were encountered between different lots of samples which were prepared at intervals over a period of 2 years. For instance, when different samples of compound *I* were stretched to 600-percent elongation at 25° C the decreases in volume observed ranged from 1.1 to 1.5 percent, with most of the values in the neighborhood of 1.2 percent. This variation is probably due, in part at least, to bloom and inhomogeneities in the rubber which would tend to cause an increase in volume on stretching. Some very erratic results which were obtained in the case of a compound vulcanized with 3 percent of tetramethylthiuram disulphide were traced by microscopic examination to particles of the accelerator which had crystallized out from the rubber. Inasmuch as the present investigation was exploratory in character, no critical study was made of

the variations between different samples or different lots of rubber compound.

V. POISSON'S RATIO

Poisson's ratio for homogeneous rubber is precisely 0.5 at low elongations where there is no change of volume on stretching, and is greater than 0.5 at high elongations where the volume decreases on stretching. Inasmuch as this change in volume is dependent on the composition, the elongation, the temperature, and the time the sample is kept stretched, all of these factors must be specified in order to give significance to any numerical value for the ratio. Most of the values for Poisson's ratio which are given in the literature are less than 0.5 since they refer to rubber-filler systems which increase in volume on stretching because of the formation of voids around the particles of filler.

Poisson's ratio has been defined for rubber by Vogt and Evans [14] as "the ratio of the percentage of lateral shrinkage of a rod to the corresponding percentage longitudinal increase, when such increase is infinitesimally small."

This may be expressed as,

$$P=-\frac{dS/S}{dL/L}, \tag{1}$$

where S is the lateral dimension of the sample at any instant, L is the length at the same instant, and dS and dL are the corresponding infinitesimal changes in the two dimensions.

This definition may be expressed on a volume basis as,

$$P=1/2-1/2\left(\frac{LdV}{VdL}\right), \tag{2}$$

where the initial volume is taken as unity and V is the volume at any instant.[15]

For purposes of illustration, Poisson's ratio has been computed from data shown in figure 6. The relative volumes 3 minutes after stretching have been taken from the different curves shown in this figure and have been plotted against the elongation to give the curve shown in figure 13. The slope of this curve is dV/dL. The numerical values of the slope have been found at several points, as indicated on the graph, and have been used for the computation of the values of

[14] W. W. Vogt and R. D. Evans, *Poisson's ratio and related properties for compounded rubber*, Ind. Eng. Chem. **15**, 1015–1018 (1923).

[15] Equation 2 can be obtained from equation 1 as follows:

$V=KLS^2$, where K is a constant. (3)

Differentiating,

$dV=2KLSdS+KS^2dL.$ (4)

Dividing equation 4 by equation 3

$dV/V=2dS/S+dL/L$ (5)

Or

$\frac{dV/V}{dL/L}=\frac{2dS/S}{dL/L}+1.$ (6)

Combining equations 6 and 1,

$$P=1/2-1/2\left(\frac{LdV}{VdL}\right).$$

Poisson's ratio which are given in table 3. The slope is 0 up to 300-percent elongation, making the ratio 0.500 for this range. Between 400- and 500-percent elongation the slope increases rapidly and at the latter elongation the ratio reaches its maximum value of 0.527; at higher elongations it decreases somewhat and drops to 0.515 at 700 percent.

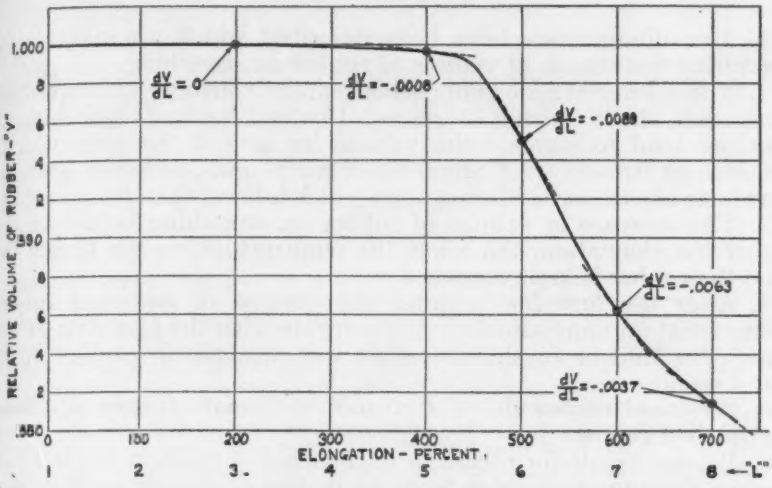

FIGURE 13.—*Elongation-volume relation for use in computing Poisson's ratio*

The data refer to samples of compound *II* stretched to the elongations indicated and held for 3 minutes at 25° C.

TABLE 3.—*Poisson's ratio for compound II stretched for 3 minutes at 25°* C

Elongation	Length, *L*	Volume, *V*	*dV/dL*	Poisson's ratio
Percent				
100	2	1.000	0.	0.500
200	3	1.000	0.	.500
300	4	1.000	0.	.500
400	5	0.9996	−.0008	.502
500	6	.995	−.0089	.527
600	7	.986	−.0063	.522
700	8	.9815	−.0037	.515

VI. INTERPRETATION OF RESULTS

Measurements of the volume changes associated with the stretching of rubber afford a simple, quantitative means of studying the fibering or crystallization which is the basis for the well-known contrast between the properties of unstretched and stretched rubber. The present investigation has been conducted from the standpoint of developing simple facts and relations and exploring the field. No attempt has, as yet, been made to coordinate the results of the volume measurements with theories of the molecular structure and the mechanism of stretching. One limitation of the present results from the standpoint of their utilization for purposes of basic theory is that none of the volume change measurements has been followed to any ultimate

or equilibrium state. The change with time *on a logarithmic scale* proceeds at a rate which shows no significant diminution for the longest periods covered by the present work. There can, of course, be no full understanding of the process of fibering until the end product has been prepared and its properties measured.

VII. SUMMARY

1. Two dilatometers have been described which are suitable for measuring the change of volume of rubber on stretching.

2. The volume of pure gum rubber remains constant up to a critical elongation, above which it decreases. Coarse fillers and other inhomogeneities tend to increase the volume because of the formation of vacuoles on stretching. Carbon-black compounds, however, decrease in volume above a critical elongation which is lower than for pure gum.

3. The decrease in volume of rubber on stretching is greater the higher the elongation, the lower the temperature, or the longer the time the rubber is kept stretched.

4. After the first few minutes the volume of stretched rubber decreases at an approximately uniform rate with the *logarithm* of the time. No final or equilibrium state was attained in periods up to 3 or 4 weeks.

5. Stretched rubber shows a greater coefficient of expansion than unstretched rubber.

6. Poisson's ratio for rubber in the absence of coarse fillers is 0.5 or greater, the numerical value being a function of the composition, the elongation, the temperature, and the time after stretching.

WASHINGTON, August 26, 1936.

U. S. Department of Commerce National Bureau of Standards

RESEARCH PAPER RP937

Part of Journal of Research of the National Bureau of Standards, Volume 17, November 1936

CHANGES IN COLOR TEMPERATURE OF TUNGSTEN-FILAMENT LAMPS AT CONSTANT VOLTAGE

By Deane B. Judd

ABSTRACT

Seasoned lamps, operated at constant voltage, gradually decrease in color temperature because of evaporation of the filament. Since the current does not decrease enough to correspond to an appreciable change in filament temperature, this decrease in color temperature is ascribed in large part to the accumulation of the familiar brown film on the inside surface of the bulb. The size and shape of the bulb are, therefore, important; each type must be separately investigated. Results are given for five types. The effect of operating seasoned lamps is a gradual decrease in color temperature, linear with time, which, like the rate of evaporation of tungsten, was found for 400-watt projection lamps to be nearly proportional to the thirtieth power of the temperature. The effect of seasoning new lamps for one hour at about rated voltage was a rise in color temperature from 3,050 to about 3,140° K, approximately half of which occurred in the first 3 minutes.

CONTENTS

	Page
I. Introduction	679
II. Theoretical considerations	680
1. Filaments of uniform diameter	681
2. Filaments of nonuniform diameter	682
III. Apparatus	685
1. Devices for operating lamps at constant voltage	685
2. Measurement of luminous flux	685
3. Measurement of color temperature	685
IV. Method	686
V. Reduction and summary of data	686
VI. Discussion and supplementary results	689
1. Dependence of lamp permanence on filament temperature	689
2. Type of lamp for color-temperature standards	690
3. Alternating-current versus direct-current operation	690
4. Correlation between luminous efficiency and color temperature of individual lamps in the life test	691
5. Effects of seasoning the lamps	692
6. Supplementary measurements of the brown deposit	692
VII. Conclusions	694

I. INTRODUCTION

When a seasoned incandescent lamp is burned at constant voltage, its chromaticity is not quite constant but changes slowly toward yellow. This chromaticity is conveniently and customarily specified by color temperature, defined as the temperature which an inclosure would need have in order to yield the same chromaticity by thermal radiation. The light output of the lamp also gradually decreases.

The present investigation was begun in 1930 with the primary purpose of discovering which of a number of types of tungsten-filament incandescent lamps was best suited for standards of color temperature. It was also expected that the study would show how much a working standard could be used before a check against a primary standard was advisable. Furthermore, the suggestion was made that measurements of luminous efficiency might serve as a check on the color-temperature constancy of lamps, and therefore an attempt has been made to correlate the decline in luminous efficiency with the decline in color temperature.

The types of lamp investigated are those which were thought of as possible best choices for color-temperature standards; table 1 gives a description of these types, the number tested, the type of current used, the initial color temperature, and the date and duration of the test.

The general plan of the investigation has been to burn the lamps at constant voltage and to measure at intervals, (1) current, (2) light output, and (3) color temperature.

It is the purpose of this paper to describe the apparatus and method and to give the essential results with some discussion of their significance.

TABLE 1.—*Types of lamp investigated, their number, duration of test, and color temperature*

Rated watts	Type of bulb	Type of filament	Number tested	Duration of test	Type of current	Initial color temperature	Test started (date)
				hr		°K	
400	Tubular, gas-filled	Monoplane	5	64	a–c	3,100	6/18/32.
			5	64	d–c	3,100	6/18/32.
			5	700	a–c	2,850	8/3/32.
			5	700	a–c	2,360	8/3/32.
500	Pear-shaped, gas-filled	Crown (C7)	5	128	d–c	2,850	5/4/31.
500	Pear-shaped, gas-filled	Circular-coil (C7A)	5	128	d–c	2,840	10/19/31.
60	Pear-shaped, vacuum	Squirrel-cage	5	128	d–c	2,360	5/4/31.
60	Pear-shaped, vacuum	Circular-coil (C9)	5	128	d–c	2,360	10/19/31.

II. THEORETICAL CONSIDERATIONS

The change in color temperature of a tungsten-filament lamp at constant voltage is ascribable to evaporation of tungsten from the filament. Such evaporation may change the color temperature of the lamp in two ways. It may cause a change in the true temperature of the filament itself, and it may change the color temperature of the lamp by a deposit on the inside of the bulb acting as a selective filter.

The properties of tungsten and tungsten filaments have been thoroughly investigated and summarized by Forsythe and Worthing[1] and by Jones and Langmuir.[2] From these investigations the change in color temperature of the filament itself, from the loss of tungsten, may be closely estimated regardless of whether or not the diameter remains uniform.

[1] W. E. Forsythe and A. G. Worthing, *The properties of tungsten and the characteristics of tungsten lamps*, Astrophys. J. **61**, 146 (1925).

[2] H. A. Jones and Irving Langmuir, *The characteristics of tungsten filaments as functions of temperature*, Gen. Elec. Rev. **30**, 310-319; 354-361; 408-412 (1927).

1. FILAMENTS OF UNIFORM DIAMETER

Consider, as is usually done, an ideal straight tungsten filament of circular cross section having a smooth, polished surface. Let there be no cooling at the leads nor any cooling by conduction to gases in contact with the filament. For such a filament of constant length, L, with a constant voltage, V, applied over this length, it has been shown by Jones and Langmuir that temperature of the filament, T, and current, I, in it are proportional to certain powers of the diameter, d, so that we may write:

$$T/T_0=(d/d_0)^n, \tag{1}$$

where n varies from 0.168 to 0.176 within the temperature range 2,300 to 3,000 °K, and

$$I/I_0=(d/d_0)^m, \tag{2}$$

where m varies from 1.80 to 1.79 within the same range. The subscript, 0, denotes the values at the beginning of the burning test.

The color temperature, θ, differs from the true temperature of the filament by only 50 to 100 degrees throughout this range of temperatures,[3] so without appreciable error for our purpose eq 1 may be written:

$$\theta/\theta_0=(d/d_0)^{0.17}. \tag{3}$$

Assume that the diameter of the filament is uniform and decreases uniformly because of evaporation from the surface and linearly with time, t, in service, thus:

$$d/d_0=1-t/t', \tag{4}$$

where t' is the time required for the complete evaporation of the filament.

For a lamp whose change in color temperature is ascribable wholly to change in true temperature of a uniform filament it could be expected from eq 3, 2, and 4 that the color temperature and current would vary with time as follows:

$$\theta/\theta_0=(1-t/t')^{0.17} \tag{5}$$

$$I/I_0=(1-t/t')^{1.8}, \tag{6}$$

that is, the color temperature should decrease approximately as the sixth root of time and the current should decrease approximately as the square.

Actual filaments, however, are not uniform to start with, and it may be readily seen that a narrow, constricted region of the filament will cause development of a "hot spot" which will be always at a higher temperature than other parts of the filament and which, barring other accidents, will ultimately cause its failure.[4] Irregularities in the filament also appear because of formation of large crystals.[5] The filaments of the lamps burned for 700 hours show considerable evidence of such crystallization.

[3] See footnote 1.
[4] R. Becker, *Lebensdauer und Wolframverdampfung*, Z. techn. Physik **6**, 309 (1925).
[5] G. R. Fonda, *Burn-out of incandescent lamps*, Gen. Elec. Rev. **32**, 206 (1929).

2. FILAMENTS OF NONUNIFORM DIAMETER

Consider changes in the original filament such that a certain fraction, f, of the length is reduced in diameter to a certain fraction, c, of the original diameter. To trace the effect of these changes in dimensions requires three separate sets of symbols as follows:

(1) Voltage, V, applied to the original filament, diameter, d_0, produces current, I_0, color temperature, θ_0, and resistivity, ρ_0.

(2) Voltage, V, applied to the diminished filament produces in the unreduced part, diameter, $d'=d_0$, a lower current, I', a lower color temperature, θ', and a lower resistivity, ρ'.

(3) And it produces in the reduced part, diameter $d=cd_0$, the same current, $I''=I'$, and, as will appear presently, a higher color temperature, θ'', and a higher resistivity, ρ''.

The resistance, R, of the partially reduced filament may be expressed in terms of the resistivities of the two component parts, thus:

$$R=\frac{L}{d_0^2}[\rho'(1-f)+\rho''(f/c^2)]. \tag{7}$$

The current flowing through the partially reduced filament is: $I''=I'=V/R$; that flowing through the original filament is: $I_0=Vd_0^2/L\rho_0$; and the ratio from eq 7 may be written

$$I''/I_0=I'/I_0=\frac{\rho_0}{\rho'(1-f)+\rho''f/c^2}. \tag{8}$$

Assuming that no heat is transferred from the narrow part of the filament to the unreduced part by conduction, we may write from the Jones and Langmuir table of relations between the variables of ideal tungsten filaments [6] for constant current, since $I''=I'$:

$$\theta''/\theta'=(d_0/d)^{0.9}=1/c^{0.9} \tag{9}$$

also:

$$\rho''/\rho'=1/c^{1.1} \tag{10}$$

The effect of introducing a narrow place in the filament is, of course, to decrease the current, but as shown below, even with this decreased current (except for f nearly unity) there is a rise in the color temperature of the narrow part of the filament.

The color temperature of the filament as a whole is a mean of the color temperatures of the two component parts. Use has been made of the red-blue ratio,[7] taking wave lengths 660 and 470 mμ for estimating the mean. The total amount of radiant energy at 660 mμ from both the narrow and unchanged parts of the filament was computed by Wien's law from the respective color temperatures, a similar total at 470 mμ found, and the ratio computed. The color temperature of the filament as a whole was taken as the temperature of the Wien radiator having this same red-blue ratio.

As an illustration of the dependence of color temperature on the degree of irregularity with which the filament decreases in diameter, there have been computed the color temperatures of five filaments each differing from the original filament by losing enough tungsten

[6] Gen. Elec. Rev. **30**, 357-358 (1927).

[7] W. E. Forsythe, *Color match and spectral distribution*, J. Opt. Soc. Am. & Rev. Sci. Instr. **7**, 1115 (1923).

to reduce the current with constant voltage, V, by 1 percent. The first of these five filaments has its diameter reduced uniformly over the entire length ($f=1$), the second is unchanged over nine-tenths of its length, but has its diameter uniformly decreased over the remaining one-tenth ($f=0.1$), and so on for $f=0.05$, 0.02, and 0.01. The details of the computation and the results are shown in table 2.

The reduction in diameter, c, required to reduce the current from I_0 to 0.99 I_0 was found from eq 8 and 10:

$$c^{3.1}=\frac{\rho' f}{\rho_0/0.99-\rho'(1-f)} \tag{11}$$

The resistivities ρ' and ρ_0 refer to filaments of the same diameter ($d'=d_0$) but the filament of resistivity, ρ', carries 1 percent less current. From relations given by Jones and Langmuir, the temperatures, and hence the color temperatures, of the filaments, are closely proportional to the 0.6 power of the current for diameter constant:

$$\theta'/\theta_0=(I'/I_0)^{0.60} \tag{12}$$

TABLE 2.—*Change in color temperature according to distribution of tungsten removed from filament*

[These computations refer to a 1 percent decrease in current, $I'/I_0=0.99$]

Fraction of original length, L, reduced in diameter	Fraction of original diameter required over fractional length, f, to produce a 1% decrease in current (see eq 14)	Fractional increase in color temperature at narrow part of filament $\frac{\theta''}{\theta_0}=\frac{0.994^*}{c^{0.9}}$	Color temperature of unchanged part of filament, θ', of narrow part, θ'', and of whole filament, $\theta_{R/B}$, for two initial color temperatures, θ_0, in °K.					
			For $\theta_0=2{,}400°$ K			For $\theta_0=2{,}800°$ K		
			θ''	θ' See note**	$\theta_{R/B}$	θ''	θ' See note**	$\theta_{R/B}$
f	c	θ''/θ_0						
1.00	0.995	0.999	2,398	--------	2,398	2,797	--------	2,797
.10	.950	1.042	2,501	2,386	2,403	2,918	2,783	2,801
.05	.909	1.084	2,602	2,386	2,407	3,035	2,783	2,804
.02	.818	1.191	2,858	2,386	2,422	3,335	2,783	2,814
.01	.724	1.330	3,192	2,386	2,460	3,724	2,783	2,840

* The factor, 0.994, is introduced because eq 3 requires θ''/θ_0 to equal 0.999 for $c=0.995$; this is a drop in color temperature with voltage and length constant due to decreased current; it does not follow from eq 9 which refers to constant current.

** The length of filament, $(1-f)$ L, unchanged in diameter has a color temperature lower than θ_0 because of the 1 percent decrease in current, thus: from eq 12: $\theta'/\theta_0=(I'/I_0)^{0.60}=0.99^{0.60}=0.994$.

and resistivity is closely proportional to the 1.2 power of the color temperature regardless of filament dimensions:

$$\rho'/\rho_0=(\theta'/\theta_0)^{1.2} \tag{13}$$

These exponents vary slowly with color temperature much as those of eq 1 and 2; but, as before, values representative of 2,800° K are used for simplicity, the errors resulting from neglect of the more accurate relations being of no consequence for the present purpose.

From eq 12 and 13 may be written:

$$\rho'/\rho_0=(I'/I_0)^{0.72}$$

which for I'/I_o equal to 0.99 is approximately 0.993. Substitution of this value in eq 11 gives the relation from which the values of c in the second column of table 2 were found:

$$c^{3.1}=0.983f/(0.017+0.983f) \tag{14}$$

It may be noted that the numerical results computed from eq 14 differ only slightly from those obtained from the simpler relation:

$$c^3=f/(0.01+f) \tag{14a}$$

found from eq 8 by neglecting the differences between ρ_o, ρ', and ρ''.

The third column gives the ratio of color temperature of the "hot spot" to the original color temperature, $\theta''/\theta°$, according to a relation found from eq 3 and 9. There are also given for two initial color temperatures, 2,400 and 2,800° K, the color temperature of the "hot spot", f, the color temperature of the remainder, $1-f$, of the filament, and the color temperature of the whole filament, $\theta_{R/B}$, estimated by the red-blue-ratio method.

It may be seen for $f=1$ that a reduction in diameter of the whole filament by 0.5 percent is required to produce a 1-percent reduction in current. This reduction may be expected to lower the color temperature by but 0.1 of 1 percent (2 or 3 degrees); this is in accord with eq 3. The remainder of the entries in the table show that the color temperature of the whole filament is relatively independent of how the reduction in diameter required to reduce the current by 1 percent is distributed, the effect of deviating from uniform reduction in diameter ($f=1$) being to raise the color temperature slightly. Only when the whole decrease is limited to one-twentieth or less of the filament length does the increase amount to more than 9° K. Such an irregularity produces a rather severe "hot spot", a locality in which the color temperature rises about 200° K above that of the remainder of the filament. The extreme restriction, $f=0.01$, was included as representative of a lamp burning out from development of a "hot spot."

These results apply to ideal straight filaments in a vacuum; most of the lamps actually tested had coiled filaments in gas-filled bulbs. It is believed, however, that the considerations apply essentially to such lamps also. We may expect therefore that the color temperature of the filament will, in general, rise slowly with continued operation, and even in the unlikely case of a very uniform filament the fractional decrease in color temperature is expected not to be any more rapid than the tenth root of the fractional decrease in current (see eq 5 and 6). This permits a considerably simplified discussion of the results which may conveniently be mentioned now. As will appear later, decreases have been found in color temperature of as much as 35° K accompanied by decreases in current up to 1 percent. From table 2 it may be seen that the maximum decrease ascribable to change in color temperature of the filament is 3° at 2,800° K. It may be concluded, therefore, that by far the largest part of the decrease in color temperature is ascribable to the accumulation of the brown film on the inside of the bulb. No further attention will be paid to possible changes in color temperature of the filament because there is no evidence that such changes have significantly influenced the experimental results.

This conclusion emphasizes, however, that size, shape, and gaseous content of the bulb determine the permanence of the lamp as a color-temperature standard. A large bulb provides a larger glass surface on which the film may be deposited with a consequent reduction in its thickness. By variation in shape of the bulb convection currents within may be controlled so that most of the film is deposited on parts of the bulb off the line of sight. Each type of lamp must therefore be separately investigated.

III. APPARATUS

The apparatus consisted of devices for operating lamps at constant voltage, and devices for measuring luminous flux and color temperature at known voltages.

1. DEVICES FOR OPERATING LAMPS AT CONSTANT VOLTAGE

For most of the work the lamps were operated on alternating current at prescribed voltages in the equipment developed for life testing of incandescent lamps. Since lamps used for standards of color temperature are customarily operated by direct current, the early tests were made with direct current until a comparison of the two methods showed little significant difference. In each case the voltage was controlled to within 0.25 volt.

2. MEASUREMENT OF LUMINOUS FLUX

The light output of each lamp was measured either by means of an 88-inch photometric integrating sphere and visual photometric equipment used in routine tests at the Bureau for many years, or by a 60-inch sphere equipped with a cesium photoelectric cell in a Sharp and Smith circuit.[8] It has been found possible, in routine measurements, to detect variations in luminous flux as small as 0.25 percent with the photoelectric photometer, which is a precision somewhat higher than was obtained with the visual photometer.

3. MEASUREMENT OF COLOR TEMPERATURE

The color temperature of the lamps was measured by comparison with lamp standards on the Nela scale of color temperature [9] according to the substitution method on the color comparator described in 1930[10] either with the flat 16° circular photometric field divided vertically in the center and viewed binocularly, or with the Lummer-Brodhun contrast photometer head with the contrast strips removed giving a $9 \times 13°$ field with a complex double-trapezoid pattern viewed monocularly. The latter more complex field gave no higher precision, but was preferred because it largely eliminated errors due to changes in chromatic sensitivity of one-half of the observer's retina relative to the other half over time intervals of the order of 10 minutes.

[8] C. H. Sharp and H. A. Smith, *Further developments in photoelectric photometers*, Trans. Illum. Eng. Soc. **21**, 434 (1928).

[9] This work was done in 1930 to 1932 prior to the establishment of the present scale of color temperature (see BS J. Research **12**, 527 (1934) RP677). The Nela scale differs so little from the present scale that no useful purpose would be served in transferring these results.

[10] D. B. Judd, *Precision of color temperature measurements under various observing conditions; A new color comparator for incandescent lamps*, BS J. Research **5**, 1161 (1930) RP252.

IV. METHOD

The method for seasoned lamps was (1) to set them for the desired initial color temperature, θ_0 (see table 1), by adjustment to voltage, V; (2) to check for possible seasoning effects by measurement of current and color temperature at this voltage immediately after this period (about 3 minutes) of adjustment; (3) to operate them at this voltage for the following time intervals, in hours, 1, 2, 4, 8, 16, 32, 64, 50, 50, 50 . . . ., continuing until the durations given in table 1 had been reached; and (4) after each such time interval to measure current, luminous flux, and color temperature.

The method for unseasoned lamps was the same, except that they were seasoned for 1 hour at 3,140° K and the check for seasoning effect was applied once during this hour after about 7 minutes, the

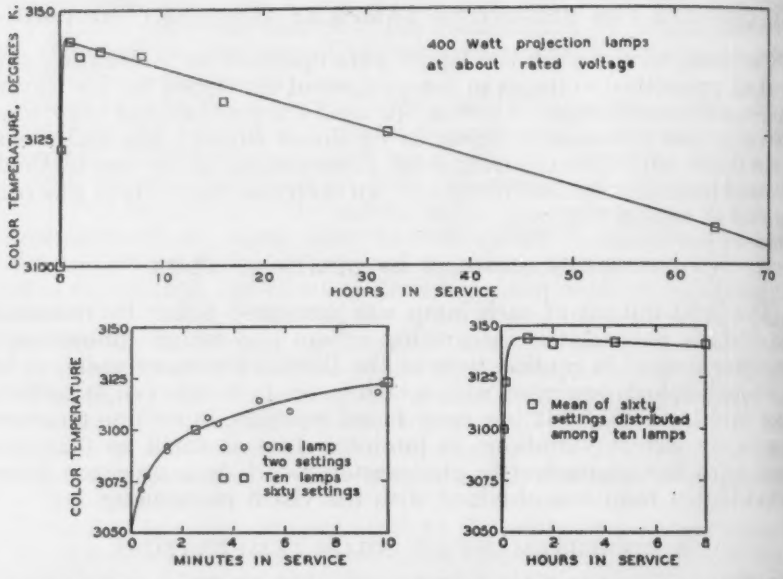

FIGURE 1.—*Color temperature of unseasoned lamps as a function of time in service.*

The color temperature rises rapidly during seasoning, then declines slowly.

initial adjustment requiring longer than 3 minutes because of the rapid rise in color temperature during initial stages of seasoning. For two lamps the seasoning effect was studied continuously for 10 minutes by settings of color temperature every 30 seconds.

V. REDUCTION AND SUMMARY OF DATA

The 400-watt lamps were taken from stock; the 60-watt, squirrel-cage filament lamps were taken from lamp sockets after actual use of unknown amount; the remainder of the lamps (see table 1) were purchased as photometric standards. As might be expected, only the lamps taken from stock showed any evidence of a seasoning effect.

Figure 1 shows typical variation of color temperature with time in service for unseasoned lamps. The seasoning effect found is a rapid

rise of 50 to 100° K in color temperature accompanied in every case, contrary to expectation, by a 1 percent decrease in current. The color-temperature rise is best shown on figure 1 by the plot with the enlarged time scale. The effect of burning seasoned lamps is a slow decline in color temperature with continued but slow decrease in current. The plot to the intermediate time scale shows that seasoning is completed sometime in the first hour of burning. This result justified the usual seasoning procedure which is to operate such lamps at about this color temperature (3,140° K) for an hour. The color temperature rises during the first minute of seasoning by an amount about equal to the decrease produced by 50 hours of burning after seasoning; hence color temperature during the initial stages of the seasoning process changes several thousand times as fast as it does during operation of a seasoned lamp. This rapid rise in color temperature is customarily ascribed to change in surface condition of the filament so as to increase within the visible spectrum the spectral emissivity of short-wave radiant energy relative to that for long wave.

Lamps other than those taken from stock showed only the gradual decrease in color temperature characteristic of seasoned lamps. It is important to note that the color-temperature–time curve closely approximates a straight line. Analysis of the data shows that the actual deviations from a straight line are not significant. For the mean of these 10 lamps, the deviations from a straight line are in each case less than 3° ; they are ascribable to experimental error, apparently in large part, because of error in control by the lamp standard of color temperature. In addition to this, the individual lamps, whose mean is represented on figure 1, gave a spread of about 20°, but this is due chiefly to uncertainty in the initial determination of voltage for 3,100° K because of the rapidity of the seasoning effect during the first 5 minutes. The curves for the individual lamps showed generally parallel courses; significant deviations could be traced to the fusing of two adjacent coils of the filament accompanied by an increase in current, to development of an unusually heavy region of brown deposit in the line of sight, or similar incidents. Significant erratic variations not accompanied by these incidents, such as reported by Howe [11] and Dziobek, [12] were not found with these lamps. The previously noted erratic variations would seem from the present tests to be ascribable to undetected sources of error; but it is possible that the present results fail to be typical because of insufficient number of lamps tested.

The other types of lamps and the same type at lower initial color temperatures likewise exhibited a decrease in color temperature not significantly nonlinear with time, though, of course, the rapidity of color-temperature change at the lower temperatures was notably less than at 3,140° K. It is concluded, therefore, that the permanence of a lamp for use as a standard of color temperature at a given voltage can be satisfactorily indicated by the average decline in color temperature per unit time.

[11] H. E. Howe, *The color temperature of the gas-filled tungsten lamp as a function of time in service*, J. Opt. Soc. Am. & Rev. Sci. Instr. **13**, 304 (1926).

[12] W. Dziobek, *Über die Verwendbarkeit der Wolfram-Vakuumlampe zu sensitometrischen Messungen*, Z. wiss. Phot. **31**, 96 (1932).

Luminous efficiency and current of the lamps studied were also found to decrease with time in a nearly linear way; this agrees with results found for gas-filled lamps used as photometric standards.[13]

The method used in reducing the data was accordingly to compute the change per hour by reference to the average current, luminous efficiency, and color temperature for the group of lamps, no further attention being paid to values for individual lamps. In the case of current the method was merely to divide the difference between the initial and final values by the number of hours the lamps had been burned; this gives a result of the right order of magnitude. But, with luminous efficiency and color temperature least-square solutions were found for the constants a and b in the expression, $a+bt$; the values of b thus found expressed as the change per hour are given in table 3, together with uncertainties of these values. The uncertainties are taken as 4.9 times the probable error obtained in the customary way from the departures of the actual data from the linear relation found by least squares. On the assumption that the lamps studied are fair samples of all lamps of the same type, these uncertainties may be interpreted as limits which would be exceeded on the average only once in a thousand such tests as these.

TABLE 3.—*Current, luminous efficiency, and color temperature for the types of lamps studied, and their time rates of change when the lamps are operated at constant voltage, V*

[See table 1, for further description of lamps]

Identification of lamp type	Voltage, V	Current, I_s	dI/dt	Luminous efficiency, e_s	de_s/dt	Color temperature, θ_s	$d\theta/dt$
	v	amp	ma/hr	lpw	lpw/hr	°K	°K/hr
Projection	110	3.82	−0.6	24.6	−0.058 ±.006	3,140	−0.6 ±0.1
	85	3.31	−.03	16.0	−.0026 ±.0004	2,850	−.06 ±.01
	52	2.54	−.003	5.7	−.00015 ±.00011	2,360	−.006 ±.005
Old standard type (C7)	110	4.20	+.04	16.5	−.0029 ±.0011	2,850	−.09 ±.03
New standard type (C7A)	100	4.08	+.02	16.1	−.0026 ±.0011	2,840	−.08 ±.03
Commercial vacuum type	105	.475	−.01	7.4	−.0018 ±.0009	2,360	−.01 ±.03
Standard vacuum type	95	.469	.00	7.4	−.0015 ±.0005	2,360	−.05 ±.04

Table 3 is a summary of these results including the uncertainties in rates of change of luminous efficiency and color temperature with duration of the test. The data cannot be correctly interpreted without a consideration of these uncertainties which in some cases are undesirably large. Note, for example, that the projection lamps were found at 2,850° K to decline in color temperature at the rate of from 0.05 to 0.07 degrees per hour, while the new standard type at about the same temperature yielded from 0.02 to 0.14 degrees. The conclusion is therefore that there is no significant difference in permanence between these two types of lamps; this is borne out by a consideration of the corresponding decline in luminous efficiency. In another example, however, the projection lamps at 2,360° K showed an average decline greater than 0.001 and less than 0.011 degree per hour, while the standard-vacuum-type lamps yielded an average between 0.01 and 0.09. The conclusion is that the superior permanence of the

[13] R. P. Teele, *Gas-filled lamps as photometric standards*, Trans. Illum. Eng. Soc. 25, 78 (1930).

projection lamps at 2,360° K to vacuum lamps at the same color temperature has been established to a high degree of probability; consideration of the corresponding results for luminous efficiency establishes this superiority beyond reasonable doubt because in this case there is no overlapping whatsoever.

In general, the uncertainty in rate of decline is greater for color temperature than for luminous efficiency. This is ascribable partly to the relatively less dependence of total luminous flux on distribution of the brown deposit on the bulb, but it is chiefly ascribable to the generally higher precision of the measurements of luminous flux. In the first part of the work, changes in the lamps could be detected much better (perhaps five times as well) by following the luminous flux than by following the color temperature. After two years of practice in technique of setting for color-temperature match and after several refinements in method and equipment, including installation of the Lummer-Brodhun contrast photometer head, it was found possible to do about equally well with either method. At the end of the work measurements of luminous flux were again found somewhat superior for tracing small changes in the lamps, the increased precision being ascribable chiefly to the substitution of the photoelectric cell for the visual photometer.

VI. DISCUSSION AND SUPPLEMENTARY RESULTS

1. DEPENDENCE OF LAMP PERMANENCE ON FILAMENT TEMPERATURE

It should first be pointed out that the rate of decline in both color temperature and luminous efficiency indicated in table 3 varies approximately according to the thirtieth power of the temperature of the filament. The rate of vaporization of tungsten[14] has a similar dependence. The results are therefore in approximate accord with the view that the decline of both color temperature and luminous efficiency of these lamps is ascribable to formation of a brown film of tungsten or some tungsten compound on the inside of the bulb. Table 4 shows a comparison of the observed values of these rates with powers of the true temperature of the filament; it indicates that within the uncertainty of the results color temperature of the lamp declines according to the twenty-third power of the temperature of the filament, and that luminous efficiency declines closely according to the thirty-first power of the temperature; but the agreement is not perfect. The indication is that even the small changes observed at color temperature 2,360° K are somewhat larger than would be expected from the rate of vaporization of tungsten. It is evident that other factors not taken into account have a significant influence on the results. Evaporation of material from the leads and filament supports may produce this effect; also the higher pressure of the gas may interfere with evaporation of tungsten from the filament at the higher temperatures.

[14] Gen. Elec. Rev. **30**, 355 (1927).

TABLE 4.—*Dependence on temperature of filament of rate of decline of luminous efficiency, ϵ, and color temperature, θ, of the lamp*

Color temperature, θ	True temperature, T	$\frac{-0.59\ T^{21}}{10^{109}}$	$\frac{d\epsilon}{dt}$	$\frac{-0.44\ T^{23}}{10^{69}}$	$\frac{d\theta}{dt}$
°K	°K		lpw/hr		°K/hr
3,140	3,046	−0.058	−0.058 ±.006	−0.59	−0.6 ±.1
2,850	2,768	−.0030	−.0026 ±.0004	−.065	−.06 ±.01
2,360	2,310	−.00003	−.00015 ±.00011	−.0010	−.006±.005

[a] Taken from data by Forsythe and Worthing (see Astrophys. J. **61**, 146 (1925)) connecting true temperature with color temperature on the Nela scale.

The fact that the color-temperature change varies more slowly with temperature (twenty-third power) than rate of vaporization (thirtieth power and higher) suggests that at the high temperatures the convection currents of gas within the bulb are such as to favor, relative to low temperatures, the deposition of tungsten off the line of sight. This explanation does not apply to luminous efficiency because the light output refers to all directions from the filament rather than only one, nor is this explanation needed because luminous efficiency declines much more closely (thirty-first power) according to rate of vaporization of tungsten.

2. TYPE OF LAMP FOR COLOR-TEMPERATURE STANDARDS

From table 3 it may be noted that the gas-filled lamps specially constructed for photometric standards were not found to be any more permanent in color temperature near 2,850° K than the 400-watt projection lamps. Indeed, the projection lamps seem to be slightly more permanent although the difference is not certain. The reverse had been expected because the projection lamps had considerably smaller bulbs which should cause a thicker brown deposit in the line of sight if the distribution of deposit were uniform. The greater permanence of the projection lamps is now ascribed to the tubular shape of the bulbs which seems to cause a greater proportion of the deposit to occur out of the line of sight.

It may also be noted from table 3 that, as is to be expected, the projection lamps are definitely more permanent at 2,360° K than the vacuum lamps tested at the same temperature.

The projection-type of lamp was therefore chosen for new standards of color temperature over the whole scale.[15] Advantages gained by this choice apart from the gain in permanence just noted are: (1) a single lamp can be used over the whole scale; (2) the projection lamps are more convenient because they are smaller and burn base down; and (3) they are cheap because they are produced in large quantities for another purpose.

3. ALTERNATING-CURRENT VERSUS DIRECT-CURRENT OPERATION

Five of the ten lamps burned at about 3,100° K were operated on direct current, the other five on alternating current. When the results on these two groups of lamps were plotted it appeared from visual inspection of the graphs that there was no significant difference

[15] H. T. Wensel, D. B. Judd, and Wm. F. Roeser, *Establishment of a scale of color temperature*, B S J. Research **12**, 527 (1934) RP677.

between the two kinds of operation. Alternating current did not, it is true, produce quite as much lowering of color temperature as direct current. For three reasons, however, this result at the time seemed incredible: (1) it had been suspected that a small effect in the reverse sense might show up because of possible fluctuations (60 per second) in temperature from alternating-current operation, the vaporizing action of which might therefore exceed that of direct-current operation at the same color temperature; (2) no difference in the decline of luminous efficiency was noted between the two groups; and (3) the difference observed seemed ascribable to chance. Hence in subsequent burning the less convenient method using direct current was given up and alternating-current burning used.

Later on, however, when the least-square analysis was applied to the data, it was found that the rather uncertain difference previously noted might be significant. Table 5 shows the result of the analysis carried out as previously described for the results presented in table 3. Note that the difference in decline of luminous efficiency is quite insignificant, but that apparently direct-current produces a significantly more rapid decline in color temperature than alternating current. No satisfactory explanation of this result has been found. From the computed uncertainties it is to be expected to occur because of pure chance only about once in ten thousand such tests as were carried out.

TABLE 5.—*Alternating-current operation compared to direct-current operation for 400-watt projection lamps at rated voltages (110 v, 3,140° K) burned base down*

Type of current	$\frac{de}{dt}$	$\frac{d\theta}{dt}$
	lpw/hr	°K/hr
a-c	−0.058±.006	−0.33±.18
d-c	−.059±.006	−.69±.12

4. CORRELATION BETWEEN LUMINOUS EFFICIENCY AND COLOR TEMPERATURE OF INDIVIDUAL LAMPS IN THE LIFE TEST

It has been proposed that measurements of luminous efficiency might be made on lamp standards of color temperature as a check on their permanence. This proposal was based on two assumptions—first, that the precision with which luminous flux may be measured is considerably superior to that with which color temperature may be measured; and second, that there is a close correlation between the two quantities. The first assumption is not very well borne out by present practice because the superiority is slight. However, the second assumption has some justification, if referred to average values for groups of lamps as may be seen from table 3, though table 5 illustrates a case of poor correlation.

Accordingly, an attempt was made for a number of the individual lamps tested to correlate luminous efficiency with color temperature. The correlation found was poor, too poor to be of any use; there was little tendency for the lamps having rapidly decreasing luminous efficiency to have rapidly decreasing color temperature as well. This lack of correlation accords with the conclusion reached from theoretical considerations (see section II) that both luminous efficiency

and color temperature decline chiefly because of the brown deposit on the inside of the bulb, and that the former decrease corresponds to the average deposit all over the bulb, the latter to the deposit which forms on that part of the bulb in the line of sight. This view suggests that an improved correlation might be obtained by measuring apparent candle power in this one direction instead of mean spherical candle power, but the permanence of lamp standards of color temperature may now be so conveniently and reliably checked by color-temperature comparison with other similar standards set aside for that purpose that further work seems not to be justified.

5. EFFECTS OF SEASONING THE LAMPS

The changes which occur during seasoning are thought to be (1) expulsion of gases from the filament and a sintering of the filament accompanied by a decrease in resistance, and (2) a surface change of the filament causing a rise in color temperature. This surface change might be merely a decrease in area causing a rise in filament temperature, or it might be a change in surface character causing an increase of emissivity in the blue relative to that for red. The result with the projection lamps at 3,100° K was unexpected because the current fell sharply, indicating a sharp increase in filament resistance. The rise in color temperature was as expected. All lamps of the twenty seasoned at 3,100° K agreed in these respects.

For the lamps constructed especially for photometric standards no rise in color temperature was found. The current, however, increased gradually throughout the 128-hour period of burning. This held true for each of the 10 lamps tested. This increase suggested that the lamps had not been thoroughly seasoned and that sintering of the filament was continuing throughout the entire period of burning at 2,850° K. Details of construction and seasoning which might account for this result are not known.

6. SUPPLEMENTARY MEASUREMENTS OF THE BROWN DEPOSIT

The results of the tests thus far discussed suggest that the color-temperature impermanence of seasoned incandescent lamps is to be ascribed to brown deposit on the inside of the bulb. The amount of deposit in the line of sight even for the lamps burned for 700 hours is too small to be certainly detected by direct visual inspection although a dark deposit usually appears near the top of the lamps even before any certain decline in color temperature is noted. The question arises, therefore, whether there is really enough brown deposit in the line of sight to account for the decline in color temperature.

Accordingly, the bulb of a lamp which had declined in color temperature about 20° K from 64 hours burning near 3,140° K was removed and the spectral transmittance [16] of the deposit determined on the König-Martens spectrophotometer [17] both for the part of the bulb in the line of sight during the color-temperature measurements and for a part of the bulb near the top which seemed to bear the heaviest deposit. The spectrophotometer provided for unidirectional illumination and viewing, the direction of both being normal to the surface of the specimen.

[16] For definition of this term, see J. Opt. Soc. Am. **10**, 177 (1925).

[17] H. J. McNicholas, *Equipment for routine spectral transmission and reflection measurements.* BS J. Research **1**, 793 (1928) RP30.

Although the lamp was chosen because of the relative uniformity of the brown deposit on its bulb, this deposit was found to be sufficiently nonuniform to cause considerable trouble in making photo-

TABLE 6.—*Spectral transmittance of brown deposit on the bulb of a lamp whose color temperature had declined about 20° K during a 64-hour period of burning near 3,140 K*

[Illuminating beam and direction of view both nearly normal to surface of deposit]

Wave length	Transmittance		Seventh root of transmittance at top of bulb
	In line of sight	At top of bulb	
mμ			
440	0.848	0.306	0.843
480	.861	.354	.861
520	.874	.400	.876
560	.886	.437	.888
600	.897	.471	.897
640	.907	.502	.906
680	.916	.533	.914

metric settings. The results shown in table 6 are values adopted from a smooth curve drawn among the points representing the actual data. The last column in the table shows the seventh root of the transmittance of the heavy deposit. It is seen that these values agree very well with the transmittance of the deposit in the line of sight. This agreement indicates (1) that the nonuniformity of the deposit has not vitiated the results, (2) that the deposit at the top of the bulb is merely a thicker layer of the same material forming the deposit in the line of sight, and (3) that the deposit at the top of the bulb is seven times as thick as that on the bulb in the line of sight.

By the red-blue-ratio method it is found that the deposit in the line of sight is sufficiently selective to reduce the color temperature of the lamp by 65° K near 3,140, and that the heavy deposit is enough for a reduction of nearly 400° K. Since the observed decline in color temperature is only 20° K, it may be concluded that the selectivity of the brown deposit is ample to account for observed changes in color temperature.

In a sense, the measurements have proved too much; they indicate that three times the observed change ought to have been found. This might be caused by (1) a rise of 45° K in the color temperature of the filament from development of a severe "hot spot", or (2) to a possible division of the observed selectivity into about two-thirds from selective scattering and one-third from selective absorption. From table 2 it is judged that the lamp would burn out from a "hot spot" severe enough to cause a rise of even half of 45° K; furthermore, no "hot spots" were observed in the burn-out of these lamps; they burned normally with an occasional fusing of adjacent coils of the filament and continued loss of filament strength due to crystallization until an accidental jar broke the filament, which would then crumble into many pieces. This rules out the first possibility.

Whether the deposit owes its measured selectivity to scattering or to absorption deserves further consideration. If the selectivity found by unidirectional illuminating and viewing normal to the surfaces of the deposit were entirely caused by selective scattering, such a deposit

would be expected to change the color temperature of the lamp not at all, since the short-wave light which is scattered by the fragment of bulb in the spectrophotometer and lost by not entering the viewing slit is saved in the measurements of color temperature because the test plate is illuminated not only by light penetrating the bulb normally along the line of sight but also by light scattered from the deposit on other parts of the bulb. Accordingly, an attempt was made to determine what part of the selectivity observed was caused by selective scattering and what part by selective absorption. What is required for measurement of the selectivity from selective absorption alone is spectral transmittance from unidirectional illumination counting in the measurement all light transmitted regardless of direction. The equivalent conditions, diffuse illumination and normal viewing, were tried by placing the sample over the sphere of the Priest-Lange reflectometer [18] and some evidence was obtained that a considerable part of the selectivity is ascribable to selective scattering, but the nonuniformity of the sample introduced too much uncertainty in the measurement to permit any quantitative conclusion.

VII. CONCLUSIONS

The results of these tests may be summarized as follows:

1. Decrease of color temperature and luminous efficiency of seasoned incandescent lamps during burning at constant applied voltage is caused by the brown deposit forming on the inside of the bulb.

2. Color temperature of a lamp declines during such burning approximately in proportion to the twenty-third power of the filament temperature.

3. Luminous efficiency declines approximately in proportion to the thirty-first power of the filament temperature.

4. No good correlation between color temperature and luminous efficiency of individual lamps in the life test was found, nor is any to be expected since the two quantities depend differently on the distribution of the brown deposit over the inside surface of the bulb.

5. The spectral transmittance of the brown deposit has been found for two thicknesses, one deposit occurring at the side of a tubular bulb, the other, apparently about seven times as thick, occurring at the top of the bulb. The spectral selectivity of this deposit is probably to be ascribed partly to selective absorption and partly to selective scattering.

6. Lamps with tubular bulbs seem to have a more constant color temperature than those with pear-shaped bulbs, probably because a greater proportion of the brown deposit on the tubular bulb occurs near the top out of the line of sight.

7. These results suggest that the permanence of lamp standards of color temperature would be increased several fold by building into the lamps a device for brushing off the deposit, but 400-watt projection lamps are already very permanent, decreasing in color temperature when burned at about 2,850° K by an average of less than one-tenth of a degree per hour.

[18] I. G. Priest, *The Priest-Lange reflectometer applied to nearly white porcelain enamels*, J Research NBS 15, 529 (1935) RP847.

The operation of the lamps at constant voltage was carried out by R. S. Hunter, and the measurements of luminous flux were made by R. P. Teele and L. E. Barbrow. Dr. J. F. Meyer aided with his knowledge of incandescent lamps and his acquaintance with the extensive literature of the subject.

WASHINGTON, August 15, 1936.

U. S. Department of Commerce National Bureau of Standards

RESEARCH PAPER RP938

Part of Journal of Research of the National Bureau of Standards, Volume 17, November 1936

THERMAL EXPANSION OF LEAD-ANTIMONY ALLOYS

By Peter Hidnert

ABSTRACT

This paper gives the results of an investigation of the linear thermal expansion of cast lead-antimony alloys containing from 2.9 to 98.0 percent of antimony. Observations were made at various temperatures between −12 and +200° C and are shown in figures 3 to 5, inclusive.

A majority of the curves obtained on cooling lie below the expansion curves obtained on heating. The deviations between these curves are particularly noticeable for the alloys containing up to 15 percent of antimony which were cast in a preheated steel mold and cooled slowly. The deviations are less noticeable for the alloys of higher antimony content which were cast either in a sand mold or a chill mold. It is probable that the deviations indicate a lack of equilibrium in the samples on account of the effect of the casting conditions or of the chemical composition.

Table 3 gives the coefficients of expansion, the change in length after heating and cooling, and the densities of the alloys.

Equations 1 to 5 give linear relations between the coefficients of expansion and the atomic percentage of antimony of the lead-antimony alloys containing from 4.8 to 97.0 atomic percent of antimony (2.9 to 95.0 percent, by weight), and show that the coefficients of expansion decrease linearly with increase in the atomic percentage of antimony. The densities of the lead-antimony alloys also decrease linearly with increase in the atomic percentage of antimony. These linear relations are typical of relations for other properties of binary alloys having structures composed of solid solution + eutectic.

The coefficients of expansion of the lead-antimony alloys cover a wide range of values. It is possible to select lead-antimony alloys that have approximately the same coefficients of expansion as iron, nickel, gold, copper, silver, aluminum, magnesium, and many of their alloys.

CONTENTS

		Page
I.	Introduction	697
II.	Previous determinations	698
III.	Materials investigated	699
IV.	Apparatus	701
V.	Results	701
VI.	Conclusions	707
VII.	References	708

I. INTRODUCTION

In 1923 determinations were made by Hidnert and Sweeney [1][1] of the linear thermal expansion of lead and lead-antimony alloys containing from 0 to 15 percent of antimony. In 1930 and 1932 Hidnert and Sweeney [2, 3] published data on the thermal expansion

[1] The numbers in brackets here and elsewhere in the text refer to the references at the end of this paper.

of lead, and in 1935 Hidnert [4] published data on the thermal expansion of monocrystalline and polycrystalline antimony.

The results reported in the present paper represent an extension of the work started in 1923, which indicated that the coefficient of expansion of lead-antimony alloys (0 to 15 percent of antimony) decreases with increase of antimony. The work was extended in order to find, if possible, a relation between thermal expansion and chemical composition for alloys containing from 0 to 100 percent of antimony.

It has been pointed out by Goodrich [5] and others that the binary alloys of lead and antimony containing up to 25 percent of antimony are of considerable commercial importance. Goodrich [5] stated that alloys containing from 3 to 5 percent of antimony are used for rifle bullets and battery plates, alloys containing from 10 to 15 percent of antimony are used in much of the lead apparatus of chemical works, alloys containing from 12.5 to 20 percent of antimony are very useful as bearing metals for light loads, and that alloys containing from 10 to 25 percent of antimony are used for type metals.

II. PREVIOUS DETERMINATIONS

Previous observers on the thermal expansion of lead-antimony alloys include Daniell [6], Calvert, Johnson and Lowe [7], Vicentini and Omodei [8], Wüst [9], Hidnert and Sweeney [1], and Broniewski and Sliwowski [10]. None of these investigations, except the last, covered the whole range of composition. The most extensive previous report is that by Broniewski and Sliwowski [10], who not only covered the entire range in composition, but also covered a wider temperature range than was used by other observers. For these reasons the data by Broniewski and Sliwowski [10] are reproduced in table 1. It will be shown subsequently that Broniewski and Sliwowski's results are in good agreement with the results of the present investigation for the antimony-rich alloys, but their results are too high for pure lead and the lead-rich alloys.

TABLE 1.—*Coefficients of expansion of annealed lead-antimony alloys (Broniewski and Sliwowski* [10])

Atomic percentage of antimony	Coefficients of linear expansion		Remarks
	a	$2b$	
	$\times 10^{-4}$	$\times 10^{-4}$	
0 (Pb)	28.92	0.02478	Each value given for a represents a coefficient of expansion or rate of expansion at 0° C, and $2b$ represents the variation of the coefficient of expansion with temperature. The coefficient of expansion at any temperature may be computed from the following equation: $a_t = a + 2bt$, where a_t is the coefficient of expansion at any temperature t between −186 and +218° C.
1.7	28.82	.01467	
5	28.59	.00900	
10	27.58	.00816	
19.1	25.98	.00796	
20	25.65	.00814	
20.5	25.61	.00794	
21.9	24.94	.00510	
30	23.72	.00350	
40	21.73	.00718	
50	20.13	.00836	
60	18.47	.00330	
70	16.69	.00532	
80	14.80	.00396	
90	12.85	.00296	
95	11.48	.00248	
100 (Sb)	10.25	.00065	

III. MATERIALS INVESTIGATED

Twenty-four samples of lead-antimony alloys containing from 2.9 to 98.0 percent of antimony were cast at this Bureau from lead of high purity (99.99 percent) and antimony with a purity of 99.8 percent or higher. Each sample was about 300 mm in length and about 10 by 10 mm in cross section. After the thermal-expansion determinations had been completed, cross sections cut from the ends and the center of each sample were polished and examined microscopically in order to determine which samples showed evidence of segregation. Throughout this paper the term segregation is used to refer to nonuniformity in structure. Density determinations and chemical analyses were made on other pieces of the samples.

Table 2 gives the chemical compositions [2] and also indicates the samples which showed segregation. Samples *989* to *1000* were cast in a preheated steel mold and cooled slowly, samples *1062* to *1148* were cast in a sand mold, and samples *1452* to *1453A* were cast in a steel chill mold.

TABLE 2.—*Cast lead-antimony alloys investigated*

Sample	Batch formula		Chemical analysis		Segregation
	Lead	Antimony	Lead	Antimony	
	Percent	*Percent*	*Percent*	*Percent*	
989			90.0	9.8	No.
990			91.0	8.8	No.
991			92.7	7.1	No.
992			92.8	7.0	No.
993			94.1	5.7	No.
994			94.9	4.9	No.
995			95.9	4.0	No.
996			96.9	2.9	No.
997			89.1	10.7	No.
998			87.9	11.9	No.
999	87	13			Yes.
1000	85	15			Yes.
1062	75	25			Yes.
1063	60	40	60.4	39.6	No.
1064	45	55	45.2	54.7	No.
1065	30	70	32.3	67.6	No.
1066	15	85	17.4	82.5	No.
1145	83	17			Yes.
1146	75	25			Yes.
1147	5	95	5.0	95.0	No.
1148	2	98	2.0	98.0	No.
1452	87	13			Yes.
1453 [a]	73	27	75.2	24.8	No.
1453A	73	27	76.2	23.8	No.

[a] Contained arsenic, less than 0.02 percent.

The samples containing from 13 to 25 percent of antimony were found to be segregated. Figure 1 shows the differences in structure observed in two portions of sample *1452*. The distribution of the antimony-rich solid solution (white particles) varies considerably in different portions of this alloy.

Figure 2 illustrates the nonuniformity of structure in sample *1062* (25 percent of antimony). The background of this figure represents

[2] Weight percentages are used in this paper, except where noted otherwise.

the eutectic composition, and the light areas are the antimony-rich solid solution present in excess of the eutectic composition.

The segregation encountered in the cast lead-antimony alloys is attributed to the following factors:

(a) The large difference in the densities of lead (11.3) and antimony (6.7).

(b) The rate of cooling.

(c) The percentage of lead and antimony.

(d) The viscosity of the liquid mixture.

As antimony is lighter than lead, and as it solidifies first, antimony crystals tend to rise to the top of the liquid.

Segregation may be avoided by increasing the rate of cooling. Samples *1062* and *1146* containing about 25 percent of antimony, cast in a preheated steel mold and a sand mold, respectively, were segregated, but samples *1453* and *1453A* containing about the same percentage of antimony, cast in a chill mold, showed no evidence of segregation.

Segregation appears to be most common with lead-antimony alloys containing a little more than the eutectic proportion of antimony (12.5 percent). Casting sample *1452*, containing about 13 percent of antimony, in a chill mold, did not prevent segregation.

Segregation is more noticeable the lower the viscosity of the liquid mixture. Plüss [11] made viscosity measurements at 292° C on lead-antimony alloys containing from 7.6 to 17.0 percent of antimony. He found that the viscosity decreases from 7.6 percent of antimony to the eutectic at 13 percent of antimony and then increases rapidly above the latter percentage.

Ewen and Turner [12] obtained marked segregation in two bars of lead-antimony alloys containing 14.6 and 23.2 percent of antimony. They stated, "It would appear that in casting alloys of this range of composition, which includes bearing metals and type metals, the casting temperature should be as low as possible if segregation is to be avoided. With higher percentages of antimony the dendritic structure effectually prevents segregation." In order to obviate the tendency of lead to collect at the bottom of the melts of lead-rich lead-antimony alloys, Goodrich [5] sealed the constituent metals in a bulb, melted them in vacuo in a tilting furnace, and agitated the melt until the first signs of solidification appeared. The alloy was then cooled slowly in the furnace, remelted and again agitated.

The equilibrium diagram obtained from the results of a number of investigations [10, 13, 14, 15, 16, 17, 18] shows that lead-antimony alloys form a eutectiferous series with limited solid solubility of antimony in lead and of lead in antimony. The eutectic is at about 13 percent of antimony and at 247° C. The solid solubility of antimony in lead increases from about 0.2 percent of antimony at 25° C. to about 2.5 percent of antimony at the eutectic temperature. There is uncertainty in regard to the solid solubility of lead in antimony. Values ranging from less than 1 percent to about 11 percent have been reported [10, 13, 17] for the limiting solid solubility at the eutectic temperature. According to Endo [17], the solid solubility of lead in antimony increases from 1 percent of lead at 0° C to 5 percent of lead at the eutectic temperature, but the results of Broniewski and Sliwowski [10] indicate that the solid solubility is about 11 percent from about 150° C to the eutectic temperature.

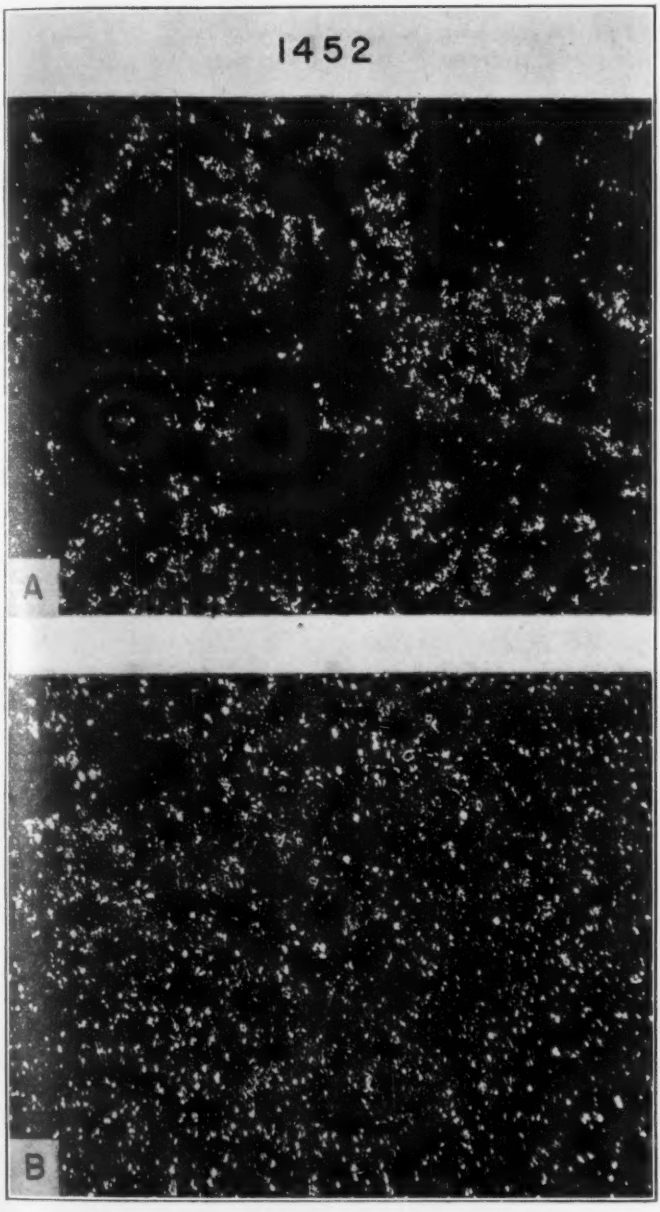

FIGURE 1.—*Typical structure of different parts of cast lead-antimony alloy showing segregation.* × *50.*

Made to contain lead 87 percent, antimony 13 percent. Etched with mixture composed of 75 parts of glacial acetic acid and 25 parts of hydrogen peroxide. *A*, One end of sample 1452; *B*, other end of sample 1452.

FIGURE 2.—*Micrograph showing the structure near the joining of the segregated and unsegregated areas of cast lead-antimony alloy.* × *50.*

Made to contain lead 75 percent, antimony 25 percent. Not etched.

IV. APPARATUS

Samples *989* to *1000* were investigated in the bath furnace described by Hidnert [19], and Souder and Hidnert [20]. Samples *1062* to *1148* were investigated in the black furnace and samples *1452* to *1453A* were investigated in the white furnace shown in figure 1 of the latter publication.

V. RESULTS

The observations obtained on heating and cooling at various temperatures between −12 and +200° C are shown in figures 3 to 5, inclusive. Each expansion curve is plotted from a different origin in order to display the individual characteristics of each curve. A majority of the curves obtained on cooling lie below the expansion curves obtained on heating. The deviations between these curves are particularly noticeable for the alloys containing up to 15 percent of antimony which were cast in a preheated steel mold and cooled slowly. The deviations are less noticeable for the alloys of higher antimony content which were cast either in a sand mold or a chill mold. It is probable that the deviations indicate a lack of equilibrium in the samples on account of the effect of the casting conditions or of the chemical composition.

Only one test was made on each sample except *1146* and *1065* (fig. 5) on which two tests were made. The results obtained on the first heating apply for cast alloys, but the data obtained on the second heating of samples *1146* and *1065* apply for alloys which had received the heat treatment incident to the first heating. As the observations on cooling nearly coincide with the expansion curves on heating in the second tests of samples *1146* and *1065*, it may be assumed that other alloys would show similar results in a second test.

Table 3 gives coefficients of linear expansion which were computed from the results indicated in figures 3 to 5, inclusive. The antimony contents are given in weight and atomic percentages. The table also shows the difference in length before and after each expansion test, and the densities of the samples after the expansion tests.

From the coefficients of expansion obtained for the temperature range from 20 to 60° C on the lead-antimony alloys containing 4.8 to 97.0 [3] atomic percent of antimony (2.9 to 95.0 percent, by weight), the following empirical equation was derived by the method of least squares:

$$_{20}a_{60}=(29.09-0.1789\mathrm{Sb})10^{-6}, \qquad (1)$$

where $_{20}a_{60}$ represents the average coefficient of linear expansion between 20 and 60° C, and Sb represents the atomic percentage of antimony (between 4.8 and 97.0 atomic percent). The probable error of a single computed value is $\pm 0.3\times10^{-6}$. In deriving the equation, the coefficients of expansion of the segregated alloys and the coefficient of expansion obtained in the second test on sample *1065*, were ignored. Only alloys that were uniform and the compositions of which were known, were used in the derivation of the equation.

[3] The alloy containing 98.8 atomic percent of antimony (98.0 percent, by weight) was excluded, for there is doubt whether or not this alloy lies outside of the region of the solid solution of lead in antimony.

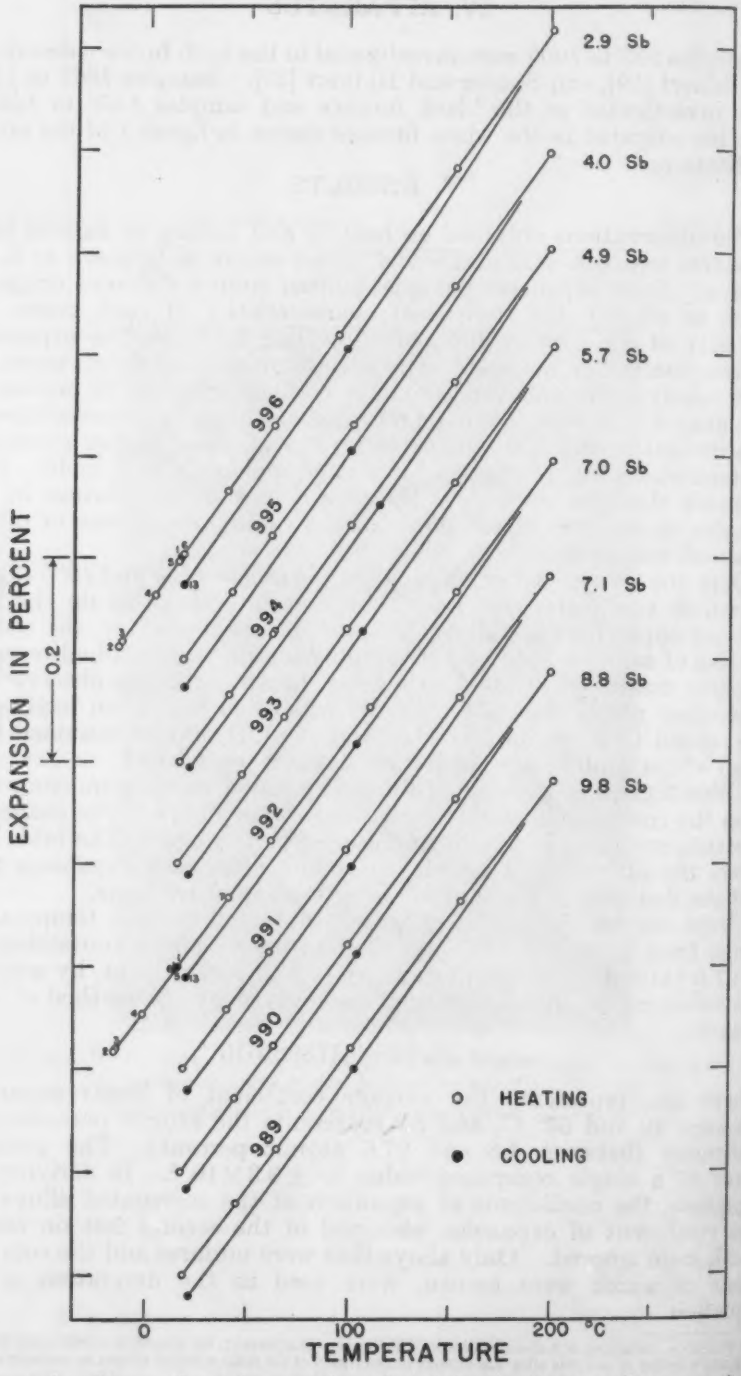

FIGURE 3.—*Linear thermal expansion of cast lead-antimony alloys containing from 2.9 to 9.8 percent of antimony.*

[1] The numbers adjoining the observations at the lower end of the expansion curves of samples *996* and *989* indicate the sequence of the observations. The tagged symbol indicates more than one observation.

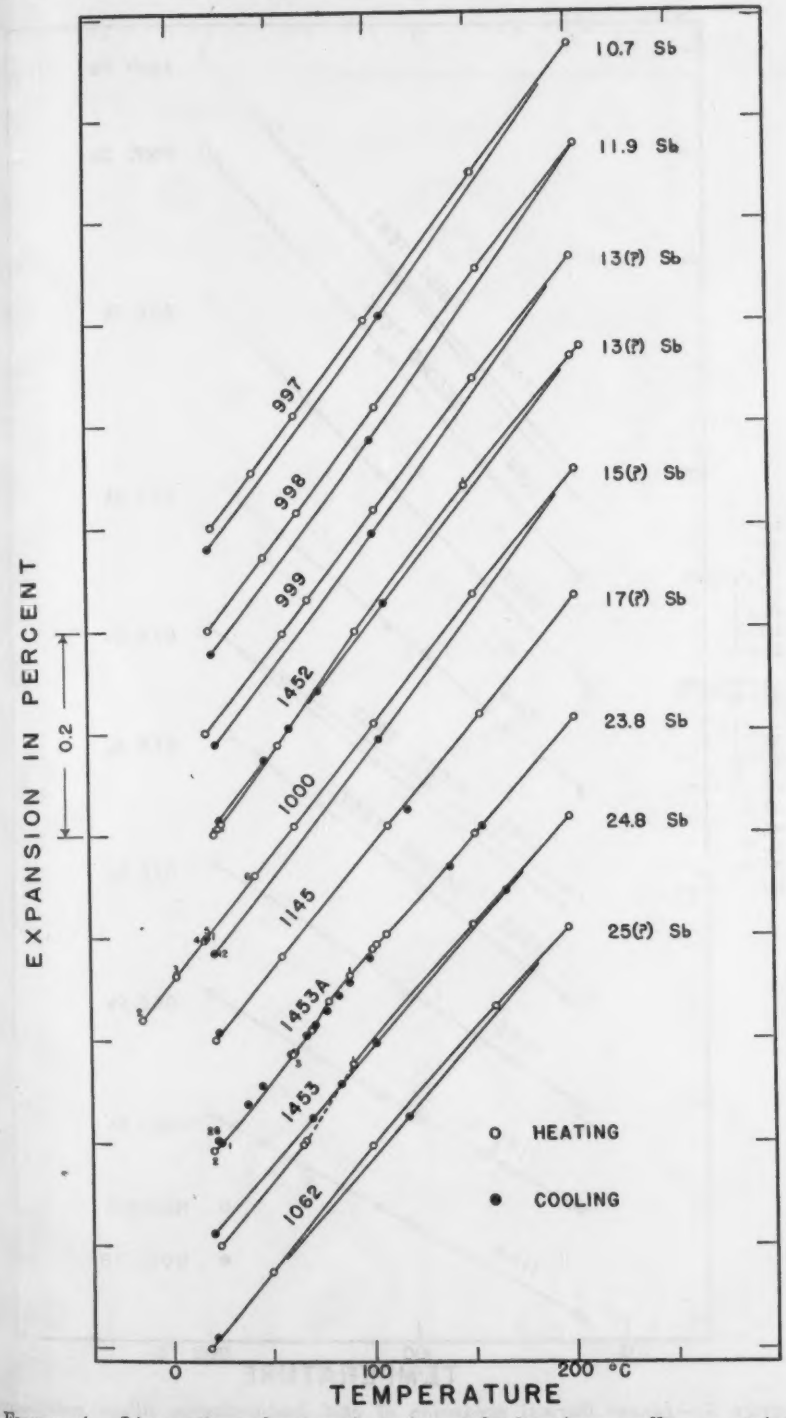

FIGURE 4.—*Linear thermal expansion of cast lead-antimony alloys containing from 10.7 to 25 percent of antimony.*

Samples *999*, *1452*, *1000*, *1145*, and *1062* are segregated. The numbers adjoining the observations at the lower end of the expansion curves of samples *1000* and *1453A* indicate the sequence of the observations. A tagged symbol indicates more than one observation.

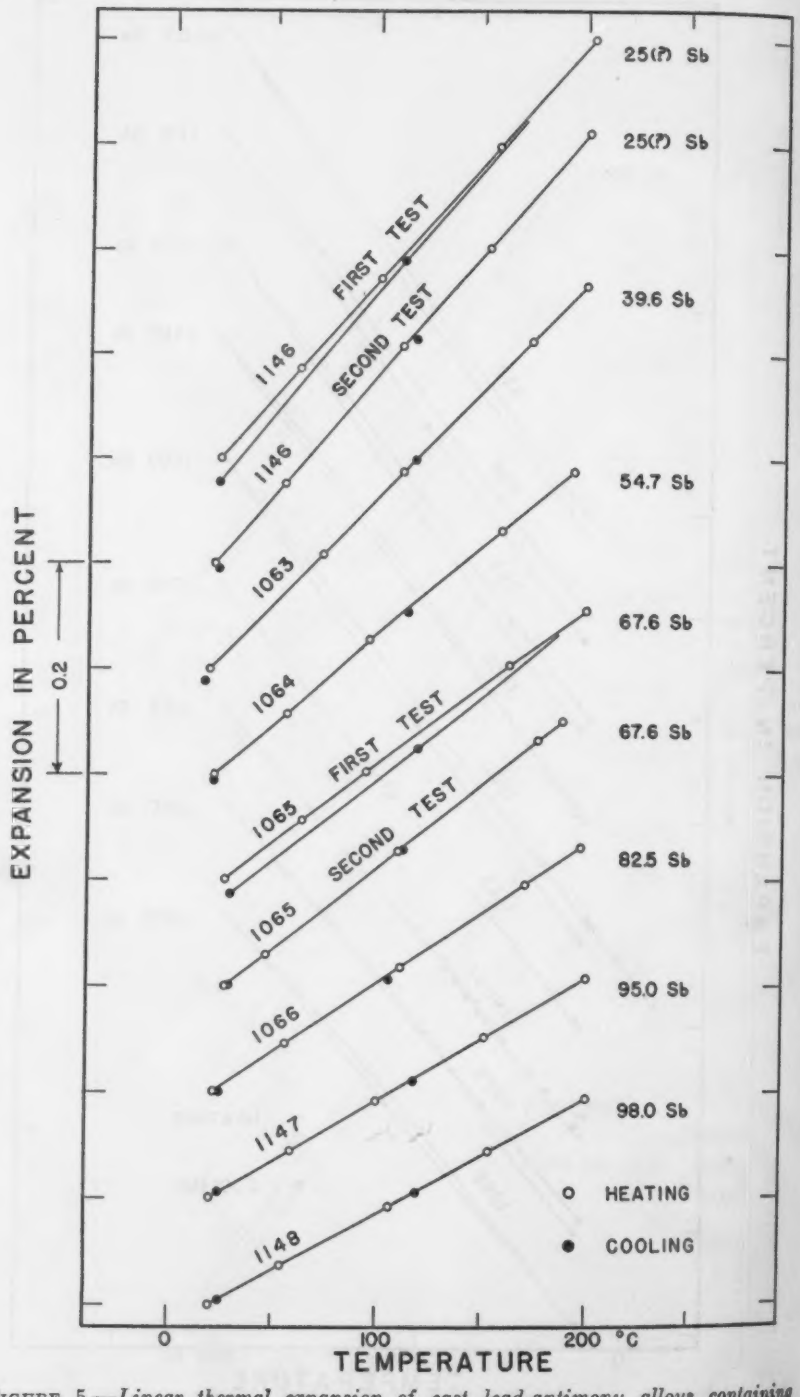

FIGURE 5.—*Linear thermal expansion of cast lead-antimony alloys containing from 25 to 98.0 percent of antimony.*

Sample *1146* is segregated.

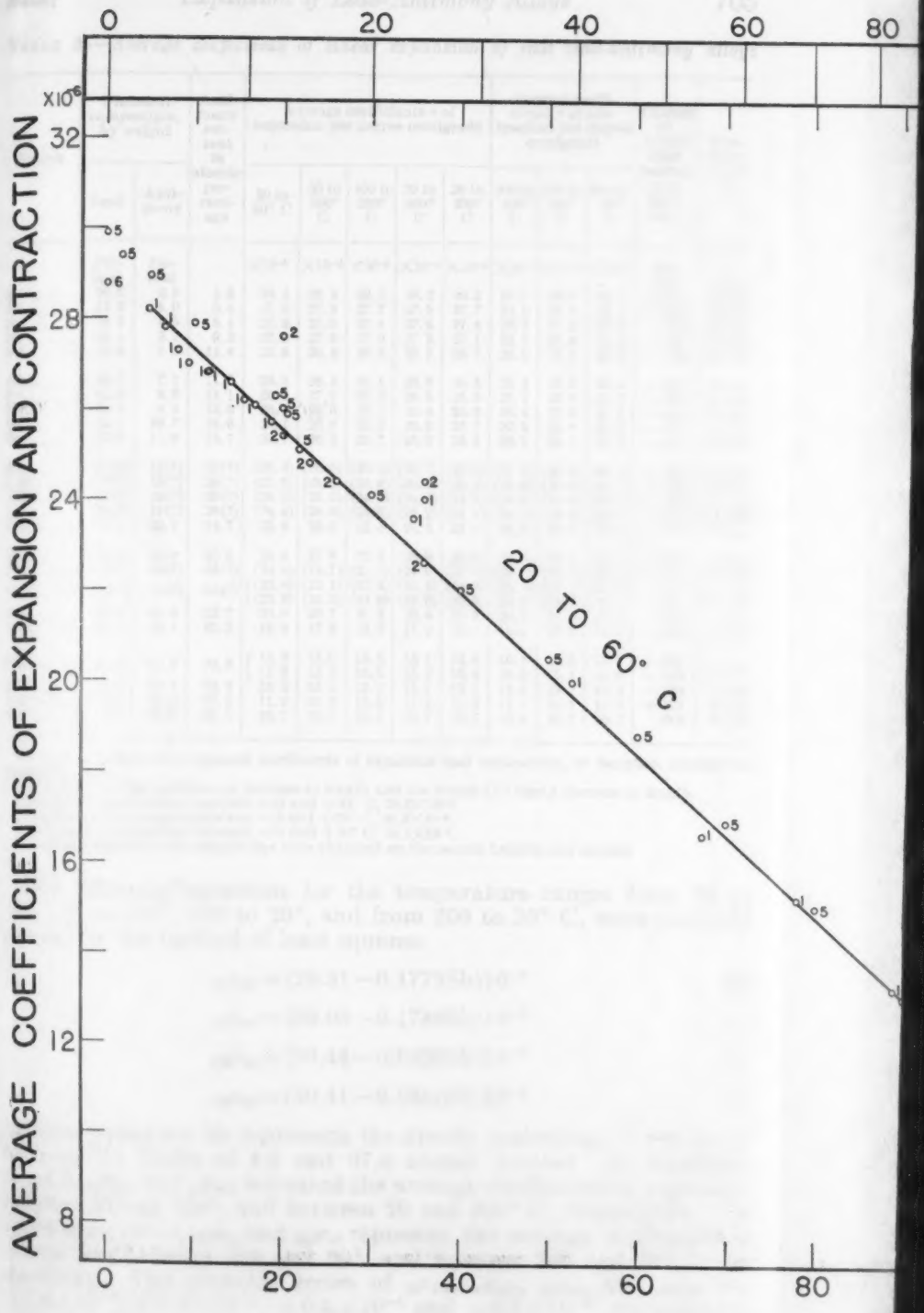
AVERAGE COEFFICIENTS OF EXPANSION AND CONTRACTION
X10⁻⁶
32
28
24
20
16
12
8
0
20
40
60
80
20 TO 60° C

FIGU

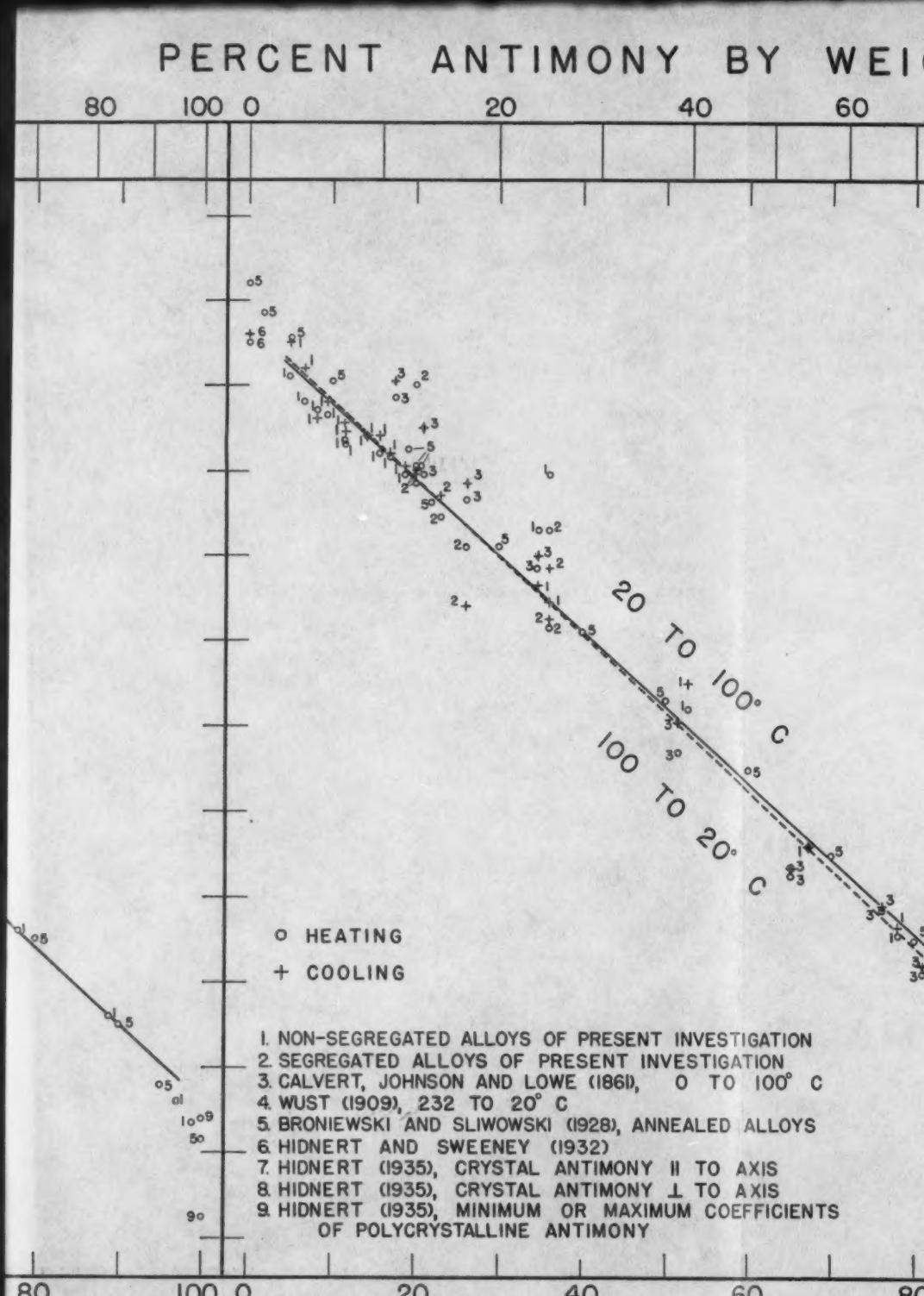
PERCENT ANTIMONY BY WEI
80 100 0 20 40 60
20 TO 100° C
100 TO 20° C
o HEATING
+ COOLING
1. NON-SEGREGATED ALLOYS OF PRESENT INVESTIGATION
2. SEGREGATED ALLOYS OF PRESENT INVESTIGATION
3. CALVERT, JOHNSON AND LOWE (1861), 0 TO 100° C
4. WUST (1909), 232 TO 20° C
5. BRONIEWSKI AND SLIWOWSKI (1928), ANNEALED ALLOYS
6. HIDNERT AND SWEENEY (1932)
7. HIDNERT (1935), CRYSTAL ANTIMONY || TO AXIS
8. HIDNERT (1935), CRYSTAL ANTIMONY ⊥ TO AXIS
9. HIDNERT (1935), MINIMUM OR MAXIMUM COEFFICIENTS OF POLYCRYSTALLINE ANTIMONY
80 100 0 20 40 60 80
ATOMIC PERCENT ANTIM

FIGURE 6.—*Relations between coefficients of expansion, coefficients of contraction, and antimony*

The straight lines represent equations 1 to 5 derived from data obtained in the present investigation on

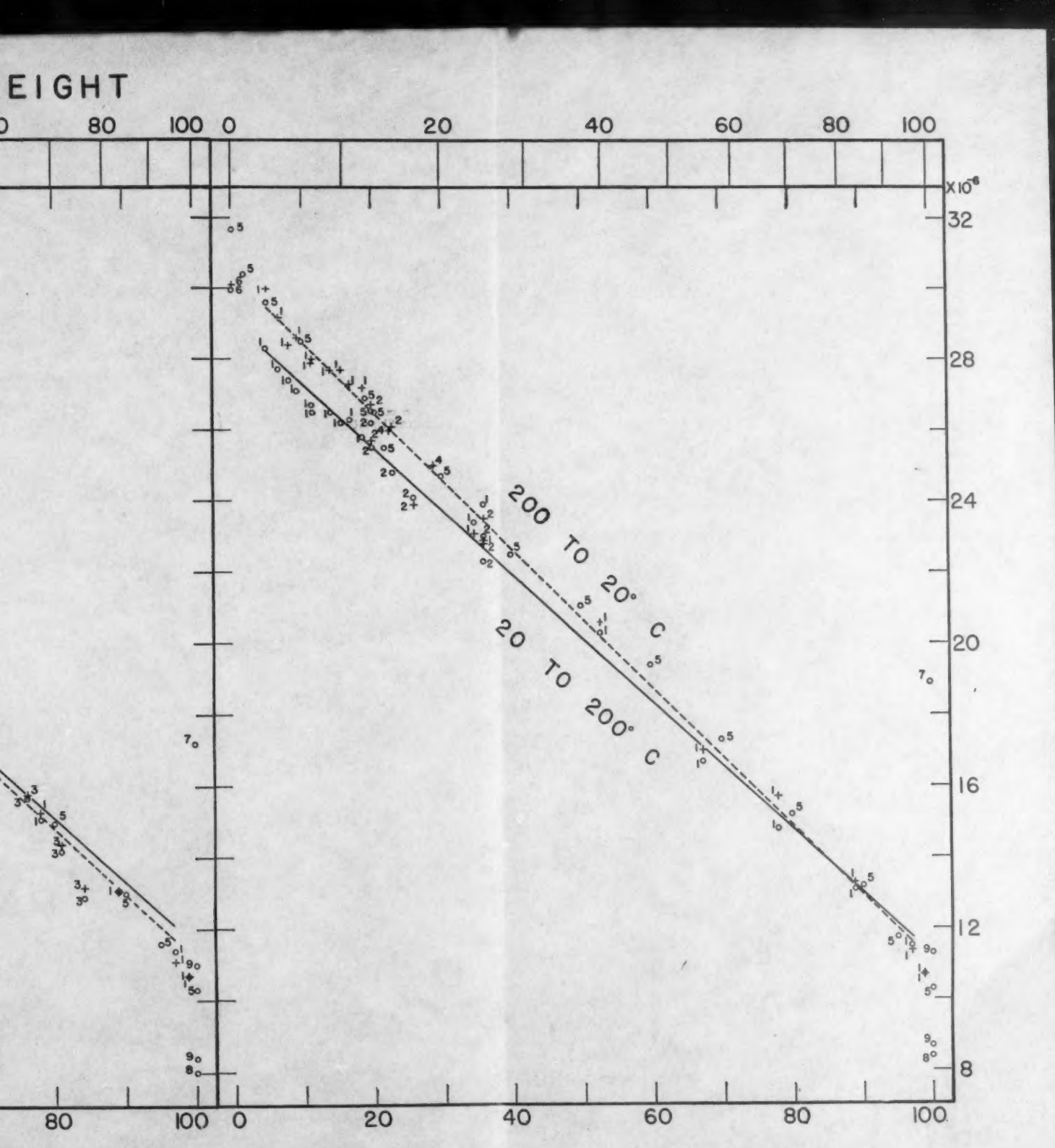

TIMONY

antimony contents of lead-antimony alloys.

tigation on nonsegregated alloys.

UNIV. OF MICH.

PERCENT ANTIMONY
0
20
40
60
ATOMIC PERCENT
0
20
40
60
AVERAGE COEFFICIENTS OF EXPANSION AND CONTRACTION
X10⁶
20 TO 60° C
HEATING
COOLING
1. NON-SEGREGATED ALLOYS OF PRESENT INVESTIGATION
2. SEGREGATED ALLOYS OF PRESENT INVESTIGATION
3. CALVERT, JOHNSON AND LURIE (1954)
4. WUST (1909), 250 TO 20° C
5. BRONIEWSKI AND SLAWINSKI (1928), ANNEALED
6. HIDNERT AND SWELNEY (1932)
7. HIDNERT (1935), CRYSTAL ANTIMONY ⊥ TO
8. HIDNERT (1935), CRYSTAL ANTIMONY ∥ TO
9. HIDNERT (1935), MINIMUM OR MAXIMUM
OF POLYCRYSTALLINE ANTIMONY

TABLE 3.—*Average coefficients of linear expansion of cast lead-antimony alloys*

Sample	Chemical composition, by weight		Antimony content in atomic percentage	Average coefficients [a] of expansion per degree centigrade					Average coefficients [a] of contraction per degree centigrade			Change in length after heating and cooling [b]	Density [a] at 25° C
	Lead	Antimony		20 to 60° C	60 to 100° C	100 to 200° C	20 to 100° C	20 to 200° C	200 to 100° C	100 to 20° C	200 to 20° C		
	Per cent	*Per cent*		×10⁻⁶	×10⁻⁶	×10⁻⁶	×10⁻⁶	×10⁻⁶	×10⁻⁶	×10⁻⁶	×10⁻⁶	*Per cent*	g/cm³
996 [c]	96.9	2.9	4.8	28.2	28.2	28.3	28.2	28.3	30.7	29.0	30.0	−0.031	10.979
995	95.9	4.0	6.6	27.8	27.4	27.7	27.6	27.7	29.9	28.4	29.2	−.029	10.975
994	94.9	4.9	8.1	27.3	27.6	27.4	27.4	27.4	29.4	27.2	28.4	−.019	10.948
993	94.1	5.7	9.3	27.0	27.6	27.0	27.3	27.1	29.3	27.6	28.6	−.027	10.880
992 [d]	92.8	7.0	11.4	26.8	25.6	26.8	26.7	26.7	28.6	27.1	27.9	−.023	10.798
991	92.7	7.1	11.5	26.8	26.4	26.5	26.6	26.5	28.9	26.9	28.0	−.021	10.766
990	91.0	8.8	14.1	26.6	27.0	26.2	26.8	26.5	28.4	26.8	27.7	−.024	10.676
989	90.0	9.8	15.6	26.2	26.6	26.0	26.4	26.2	28.4	26.8	27.7	−.028	10.598
987	89.1	10.7	16.9	26.1	26.6	26.3	26.3	26.3	27.9	26.4	27.3	−.017	10.478
998	87.9	11.9	18.7	25.7	26.2	25.7	25.9	25.8	28.1	26.1	27.2	−.027	10.458
999	87(?)	13(?)	20(?)	(25.4)	(26.0)	(25.3)	(25.7)	(25.5)	(27.3)	(26.0)	(26.7)	−.022	(10.415)
1458	87(?)	13(?)	20(?)	(27.6)	(28.4)	(24.8)	(28.0)	(26.2)	(25.5)	(25.9)	(25.7)	+.006	(10.381)
1000 [e]	85(?)	15(?)	23(?)	(24.8)	(25.0)	(24.7)	(24.9)	(24.8)	(26.8)	(25.4)	(26.1)	−.025	(10.269)
1145	83(?)	17(?)	26(?)	(24.4)	(24.0)	(24.0)	(24.2)	(24.1)	(24.8)	(22.8)	(23.9)	+.002	(10.138)
1483A	76.2	23.8	34.7	23.6	25.6	22.4	24.6	23.4	23.0	23.3	23.1	+.006	9.626
1483	75.2	24.8	36.0	24.0	27.9	22.3	25.9	23.9	22.8	22.9	22.9	+.019	9.676
1062	75(?)	25(?)	36(?)	(24.4)	(24.7)	(21.7)	(24.6)	(23.0)	(23.1)	(22.5)	(22.8)	+.003	(9.598)
1148 [f]	75(?)	25(?)	36(?)	(22.6)	(22.1)	(22.4)	(22.3)	(22.3)	(23.4)	(23.7)	(23.5)	−.021	(9.683)
				(22.8)	(23.2)	(22.9)	(23.0)	(22.9)	(23.9)	(22.9)	(23.4)	−.010	
1063	60.4	39.6	52.7	20.0	20.7	20.2	20.4	20.3	20.4	21.0	20.6	−.007	8.333
1064	45.2	54.7	67.3	16.6	17.8	16.3	17.2	16.7	16.8	17.2	17.0	−.005	8.190
1065 [f]	32.3	67.6	78.0	15.2	15.0	14.5	15.1	14.8	16.1	15.3	15.7	−.017	7.649
				15.0	15.4	15.5	15.2	15.4	16.0	15.1	15.6	−.002	
1066	17.4	82.5	88.9	13.2	13.1	13.1	13.1	13.1	13.6	13.1	13.3	−.004	7.124
1147	5.0	95.0	97.0	11.2	11.6	11.5	11.4	11.5	11.7	11.1	11.4	+.001	6.702
1148	2.0	98.0	98.8	10.7	10.7	10.8	10.7	10.7	10.8	10.7	10.7	.000	6.682

[a] Values in parentheses represent coefficients of expansion and contraction, or densities obtained on segregated alloys.
[b] The plus (+) sign indicates an increase in length and the minus (−) sign a decrease in length.
[c] Coefficient of expansion between −12 and +20° C, 28.0×10⁻⁶.
[d] Coefficient of expansion between −12 and +20° C, 26.3×10⁻⁶.
[e] Coefficient of expansion between −12 and +20° C, 24.5×10⁻⁶.
[f] Coefficients given on the second line were obtained on the second heating and cooling.

The following equations for the temperature ranges from 20 to 100°, 20 to 200°, 100 to 20°, and from 200 to 20° C, were similarly derived by the method of least squares:

$$_{20}a_{100} = (29.31 - 0.1773\text{Sb})10^{-6} \quad (2)$$

$$_{20}a_{200} = (29.08 - 0.1786\text{Sb})10^{-6} \quad (3)$$

$$_{100}a_{20} = (29.44 - 0.1826\text{Sb})10^{-6} \quad (4)$$

$$_{200}a_{20} = (30.41 - 0.1941\text{Sb})10^{-6} \quad (5)$$

In these equations Sb represents the atomic percentage of antimony between the limits of 4.8 and 97.0 atomic percent. In equations 2 and 3, $_{20}a_{100}$ and $_{20}a_{200}$ represent the average coefficients of expansion between 20 and 100°, and between 20 and 200° C, respectively. In equations 4 and 5, $_{100}a_{20}$ and $_{200}a_{20}$ represent the average coefficients of contraction between 100 and 20°, and between 200 and 20° C, respectively. The probable errors of $_{20}a_{100}$, $_{20}a_{200}$, $_{100}a_{20}$, and $_{200}a_{20}$ are $\pm 0.6\times10^{-6}$, $\pm 0.3\times10^{-6}$, $\pm 0.3\times10^{-6}$ and $\pm 0.2\times10^{-6}$, respectively.

Figure 6 shows the relations between the coefficients of expansion and the antimony contents of cast lead-antimony alloys. Values for lead [3] and for monocrystalline and polycrystalline antimony [4] are included in the figure. Equations 1, 2, and 3 are represented in figure 6 by solid lines, and equations 4 and 5 by dashed or broken lines. Values obtained from previous investigators are included in this figure for comparison. Broniewski and Sliwowski's [10] values for lead and the lead-rich lead-antimony alloys appear to be too high. Their coefficients of expansion for lead are appreciably higher than nearly all of the results reported by other investigators.

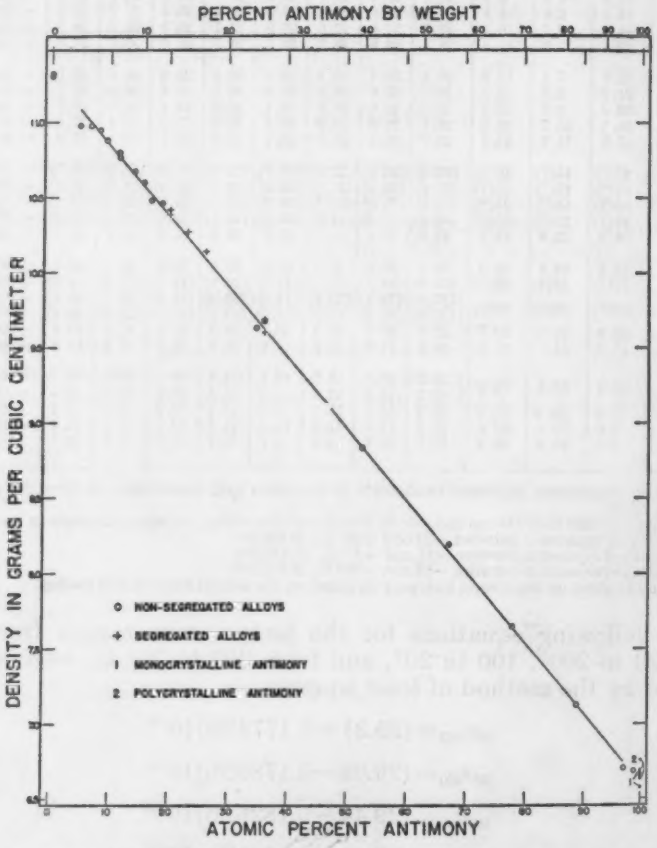

FIGURE 7.—*Relation between densities and antimony contents of lead-antimony alloys.*

Equations 1 to 5 and the straight lines in figure 6 show that the coefficients of expansion of the lead-antimony alloys decrease linearly with increase in the antimony content from about 5 to 97 atomic percent (3 to 95 percent, by weight). These alloys, which lie between the solid solutions at the lead end and the antimony end of the equilibrium diagram, consist of an excess of one or the other solid solution.

Some deviations from these linear relations were anticipated at both ends of the equilibrium diagram. At the lead end the deviations are slight for the ranges from 20 to 60° C and from 20 to 100° C, but the deviation is 0.9×10^{-6} for the range from 20 to 200° C. The deviations are more evident near the antimony end of the diagram for the antimony-richest alloy and for pure antimony.

The coefficients of expansion of the lead-antimony alloys cover a wide range of values. It is possible to select lead-antimony alloys that have approximately the same coefficients of expansion as iron, nickel, gold, copper, silver, aluminum, magnesium, and many of their alloys, at temperatures below 200° C.

Figure 7 shows the relation between the densities and the antimony contents of the lead-antimony alloys investigated. Values for lead [3] and for monocrystalline and polycrystalline antimony [4] are included in the figure. The straight line shows that the density also decreases linearly with increase in the antimony content (atomic percentage) of the lead-antimony alloys.

The linear relations between the coefficients of expansion, or density, and the chemical composition (atomic percentage) are typical of relations for other properties of binary alloys having structures composed of solid solution+eutectic.

VI. CONCLUSIONS

1. A majority of the curves obtained on cooling lie below the expansion curves obtained on heating. The deviations between these curves are particularly noticeable for the lead-antimony alloys containing up to 15 percent of antimony which were cast in a preheated steel mold and cooled slowly. The deviations are less noticeable for the alloys of higher antimony content which were cast either in a sand mold or a chill mold. It is probable that the deviations indicate a lack of equilibrium in the samples on account of the effect of the casting conditions or of the chemical composition.

2. The following equations give the relations between the coefficients of expansion and the chemical composition of the lead-antimony alloys investigated.

$$ {}_{20}a_{60} = (29.09 - 0.1789\mathrm{Sb})10^{-6} \pm 0.3 \times 10^{-6} \quad (1) $$

$$ {}_{20}a_{100} = (29.31 - 0.1773\mathrm{Sb})10^{-6} \pm 0.6 \times 10^{-6} \quad (2) $$

$$ {}_{20}a_{200} = (29.08 - 0.1786\mathrm{Sb})10^{-6} \pm 0.3 \times 10^{-6} \quad (3) $$

$$ {}_{100}a_{20} = (29.44 - 0.1826\mathrm{Sb})10^{-6} \pm 0.3 \times 10^{-6} \quad (4) $$

$$ {}_{200}a_{20} = (30.41 - 0.1941\mathrm{Sb})10^{-6} \pm 0.2 \times 10^{-6} \quad (5) $$

In these equations Sb represents the atomic percentage of antimony between 4.8 and 97.0 atomic percent (2.9 to 95.0 percent of antimony by weight). In equations 1, 2, and 3, ${}_{20}a_{60}$, ${}_{20}a_{100}$, and ${}_{20}a_{200}$ represent the average coefficients of expansion between 20 and 60°, 20 and 100°, and between 20 and 200° C, respectively. In equations 4 and 5, ${}_{100}a_{20}$ and ${}_{200}a_{20}$ represent the average coefficients of contraction between 100 and 20°, and between 200 and 20° C, respectively.

The last term in each equation indicates the probable error of the coefficient of expansion. These equations show that the coefficients of expansion decrease linearly with increase in the atomic percentage of antimony.

3. The densities of the lead-antimony alloys also decrease linearly with increase in the atomic percentage of antimony.

4. The linear relations between the coefficients of expansion, or density, and the chemical composition (atomic percentage) are typical of relations for other properties of binary alloys having structures composed of solid solution+eutectic.

5. The coefficients of expansion of the lead-antimony alloys cover a wide range of values. It is possible to select lead-antimony alloys that have approximately the same coefficients of expansion as iron, nickel, gold, copper, silver, aluminum, magnesium, and many of their alloys.

VII. REFERENCES

The numbers in brackets are the citation numbers given throughout this paper for the references herein.

[1] Data by Hidnert and Sweeney obtained in 1923 on the linear thermal expansion of one sample of cast lead and various cast lead-antimony alloys between 20 and 60° C were published in 1924 by Vinal, Storage Batteries (John Wiley & Sons, Inc., New York, N. Y.).
[2] Hidnert and Sweeney, Phys. Rev. **10,** 296 (1930).
[3] Hidnert and Sweeney, BS J. Research **9,** 703 (1932) RP500.
[4] Hidnert, J. Research NBS **14,** 523 (1935) RP784.
[5] Goodrich, Trans. Faraday Soc. **25,** 531 (1929).
[6] Daniell, Phil. Mag. [3] **1,** p. 197, 261 (1832).
[7] Calvert, Johnson, and Lowe, Chem. News, **3,** p. 315, 357, 371 (1861).
[8] Vicentini and Omodei, Rendiconti della R. Accad. dei Lincei **4,** 1° Sem., p. 718; 2° Sem., p. 19 (1888).
[9] Wüst, Metallurgie, **6,** 769 (1909).
[10] Broniewski and Sliwowski, Rev. Mét. **25,** 397 (1928).
[11] Plüss, Z. anorg. allgem. Chem. **93,** 1 (1915).
[12] Ewen and Turner, J. Inst. Metals **4,** 128 (1910).
[13] Gontermann, Z. anorg. Chem. **55,** 419 (1907).
[14] Dean, Hudson, and Fogler, J. Ind. Eng. Chem. **17,** 1246 (1925).
[15] Schumacher and Nix, Proc. Inst. Metals Div., Am. Inst. Min. Met. Eng., p 195 (1927).
[16] Schumacher and Bouton, J. Am. Chem. Soc. **49,** 1667 (1927).
[17] Endo, Sci. Rep. Tohôku Imperial Univ., Series 1, **16** (no. 2), 201 (1927).
[18] Obinata and Schmid, Metallwirtschaft **12,** 101 (1933).
[19] Hidnert, Sci. Pap. BS **17,** 91 (1922) S410.
[20] Souder and Hidnert, Sci. Pap. BS **21,** 1 (1926) S524.

The author expresses his appreciation to H. W. Bearce, W. Souder, and J. G. Thompson for valuable suggestions; to J. R. Freeman, Jr., and C. M. Saeger, Jr., for casting the lead-antimony alloys; to H. A. Buchheit and W. D. Mogerman for the chemical analyses; to E. L. Peffer and Miss E. E. Hill for the density determinations; and to J. Burks for assistance in the preparation of the figures.

Washington, May 21, 1936.

U. S. Department of Commerce National Bureau of Standards

RESEARCH PAPER RP939

Part of Journal of Research of the National Bureau of Standards, Volume 17, November 1936

SOLUBILITY OF MERCUROUS SULPHATE IN SULPHURIC-ACID SOLUTIONS

By D. Norman Craig, George W. Vinal, and Francis E. Vinal

ABSTRACT

Although mercurous sulphate has been the subject of many papers, particularly papers relating to its use in standard cells, the information available in the technical literature about its solubility in dilute solutions of sulphuric acid is somewhat conflicting and incomplete. New determinations have been made, therefore, of the solubility of the salt at 28° C and at 0° C. About half of the determinations at each temperature were made on solutions which were brought to saturation from an undersaturated state and the others from an initially supersaturated state. The mercury was determined electrolytically. Each solution was tested after electroylysis for residual mercury. Errors which might arise from the presence of mercuric mercury were shown to be within the limit of experimental error of the determinations. The acid concentration of the solutions ranged from 0.001 to 4 molar. Tables are given for the solubility of the salt in these solutions. The trend of the curves is discussed and comparisons are made with data previously obtained by others.

CONTENTS

I. Introduction 709
II. Experimental procedure 711
1. Materials 711
2. Saturation of solutions 711
3. Determination of mercury 711
4. Determination of sulphuric acid 712
III. Experimental results 712
1. Acid solutions 712
2. "Water" solutions 713
IV. Solubility of mercurous sulphate at regular intervals of sulphuric-acid concentration 716
V. Discussion of results 717
VI. Comparison with previous determinations 719
VII. References 720

I. INTRODUCTION

Although mercurous sulphate has been the subject of many papers, particularly papers relating to its use in standard cells, further study of its properties was deemed to be desirable as part of a larger program of work on standard cell materials and construction. The solubility of mercurous sulphate in water and in dilute solutions of sulphuric acid has been measured by a considerable number of previous experimenters.

Gouy [1] [1] studied the hydrolysis of mercurous sulphate and determined its solubility in water. Cox [2], using Gouy's data and some of his own, concluded that between mercurous sulphate, Hg_2SO_4, and mercurous oxide, Hg_2O, only one solid phase exists, namely, a basic sulphate. Hager and Hulett's [3] results, as well as those of Gouy, showed that the "equilibrium water" has an acidity equivalent to 0.001 molar sulphuric acid. This is in close agreement with the values obtained in the present work, 0.00108 molar at 28° C and 0.00099 at 0° C. Hager and Hulett, however, argued that a 0.001 molar sulphuric acid solution is not as effective in preventing hydrolysis of the salt as the equilibrium water, which they found to be 0.002 molar in respect of $HgHSO_4$.

The solubility of mercurous sulphate in water and in dilute solutions of sulphuric acid was measured by Hulett [4] with precision which merited more recognition than it has received. Results of the present work calculated to 25° C from 28° C are in close agreement with his, assuming that the change in solubility with temperature is linear over this small temperature interval.

Drucker's [5] four determinations, which are the basis of values given in the International Critical Tables (see page 720), are not entirely consistent with Hulett's results. Drucker's data indicated a greater solubility of mercurous sulphate in acid solutions of 0.05 molar than in other solutions immediately above and below this concentration. Hulett, on the other hand, found the solubility to be a minimum for acid solutions in this range.

Some of the earlier determinations lack sufficient data on methods of arriving at saturation equilibrium and others, such as the comprehensive determinations of Smith [7], lack information as to the temperature. There appear to be no systematic data on the effect of temperature on solubility of mercurous sulphate. These and other determinations are discussed in a later section of the paper.

For the present work, an electrolytic method of determining the mercury in solutions which were brought to saturation after prolonged mechanical stirring, was chosen. Each solution was tested after electrolysis for residual mercury.

About half of the determinations were made on solutions which were brought to saturation equilibrium from an undersaturated state, and the others were from an initially supersaturated state. We have not been unmindful of the possibility that small amounts of mercuric mercury might be included in these determinations. However, the precautions which were taken to reduce the mercuric ion to its equilibrium value with the mercurous ion in the presence of free mercury the error produced by the -ic ion is shown by the results to be less than the estimated experimental error of the work.

A series of measurements was made on solutions ranging in acidity from 0.001 to 4 molar at 28° C, which is the temperature at which the primary standard for the volt is maintained, and a similar series of measurements at 0° C.

[1] Numbers in brackets refer to references at end of the paper.

II. EXPERIMENTAL PROCEDURE

1. MATERIALS

The mercurous sulphate was part of a gray sample prepared for use in standard cells. It was made electrolytically from new mercury which had been distilled twice under reduced pressure by Hulett's [8] method. The current during electrolysis was equivalent to 2 amp/dm^2. Other details of the process were essentially the same as those previously described by Wolff and Waters [9]. Since the time of its preparation in 1931 the mercurous sulphate was preserved in the dark under a portion of the acid electrolyte used in its preparation. Although this sample of mercurous sulphate contained an appreciable amount of free mercury, all of the saturated solutions were prepared with the addition of more free mercury.

The sulphuric acid conformed to the requirements recommended by a committee [10] of the American Chemical Society for reagent grade acid.

2. SATURATION OF SOLUTIONS

The saturation of the solutions was accomplished by agitating them mechanically with Pyrex-glass stirrers in 500-ml Pyrex flasks containing free mercury. At 28° C the temperature was controlled to ± 0.02° C by a water thermostat. At 0° C the temperature was controlled by large dewar flasks containing a mixture of ice and water. The experimental results at both temperatures include values obtained by approaching the saturation equilibrium from a condition of incomplete saturation and from supersaturation.

After agitating the solutions for 72 hours, the stirrers were removed and the flasks were allowed to stand at their respective temperatures until the solutions were clear. This usually required 48 hours. The samples of the supernatant solutions were carefully removed by pressure, the lower end of the delivery tube in each case projecting into the liquid no farther than was required to deliver 100 to 150 ml samples. After each sample was removed it was carefully inspected, and if found to be entirely clear it was then weighed to 0.1 g.

3. DETERMINATION OF MERCURY

The mercury content was determined by electrolytic deposition on platinum-gauze electrodes 3.5 by 3.5 cm. Two pieces of platinum foil, one on either side of the gauze electrode, served as anodes. After electrolyzing the solutions for a period of 40 to 48 hours, the electrolysis was stopped by removing the cathodes, which were then washed promptly and suspended in a desiccator containing P_2O_5 and free mercury. No difficulty was experienced with mercury dropping from the gauze. Repeated weighings indicated that the cathodes reached constant weight after hanging in the desiccator for 3 hours.

The water used in rinsing the cover glasses and the cathodes was caught in the respective beakers containing the electrolyzed solutions. Each solution was then weighed and divided into two portions. One portion was used to test for mercury by H_2S, and the other portion

was titrated to determine the sulphuric acid. It was found that the removal of the mercury was generally complete except in the more concentrated sulphuric acid solutions. Small corrections were therefore necessary in such cases. These corrections were determined with H_2S turbidimetrically by comparison with solutions of the same acid concentration containing known amounts of mercury.

4. DETERMINATION OF SULPHURIC ACID

The sulphuric-acid content of each portion of solution titrated was multiplied by the proper factor to give the total sulphuric-acid content of the electrolyzed sample. The H_2SO_4 equivalent of the mercury was then subtracted from the total sulphuric acid and the weight fraction of the free sulphuric acid in the original solution was calculated. The density of the original solution was then calculated, using the tables in the International Critical Tables. The volume of the original solution and sulphuric-acid molarity could then be calculated, as well as the weight of mercury per 100 ml.

The method for determining sulphuric acid described above was applied to all the solutions. It is referred to in this paper as method *A*. A second method, *B*, was applied to some of the solutions below 0.01 molar acid. This method served as a valuable check on method *A*.

Method *B* consisted in adding 2 ml of a 5-percent KCl solution to a weighed portion of the solution containing the dissolved Hg_2SO_4. After coagulation of the Hg_2Cl_2, the sulphuric-acid content of the solution was determined by titration. In the determinations by method *B* no correction was required as indicated for method *A*, in which allowance was made for the formation of sulphuric acid by the electrolytic deposition of the mercury. The agreement between the two methods, as shown in table 3, may be considered to indicate, within experimental error, that the mercury was in solution as mercurous mercury. Additional titrations by both methods of other solutions below 0.01 molar acid led to the same conclusion. No comparisons were made in solutions above 0.01 molar. Hulett [4] reported the ratio of Hg(ous) Hg(ic) to be 200:1 in sulphuric-acid solutions saturated with Hg_2SO_4. The ratio indicates that 0.5 percent of the mercury is present as mercuric ion. Accordingly, it would be expected that the electrolytic deposition of the mercury would give values slightly greater than those obtained by precipitating the mercury as calomel. The difference, however, is probably smaller than our average experimental error.

III. EXPERIMENTAL RESULTS

1. ACID SOLUTIONS

The weight of mercury in 100 ml of each solution at 28° C, determined directly from the experimental data, is given in table 1 as observed values, together with the acid molarity of the respective solutions. Columns 3, 5, and 6 of this table need not be considered now. They relate to smoothed curves, shown in figure 1, which are discussed on page 716. Corresponding data are given in table 2 for determinations made at 0° C. The direction from which the satura-

tion equilibrium was approached is indicated in these tables by *D* ("down" points) if approached from a supersaturated condition and by *U* ("up" points) if approached from an unsaturated condition.

TABLE 1.—*Experimental data at 28° C and comparison with the smoothed curve, figure 1*

Molarity H_2SO_4	Weight of Hg per 100 ml		Direction	Difference	Difference
	Observed	From curve			
	Gram	*Gram*		*Gram*	*Percent*
0.00107	0.0507	0.0504	*D*	+0.0003	+0.6
0.00109	.0501	.0504	*U*	−.0003	−.6
0.00150	.0490	.0493	*D*	−.0003	−.6
0.00152	.0495	.0491	*U*	+.0004	+.8
0.00202	.0465	.0464	*D*	+.0001	+.2
0.00198	.0461	.0464	*U*	−.0003	−.6
0.00304	.0424	.0423	*D*	+.0001	+.2
0.00307	.0420	.0422	*U*	−.0002	−.5
0.00519	.0369	.0371	*D*	−.0002	−.5
0.00518	.0371	.0371	*U*	.0000	.0
0.01046	.0340	.0336	*D*	+.0004	+1.2
0.01043	.0337	.0336	*U*	+.0001	+.3
0.02908	.0314	.0313	*D*	+.0001	+.3
0.02906	.0312	.0313	*U*	−.0001	−.3
0.04854	.0318	.0321	*D*	−.0003	−.9
0.04838	.0325	.0321	*U*	+.0004	+1.2
0.1042	.0343	.0346	*D*	−.0003	−.9
0.1035	.0343	.0346	*U*	−.0003	−.9
0.1583	.0360	.0365	*D*	−.0005	−1.4
0.1576	.0375	.0365	*U*	+.0010	+2.7
0.4121	.0423	.0425	*D*	−.0003	−.7
0.4102	.0427	.0425	*U*	+.0002	+.5
0.7185	.0460	.0462	*D*	−.0002	−.4
0.6825	.0463	.0460	*U*	+.0003	+.7
1.466	.0454	.0455	*D*	−.0001	−.2
1.370	.0461	.0460	*U*	+.0001	+.2
2.142	.0393	.0395	*D*	−.0002	−.5
2.487	.0357	.0357	*U*	.0000	.0
3.550	.0232	.0232	*D*	.0000	.0
3.560	.0234	.0233	*U*	+.0001	+.4
Average of "downs"				±.0002$_5$	
Average of "ups"				±.0002$_5$	
Average of all determinations				±.0002$_4$	±.6

2. "WATER" SOLUTIONS

The observed weights of mercury per 100 ml of "water" solutions and the molarity of the sulphuric acid resulting from hydrolysis are given in tables 3 and 4 for solutions saturated at 28° C and at 0° C, respectively. In the preparation of these solutions water only was added to the mercurous sulphate; they are therefore referred to as "water" solutions. After removal of the portions for the determinations marked *1D* and *1U* the remaining solutions were again agitated and allowed to clear. The portions removed at this time were designated as *2D* and *2U*. Determinations indicated by primes were made after a second or third addition of water.

TABLE 2.—*Experimental data at 0° C and comparison with the smoothed curve, figure 1*

Molarity H_2SO_4	Weight of Hg per 100 ml		Direction	Difference	Difference
	Observed	From curve			
	Gram	*Gram*		*Gram*	*Percent*
0.00099	0.0350	0.0352	*D*	−0.0002	−0.6
0.00098	.0354	.0353	*U*	+.0001	+.3
0.00155	.0313	.0311	*D*	+.0002	+.6
0.00157	.0309	.0311	*U*	−.0002	−.6
0.00310	.0257	.0256	*D*	+.0001	+.4
0.00309	.0255	.0256	*U*	−.0001	−.4
0.00520	.0229	.0223	*D*	+.0006	+2.7
0.00527	.0215	.0221	*U*	−.0006	−2.7
0.01014	.0200	.0197	*D*	+.0003	+1.5
0.01036	.0195	.0196	*U*	−.0001	−.5
0.01838	.0182	.0183	*D*	−.0001	−.5
0.01861	.0182	.0183	*U*	−.0001	−.5
0.07223	.0185	.0180	*D*	+.0005	+2.8
0.09098	.0176	.0181	*U*	−.0005	−2.8
0.2877	.0213	.0211	*D*	+.0002	+.9
0.3380	.0214	.0217	*U*	−.0003	−1.4
0.7266	.0248	.0245	*D*	+.0003	+1.2
0.7608	.0242	.0246	*U*	−.0004	−1.6
0.9816	.0250	.0249	*D*	+.0001	+.4
0.9816	.0247	.0249	*U*	−.0002	−.8
1.383	.0248	.0243	*D*	+.0005	+2.1
1.595	.0233	.0237	*U*	−.0004	−1.7
2.479	.0179	.0179	*D*	.0000	.0
2.587	.0173	.0173	*U*	.0000	.0
4.229	.0068	.0068	*D*	.0000	.0
4.180	.0067	.0067	*U*	.0000	.0
Average of "downs"				$\pm.0002_4$	
Average of "ups"				$\pm.0002_3$	
Average of all determinations				$\pm.0002_3$	±1.0

The sulphuric-acid molarities given in tables 3 and 4 indicate that normal and basic mercurous sulphate may be present as solids at 28° C in equilibrium with sulphuric-acid solutions of 0.00108 molar and at 0° C in solutions of 0.00099 molar. These values indicate that the acid concentration in equilibrium with the normal and basic solid increases with temperature. Hulett [4] reported that a solution formed at 25° C by the addition of water to mercurous sulphate contained 0.00235 mole of mercurous mercury and 0.00225 mole of SO_4 and that repeated additions of water gave the same result. These results indicate that his saturated solution at 25° C contained 0.00107 mole of free sulphuric acid as compared with our value of 0.00108 at 28° C.

The formation of a greenish-yellow color by the addition of water to mercurous sulphate was observed in these experiments. This has been reported by many previous investigators. According to Gouy [1] the greenish-yellow color is due to the formation of basic mercurous sulphate and according to his analysis this has the composition $Hg_2OHg_2SO_4H_2O$. Hulett [4] reported that his analysis of the completely hydrolyzed material confirmed the composition reported by Gouy, but that his product was grayish white rather than yellow.

TABLE 3.—*Solubility, 28° C, of mercurous sulphate added to water*

Experiment	Molarity of H_2SO_4 [a]		Weight of Hg per 100 ml	Deviation
	Method *A*	Method *B*		
			Gram	*Gram*
1*D*	0.00110		0.0503	+0.0001
2*D*	.00106	0.00106	.0509	+.0007
1′*D*	.00104		.0512	+.0010
2′*D*	.00109	.00111	.0506	+.0004
Average of "downs"	.00107	.00108	.0507	
1*U*	.00109		.0492	−.0010
2*U*	.00108	.00107	.0500	−.0002
1′*U*	.00111		.0495	−.0007
2′*U*	.00110	.00110	.0501	−.0001
Average of "ups"	.00109	.00109	.0497	
Average of all determinations	.00108	.00108	.0502	±.0005

[a] Molarity of acid after saturation with mercurous sulphate.

TABLE 4.—*Solubility, 0° C, of mercurous sulphate added to water*

Experiment	Molarity [1] H_2SO_4	Weight of Hg per 100 ml	Deviation
		Gram	*Gram*
1*D*	0.00102	0.0348	−0.0004
2*D*	.00103	.0342	−.0010
1′*D*	.00094	.0360	+.0008
2′*D*	.00098	.0344	−.0008
1″*D*	.00099	.0357	+.0005
Average of "downs"	.00099	.0350	
1*U*	.00099	.0360	+.0008
2*U*	.00099	.0352	.0000
1′*U*	.00092	.0353	+.0001
2′*U*	.00100	.0350	−.0002
1″*U*	.00096	.0362	+.0010
2″*U*	.00102	.0347	−.0005
Average of "ups"	.00098	.0354	
Average of all determinations	.00099	.0352	±.0006

[1] Molarity of acid after saturation with mercurous sulphate.

Other experimenters have reported the hydrolyzed salt to be yellow or yellowish green. In our own experiments we have found that various samples of mercurous sulphates, including white and gray modifications, all become greenish yellow when treated with successive portions of water. The greenish yellow color appears to be characteristic of the hydrolyzed mercurous salt and distinguishes it from hydrolyzed mercuric sulphate, which is bright yellow. There is, however, some variation in color of partially hydrolyzed mercurous salt dependent on the source of the sample and the extent of the treatment. Our own observations are in accord with those of Gouy.

After many washings the hydrolyzed salt becomes finer and the free mercury initially present in a very finely divided state in gray samples is released and coalesces into a relatively large single drop. The yellowish coloration of hydrolyzed mercurous sulphate cannot be regarded as sufficient evidence of the presence of mercuric salt.

When base was added to hydrolyzed mercury sulphates, further color changes were noted as a result of the formation of oxides. Hydrolyzed mercurous sulphate became a dirty brown or black, while mercuric sulphate became an orange color, due perhaps to a mixture of the red and yellow modifications of mercuric oxide.

IV. SOLUBILITY OF MERCUROUS SULPHATE AT REGULAR INTERVALS OF SULPHURIC-ACID CONCENTRATION

Since the experimental determinations reported in tables 1 and 2 were made at acid concentrations which have no simple relation to each other, all of the data were plotted and the solubility read from the curves at regular intervals. To avoid errors which might result from drawing a single curve, three separate plots on large scales in several sections were made, using the molarity of the acid concentration, the square root of the molarity and the logarithm of the molarity as abscissas. The average solubility was then calculated from the readings made of these three plots. These are considered the best data and they are given in table 5. No value is given for 0.001 molar solution at 28° C because of the formation of the basic salt at 0.00108 molar acid.

TABLE 5.—*Solubility of mercurous sulphate in solutions of sulphuric acid*

H_2SO_4 Molarity at t° C	Weight of Hg per 100 ml		H_2SO_4 Molarity at t° C	Weight of Hg per 100 ml	
	t=28° C	t=0° C		t=28° C	t=0° C
	Gram	*Gram*		*Gram*	*Gram*
0.001	----------	0.0351	0.100	0.0344	0.0183
.002	0.0463	.0290	.200	.0379	.0198
.003	.0424	.0259	.300	.0403	.0212
.004	.0395	.0239	.400	.0423	.0224
.005	.0373	.0224	.500	.0438	.0233
.006	.0360	.0215	.600	.0451	.0239
.007	.0351	.0208	.700	.0461	.0244
.008	.0346	.0203	.800	.0467	.0247
.009	.0341	.0200	.900	.0470	.0248
.010	.0338	.0197	1.000	.0470	.0249
.020	.0318	.0182	1.500	.0452	.0240
.030	.0313	.0179	2.000	.0409	.0216
.040	.0317	.0178	2.500	.0354	.0179
.050	.0322	.0178	3.000	.0294	.0139
.060	.0327	.0178	3.500	.0238	.0105
.070	.0332	.0179	4.000	----------	.0078
.080	.0337	.0180	----------	----------	----------
.090	.0341	.0181	----------	----------	----------

The smoothed values were then plotted against the logarithms of the respective molarities to obtain the curves shown in figure 1. The individual points, which were plotted for the purpose of drawing these curves are not shown in the figure, but we have plotted the actual experimental determinations to show their deviations from the smoothed data. These deviations afford a means of estimating the accuracy of individual determinations. For each point the deviation in grams from the smoothed curve has been read and tabulated in tables 1 and 2. The average deviations are about 0.0002 g at 28° C and at 0° C. The percentage deviations, however, are larger at 0° C

because the total amount of mercury involved in each of these determinations is smaller than for corresponding determinations at 28° C.

V. DISCUSSION OF RESULTS

The data given in table 5 and in figure 1 show definite maxima and minima for the solubility. Each curve for a specified temperature shows that three different solutions with the same mercury content are possible. At 28° C the curve passes through a maximum at 1

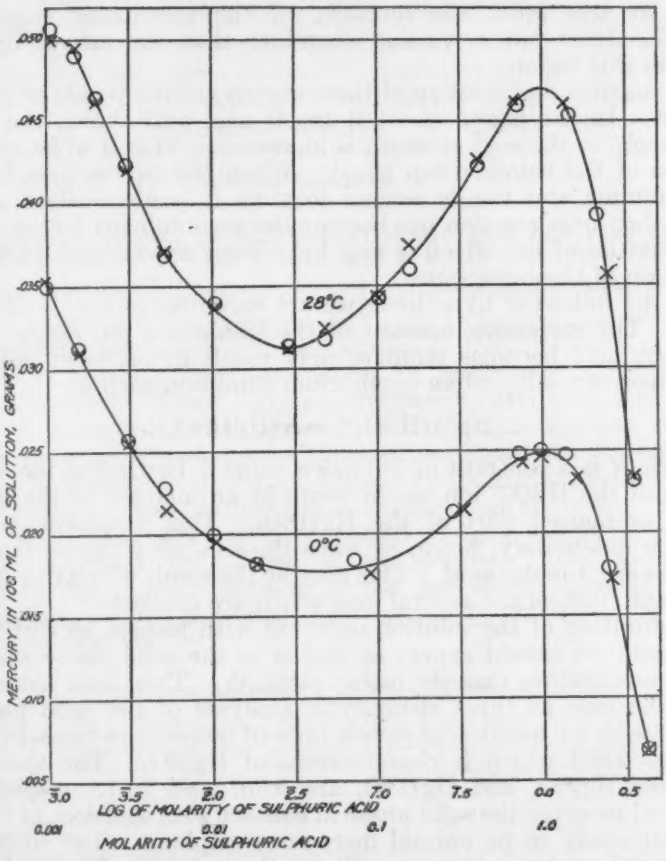

FIGURE 1.—*Solubility of mercurous sulphate in sulphuric acid solutions.*

Circles represent equilibrium approached from supersaturated solutions and crosses from undersaturated solutions.

molar acid and a minimum at 0.03 molar acid. The 0° C curve also shows a maximum at 1 molar acid and a minimum at 0.04 molar acid.

A noteworthy difference between the curves for 28° C and 0° C occurs in the region of the most dilute acid solutions. It is in this region that the molarity of the mercurous sulphate is approximately equal to the molarity of the acid. Below 0.0015 molar acid (log $\bar{3}$.176) a marked change in slope of the curve at 28° C occurs. The

solubility at 0.00108 molar acid (log $\bar{3}.033$) is much less than would be predicted by an extrapolation of other portions of the curve. At the acid molarity of 0.00108, the molarity of Hg_2SO_4 is 0.00125; that is, the molarity of the mercury salt exceeds that of the acid. It is in this region that the maximum buffer action of any dissolved hydrolyzed mercurous salt would be expected.

A different condition exists in the measurements at 0° C. There is no point on this curve where the molarity of the mercurous sulphate equals the molarity of the acid. The hydrolysis point has shifted toward the weaker acid concentrations and lies below 0.001 molar acid. At this point the molarity of the mercurous sulphate is 0.00087. It is not surprising therefore that the curves differ in shape in this region.

The maxima and minima of these curves are the points of greatest interest. In the region of 0.001 molar acid and above, the curves fall steeply as the acid strength is increased. This is to be expected because of the common ion effect. When the curves pass through their minima and rise to second maxima it is obviously true that some other ionic reaction has become the predominant factor. Until the activities of the effective ions have been determined no one can be certain of these reactions.

For the following hypothesis we are indebted to Dr. D. A. MacInnes. The increasing amount of the bisulphate ion HSO_4^- as the sulphuric acid becomes stronger may result in increased solubility of the mercury salt and an equilibrium condition such as

$$(Hg^+)(HSO_4^-) = K(HgHSO_4),$$

in which K is a constant of unknown value. Increasing the concentration of the HSO_4^- ion would result in an increase in the solution of the un-ionized part of the $HgHSO_4$. This condition does not continue indefinitely, however, since the solubility curves fall again after passing 1 molar acid. This may be the result of relative changes in the activities of the several ions which are present.

If saturation of the solution occurred with respect to $HgHSO_4$ at molar acid we should expect to find it in the solid phase when the acid concentration exceeds molar strength. This does not appear to be the case as three electrolytic analyses of the solid phase in contact with 3.1 molar acid gave a ratio of mercury to the solid phase equal to 0.804 which is characteristic of Hg_2SO_4. The theoretical ratios for Hg_2SO_4 and $HgHSO_4$ are 0.807 and 0.673, respectively. Hulett [4] reported the solid phase in contact with solutions of 1 molar acid and above to be normal mercurous sulphate. The controlling ion beyond molar acid may still be the sulphate, SO_4^{--}. Hulett, however, considers the solid phase in contact with solutions below 1 molar acid to be a mixture of the normal and basic salts. This is not in accord with our observations. Our electrolytic determinations of the ratio of mercury to sulphate in portions of the solid phase removed from contact with the dilute acid solutions, where the tendency to hydrolyze should be greater, gave the results reported in table 6. These results indicate that the solid phase is not a mixture of the two salts, but Hg_2SO_4 alone. Equilibrium conditions would not preclude the possibility of hydrolyzed salt in solution when the acid concentration is above 0.001 molar, but our results indicate that the

hydrolyzed salt can not be present in sufficient amount to cause a change in the solid phase.

Small portions of the solid phase were removed from typical solutions covering acidities from the lowest to the highest concentration. The crystal form of these samples was examined microscopically by Dr. C. P. Saylor, who reported all were of the same crystalline modification.

TABLE 6

Molarity of acid, H_2SO_4	Ratio Hg to SO_4
0.0013	4.15
0.002	4.19
0.0025	4.12
0.003	4.18
Theoretical ratio for Hg_2SO_4	4.18
Theoretical ratio for $Hg_3O_2SO_4H_2O$	8.36
Theoretical ratio for $HgHSO_4$	2.09

VI. COMPARISON WITH PREVIOUS DETERMINATIONS

Hulett's [4] determinations at 25° C. and the present results at 28° C differ so little as to temperature that we have reduced our solubilities by 3/28 of the respective differences between measurements at 28° C. and at 0° C. Such a procedure cannot be justified for large temperature differences. Table 7 gives a comparison of Hulett's results at 25° C. with our results calculated to 25° C. One figure in Hulett's original table, 0.0424, has been changed to 0.0434, as the former is apparently a numerical error. The latter figure, 0.0434, was calculated from his basic data given in column 2 of his table. Table 7 shows agreement between his results and ours within 1 percent, although materials from different sources were used, different methods of determining mercury were employed, and errors of weighing and titrating are included as well as the uncertainty which may be caused by the mercuric ion.

TABLE 7.—*Comparison of results with those of Hulett*

[NBS results were calculated to 25° C from 28° C]

Molarity H_2SO_4	Weight of Hg per 100 ml		Difference NBS—Hulett
	NBS, 25° C	Hulett, 25° C	
	Gram	*Gram*	*Gram*
0.004	0.0378	0.0376	+0.0002
0.010	.0323	.0321	+.0002
0.020	.0303	.0305	−.0002
0.050	.0307	.0307	.0000
0.100	.0327	.0325	+.0002
0.200	.0360	.0352	+.0008
0.250	.0371	.0365	+.0006
0.333	.0389	.0392	−.0003
0.500	.0416	.0416	.0000
1.000	.0446	.0442	+.0004
1.333	.0439	.0434	+.0005
2.000	.0388	.0386	+.0002
Average			±.0003

Summers and Gardner [11] measured the solubility of mercurous sulphate at 100° C, and compared it with other measurements at 25° C. There is an apparent error in the position of their decimal point, however, which makes the scale of ordinates of their figure 1 ten times too much for their 25° C curve. The scale evidently should be 1.0, 2.0, ... etc. To make a comparison of their measurements with ours it is necessary to convert the molalities given by them to molarities, which is the method we have used for expressing the concentration of acid. Because of the large temperature difference between their work and ours, no simple assumption about the effect of temperature on solubility is warranted. It is evident that the effect of temperature on solubility of mercurous sulphate does not follow a linear relationship.

Drucker's [12] measurements are often quoted and are the basis of values reported in the International Critical Tables [6]. Here, again there is some uncertainty. Drucker reports his acid concentrations as normalities, but the solubilities of Hg_2SO_4 as molarities. Drucker's figures are copied in the Critical Tables, but the concentration of the mercury salt is given in terms of normality instead of molarity, which makes the values reported there one-half as large as Drucker originally reported them. Drucker's determinations of the solubility of mercurous sulphate in water and in 0.1 molar acid agree very closely with our results, but his two other determinations differ by several milligrams.

No comparison with Smith's [7] results can be made since the temperature of his determinations is not known.

A few other determinations have appeared in the literature including those of Wright and Thompson [13], Traube [14], Gouy [1], Wilsmore [15], Cox [2], and Barre [16].

These determinations cover a very limited range. In some cases essential details, such as temperature or methods, are not adequately described. We have not attempted to compare our results with theirs. Of the earlier determinations only Hulett's measurements fulfill all the requirements which we believe are essential.

VII. REFERENCES

[1] Gouy, Compt. Rend. **130,** 1399 (1900).
[2] Cox, Z. anorg. Chem. **40,** 178 (1904).
[3] Hager and Hulett, J. Phys. Chem. **36,** 2095 (1932).
[4] Hulett, Trans. Int. Elec. Cong., St. Louis, **2,** 109 (1904); Trans. Am. Electrochem. Soc. **6,** 109 (1904).
[5] Drucker, Z. anorg. Chem. **28,** 361 (1901).
[6] Int. Crit. Tables **4,** 339 (1928).
[7] Smith, Glazebrook's Dictionary Applied Physics **2,** 267 (1922).
[8] Hulett, Phys. Rev. **33,** 307 (1911).
[9] Wolff and Waters, Bul. BS 4, 18 (1907) S70.
[10] Ind. Eng. Chem. **17,** 756 (1925).
[11] Summers and Gardner, Trans. Am. Electrochem. Soc. **56,** 144 (1929).
[12] Drucker, Z. anorg. Chem. **28,** 362 (1901).
[13] Wright and Thompson, Phil. Mag. **17,** 288 (1884); **19,** 1 (1885).
[14] Traube, Z. anorg. Chem. **8,** 22 (1895).
[15] Wilsmore, Z. Phys. Chem. **35,** 305 (1900).
[16] Barre, Ann. chim. phys. **24,** 203 (1911).

WASHINGTON, August 28, 1936.

U. S. Department of Commerce National Bureau of Standards

RESEARCH PAPER RP940

Part of Journal of Research of the National Bureau of Standards, Volume 17, November 1936

EBULLIOMETRIC AND TONOMETRIC STUDY OF NORMAL ALIPHATIC ALCOHOLS

By Mieczysław Wojciechowski [1]

ABSTRACT

The following normal aliphatic alcohols: methanol, ethanol, *n*-propanol, *n*-butanol, and *n*-amyl alcohol, were prepared in a state of high purity. By the use of Świętoslawski's ebulliometric technique, and the comparative method of measurements using water as a reference liquid, their normal boiling points and coefficients of increase of boiling point with increase of pressure, $\frac{dt}{dp}$, expressed in degrees centigrade per millimeter of mercury, were determined. The following numerical data were obtained: methanol—boiling point 64.509° C; $\frac{dt}{dp}=0.0331$; ethanol—boiling point, 78.325° C; $\frac{dt}{dp}=0.0334$; *n*-propanol—boiling point 97.209; $\frac{dt}{dp}=0.0344$; *n*-butanol—boiling point, 117.726; $\frac{dt}{dp}=0.0372$; *n*-amyl alcohol—boiling point, 138.06; $\frac{dt}{dp}=0.0402$. Beginning with *n*-propanol, the introduction of a CH_2 group into the chain of a normal aliphatic alcohol molecule has a specific effect, increasing $\frac{dt}{dp}$ by a constant value of 0.0029—the same amount as in the case of aliphatic hydrocarbons.

The ebulliometric control of purity of the preparations, the use of substances of extreme purity, and the application of the method of comparative measurements ensure the accuracy of the results reported.

CONTENTS

	Page
I. Introduction	721
II. Method of measurements	722
III. Purification of substances	722
1. Methanol	722
2. Ethanol	722
3. *n*-Propanol	723
4. *n*-Butanol	723
5. *n*-Amyl alcohol	723
IV. Experimental results	723
V. Conclusions	725
VI. References	726

I. INTRODUCTION

In a previous paper [1][2], it was shown that in the homologous series of normal saturated hydrocarbons from *n*-pentane to *n*-octane, inclusive, the coefficient of increase of boiling point with pressure,

[1] Guest Worker, from the Polytechnic Institute, Warsaw, Poland.

[2] The figures in brackets throughout this paper refer to the numbered references listed at the end of the paper.

$\frac{dt}{dp}$, is a linear function of the molecular weight, and the introduction of a CH_2 group into the chain of the molecule has a specific effect, increasing this coefficient by 0.0029 degree centigrade per millimeter of mercury. In this paper a similar investigation of the relationship between the molecular weights of normal aliphatic alcohols and their respective values of the coefficient $\frac{dt}{dp}$ is described. In addition, there are reported the normal boiling points of the following alcohols: methanol, ethanol, *n*-propanol, *n*-butanol, and *n*-amyl alcohol.

II. METHOD OF MEASUREMENTS

Świętosławski's ebulliometric technic [2] and his comparative method of measurements [3] with water as a reference liquid, briefly described in the paper on hydrocarbons, were employed for the determination of boiling points and the coefficient $\frac{dt}{dp}$.

The sensitive ebulliometric test of purity [4] of substances and the use of preparations of high purity ensure the accuracy of the values reported.

The boiling points were measured with a platinum-resistance thermometer having a coiled filament and potential terminals [5], kindly furnished by C. H. Meyers.

The normal boiling points were calculated by the use of the formula [1]:

$$t_s = t_s' + \frac{dt_s}{dt_w}(100 - t_w'),$$

where t_s represents the normal boiling point of the substance under investigation; t_s' the boiling point actually measured; t_w' the boiling point of water actually measured under the same pressure as that of the substance; and $\frac{dt_s}{dt_w}$ the ratio of the coefficients $\frac{dt}{dp}$.

III. PURIFICATION OF SUBSTANCES

1. METHANOL

Two liters of the best available commercial methanol of reagent grade was distilled in a 40-bulb Świętosławski improved distilling column [6], and three middle fractions of 200 ml each, which distilled in the limits of 0.001° C, were used for the measurements. These preparations were found to have a difference of 0.001 and 0.002° C. between the boiling point and condensation temperature in the differential ebulliometer of standardized dimensions, and were accordingly of the highest degree of purity on Świętosławski's scale for characterizing the purity of liquid substances and of azeotropic mixtures.

2. ETHANOL

The best commercial absolute alcohol was dehydrated and purified by azeotropic distillation from an efficient column, using benzene as an azeotropic agent. Two fractions of the middle part of the dis-

tillate, which distilled at constant temperature, were used for the determination of boiling point and $\frac{dt}{dp}$ ratio. Preparations thus obtained were of the fifth (highest) degree of purity on Świętosławski's scale, having a Δt, difference between boiling point and condensation temperature, equal to 0.001° C.

3. *n*-PROPANOL

n-Propanol was purified by azeotropic distillation, using benzene as an azeotropic agent. The middle fraction was of the fourth degree of purity, having Δt=0.006° C. Another azeotropic distillation of a commercial preparation of *n*-propanol also resulted in a product of the fourth degree of purity, having Δt=0.014° C.

4. *n*-BUTANOL

By a simple distillation of a commercial preparation in the 40-bulb column, two preparations of the highest purity, having Δt=0.001 and 0.003° C, were obtained.

5. *n*-AMYL ALCOHOL

Commercial *n*-amyl alcohol was distilled in the 40-bulb column. The samples thus obtained were of the fourth and third degree of purity, having Δt equal to 0.020 and 0.024° C.

IV. EXPERIMENTAL RESULTS

The data obtained in the present work for the boiling points of five normal aliphatic alcohols are given in table 1.

To calculate the boiling points of the substances that were not of the fifth degree of purity on Świętosławski's scale, a method of extrapolation [7] previously reported, was used.

Table 2 contains a comparison of the author's data for boiling point and the coefficient, $\frac{dt}{dp}$, of the alcohols investigated, with those previously reported.

TABLE 1.—*Normal boiling point data for five normal aliphatic alcohols*

Substance	Preparation number	t	Degree of purity	Normal boiling point	Normal boiling point extrapolated
		°C		°C	°C
Methanol	1	0.002	V	64.508	64.50
	2	.001	V	64.509	
	3	.001	V	64.509	
Ethanol	1	.001	V	78.325	78.32
	2	.001	V	78.325	
n-Propanol	1	.006	IV	97.186	97.20
		.014	IV	97.149	
n-Butanol	1	.001	V	117.726	117.72
	2	.003	V	117.719	
n-Amyl alcohol	1	.020	IV	137.953	138.0
	2	.025	III	137.924	

TABLE 2.—*Comparison of determinations obtained by various observers*

Substance	Author	Boiling point	$\left(\frac{dt}{dp}\right)_{p=760}$
		°C	°C/mm Hg
Methanol	G. C. Schmidt [8]	66.9	0.0350
	A. Doroszewski [41]	64.53	
	A. Doroszewski and J. Poljanski [16]	64.57	
	J. Timmermans and Hennaut-Roland [9]	64.65	.035
	J. A. V. Butler, D. W. Thomson, and W. H. MacLennan [10].	64.46	
	M. Wojciechowski	64.500	.0331
Ethanol	D. Mendelejew [11]	78.303	
	W. Ramsay and S. Young [12]	78.30	
	G. C. Schmidt [8]	78.3	.0342
	W. Ramsay and J. Shields [13]	78.3	.0334
	E. Beckmann and P. Fuchs [14]	78.6	.0346
	W. A. Noyes and R. R. Warfel [15]	78.33	
	A. Doroszewski and J. Poljanski [16]	78.35	
	J. Wade and R. M. Merriman [17]	78.39	
	T. W. Richards and L. B. Coombs [18]	78.42	
	R. F. Brunel, J. L. Crenshaw, and E. Tobin [19].	78.30	
	W. Pratolongo [20]	78.30	
	W. Świętosławski, A. Zmaczynski, and J. Usakiewicz [21].	78.318 to 78.320	
	L. Harris [22]	78.37	
	M. Wojciechowski	78.325	.0334
n-Propanol	W. Brühl [23]	97.3 to 97.5	
	W. H. Perkin [24]	98.0	
	W. Ramsay and S. Young [25]	97.4	
	G. C. Schmidt [8]	96.9	.0350
	H. Landolt and H. Jahn [26]	96.1	
	E. Beckmann and P. Fuchs [14]	95.7	.0358
	E. H. Loomis [27]	97.2	
	S. Young and E. C. Fortley [28]	97.19	
	J. Holmes and P. J. Lagemann [29]	97.2 to 97.4	
	A. Doroszewski and T. Rozdestwienski [30]	97.26	
	R. F. Brunel, J. L. Crenshaw, and E. Tobin [19].	97.19	
	V. C. G. Trew and G. M. C. Watkins [31]	96.6 (p=744)	
	J. A. V. Butler, D. W. Thomson, and N. H. MacLennan [10].	97.19±0.02	
	J. Timmermans and Y. Delcourt [32]	97.15	.38 (10 mm of Hg)
	M. Wojciechowski	97.209	.0344
n-Butanol	G. W. A. Kahlbaum [33]	117.6	.0350
	A. Doroszewski and Z. Dworzanczyk [34]	117.1	
	R. F. Brunel, J. L. Crenshaw, and E. Tobin [19].	117.1	
	J. Timmermans and F. Martin [35]	118.0	.037
	C. P. Smyth and W. S. Walls [36]	117.2 to 117.4	
	V. C. G. Trew and G. M C. Watkins [31]	117.25	
	R. C. Ernst, E. E. Litkenhous, and J. W. Spanger [37].	117.69	
	J. A. V. Butler, D. W. Thomson, and W. H. MacLennan [10].	117.71	
	T. J. Webb and C. H. Lindsley [38]	118.0	
	M. Wojciechowski	117.726	.0372
n-Amyl alcohol	G. Lievens [39]	137.95	.037
	T. Timmermans and Hennaut-Roland [40]	138.25	
	J. A. V. Butler, D. W. Thomson, and W. H. MacLennan [10].	137.60 to 177.70	
	M. Wojciechowski	138.06	.0402

In table 3 are given the values of $\frac{dt}{dp}$ for the alcohols investigated, and the ratios, $\frac{dt_s}{dt_w}$, of these coefficients to that of water.

TABLE 3.—*Data for* $\frac{dt}{dp}$ *for five normal aliphatic alcohols*

Substance	$\frac{dt_s}{dt_w}$	Boiling point of water	$\left(\frac{dt}{dp}\right)_{p=760}$	Difference between coefficients $\frac{dt}{dp}$
		°C	°C/mm Hg	
Methanol	0.8909	100.175	0.0331	
	.9073	97.634		0.0003
Ethanol	.9030	100.881	.0334	
	.9035	98.157		.0010
n-Propanol	.9231	101.043	.0344	
	.9431	98.036		.0028
n-Butanol	1.0039	100.690	.0372	
	1.0058	97.201		.0030
n-Amyl alcohol	1.0887	101.086	.0402	
	1.0840			

V. CONCLUSIONS

The values of the coefficients $\frac{dt}{dp}$ of *n*-amyl alcohol and *n*-propanol are probably slightly affected by impurities in the preparations used in the measurements, but not enough to obscure the specific effect of each CH_2 group introduced into the chain of the alcohol molecule.

From table 3 it is obvious that the increase of $\frac{dt}{dp}$ is not constant up to *n*-propanol. Beginning with *n*-propanol the introduction of each CH_2 group into the chain of the molecule of a normal aliphatic alcohol is accompanied by the same increment in $\frac{dt}{dp}$. The average increment for the alcohols is 0.0029° C. per millimeter of mercury, exactly the same as in the case of the normal aliphatic hydrocarbons. The irregularities observed in the case of alcohols up to *n*-propanol are probably caused by the high degree of association of the molecules of these compounds.

The data previously reported on the normal aliphatic hydrocarbons, together with the data presented in this paper, suggest the following generalization: In any organic molecule containing a normal alkyl group of more than some small number n of carbon atoms, the addition of a CH_2 group to the normal alkyl group to form the next higher normal alkyl group results in an increase of 0.0029° C. per millimeter of mercury in the coefficient $\frac{dt}{dp}$ at the normal boiling point. The data reported in this paper indicate that for the normal aliphatic alcohols $n=2$, while the data reported in the paper [1] on the normal aliphatic hydrocarbons indicate that for these compounds n is not greater than 4. It is possible that $\frac{dt}{dp}$ may be an additive property,

the value of which may be calculated by taking the sum of the values corresponding to all atoms in the molecule of a given compound. Further work is in progress to determine whether this generalization is applicable to other series of compounds.

The author tenders his thanks to H. Matheson for his assistance in purifying some of the substances. He also expresses his gratitude to Polish Fundusz Kultury Narodowej w Warszawie (Polish Fund of National Culture in Warsaw) for financial aid.

VI. REFERENCES

[1] M. Wojciechowski, J. Research NBS **17,** 453, —, — (1936) RP921.
[2] W. Świętosławski, Ebuljometrja, Warszawa (1935) Ebulliometry 1936, Kara im. Miauswskiego, Jagielloniau University Press, Krakow.
[3] W. Świętosławski, J. chim. phys. **27,** 496 (1930); Roczniki Chem. **9,** 266 (1929).
[4] W. Świętosławski, IX Congreso Int. Quim. Pura Aplicada, Madrid, **2,** 13, (1934).
[5] C. H. Meyers, BS, J. Research **9,** 807 (1932) RP508.
[6] W. Świętosławski, J. chim. phys. **27,** 329 (1930). Bul. Soc. Chim. France **4,** 49, 1563 (1931).
[7] M. Wojiechowski and E. R. Smith, Nature, **138,** 30 (1936).
[8] G. C. Schmidt, Z. phys. Chem. **8,** 628 (1891).
[9] J. Timmermans and Hennaut-Roland, J. Phys. Chem. **27,** 401 (1930).
[10] J. A. V. Butler, D. W. Thomson, and W. H. MacLenan, J. Chem. Soc. 674 (1933).
[11] D. Mendelejew, Z. Chem. 257 (1865).
[12] W. Ramsay and S. Young, J. Chem. Soc. **47,** 654 (1885).
[13] W. Ramsay and J. Shields, Z. phys. Chem. **12,** 461 (1893).
[14] E. Beckmann and P. Fuchs, Z. phys. Chem. **18,** 495 (1895).
[15] W. A. Noyes and R. R. Warfel, J. Am. Chem. Soc. **23,** 465 (1901).
[16] A. Doroszewski and J. Poljanski, Z. phys. Chem. **73,** 192 (1910).
[17] J. Wade and R. M. Merriman, J. Chem. Soc. **97,** 1002 (1911).
[18] T. W. Richards, and L. B. Coombs, J. Am. Chem. Soc. **37,** 1667.(1915)
[19] R. F. Brunel, J. L. Crenshaw and E. Tobin, J. Am. Chem. Soc. **43,** 561 (1921)
[20] U. Pratolongo, Atti. Accad. Lincei **30,** II, 419.
[21] W. Swiętoslawski, A. Zmaczynski and J. Usakiewicz, Compt. rend. **194,** 357 (1932).
[22] L. Harris, J. Am. Chem. Soc. **55,** 1942 (1933).
[23] W. Brühl, Liebigs Ann. Chem. **200,** 173 (1879).
[24] W. H. Perkin, J. Chem. Soc. **45,** 466 (1884).
[25] W. Ramsay and S. Young, Phil. Trans. **180,** 140 (1889).
[26] H. Landolt and H. Jahn, Z. phys. Chem. **10,** 288 (1892).
[27] E. H. Loomis, Z. phys. Chem. **32,** 594 (1900).
[28] S. Young and E. C. Fortey, J. Chem. Soc. **81,** 725 (1902).
[29] T. Holmes and P. J. Lagemann, J. Chem. Soc. **95,** 1936 (1909).
[30] Z. Doroszewski and J. Rozdestwienski, J. Russ. Phys. Chem. Soc. **40,** 1428.
[31] V. C. G. Trew and G. M. C. Watkins, Trans. Faraday Soc. **29,** 1310 (1933).
[32] J. Timmermans and Y. Delcourt, J. chim. phys. **31,** 85 (1934).
[33] G. W. A. Kahlbaum. Z. phys. Chem. **26,** 577 (1898).
[34] A. Doroszewski and Z. Dworzanczyk, J. Russ. Phys. Chem. Soc. **40,** 887.
[35] J. Timmermans and F. Martin, J. chim. phys. **25,** 411 (1928).
[36] C. P. Smyth and W. S. Walls, J. Am. Chem. Soc. **53,** 2117 (1931).
[37] R. C. Ernst, E. E. Litkenhous and J. W. Spanger, J. phys. Chem. **36,** 842 (1932).
[38] T. J. Webb and C. H. Lindsley, J. Am. Chem. Soc. **56,** 874 (1934).
[39] G. Lievens, Bul. Soc. chim. Belg. **33,** 122 (1924).
[40] J. Timmermans and Hennaut-Roland, J. chim. phys. **29,** 529 (1932).
[41] A. Doroszewski, J. Russ. phys. chem. Soc. **41,** 962.

WASHINGTON, August 24, 1936.

U. S. DEPARTMENT OF COMMERCE NATIONAL BUREAU OF STANDARDS

RESEARCH PAPER RP941

Part of Journal of Research of the National Bureau of Standards, Volume 17, November 1936

THE SYSTEM LIME—BORIC OXIDE—SILICA

By E. P. Flint* and Lansing S. Wells

ABSTRACT

The equilibrium diagram for the system $CaO–B_2O_3–SiO_2$, constructed from data on 200 ternary compositions, is presented. The portion of the diagram immediately adjacent to the binary system $B_2O_3–SiO_2$ is incomplete. A unique feature of the system is the appearance of an area of liquid immiscibility extending across the diagram from the lime-silica side to the lime-boric oxide side and crossing the fields of silica, monocalcium borate, and calcium diborate. A newly established ternary compound, $5CaO.B_2O_3.SiO_2$, melts congruently at 1,419° C. Tricalcium silicate does not appear at the liquidus in the ternary system. Dicalcium silicate forms partial solid solutions with calcium borates whereby the α-β inversion temperature is lowered by a maximum of 190° C.

CONTENTS

	Page
I. Introduction	727
II. General procedure	729
1. Preparation and analysis of mixtures	729
2. Apparatus and methods	730
III. The stability fields	731
1. $CaO.SiO_2$	731
2. $3CaO.2SiO_2$	733
3. $2CaO.SiO_2$	733
4. CaO	737
5. $5CaO.B_2O_3.SiO_2$	737
6. $3CaO.B_2O_3$	738
7. $2CaO.B_2O_3$	739
8. $CaO.B_2O_3$	741
9. $CaO.2B_2O_3$	742
10. SiO_2	742
IV. The two-liquid area	743
V. Characteristics of the fusion surfaces	745
VI. Crystallization curves intersecting the two-liquid area	748
VII. Applications	749
VIII. Summary	750
IX. References	751

I. INTRODUCTION

The existence of liquid immiscibility in binary systems of boric oxide with oxides of certain of the alkaline earths and other divalent elements was early established in phase equilibrium investigations [1].[1] It was not recognized until much later that liquid immiscibility

* A part of this paper was presented by E. P. Flint to the Graduate School of the University of Maryland, represented by Dr. M. M. Haring, in partial fulfillment of the requirements of the degree of Doctor of Philosophy, June 1936.

[1] Figures in brackets here and elsewhere throughout the text refer to references at the end of this paper.

of a similar type occurs in the corresponding binary systems of silica [2]. The system $CaO–B_2O_3–SiO_2$ is the first ternary system investigated to include both B_2O_3 and SiO_2 as components, and also furnishes the first example of a type of liquid immiscibility in ternary oxide systems wherein the immiscibility region crosses more than one field of primary crystallization.

The system $CaO–B_2O_3–SiO_2$ is a fundamental one in ceramics, for the high silica–boric oxide portion may serve as a starting point for investigations of borosilicate glasses, enamels, and ceramic glazes. The initial motive for the present study was furnished by observations of the effect of small quantities of boric oxide on calcium silicates occurring in portland cement, which apparently indicated the possibility of producing a "well-burned" clinker at a relatively low tem-

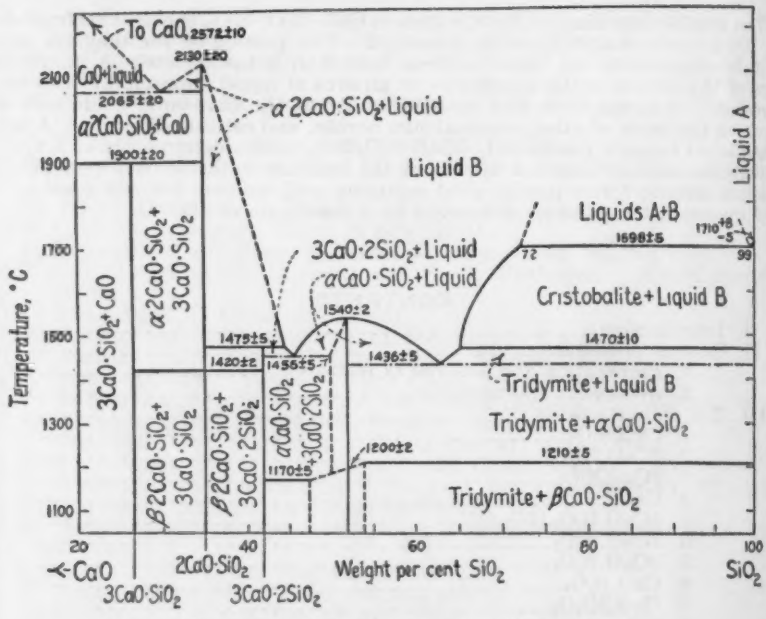

FIGURE 1.—*The binary system* CaO–SiO.

(See literature references [2, 7, 8, 9])
(Reproduced from that given by F. P. Hall and H. Insley, J. Am. Ceram. Soc. 16 p. 492, fig. 37 (1933))

perature. This paper represents the completion of a program first outlined in 1930 and reported on at intervals subsequently [3].

Previous investigations have supplied most of the necessary data on the components and the three binary systems which they form.

The melting point of lime was determined by Kanolt [4] as 2,572° C and by Schumacher [5] as 2,576° C. Taylor and Cole [6] in 1934 reported having prepared crystalline boric oxide and gave its melting point as 294° C. Silica, as cristobalite, melts at 1,713° C [2].

The binary system lime–silica (fig. 1) has been investigated by Day, Shepherd, and Wright [7]; Rankin and Wright [8]; Ferguson and Merwin [9]; and Greig [2].

Phase equilibria in the system lime–boric oxide (fig. 2) were established by Carlson [10].

Only limited information on the system B_2O_3–SiO_2 is available and the course of the liquidus is unknown. Greig [2], and Cousen and Turner [11] have demonstrated the probability that the liquids formed by these oxides are miscible in all proportions. The latter authors found that the thermal expansion and density-composition curves of boric oxide—silica glasses gave no indication of the formation of compounds and concluded that the oxides form only simple solutions.

Morey, and Morey and Ingerson [12] have reported briefly on the melting of danburite, $CaO.B_2O_3.2SiO_2$, the only known naturally occurring calcium borosilicate. This mineral was found to melt with the formation of two ternary liquid layers. Some general characteristics of the immiscibility region of the system

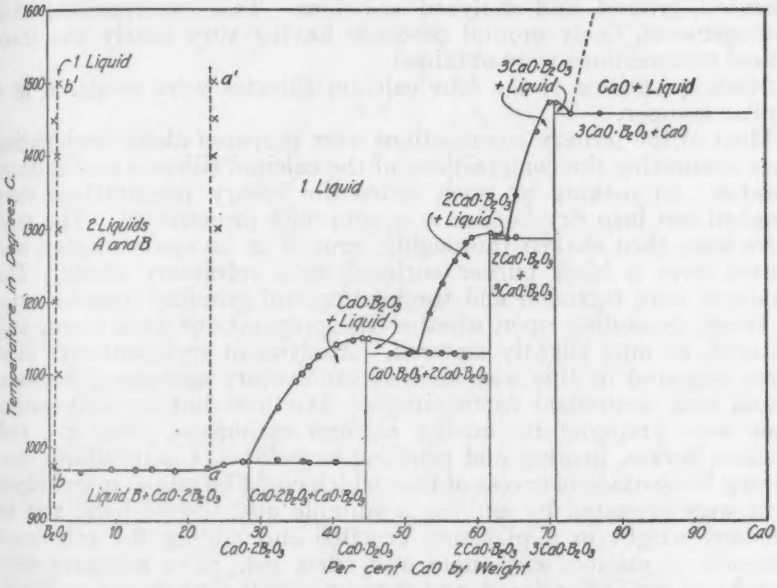

FIGURE 2.—*The binary system* CaO–B_2O_3.

(Reproduced from fig. 2 of reference [0])

CaO–B_2O_3–SiO_2, within which the composition of danburite lies, have also been pointed out by these investigators.

II. GENERAL PROCEDURE

1. PREPARATION AND ANALYSIS OF MIXTURES

Calcium carbonate, boric acid, and silica gel were used as starting materials.

The calcium carbonate was of reagent quality for alkali determinations. Analyses showed 56.06 percent of CaO (theoretical for $CaCO_3$=56.08 percent of CaO). Impurities in the boric acid were reported by the Chemistry Division of the National Bureau of Standards as follows: Fe<0.001 percent; SO_3<0.01 percent; Cl<0.001 percent. The silica gel was a commercial granular product

which was purified by boiling with concentrated nitric acid and subsequently thoroughly washed and dried. Treatment with hydrofluoric and sulfuric acids gave 0.04 percent of nonvolatile material based on the weight of the ignited silica.

Boric acid volatilizes appreciably on heating and boric oxide, though much less volatile, is extremely hygroscopic and difficult to handle. It was, therefore, considered advantageous in preparing the ternary compositions to add boric oxide already combined with lime. For this purpose the four calcium borates were prepared by mixing boric acid in excess with calcium carbonate and fusing or sintering. All heat treatments were made in covered platinum containers. The products were ground in an agate mortar, their ignition losses and lime contents determined, and the latter brought to the theoretical values by the addition of calcium carbonate. They were then reheated, ground, and analyzed as before. This was repeated until homogeneous, finely ground products having very nearly the theoretical compositions were obtained.

Stock quantities of the four calcium silicates were prepared in a similar manner.

Most of the ternary compositions were prepared along conjugation lines connecting the compositions of the calcium silicates and calcium borates. In making up such series the binary preparations were weighed out into dry bottles in appropriate proportions. The mixtures were then shaken thoroughly, ground in an agate mortar, and heated over a blast burner enclosed in a refractory shield. The products were reground and the heating and grinding repeated once or twice, depending upon whether the preparations were fused, well sintered, or only slightly sintered. Analysis of representative mixtures prepared in this way showed satisfactory agreement between actual and theoretical compositions. Mixtures not on conjugation lines were prepared by mixing calcium carbonate, silica gel, and calcium borate, heating and grinding as before. Compositions containing boric oxide in excess of that which could be added in combined form were prepared by igniting a suitable quantity of boric acid to constant weight in a platinum crucible and adding the calculated amounts of calcium carbonate and silica gel. The mixtures were then fused, ground, refused, and reground twice, and finally analyzed.

Analytical determinations were made of ignition loss, silica, and lime; boric oxide was obtained by difference. Half-gram samples were decomposed by 1:1 hydrochloric acid, evaporated almost to dryness and the moist residue evaporated three times with 10-ml portions of methyl alcohol to remove the boric acid. Silica was then determined by double dehydration in the usual way and lime precipitated as calcium oxalate, which was ignited to the oxide and weighed.

2. APPARATUS AND METHODS

The behavior of the ternary preparations on heating or on crystallization from their melts was studied by means of a vertical tube resistance furnace [13] wound with 80-percent platinum—20-percent rhodium wire. Temperatures were measured by platinum—platinum-rhodium thermocouples in conjunction with a precision potentiometer and galvanometer. The single thermocouples used were calibrated frequently against the melting points of potassium sulphate,

1,069.1° C; monocalcium borate, 1,154° C; diopside, 1,391.5° C; and monocalcium silicate, 1,544° C. The differential thermocouple used in heating curves was calibrated against potassium sulphate, 1,069.1° C; dicalcium borate, 1,304° C; and monocalcium silicate, 1,544° C.

The quenching method [14] was used principally for investigation of the ternary mixtures. Phases present in quenched samples were identified with the petrographic microscope. However, for the majority of compositions in the high-lime portion of the diagram this method was not applicable, as crystallization occurred during quenching. The melting behavior of such mixtures was determined by means of heating curves.

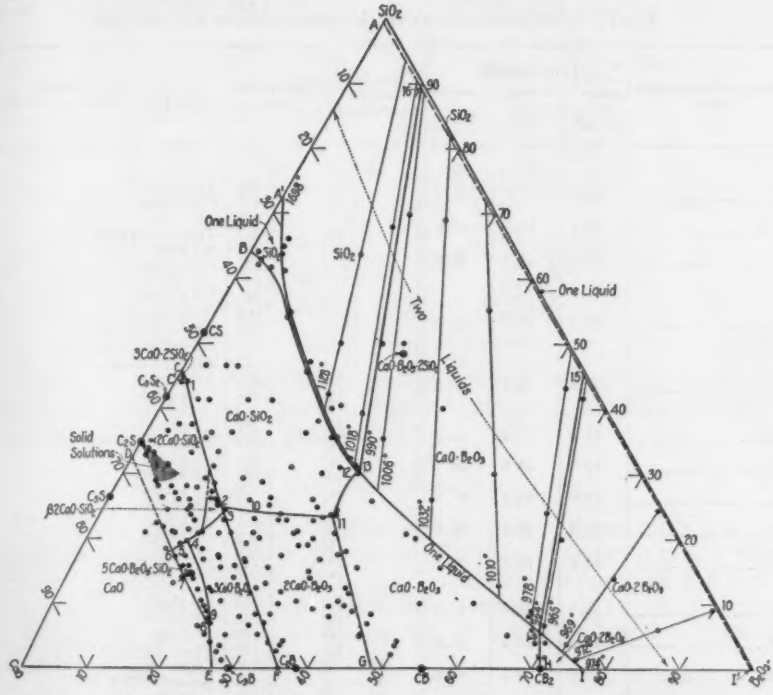

FIGURE 3.—*Triangular concentration diagram of the system* $CaO–B_2O_3–SiO_2$ *giving the compositions investigated and the limits of the stability fields in weight percent.*

III. THE STABILITY FIELDS

1. $CaO.SiO_2$

The compositions determining the area within which monocalcium silicate occurs as a primary phase (B–12–11–10–2–1–C, fig. 3) are listed in table 1. Column 5 gives the length of heat treatment of each charge in the furnace before quenching. The last column shows the results of microscopic examinations on the quenched samples. Formulas of binary and ternary compounds given in this and other tables are abbreviated by designating each component oxide by its first letter, C for CaO; B for B_2O_3; and S for SiO_2. The data in table 1 serve to fix the liquidus temperatures within sufficiently narrow limits and, for some compositions such as no. 4, the temperatures of boundaries and of quintuple points or eutectics.

Crystallization from melts in the monocalcium silicate field occurred readily except in the case of a few compositions located near the monocalcium borate boundary and the lower part of the silica boundary. Charges of these compositions were held overnight to insure attainment of equilibrium.

No marked variation in the indices of α–$CaO.SiO_2$ from the values of the pure compound was observed. The possible existence of solid solutions with calcium borates and their effect on the alpha-beta inversion of monocalcium silicate have not been investigated and therefore no attempt is made in figure 3 to indicate a boundary between the fields of alpha- and beta-monocalcium silicate.

TABLE 1.—*Compositions in the monocalcium silicate field*

Composition number	Composition			Time held before quenching	Temperature	Phases present (C=CaO, B=B_2O_3, S=SiO_2)
	CaO	B_2O_3	SiO_2			
	%	%	%	hr	°C	
1	46.3	7.1	46.6	¼	1,418	All glass.
				¼	1,415	CS+glass.
2	44.4	14.3	41.3	2	1,305	All glass.
				¾	1,301	Trace CS+glass.
3	42.4	21.4	36.2	4	1,177	All glass.
				4	1,170	CS+glass.
4	40.4	28.6	31.0	17	1,043	All glass.
				17	1,041	CS+glass.
				17	998	CS+glass.
				17	993	CS+CB+glass.
				17	978	CS+CB+glass.
				17	976	All crystalline.
5	47.9	5.5	46.6	¼	1,460	All glass.
				¼	1,454	CS+glass.
6	47.6	11.1	41.3	¼	1,372	All glass.
				¼	1,365	Trace CS+glass.
7	47.2	16.6	36.2	¼	1,285	All glass.
				¼	1,283	CS+glass.
8	46.8	22.2	31.0	¼	1,178	All glass.
				¼	1,173	CS+glass.
9	46.4	27.7	25.9	¼	1,095	All glass.
				¼	1,090	CS+glass.
10	46.4	28.8	24.8	¼	1,046	All glass.
				¼	1,039	CS+glass.
11	52.3	11.5	36.2	¼	1,353	All glass.
				¼	1,348	CS+glass.
12	55.0	19.2	25.8	¼	1,198	All glass.
				¼	1,193	Trace CS+glass.
13	50.5	2.9	46.6	h. c.[a]	1,494	Liquidus.
				h. c.	1,119	Eutectic (2).[b]
14	51.7	4.4	41.4	h. c.	1,459	Liquidus.
				h. c.	1,118	Eutectic (2).
15	52.8	5.8	41.4	¼	1,440	All glass.
				¼	1,437	CS+glass.
16	55.0	8.8	36.2	¼	1,326	All glass.
				¼	1,323	CS+glass.
17	57.3	11.7	31.0	¼	1,233	All glass.
				¼	1,230	CS+glass.
18	58.4	13.2	28.4	¼	1,179	All glass.
				¼	1,175	CS+glass.
				¼	1,144	CS+glass.
				¼	1,136	CS+C_2S+glass.
19	56.3	8.3	35.4	¼	1,336	All glass.
				¼	1,334	CS+glass.
20	55.6	11.1	33.3	¼	1,318	All glass.
				¼	1,316	CS+glass.

[a] "h. c." indicates data obtained by heating curves. Under the column headed "phases present" the data given in such cases represent interpretations placed on breaks in heating curves.

[b] Numbers in parentheses in all the tables refer to points or boundaries in figure 3.

TABLE 1.—*Compositions in the monocalcium silicate field*—Continued

Composition number	Composition			Time held before quenching	Temperature	Phases present (C=CaO, B=B_2O_3, S=SiO_2)
	CaO	B_2O_3	SiO_2			
	%	%	%	hr	°C	
21	54.2	16.6	29.2	¼	1,258	All glass.
				¼	1,256	CS+glass.
22	52.8	22.2	25.0	¼	1,148	All glass.
				¼	1,145	CS+glass.
23	46.3	28.7	25.0	¾	1,058	All glass.
				1	1,055	CS+glass.
24	43.2	26.8	30.0	½	1,087	All glass.
				1	1,079	Trace CS+glass.
25	36.0	2.0	62.0	¼	1,413	All glass.
				¼	1,406	CS+glass.
26	36.0	10.0	54.0	¾	1,278	All glass.
				½	1,271	CS+SiO_2+glass.
27	37.6	16.8	45.6	17	1,191	All glass.
				½	1,183	CS+glass.
28	39.7	22.2	38.1	17	1,112	All glass.
				17	1,108	CS+glass.
29	39.2	25.2	35.6	17	1,067	All glass.
				17	1,062	CS+glass.
30	54.4	1.5	44.1	¼	1,450	All glass.
				¼	1,448	CS+glass.
				½	1,435	CS+trace C_2S+glass.
31	52.0	19.4	28.6	¼	1,207	All glass.
				¼	1,204	CS+glass.
32	52.0	21.8	26.2	¼	1,164	All glass.
				¼	1,162	CS+glass.
33	45.2	31.2	23.6	17	1,028	All glass.
				17	1,020	CS+glass.

Figure 4I shows the binary system $CaO.SiO_2$–$2CaO.B_2O_3$, and figures 4J and 4K, the pseudobinary systems $CaO.SiO_2$–$CaO._2B_2O_3$ and $CaO.SiO_2$–$CaO.B_2O_3$, respectively.

2. $3CaO.2SiO_2$

Tricalcium disilicate crystallizes as a primary phase within a very restricted area (C–1–C′, fig. 3), being obtained only from melts which contain less than 2 percent of B_2O_3. Quenches on composition no. 34 in this field (54.5 percent of CaO, 0.6 percent of B_2O_3, 44.9 percent of SiO_2) gave a liquidus temperature of 1,457° C and a C_3S_2–CS boundary temperature of 1,453° C.

3. $2CaO.SiO_2$

Dicalcium silicate forms solid solutions with the calcium borates and the partial limits of these solutions are indicated by the shaded area in figure 3. The compositions prepared in the dicalcium silicate field (C′–1–2–3–4–5–6–D, fig. 3) are given in table 2.

Compositions 41, 42, 46, 47, 48, 49, 50, 51, 52, 54, 55, 56, 57, 60, 61, 62, and 63 show the effect of solid solution on the alpha-beta inversion of dicalcium silicate, which normally occurs at 1,420° C, as is shown in figure 5. Lowering of this temperature by a maximum of 190° C was observed. If this lowering is assumed to be due entirely to solid solution of the calcium borates, no further change in the inversion temperature should occur when a saturated solid solution is formed. Furthermore, heating curves on compositions containing less than the saturation amount of solid solution should exhibit no eutectic or boundary breaks. This was found to be the

case for mixtures containing less than approximately 15 percent of added monocalcium borate, 20 percent of added dicalcium borate, and 35 percent of added pentacalcium borosilicate, and solid solution is therefore placed at these limits. It is of interest that these percentages represent approximately the same mole fractions of the

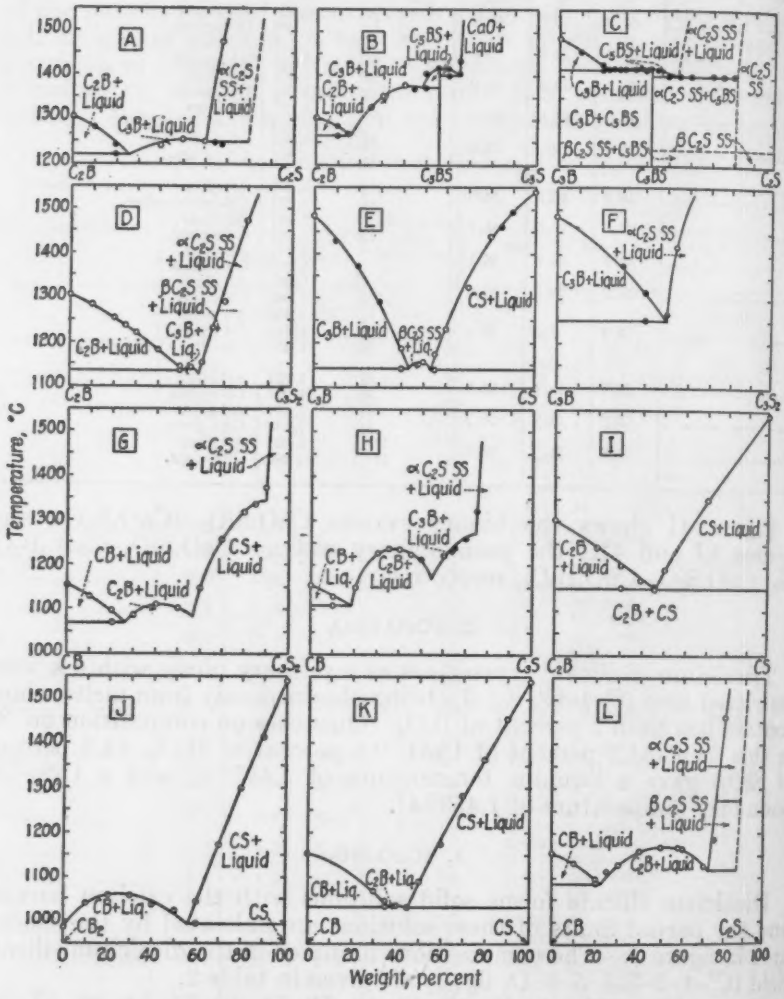

FIGURE 4.—*Binary and pseudobinary systems investigated in the system* $CaO–B_2O_3–SiO_2$.

(*SS*=solid solution.)

respective compounds in the solid solutions: a mole fraction of 0.19 for monocalcium borate and dicalcium borate, and of 0.18 for pentacalcium borosilicate. Lowering of the inversion temperature to about 1,270° C occurs in the monocalcium borate solid solutions, and to about 1,230° C in solid solutions of the other two compounds. The extent of the solid solution area from the C_2S–C_3BS and C_2S–CB

conjugation lines toward the $CaO–SiO_2$ side line has not been determined.

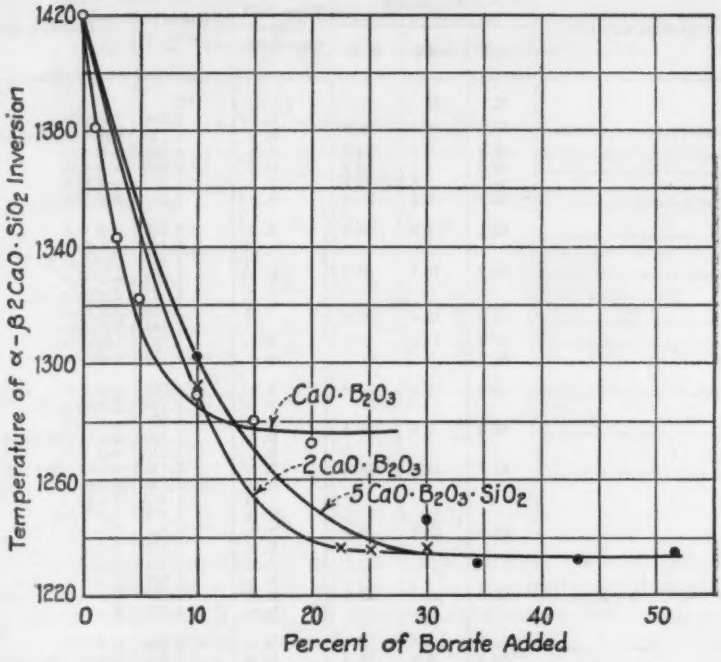

FIGURE 5.—*Effect of solid solution on the α–β inversion of dicalcium silicate.*

TABLE 2.—*Compositions in the dicalcium silicate field*

Composition number	Composition			Time held before quenching	Temperature	Phases present
	CaO	B_2O_3	SiO_2			
	%	%	%	hr	°C	
				¼	1,382	All glass.
				¼	1,373	Trace C_2S+glass.
35	57.0	5.5	37.5	¼	1,345	C_2S+CS+glass.
				h. c.	1,343	Boundary (1–2).
				h. c.	1,125	Eutectic (2).
36	58.7	3.8	37.5	h. c.	1,382	Boundary (1–2).
				¼	1,491	All glass.
37	59.0	7.7	33.3	¼	1,473	C_2S+glass.
				h. c.	1,293	Boundary (1–2).
				1	1,319	All glass.
38	59.3	11.5	29.2	¼	1,311	C_2S+glass.
				h. c.	1,185	Boundary (1–2).
				¼	1,234	All glass.
39	59.5	13.4	27.1	¼	1,226	C_2S+glass.
				¼	1,157	All glass.
40	59.7	15.3	25.0	¼	1,151	C_2S+glass.
				h. c.	1,271	α–β C_2S.
41	62.4	9.5	28.1	h. c.	1,165	Boundary (3–4).
				h. c.	1,120	Eutectic (2).
				h. c.	1,251	α–β C_2S.
42	63.0	11.0	26.0	h. c.	1,122	Eutectic (2).
				h. c.	1,241	α–β C_2S.
43	63.3	11.7	25.0	h. c.	1,127	Quintuple point (3).
				¼	1,421	All glass.
				¼	1,413	C_2S+glass.
44	64.0	13.5	22.5	h. c.	1,245	Boundary (3–4).
				h. c.	1,133	Quintuple point (3).
				h. c.	1,122	Eutectic (2).

TABLE 2.—*Compositions in the dicalcium silicate field*—Continued

Composition number	Composition			Time held before quenching	Temperature	Phases present
	CaO	B_2O_3	SiO_2			
	%	%	%	hr	°C	
45	64.5	14.7	20.8	h. c.	1,266	Liquidus.
				h. c.	1,125	Quintuple point (3).
46	64.9	0.6	34.5	h. c.	1,390	α-β C_2S.
47	64.5	1.7	33.8	h. c.	1,343	α-β C_2S.
48	64.1	2.8	33.1	h. c.	1,322	α-β C_2S.
49	63.1	5.5	31.4	h. c.	1,289	α-β C_2S.
50	62.1	8.3	29.6	h. c.	1,280	α-β C_2S.
51	61.0	11.1	27.9	¼	1,465	All glass.
				¼	1,461	C_2S+glass.
				h. c.	1,272	α-β C_2S.
				h. c.	1,117	Eutectic (2).
52	60.0	13.8	26.2	¼	1,188	All glass.
				¼	1,184	C_2S+glass.
53	59.5	15.0	25.5	h. c.	1,122	Liquidus.
54	64.8	3.8	31.4	h. c.	1,292	α-β C_2S.
55	64.4	8.6	27.0	h. c.	1,236	α-β C_2S.
				h. c.	1,120	Eutectic (2).
56	64.3	9.6	26.1	h. c.	1,235	α-β C_2S.
				h. c.	1,126	Quintuple point (3).
				h. c.	1,236	α-β C_2S.
57	64.1	11.5	24.4	h. c.	1,129	Quintuple point (3).
				h. c.	1,120	Eutectic (2).
				¼	1,477	All glass.
				½	1,472	C_2S+glass.
58	64.0	12.4	23.6	h. c.	1,244	Boundary (3-4).
				h. c.	1,127	Quintuple point (3).
				h. c.	1,121	Eutectic (2).
				h. c.	1,247	Boundary (3-4).
59	63.9	13.4	22.7	h. c.	1,131	Quintuple point (3).
				h. c.	1,119	Eutectic (2).
60	66.1	5.1	28.8	h. c.	1,246	α-β C_2S.
61	66.2	5.9	27.9	h. c.	1,403	Binary eutectic (5).
				h. c.	1,231	α-β C_2S.
62	66.5	7.3	26.2	h. c.	1,400	Binary eutectic (5).
				h. c.	1,232	α-β C_2S.
63	66.8	8.8	24.4	h. c.	1,403	Binary eutectic (5).
				h. c.	1,234	α-β C_2S.
64	67.4	11.7	20.9	h. c.	1,400	Binary eutectic (5).
				h. c.	1,262	Quintuple point (4).
65	67.6	13.2	21.4	h. c.	1,399	Binary eutectic (5).
				h. c.	1,266	Quintuple point (4).
66	68.6	9.7	21.7	h. c.	1,400	Eutectic (6).
67	66.4	13.9	19.7	h. c.	1,323	Liquidus.
				h. c.	1,258	Boundary (3-4).
68	59.5	14.6	25.9	¼	1,159	All glass.
				¼	1,155	C_2S+glass.
69	55.3	0.7	44.0	¼	1,459	All glass.
				¼	1,455	Trace C_2S+glass.

Pseudo-binary systems of $2CaO.SiO_2$ with $2CaO.B_2O_3$ and $CaO.B_2O_3$ are shown in figures 4A and 4L, respectively; and the true binary system formed by $2CaO.SiO_2$ and $5CaO.B_2O_3.SiO_2$ is given in figure 4C.

Dicalcium silicate, crystallized from melts, had the appearance of rounded grains usually imbedded in glass, making an exact determination of the indices difficult. A marked lowering of the indices was observed, however. Thus composition 18, table 1 (58.4 percent of CaO, 13.2 percent of B_2O_3, 28.4 percent of SiO_2), which lies just inside the monocalcium silicate field, when held below the temperature of secondary crystallization, gave spherules of C_2S having an average index only slightly above the 1.65 index of the glass in which they were imbedded (normal indices of β–$2CaO.SiO_2$: $\alpha=1.717$; $\gamma=1.735$).

The field of β–$2CaO.SiO_2$ has been located in figure 3 in accordance with the lowest temperatures found for the alpha-beta inversion.

4. CaO

The compositions prepared in the lime field (D–6–7–8–E–CaO, fig. 3) and melting data obtained by heating curves are given in table 3. Quenches were also made on these compositions to establish the primary phase.

TABLE 3.—*Compositions in the lime field*

Composition number	Composition			Temperature [a]	Phases present
	CaO	B_2O_3	SiO_2		
	%	%	%	°C	
70	69.3	8.3	22.4	1,398	Eutectic (6).
71	71.3	7.7	21.0	1,399	Do.
72	69.1	11.5	18.4	1,398	Do.
73	69.5	13.4	17.1	1,435	Liquidus.
				1,406	Boundary (6–7–8).
74	71.3	23.4	5.3	1,412	Boundary (8–E).
75	71.5	21.9	6.6	1,410	Do.
76	70.0	16.1	13.9	1,413	Binary eutectic (7).
77	71.5	15.3	13.2	1,412	Do.

[a] Obtained from heating curves.

5. $5CaO.B_2O_3.SiO_2$

Pentacalcium borosilicate is the only ternary compound found to possess a field (4–5–6–7–8–9, fig. 3) in the ternary diagram. It may be considered as formed by the combination of dicalcium silicate with tricalcium borate, mole for mole; or by the combination of tricalcium silicate with dicalcium borate, mole for mole. Tricalcium silicate does not occur as a primary phase in this sytem, the ternary compound occupying the region where it might be expected to appear.

The compound, $5CaO.B_2O_3.SiO_2$, melts congruently at 1,419° C. The optical properties [15] are: biaxial negative with moderate optic axial angle; $\alpha=1.666 \pm 0.003$, $\beta=1.682 \pm 0.003$, $\gamma=1.690 \pm 0.003$. Polysynthetic twinning is extremely common. The optic axial angle appears to be variable, probably because of twinning. The compound appears in irregular or rounded grains without definite crystal outline.

Pentacalcium borosilicate forms true binary systems with dicalcium silicate, tricalcium borate (fig. 4C), and lime. In accordance with the theorem of Alkemade [16] the maximum temperature on the boundary 4–5–6 (fig. 3) was found to occur at the binary eutectic (point 5); the maximum on boundary 6–7–8 at the binary eutectic (point 7); and the maximum on boundary 4–9–8 at the binary eutectic (point 9).

Complete crystallization of most charges in this field occurred on quenching; hence melting data were obtained exclusively by heating curves. The results are listed in table 4.

Possible solid solution of $2CaO.SiO_2$ in $5CaO.B_2O_3.SiO_2$ was not indicated.

TABLE 4.—*Compositions in the pentacalcium borosilicate field*

Composition number	Composition			Temperature [a]	Phases present
	CaO	B_2O_3	SiO_2		
	%	%	%	°C	
78	67.9	14.7	17.4	1,400	Binary eutectic (5).
79	68.2	16.1	15.7	1,415	Liquidus.
80	68.4	17.0	14.6	1,419	Do.
81	68.5	17.6	13.9	1,414	Do.
82	68.8	19.0	12.2	1,417	Do.
83	69.0	20.5	10.5	1,415	Do.
				1,262	Quintuple point (4).
84	69.2	21.2	9.6	1,415	Binary eutectic (5).
85	69.3	22.0	8.7	1,417	Liquidus.
86	68.9	15.3	15.8	1,417	Do.
				1,401	Boundary (5-7-8).
87	67.7	19.1	13.2	1,406	Liquidus.
				1,373	Boundary (8-9-4).
88	69.2	16.5	14.3	1,414	Liquidus.

[a] Obtained from heating curves.

6. $3CaO.B_2O_3$

Heating curves on a tricalcium borate preparation having very nearly the theoretical composition (by analysis: 70.74 percent of CaO, 29.26 percent of B_2O_3; theoretical: 70.73 percent of CaO; 29.27 percent of B_2O_3) gave its melting temperature as 1,488° C, a value 9° higher than that reported by Carlson [10] for this compound.

In this field (E–8–9–4–3–F, fig. 3) most of the melting data were secured by heating curves, owing to difficulties caused by quench crystallization. The data are given in table 5.

TABLE 5.—*Compositions in the tricalcium borate field*

Composition number	Composition			Time held before quenching	Temperature	Phases present
	CaO	B_2O_3	SiO_2			
	%	%	%	hr	°C	
89	68.5	26.3	5.2	h. c.	1,429	Liquidus.
				h. c.	1,120	Quintuple point (3).
90	66.3	23.4	16.3	h. c.	1,370	Liquidus.
				h. c.	1,124	Quintuple point (3).
91	64.0	20.5	15.5	h. c.	1,291	Liquidus.
				h. c.	1,129	Quintuple point (3).
92	61.7	17.6	20.7	¼	1,191	All glass.
				¼	1,185	C_3B+glass.
				½	1,147	C_3B+glass.
				½	1,140	C_3B+C_2S+glass.
93	59.9	17.2	22.9	¼	1,150	All glass.
				¼	1,143	Trace C_3B+glass.
94	67.0	20.5	12.5	h. c.	1,375	Liquidus.
				h. c.	1,123	Quintuple point (3).
95	65.8	17.5	16.7	h. c.	1,316	Liquidus.
				h. c.	1,253	Boundary (3-4).
				h. c.	1,123	Quintuple point (3).
96	63.8	15.3	20.9	¼	1,252	All glass.
				¼	1,248	C_3B+C_2S+glass.
				h. c.	1,125	Quintuple point (3).
				h. c.	1,118	Eutectic (2).
97	63.4	19.2	17.4	¼	1,257	All glass.
				¼	1,252	C_3B+glass.
98	63.1	23.0	13.9	¼	1,243	All glass.
				½	1,239	C_3B+glass.

TABLE 5.—*Compositions in the tricalcium borate field*—Continued

Composition number	Composition			Time held before quenching	Temperature	Phases present
	CaO	B_2O_3	SiO_2			
	%	%	%	hr	°C	
99	70.2	26.3	3.5	h. c.	1,456	Liquidus.
100	69.6	23.4	7.0	h. c.	1,428	Do.
				h. c.	1,416	Binary eutectic (9).
101	69.5	22.7	7.8	h. c.	1,416	Liquidus.
102	65.0	16.6	18.4	h. c.	1,261	Do.
				h. c.	1,122	Quintuple point (3).
103	63.5	19.4	17.1	h. c.	1,239	Liquidus.
				h. c.	1,122	Quintuple point (3).
104	62.0	22.2	15.8	¼	1,226	All glass.
				¼	1,219	C_3B+glass.
105	67.1	21.1	11.8	h. c.	1,371	Liquidus.
				h. c.	1,123	Quintuple point (3).
106	66.5	23.0	10.5	¾	1,384	All glass.
				2	1,374	C_3B+glass.
				h. c.	1,126	Quintuple point (3).
107	65.3	26.8	7.9	¼	1,354	All glass.
				¼	1,351	C_3B+glass.
				h. c.	1,170	Boundary (F-3).
108	64.7	28.7	6.6	h. c.	1,330	Liquidus.
109	64.1	30.6	5.3	h. c.	1,245	Boundary (F-3).
110	70.9	27.8	1.3	h. c.	1,476	Liquidus.
				h. c.	1,404	Eutectic (8).
111	71.0	26.4	2.6	h. c.	1,456	Liquidus.
				h. c.	1,404	Eutectic (8).
112	71.1	24.9	4.0	h. c.	1,441	Liquidus.

7. $2CaO.B_2O_3$

Dicalcium borate forms a true binary system with monocalcium silicate (fig. 4I) and accordingly boundary 2–11 (fig. 3) shows a maximum temperature at point 10, as determined by a heating curve on composition 124, and quenches on composition 125, table 6.

TABLE 6.—*Compositions in the dicalcium borate field*

Composition number.	Composition			Time held before quenching	Temperature	Phases present
	CaO	B_2O_3	SiO_2			
	%	%	%	hr	°C	
113	62.9	34.5	2.6	h. c.	1,287	Liquidus.
				h. c.	1,266	Boundary (F-3).
114	63.5	32.6	3.9	h. c.	1,270	Liquidus.
115	62.0	34.5	3.5	h. c.	1,281	Liquidus.
116	62.4	30.6	7.0	h. c.	1,240	Liquidus.
				2	1,221	C_3B+trace C_3B+glass.
117	71.3	34.5	4.2	½	1,287	All glass.
				½	1,280	C_3B+glass.
118	61.0	30.7	8.3	¼	1,256	All glass.
				¼	1,248	C_3B+glass.
119	60.9	28.7	10.4	¼	1,239	All glass.
				¼	1,235	C_3B+glass.
120	60.7	26.8	12.5	¼	1,225	All glass.
				¼	1,221	Trace C_3B+glass.
121	60.3	23.0	16.7	¼	1,184	All glass.
				¼	1,180	C_3B+glass.
122	60.0	19.2	20.8	¼	1,151	All glass.
				¼	1,142	Trace C_3B+glass.
				¼	1,136	C_3B+C_3B+glass.
123	59.1	31.0	9.9	h. c.	1,243	Liquidus.
124	57.7	26.8	15.5	h. c.	1,203	Liquidus.
				h. c.	1,153	Binary eutectic (10).
125	55.7	21.3	23.0	¼	1,155	All glass.
				¼	1,153	C_3B+glass.
				¼	1,150	C_3B+CS+glass.

TABLE 6.—*Compositions in the dicalcium borate field*—Continued

Composition number.	Composition			Time held before quenching	Temperature	Phases present
	CaO	B_2O_3	SiO_2			
	%	%	%	hr	°C	
126	52.4	32.6	15.0	¼	1,180	All glass.
				¼	1,172	C_2B+glass.
127	49.4	30.6	20.0	¼	1,097	All glass.
				¼	1,095	C_2B+glass.
128	50.4	44.3	5.3	¼	1,153	All glass.
				¼	1,150	C_2B+glass.
129	53.3	38.8	7.9	¼	1,230	All glass.
				¼	1,224	C_2B+glass.
130	54.8	36.0	9.2	¼	1,240	All glass.
				¼	1,236	C_2B+glass.
131	56.3	33.2	10.5	3	1,241	All glass.
				4	1,233	C_2B+glass.
132	57.7	30.5	11.8	1¼	1,226	All glass.
				½	1,223	C_2B+glass.
133	59.1	27.7	13.2	h. c.	1,214	Liquidus.
134	49.8	41.5	8.7	¼	1,122	All glass.
				¼	1,115	Trace C_2B+glass.
135	50.8	38.8	10.4	¼	1,134	All glass.
				¼	1,131	Trace C_2B+glass.
136	52.8	33.2	14.0	¼	1,162	All glass.
				¼	1,158	C_2B+glass.
				h. c.	1,017	Quintuple Point (11).
137	54.9	27.7	17.4	¼	1,170	All glass.
				¼	1,168	C_2B+glass.
				h. c.	1,120	Boundary (2-11).
138	56.5	23.4	20.1	¼	1,177	All glass.
				¼	1,169	C_2B+glass.
139	56.9	22.2	20.9	¼	1,170	All glass.
				¼	1,163	C_2B+glass.
140	59.0	16.6	24.4	¼	1,128	All glass.
				¼	1,126	C_2B+glass.
				¼	1,119	C_2B+C_2S+glass.
141	48.7	38.8	12.5	¼	1,089	All glass.
				¼	1,085	Trace C_2B+glass.
142	50.1	33.2	16.7	¼	1,112	All glass.
				¼	1,111	C_2B+glass.
143	51.5	27.7	20.8	¼	1,104	All glass.
				¼	1,102	C_2B+glass.
144	46.1	33.2	20.7	¼	1,039	All glass.
				¼	1,037	C_2B+glass.
145	46.3	30.4	23.3	¼	1,035	All glass.
				¼	1,027	C_2B+CS+glass.
				¼	1,037	All glass.
146	47.2	35.2	17.5	¼	1,033	C_2B+glass.
				¼	1,030	C_2B+CB+glass.
147	50.8	28.1	21.0	¼	1,109	All glass.
				¼	1,107	C_2B+glass.
148	52.6	24.6	22.8	¼	1,128	All glass.
				¼	1,123	C_2B+glass.
				¼	1,139	All glass.
149	50.7	44.3	5.0	¼	1,132	C_2B+glass.
				¼	1,105	C_2B+CB+glass.
150	51.6	38.9	9.5	¼	1,164	All glass.
				¼	1,159	C_2B+glass.
151	50.2	40.1	9.7	h. c.	1,130	Liquidus.
152	48.6	39.7	11.7	¼	1,083	All glass.
				¼	1,080	C_2B+glass.
				¼	1,075	C_2B+CB+glass.
153	51.8	29.2	19.0	¼	1,134	All glass.
				¼	1,129	C_2B+glass.
154	50.5	30.5	19.0	¼	1,113	All glass.
				¼	1,108	C_2B+glass.
155	58.7	22.2	19.1	¼	1,172	All glass.
				¼	1,170	C_2B+glass.
156	48.0	29.3	22.7	¼	1,054	All glass.
				¼	1,052	C_2B+glass.
157	51.7	25.5	22.8	¼	1,127	All glass.
				¼	1,121	C_2B+glass.
				¼	1,107	C_2B+CS+glass.
158	51.9	24.3	23.8	¼	1,125	All glass.
				¼	1,124	Trace C_2B+glass.
				¼	1,117	C_2B+CB+glass.

8. $CaO.B_2O_3$

Monocalcium borate is obtained from melts as lath-shaped crystals occasionally showing hexagonal outline. Sluggish crystallization of some compositions containing the higher percentages of silica in this field necessitated holding the charges overnight. Data relative to the monocalcium borate field are given in table 7.

About one-third of the monocalcium borate field (G–11–12–13–14–H, fig. 3) lies in the one-liquid area, and about two-thirds (13–16–15–14, fig. 3) in the immiscibility region. The boundary of the field in the one-liquid area proceeding inward from the SiO_2–B_2O_3 side line was not determined.

The composition corresponding to that of the mineral danburite, $CaO.B_2O_3.2SiO_2$, is located within the immiscibility portion of the monocalcium borate field.

TABLE 7.—*Compositions in the monocalcium borate field*

Composition number	Composition			Time held before quenching	Temperature	Phases present
	CaO	B_2O_3	SiO_2			
	%	%	%	hr	°C	
159	47.5	49.9	2.6	¼	1,131	All glass.
				¼	1,129	CB+glass.
				¼	1,110	CB+C_3B+glass.
160	46.7	49.8	3.5	¼	1,134	All glass.
				¼	1,132	CB+glass.
161	48.7	44.3	7.0	¼	1,099	All glass.
				¼	1,096	CB+glass.
				¼	1,087	CB+C_3B+glass.
162	46.0	49.8	4.2	¼	1,131	All glass.
				¼	1,128	CB+glass.
163	47.4	44.3	8.3	¼	1,099	All glass.
				¼	1,096	CB+glass.
				¼	1,070	CB+C_3B+glass.
164	45.7	38.8	15.5	¼	1,071	All glass.
				¼	1,067	CB+glass.
165	45.9	36.0	18.1	¼	1,046	All glass.
				¼	1,043	CB+glass.
				¼	1,035	CB+C_3B+glass.
166	40.1	49.9	10.0	17	1,111	All glass.
				17	1,104	CB+glass.
167	35.7	44.3	20.0	17	1,045	All glass.
				17	1,041	CB+glass.
168	30.6	64.2	5.2	17	1,041	All glass.
				17	1,036	CB+glass.
169	32.6	57.1	10.3	17	1,058	All glass.
				17	1,053	CB+glass.
				17	1,013	CB+2 glasses.
170	34.6	49.9	15.5	17	1,059	All glass.
				17	1,053	CB+glass.
				17	1,026	CB+2 glasses.
171	36.5	42.8	20.7	17	1,041	All glass.
				3½	1,033	CB+glass.
172	38.5	35.7	25.8	17	1,023	All glass.
				17	1,017	CB+glass.
173	38.4	31.6	30.0	17	991	All glass.
				17	984	CB+SiO_2+glass.
174	28.0	70.0	2.0	½	993	All glass.
				½	989	Trace CB+glass.
175	27.5	68.5	4.0	½	981	All glass.
				½	979	CB+glass.
176	26.9	67.1	6.0	¼	971	All glass.
				½	969	CB+glass.
177	44.4	32.0	23.6	17	1,018	All glass.
				17	1,017	CB+glass.
178	44.0	31.6	24.4	1½	1,027	All glass.
				1½	1,017	Trace CB+glass.
179	26.4	65.6	8.0	1½	976	Two glasses.
				1½	968	CB+glass.

9. $CaO.2B_2O_3$

Only a small portion of the calcium diborate field (H–14–I, fig. 3) lies within the one-liquid region; compositions in the area 14–15–I′–I melt with the formation of two liquids. The boundary of the field in the one-liquid area extending inward from the SiO_2–B_2O_3 side line was not determined.

The liquidus temperatures of two compositions, 180 (27.3 percent of CaO, 70.9 percent of B_2O_3, 1.8 percent of SiO_2) and 181 (26.2 percent of CaO, 69.9 percent of B_2O_3, 3.9 percent of SiO_2), in the area H–14–I, are 982° C and 967° C, respectively.

10. SiO_2

This field is distorted in a curious manner by the occurrence of liquid immiscibility. It consists of a portion (A′–B–12–13) in the one-liquid area, a large region (A′–13–16–A) in the two-liquid area, and probably a narrow strip in the one-liquid area along the SiO_2–B_2O_3 side of the triangle extending an undetermined distance toward the B_2O_3 vertex.

In the melts studied (table 8) silica appeared as tridymite imbedded in the high-index glass.

TABLE 8.—*Compositions in the silica field*

Composition number	Composition			Time held before quenching	Temperature	Phases present
	CaO	B_2O_3	SiO_2			
	%	%	%	hr	°C	
182	35.0	1.0	64.0	2	1,425	All glass.
				1	1,417	SiO_2+CS+glass.
183	35.2	2.0	62.8	2	1,411	All glass.
				1	1,405	Trace SiO_2+glass.
				1	1,400	SiO_2+CS+glass.
184	34.4	4.0	61.6	1	1,388	All glass.
				½	1,380	SiO_2+glass.
				½	1,373	SiO_2+CS+glass.
185	31.2	4.0	64.8	1	1,370	SiO_2+two glasses.
				½	1,364	SiO_2+CS+glass.
186	32.0	4.4	63.6	1	1,465	Two glasses.
				1	1,457	SiO_2+glass.
				1	1,365	SiO_2+glass.
				1	1,357	SiO_2+CS+glass.
187	32.8	6.0	61.2	1	1,392	Two glasses.
				1	1,385	SiO_2+glass.
				¼	1,332	SiO_2+glass.
				¼	1,327	SiO_2+CS+glass.
188	35.2	10.0	54.8	1	1,292	Two glasses.
				¾	1,287	SiO_2+glass.
				1	1,276	SiO_2+glass.
				1½	1,271	SiO_2+CS+glass.
189	36.3	15.5	47.2	½	1,223	Two glasses.
				1	1,218	SiO_2+glass.
				½	1,205	SiO_2+glass.
				1½	1,197	SiO_2+CS+glass.
190	37.0	23.0	40.0	4	1,113	Two glasses.
				4	1,108	SiO_2+glass.
191	35.6	24.0	40.4	17	1,071	Two glasses.
				17	1,063	SiO_2+glass.
192	38.4	26.0	35.6	17	1,057	Two glasses.
				17	1,048	SiO_2+glass.
193	38.2	29.4	32.4	17	1,038	Two glasses.
				17	1,031	SiO_2+glass.
				17	1,010	SiO_2+glass.
				17	1,006	SiO_2+CS+glass.
194	38.2	30.4	31.4	17	1,019	Two glasses.
				17	1,012	SiO_2+glass.
				17	1,003	SiO_2+glass.
				17	1,000	SiO_2+CS+glass.
195	37.8	31.4	30.8	17	995	Two glasses.
				17	991	SiO_2+glass.
				17	989	SiO_2+CB+glass.

The exact concentration intervals between the two-liquid boundary and the silica-monocalcium silicate boundary have not been accurately determined, but probably are represented fairly closely by the region between the curves A′–13 and B–12 in figure 3.

IV. THE TWO-LIQUID AREA

The appearance of liquid immiscibility in a ternary system reduces the maximum possible number of solid phases within such an area by one. Hence, no ternary eutectics can occur in an immiscibility region, and fields entering it must persist until liquid miscibility is again encountered. Moreover, boundaries between fields must be straight lines of constant temperature in the immiscibility area. The course of crystallization in this region is quite different from that in the one-liquid area.

Liquid immiscibility of the type found in the system CaO–B_2O_3–SiO_2 probably occurs also in ternary systems of B_2O_3 and SiO_2 with MgO, SrO, ZnO, FeO, CoO, and NiO, as these last six oxides, like CaO, form binary systems with both B_2O_3 and SiO_2 in which liquid immiscibility occurs [1, 2]. Analogies are also to be found in certain organic systems such as the system water-phenol-aniline investigated by Schreinemakers [17].

Studies were made of the compositions of immiscible liquids formed by the melting of mixtures within the area A–A′–13–14–I–I′, figure 3. The results are listed in table 9.

TABLE 9.—*Tie-line compositions in the immiscibility area*

Composition number	Compositions									Time held before quenching	Temperature	Phases present
	Initial			High SiO_2 glass			Low SiO_2 glass					
	CaO	B_2O_3	SiO_2	CaO	B_2O_3	SiO_2	CaO	B_2O_3	SiO_2			
	%	%	%	%	%	%	%	%	%	hr	°C	
196	30.8	19.2	50.0	21.4	15.0	63.6	36.4	21.4	42.2	7	1,132	Two glasses.
										4	1,125	SiO_2 + glass.
197	25.2	24.8	50.0	15.1	17.1	67.8	33.3	27.4	39.3	17	1,021	Two glasses.
										17	1,014	SiO_2 + glass.
198	22.3	27.7	50.0	11.8	18.4	69.8	32.4	32.2	35.4	17	1,012	Two glasses.
										17	1,003	CB + glass.
199	22.0	38.0	40.0	7.4	23.8	68.8	30.6	43.5	25.9	17	1,035	Two glasses.
										17	1,029	CB + glass.
200	20.1	49.9	30.0	8.3	36.6	55.1	28.1	59.1	12.8	17	1,014	Two glasses.
										17	1,006	CB + glass.
201	16.0	60.0	24.0	3.9	52.8	43.3	25.6	65.5	8.9	17	980	Two glasses.
										17	977	CB + glass.
202	16.0	64.0	20.0	2.2	56.1	41.7	24.9	68.3	6.8	2½	967	Two glasses.
										3	965	Trace CB_2 + glass.
203	12.0	74.0	14.0	0.8	74.9	24.3	23.4	72.8	3.8	2	964	CB_2 + CB + glass.
										2	970	Two glasses.
204	10.0	84.0	6.0	0.9	89.9	9.2	23.3	75.2	1.5	2	968	CB_2 + glass.
										2	973	Two glasses.
										½	970	CB_2 + glass.

These compositions were prepared as described under section II, 1. They were fused three times, with intermediate grinding and mixing. After the third fusion the resulting glasses were broken into coarse fragments, and those of the high-silica glass separated from those of the low-silica glass. The two glasses were easily distinguishable and there was no difficulty in making this separation. Samples were

then analyzed and quench determinations made on the low-silica glasses.

Complete separation of the two liquids was not obtained in any case, but it is evident that the initial composition of the mixture and the compositions of the two liquids resulting must lie on a straight line regardless of the degree of separation, unless the initial composition is changed during the fusions. The intersections of this line, which is a tie line, with the boundaries of the immiscibility area give the compositions of the conjugate liquids.

Two tie-line compositions were prepared in the silica field. On melting, the high-silica layer formed a very viscous liquid which remained at the center of the crucible and the low-silica liquid flowed to the sides. Separation was very incomplete as the analyses show. The high-silica liquid, because of its high viscosity, tended to retain a considerable amount of the low-silica liquid.

Much better separations were obtained in the monocalcium borate field where four tie-line compositions were prepared. The liquidus temperature of composition 199 (1,032°C) is the maximum temperature for the immiscibility portion of the monocalcium borate field.

The tie lines in the calcium diborate field have a fan-shaped distribution as figure 3 shows. The liquids in this field separated almost completely. Quenches on composition 202 fix the temperature of the quintuple line 14–15 separating the fields of calcium diborate and monocalcium borate. Quenches on a binary composition (12 percent of CaO, 88 percent of B_2O_3) gave 974° C for the temperature of the liquidus, a value 3° higher than that reported by Carlson [10].

In an attempt to establish the phase formed on secondary crystgllization at the calcium diborate boundary in the one-liquid area along the SiO_2–B_2O_3 side line, a charge of the high-silica glass from composition 203 was held for 11 days at 525° C. The charge was found still to consist of undevitrified glass.

A striking feature of the immiscibility area is the marked increase in concentration of lime in the less siliceous liquids (of compositions represented by the curve A′–13–14–I, fig. 3), proceeding toward the interior of the diagram from either the lime-silica system or the lime-boric oxide system. The maximum concentration of lime in the ternary liquids is about 38.5 percent, which is 11 percent higher than the lime content of the corresponding lime-silica liquid (A′, fig. 3) and 15 percent higher than that of the lime-rich layer in the lime-boric oxide system (I, fig. 3). A similar observation was made by Morey and Ingerson [12].

Whether any appreciable increase in the lime concentration of the more siliceous ternary liquids (represented by the line A–16–15–I′, fig. 3) occurs has not been determined, but the analyses on compositions 203, 204, and 205 indicate that the concentration change is probably small. Owing to lack of further information the compositions of the more siliceous liquids in the ternary diagram have been indicated by a dotted line connecting the compositions of the high-silica and high-boric oxide liquids in the respective binary systems.

The maximum divergence in composition of the two liquids occurs in the monocalcium borate field, as inspection of the length of tie lines in figure 3 will show.

V. CHARACTERISTICS OF THE FUSION SURFACES

Isotherms showing temperatures of complete melting have been inserted in figure 6. The positions of the isotherms were determined by points read off the diagrams of figure 4 at 50 and 100° C intervals and also by melting data for other compositions not on conjugation lines.

In general, it may be said that the portion of the diagram to the left of the two-liquid boundary A′–13–14–I is of the usual type encountered in ternary oxide systems. To the right of that boundary the liquidus presents unusual features.

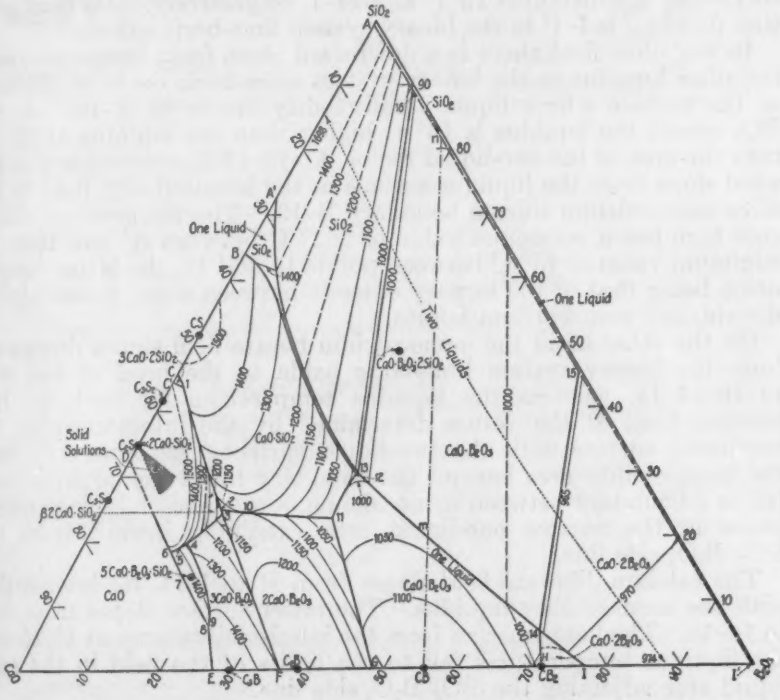

FIGURE 6.—*Triangular concentration diagram of the system* $CaO–B_2O_3–SiO_2$ *with isotherms showing temperatures of complete melting.*

In a solid model where temperature is plotted on a scale perpendicular to the concentration triangle as a base, the liquidus of the immiscibility region appears as a curved surface capable of being generated by a rotating, horizontal line of variable length [18]. In the silica field the line moves downhill, one end traversing the distance A–16 while the other end passes from A′ to 13. Successive positions of the line (from 1,698 to 990° C) are isotherms and tie lines, and its final position before leaving the field represents an invariant condition where two liquids of compositions given by points 13 and 16, two solids (silica and monocalcium borate), and vapor are in equilibrium.

Passing into the monocalcium borate field the line moves uphill assuming successively higher positions until it reaches mn, the maximum height on the surface in this region (1,032° C). In this position a plane passed through the line and perpendicular to the base will include the composition corresponding to monocalcium borate. From mn the line proceeds downhill, one end traversing the distance n–15 and the other the distance m–14. On reaching a minimum temperature (964° C) at 14–15 it represents an invariant condition wherein monocalcium borate, calcium diborate, and two liquids of compositions 14 and 15 are in equilibrium with vapor.

Entering the calcium diborate field, the line moves uphill, the ends traversing the distances 15–I′ and 14–I, respectively. Its final position (974° C) is I–I′ in the binary system lime-boric oxide.

In the silica field there is a downward slope from temperatures at the silica liquidus in the binary system silica-boric oxide to the level of the surface where liquid immiscibility starts at A–16. At the SiO_2 vertex the liquidus is 15° C higher than the liquidus at A. In turn the area of the one-liquid region A′–13–12–B represents a downward slope from the liquidus surface in the immiscibility field to the silica-monocalcium silicate boundary B–12. The temperature difference here has a maximum value of 262° C between A′ and B and a minimum value of 13° C between points 13 and 12, the latter composition being that of the ternary eutectic between silica, monocalcium silicate, and monocalcium borate.

On the other hand the monocalcium borate field slopes downward from the binary system lime-boric oxide to the level of the area 13–16–15–14, wherein the liquidus temperature for each tie line remains fixed at the values determined by the intersection of the one-liquid surface with the two-liquid surface. On emerging from the immiscibility area beyond the boundary 15–16 the liquidus must fall to a boundary between monocalcium borate and an undetermined phase in the narrow one-liquid area extending inward from the SiO_2–B_2O_3 side line.

The calcium diborate field slopes from H to I–14, its intersection with the immiscibility liquidus. The latter surface slopes from I–I′ to 14–15. The field emerges from the immiscibility area at I′–15 and the liquidus temperatures fall to the limits of the field in the one-liquid area adjoining the SiO_2–B_2O_3 side line.

Figure 7 represents projections of the boundary curves of the solid model on planes vertical to the base. Boundaries between different fields are shown and also boundaries between the one- and two-liquid portions of fields (A′–13; 13–14; and 14–I). The numbers and letters by which the boundaries are designated correspond to those in figures 3 and 6.

It is seen in figure 7 that there are four boundary curves (4–6; 6–8; 8–4; and 2–11) separating fields of primary crystallization which exhibit a maximum temperature. The maxima in these curves correspond to the temperatures of eutectics in the respective binary systems. Boundaries A′–13; 13–14; and 14–I enable one to visualize partially the general contours of the surfaces in the immiscibility region.

The compositions and temperatures of eutectics and quintuple points and other significant data are contained in table 10.

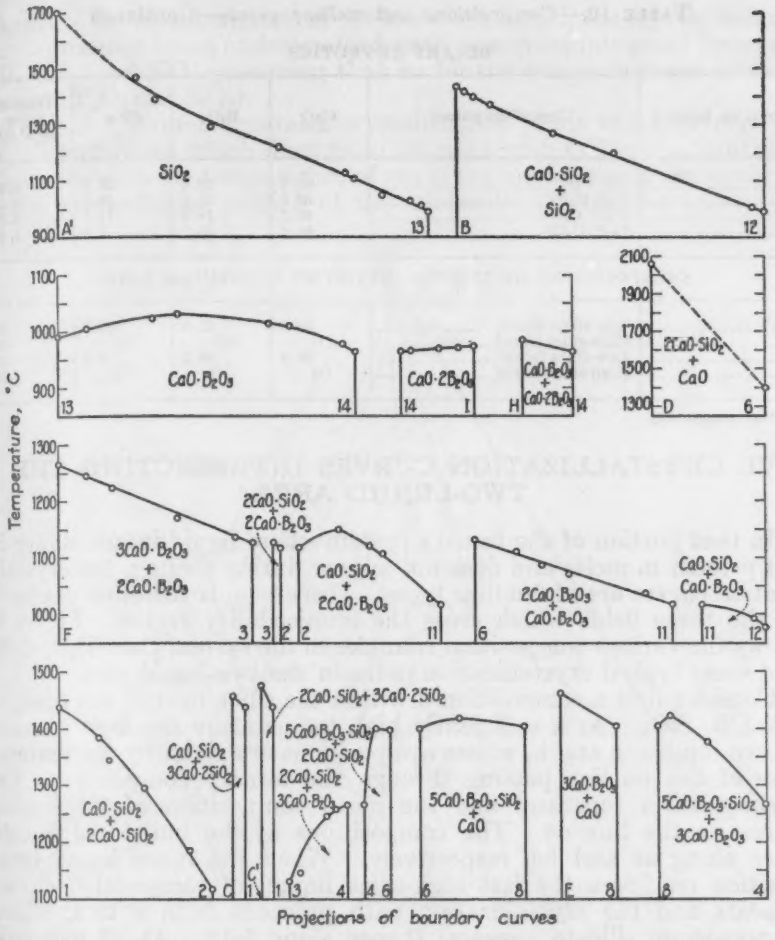

FIGURE 7.—*Temperature-concentration diagrams of boundary curves in the system* $CaO–B_2O_3–SiO_2$.

TABLE 10.—*Compositions and melting points*

TERNARY EUTECTICS

Point no. figure 6	Crystalline phases	CaO	B_2O_3	SiO_2	Temperature (± 5° C)
		%	%	%	°C
2	CS, C_2S, C_3B	59.2	16.0	24.8	1,118
6	C_3S, CaO, C_3BS	69.2	12.6	18.2	1,398
8	CaO, C_3BS, C_3B	70.0	23.2	6.8	1,404
12	CS, CB, SiO_2	38.3	31.5	30.2	977

QUINTUPLE POINTS, NOT EUTECTICS

1	CS, C_3S_2, C_3S	54.6	1.5	43.9	1,436
3	C_3S, C_3B, C_2B	59.4	16.6	24.0	1,128
4	C_3S, C_3BS, C_3B	66.2	14.1	19.7	1,266
11	CS, C_2B, CB	45.0	31.7	23.3	1,017

TABLE 10.—*Compositions and melting points*—Continued

BINARY EUTECTICS

Point no. figure 6	Crystalline phases	CaO	B_2O_3	SiO_2	Temperature (± 5° C)
10	CS, C_3B	55.4	20.4	24.2	1,120
5	C_3S, C_3BS	67.7	13.3	19.0	1,400
7	CaO, C_3BS	69.7	16.2	14.1	1,412
9	C_3B, C_3BS	69.4	22.8	7.8	1,415
	COMPOSITIONS OF LIQUIDS JOINED BY QUINTUPLE LINES				
13	Low-silica liquid	38.0	31.6	30.4	990
16	High-silica liquid	(a)	(a)	(a)	990
14	Low-silica liquid	26.0	68.2	5.8	994
15	High-silica liquid	(a)	(a)	(a)	994

a Not determined.

VI. CRYSTALLIZATION CURVES INTERSECTING THE TWO-LIQUID AREA

In that portion of the ternary system where liquid immiscibility is not present in melts and does not appear during cooling, the crystallization curves are of familiar types. Discussion is therefore confined to the three fields which cross the immiscibility region. Figure 8 shows the various composition triangles in the system $CaO–B_2O_3–SiO_2$ and some typical crystallization paths in the two-liquid area.

Consider first a composition d within the silica field of the triangle CS, CB, SiO_2. At a sufficiently high temperature the melt consists of two liquids, a and b, whose compositions are given by the extremities of the tie line passing through the ternary composition. On cooling, silica separates and the mean composition of the liquids alters on the line de. The compositions of the individual liquids alter along ac and be, respectively. When the mean liquid composition reaches e the last high-silica liquid, of composition c, disappears and the crystallization path proceeds from e to f, where monocalcium silicate appears; thence along f–12. At 12 monocalcium borate crystallizes and liquid disappears.

Composition h, at a sufficiently high temperature, consists of two liquids, g and i. On cooling, with separation of silica, the mean composition of the liquids alters along hj. At j monocalcium borate crystallizes and the temperature remains constant while the mean composition of the liquids changes along j–13, accompanied by separation of monocalcium borate and silica in a constant ratio of a composition given by the intersection of the line 13–16 with the $CB–SiO_2$ conjugation line. When the mean liquid composition reaches point 13 the last high-silica liquid disappears and the crystallization curve follows the boundary 13–12 with falling temperature. At the ternary eutectic (point 12) monocalcium silicate crystallizes and liquid disappears.

Melt r in the composition triangle CB, CB_2, SiO_2 consists of two liquids, o and k. On cooling, monocalcium borate crystallizes and the mean liquid composition alters from r to p. At p silica appears, and from p to 16, liquids 13 and 16, silica and monocalcium borate are

present. On disappearance of the low-silica liquid, the crystallization curve proceeds by an undetermined path to a quintuple point between CB, CB_2, and SiO_2 (assuming that no binary compounds are formed between B_2O_3 and SiO_2).

The line CB–m–n separates crystallization paths which diverge to its left and those which diverge to its right with falling temperature. This is because the temperature of mn is the maximum of the liquidus in the immiscibility portion of the monocalcium borate field.

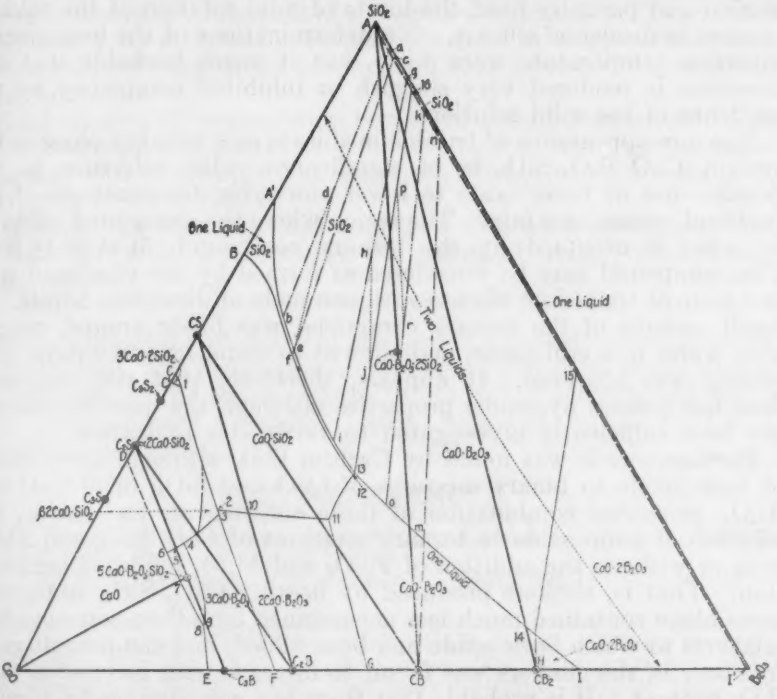

FIGURE 8.—*Composition triangles in the system* $CaO–B_2O_3–SiO_2$ *and some typical crystallization paths in the two-liquid area.*

Crystallization curves in the composition triangle CB_2, SiO_2, B_2O_3 are of types similar to those already discussed and will end at the ternary eutectic of these three compounds (again assuming the absence of binary compounds between B_2O_3 and SiO_2).

VII. APPLICATIONS

Dicalcium silicate occurs in portland cement in the unstable beta modification which possesses desirable hydraulic properties, whereas, in its low-temperature gamma modification, the compound is practically nonhydraulic. The beta-gamma inversion for the pure compound normally occurs at 675° C with such rapidity that it is difficult to prepare the beta form in appreciable quantities even on quenching from temperatures of over 1,000° C. However, it was first noticed by Bates and Klein [19] that the presence of less than 1 percent of B_2O_3 or Cr_2O_3 prevented the inversion and that the former oxide

seemed to effect a marked lowering of the fusion temperature of the compound.

Further studies carried on by E. T. Carlson of this Bureau [20] showed that progressive lowering of the alpha-beta inversion temperature of dicalcium silicate occurred on the addition of 0.5 to 5 percent of B_2O_3 to the compound. Lowering of the indices of dicalcium silicate was also noted. It was concluded that these effects probably indicated solid solution of boric oxide in the silicate.

The results of the present investigation have verified this conclusion and partially fixed the limits of solid solution of the calcium borates in dicalcium silicate. No determinations of the beta-gamma inversion temperature were made, but it seems probable that this inversion is rendered very sluggish or inhibited completely by the existence of the solid solutions.

The non-appearance of tricalcium silicate as a primary phase in the system CaO–B_2O_3–SiO_2 is of significance, with reference to the possible use of boric oxide to lower clinkering temperatures of the portland cement raw mix. The region where this compound might be expected is occupied by the ternary compound, $5CaO.B_2O_3.SiO_2$. This compound may be considered as formed by the combination of one mole of tricalcium silicate with one mole of dicalcium borate. A small amount of the ternary compound was finely ground, gauged with water to a stiff paste, and allowed to stand for some days. No setting was observed. It appears, therefore, that the compound does not possess hydraulic properties although the question has not yet been sufficiently investigated to verify this indication.

Furthermore it was found by Carlson that, although the addition of boric oxide to binary mixtures of CaO and SiO_2, or of CaO and Al_2O_3, promoted combination of these constituents on heating, the addition of boric oxide to ternary mixtures of CaO, SiO_2, and Al_2O_3, with or without the addition of Fe_2O_3 and MgO, inhibited combination. That is, clinkers produced by heating CaO, SiO_2, Al_2O_3 mixtures alone contained much less uncombined lime than corresponding mixtures to which boric oxide had been added, and the percentage of free lime in the clinkers was found to increase with increase in their B_2O_3 content. It is probable that there is a considerable broadening of the lime field at various B_2O_3 levels in the quaternary system CaO–Al_2O_3–SiO_2–B_2O_3.

The above considerations indicate that the addition of appreciable quantities of boric oxide to the portland cement raw mix would not be desirable.

The high-silica low-lime portion of the diagram is of interest in connection with the constitution of borosilicate glasses. This aspect of the problem and the effect of addition of alkali oxide upon the liquid immiscibility are being studied elsewhere [12].

VIII. SUMMARY

The foregoing investigation of the system CaO–B_2O_3–SiO_2 has disclosed a type of liquid immiscibility not encountered in other ternary oxide systems. Whereas in previous instances immiscibility was confined to one field only, in this system compositions in any one of three fields may melt with the formation of two liquids. The fields of silica, monocalcium borate, and calcium diborate were found to be

largely within the immiscibility area which extends in the triangular diagram from the immiscibility region in the lime–boric oxide system to that in the lime-silica system. The width of the area broadens very considerably in proceeding toward the interior of the triangular diagram.

Unusual features of the fusion surfaces in this system were discussed.

One new compound, pentacalcium borosilicate, $5CaO.B_2O_3.SiO_2$, melting at 1,419° C, was found. Tricalcium silicate does not appear at the liquidus in the system. The region in which it might be expected is occupied by the field of the ternary compound. The mineral danburite, $CaO.B_2O_3.2SiO_2$, was not obtained as a crystalline phase, its composition lying in the immiscible liquid portion of the monocalcium borate field.

Solid solution of monocalcium borate, dicalcium borate, and pentacalcium borosilicate occurs in dicalcium silicate, causing the alpha-beta inversion temperature of dicalcium silicate to be lowered by a maximum of about 190° C.

The evidence indicates that additions of small quantities of boric oxide to the portland cement raw mix before "burning" would not be advantageous.

The authors take pleasure in acknowledging their indebtedness to E. T. Carlson, who began this investigation, and from whose data on 35 compositions the binary system $2CaO.B_2O_3$–$CaO.SiO_2$ and part of the pseudo-binary systems $2CaO.B_2O_3$–$CaO.SiO_2$, $CaO.B_2O_3$–$2CaO.SiO_2$, are constructed.

IX. REFERENCES

[1] W. Guertler, *On the limits of miscibility of boric oxide and borates in melts*, Z. anorg. Chem. **40**, 225–53 (1904).

[2] J. W. Greig, *Immiscibility in silicate melts*, Am. J. Sci. [5], **13**, 1–44, 133–54 (1927).

[3] *Effect of boric acid on the clinkering of portland cement*, BS Tech. News Bul. 157, p. 46 (May 1930). *The system* CaC–B_2O_3, BS Tech. News Bul. 186, p. 94 (Oct. 1932). E. T. Carlson, *The system* CaO–B_2O_3, BS J. Research, **9**, 825–32 (1932). *The system* CaO–B_2O_3–SiO_2, BS Tech. News Bul. 209, p. 88 (Sept. 1934). *The system* CaO–B_2O_3–SiO_2, BS Tech. News Bul. 230, p. 49 (June 1936).

[4] C. W. Kanolt, *The melting points of some refractory oxides*, Bul. BS **10**, 295–313 (1914) S212.

[5] E. E. Schumacher, *The melting points of barium, strontium, and calcium oxides*, J. Am. Chem. Soc. **48**, 396–405 (1926).

[6] N. W. Taylor and S. S. Cole, *Crystalline boric oxide*, J. Am. Chem. Soc. **56**, 1648–49 (1934). S. S. Cole and N. W. Taylor, *The system* Na_2O–B_2O_3, I. *Preparation of crystalline* B_2O_3 *and some of its physical properties*, J. Am. Ceram. Soc. **14**, 55–58 (1935).

[7] A. L. Day, E. S. Shepherd, and F. E. Wright, *The lime-silica series of minerals*, Am. J. Sci. [4], **22**, 265–302 (1906).

[8] G. A. Rankin and F. E. Wright, *The ternary system* CaO–Al_2O_3–SiO_2, Am. J. Sci. [4], **39**, 1–79 (1915).

[9] J. B. Ferguson and H. E. Merwin, *The ternary system* CaO–MgO–SiO_2, Am. J. Sci. [4], **48**, 81–123 (1919).

[10] E. T. Carlson, *The system* CaO–B_2O_3, BS J. Research **9**, 825–832 (1932) RP 510.

[11] A. Cousen and W. E. S. Turner, *Studies of the glasses boric oxide-silica*, J. Soc. Glass Tech., Trans. **12**, 169–190 (1928).

[12] G. W. Morey, *The effect of boric oxide on the devitrification of the soda-lime-silica glasses. The quaternary system* Na_2O–CaO–B_2O_3–SiO_2, J. Am. Ceram. Soc. **15**, 457–475 (1932). G. W. Morey and Earl Ingerson, *The melting ofdanburite*, J. Mineralogical Soc. Am. **21**, 194 (1936).

[13] H. S. Roberts, *The Geophysical Laboratory furnace thermostat*, J. Opt. Soc. Am. Rev. Sci. Instr. **11**, 171–186 (1925).
[14] E. S. Shepherd, G. A. Rankin, and F. E. Wright, *Binary systems of alumina with silica, lime, and magnesia*, Am. J. Sci. [4] **28**, 293 (1909).
[15] Determined by Dr. Herbert Insley of the National Bureau of Standards.
[16] W. D. Bancroft, The Phase Rule, p. 149; (published by J. Phys. Chem., 1897).
[17] F. A. H. Schreinemakers, *Equilibrium in the system water-phenol-aniline*. II, Z. phys. Chem. **30**, 460–480 (1899).
[18] Cf. J. W. Greig, *Immiscibility in silicate melts*, Am. J. Sci. [5] **13**, 32 (1927).
[19] P. H. Bates and A. A. Klein, *Properties of the calcium silicates and calcium aluminate occurring in normal portland cement*, Tech. Pap. BS8,, (1917) T78.
[20] E. T. Carlson, unpublished data.

WASHINGTON, July 15, 1936.

U. S. Department of Commerce National Bureau of Standards

RESEARCH PAPER RP942

Part of Journal of Research of the National Bureau of Standards, Volume 17, November 1936

CARE OF FILMSLIDES AND MOTION-PICTURE FILMS IN LIBRARIES[1]

By Charles G. Weber and John R. Hill[2]

ABSTRACT

The stability of cellulose acetate film used as filmslides is being studied to determine its suitability for preserving records in libraries. Cellulose nitrate motion-picture films are being tested to find the best conditions for preserving this type of film. The control of moisture content is essential to prevent brittleness in acetate films, and scratching of the emulsion appears to be a problem involved in the use of filmslides in reading projectors. Frequent cleaning is important. Nitrate motion-picture films are not permanent because the cellulose nitrate is unstable. They can be best preserved by storing in a dry atmosphere, at low temperature, in such manner that products of decomposition are permitted to escape freely. The storage of nitrate films requires very exacting fire-prevention measures.

CONTENTS

	Page
I. Introduction	753
II. Effects of atmospheric variations on films	754
1. Moisture content	754
2. Flexibility	755
3. Expansion and contraction	757
III. Scratching of filmslides	758
IV. Cleaning of films and filmslides	758
V. Problems in the storage of cellulose nitrate film	759
VI. Summary	760

I. INTRODUCTION

Progress made in the use of photographic film for copying, in miniature, important reference records, and the apparent certainty of widespread expansion in the use of films for many classes of library records, make the care and preservation of films a problem of immediate importance to librarians. The term filmslide is applied to films used for projecting enlarged still pictures on a screen for comfortable reading. They can be either in roll or card form. Two kinds of film are available for this purpose: first, cellulose nitrate, which is very inflammable and chemically unstable and, second, cellulose acetate ("safety film"), which is slow-burning and chemically

[1] This study was made with the assistance of a fund granted by the Carnegie Corporation to the National Research Council, and a fund allotted by the National Archives, and with the advice of the following committee, appointed by the National Research Council: R. C. Binkley, National Association of Learned Societies; J. G. Bradley, National Archives; E. K. Carver, Eastman Kodak Co.; H. T. Cowling, representing the Society of Motion Picture Engineers; V. B. Sease, Du Pont Film Corporation; F. W. Willard, National Research Council; and H. M. Lydenberg, chairman, New York Public Library. The Film Preservation Committee of the Society of Motion Picture Engineers has been very helpful also.

[2] Research Associate at the National Bureau of Standards, representing the National Research Council.

stable. Both kinds have been used for copying documents in miniature, but at present only safety film is in general use for this purpose. Acetate film presents no greater fire hazard than ordinary paper, and although the safety film now used is a comparatively new material, it has been found in tests at the National Bureau of Standards [3] to be very stable, if properly made and processed. However, the preservation of acetate film requires control of moisture content.

Cellulose nitrate is in general use in the motion-picture industry chiefly because cellulose acetate is more brittle when dry, curls more in service, and is slightly plastic when wet, consequently, it is not entirely satisfactory for continuous machine development. The samples tested were furnished by the three principal domestic manufacturers of motion-picture films, and were said to be representative of current commercial products. No materials of foreign manufacture were tested.

The National Archives and other depositories interested in the storage of valuable motion-picture films have special problems due to the highly inflammable character of the base. The base of this type of film is a mixture of cellulose nitrate and camphor. It is chemically unstable and highly combustible.

II. EFFECTS OF ATMOSPHERIC VARIATIONS ON FILMS

The effects of variations in relative humidity of the surrounding air were determined by studying the properties of film over a wide range of relative humidities at constant temperature. The properties tested were: Moisture content, and its effect on flexibility as determined by the Pfund [4] type of folding-endurance tester; and dimensional changes. Inasmuch as the experience of film users has indicated that acetate film is much more susceptible to atmospheric changes than nitrate film, the relative behavior of these two types is significant. The films were conditioned for 24 hours in all instances, because both types of film were found to reach practically constant weight within that time. The tests were made on films secured from three domestic manufacturers who stated that the films were representative commercial products.

1. MOISTURE CONTENT

The moisture contents of cellulose acetate and cellulose nitrate film, in common with other hygroscopic substances, tend to follow the relative humidity of the surrounding atmosphere. With films, changes of moisture content affect the flexibility and cause dimensional changes. Hence, the relationship between relative humidity and moisture content is of interest in that it gives the basis for explanation of the physical reactions of the films to moisture changes. This relationship is shown graphically in figure 1. The data on moisture content of films are based on oven-dry weights. Oven-dry weight was obtained by heating for 1 hour at 100° C, with a slight correction for permanent loss in weight which was due to loss of volatile material.

[3] Detailed information on the stability of films will be contained in a separate article now in preparation.
[4] This type of folding tester developed by A. H. Pfund, Johns Hopkins University, for the DuPont Film Corporation, was used in the study at the Bureau after it was found to give more reproducible results than did folding testers used for paper.

The graph shows absorption and loss of moisture for both acetate and nitrate films with emulsion. These curves are similar in general form to adsorption-desorption curves for paper.[5] It will be noted that there are two curves for each type of film, which is because the moisture content of a hygroscopic substance varies according to the direction of approach to the hygrometric condition. Hence, we have one curve for absorption, that is, ascending from a dry initial condition, and one curve for descending values. This variation in moisture

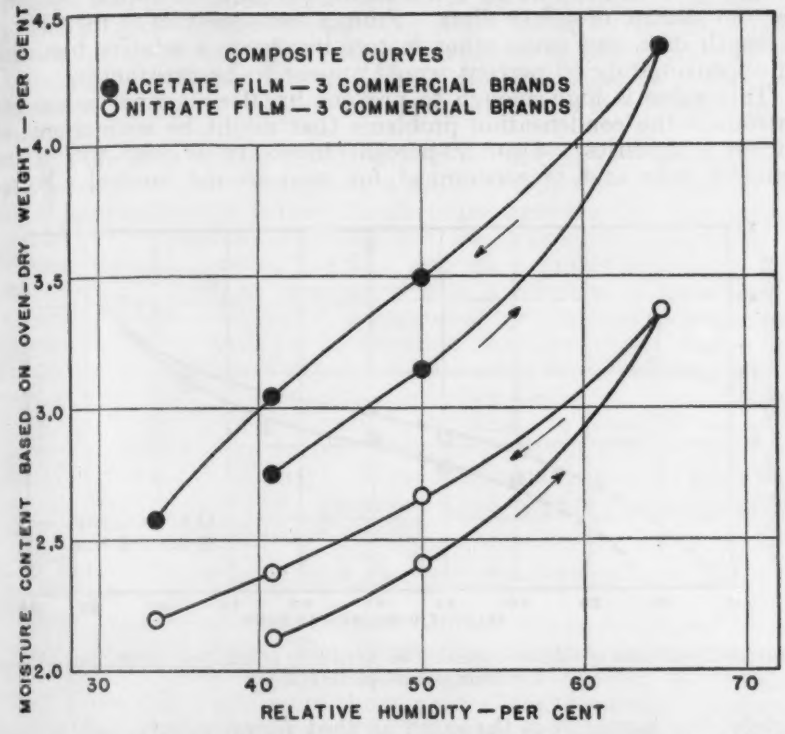

FIGURE 1.—*Relationship between relative humidity and moisture content of cellulose acetate and cellulose nitrate motion-picture film.*

content, as influenced by the history of conditioning, is known as hysteresis.

2. FLEXIBILITY

The relationship between folding endurance and relative humidity was found to be fairly regular for both acetate and nitrate film. The loss of folding strength with decreasing relative humidity was more rapid for acetate than for nitrate, which apparently explains why brittleness difficulties are more frequently encountered in the use of safety film. The relationship between the hygrometric condition and flexibility of both acetate film and nitrate film is shown in figure 2. Data were obtained for the relative-humidity range from 30 to 85 percent, as shown by the curves. Extension of the curves below 30-percent relative humidity by extrapolation is shown by the broken

[5] BS J. Research 12, 53 (1934) RP633.

lines. The only data for this region were obtained on film dried over calcium chloride in a desiccator. Neither type would withstand folding under these conditions, indicating complete loss of folding endurance before zero relative humidity was reached. The extrapolation would indicate extreme brittleness of the acetate film at about 15-percent relative humidity and below. This agrees with the experience of users Hence, since 15 percent is within the range of humidity encountered during the winter season, in heated rooms with no humidity control, some air-conditioning precautions appear essential for the storage of safety films. From a consideration of the folding-strength data and some other factors involved, a relative humidity of approximately 50 percent would appear to be satisfactory.

This value is high enough to prevent brittleness, and it does not introduce the condensation problems that might be encountered at higher humidities. Also, 50-percent humidity is well within the comfort zone and is economical for year-around control. Fortu-

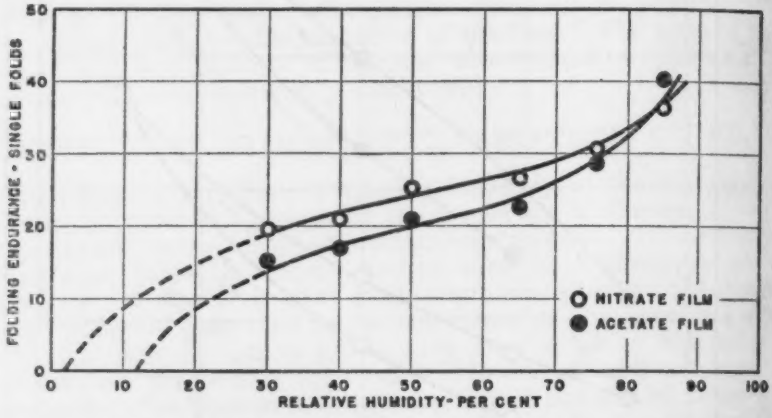

FIGURE 2.—*Effects of relative humidity on flexibility of cellulose acetate and cellulose nitrate motion-picture film.*

nately, this humidity is the same as that found satisfactory for the preservation of books in libraries;[6] therefore the use of filmslides presents no storage problems for libraries provided with air conditioning.

In libraries without conditioned air, satisfactory conditioning of films can be accomplished by means of humidification in small closed rooms or cabinets. Small closed rooms can be humidified with simple, relatively inexpensive air-conditioning units. This method has been employed successfully at the Library of Congress for filmslide storage space. Cabinets or small vaults can be humidified by using open vessels of the proper salt solution. A saturated solution of sodium dichromate, $Na_2Cr_2O_7.2H_2O$, because it gives 52-percent relative humidity at 68° F, should prove very satisfactory for the purpose. The solution should be exposed in shallow vessels with fans blowing air across the surface to promote the circulation of air. Inasmuch as considerable water may be absorbed from the air, an excess of dichromate should always be used to ensure saturation.

[6] BS Misc. Pub. M144 (1933).

Acetate filmslides should be stored in the conditioned chamber when not in actual use. In order to ensure sufficient contact with the humidified air to permit films to regain the moisture lost during projection, they should be stored in open reels without cans. When placed in the humidity room, all tightly wound rolls should be loosened and hung exposed so that the air will have free access to all parts of the film.

Successive projections drive out the film moisture more rapidly than it can be regained while tightly wound, and film in frequently used rolls may become brittle even when stored in the humidified atmosphere between projections, unless proper precautions are taken. Acetate film that has become brittle through excessive drying will regain its flexibility without permanent damage if the moisture is restored.

Moisture penetrates a tightly wound roll of film very slowly and it will require weeks to recondition a roll of brittle film properly, if the roll is not loosened to permit the air to get between the convolutions of film. Thorough conditioning can be accomplished in 10 to 30 minutes time by passing the film through a humid chamber or by other methods such as moistening with a mixture of water and a water-miscible volatile liquid as suggested by Crabtree and Carlton.[7] However, such methods are inconvenient for the average library, and are not considered necessary for conditioning the small rolls of film used as filmslides. Nitrate film has better folding endurance at low humidity than acetate film, and is less prone to break in use when dry. Hence, humidity control is less essential for nitrate film from the standpoint of flexibility. Filmslides in card or strip form that are not subject to winding on reels do not require moisture-content control if carefully handled when dry.

3. EXPANSION AND CONTRACTION

All changes of moisture content of films are accompanied by expansion or contraction. The dimensional changes resulting are not important to users of filmslides, except as uneven dimensional changes may cause curling of the films, and that is rarely sufficiently pronounced to give serious difficulty in a well-designed projector. The relationship between moisture-content increase and expansion of films is shown in figure 3. It will be noted that there is little difference between the two types of films as regards changes of dimensions per unit of moisture change. However, the moisture-content changes accompanying atmospheric variations are greater for acetate film as shown in figure 1. Furthermore, the acetate film always tends to curl more than the nitrate. While the expansion and contraction of film is considered a serious problem in film processing it does not often give trouble in the projection of films, as standard sprockets are made to allow for a shrinkage up to 1.5 percent.

Film shrinkage not caused by loss of moisture is caused by loss of volatile material. With acetate film this is confined to the loss of some traces of solvents, and possibly some plasticizer, during the first 6 months, after which there is no further measurable permanent change. Nitrate film shrinks more or less continuously throughout

[7] Trans. Soc. Motion Picture Engrs. no. 30 (1927).

its life because of the loss of solvents and of volatile decomposition products. Thus, printing from old nitrate negative will often require pulling the film down frame by frame in step printers, because the shrinkage will cause too much creep for continuous printing.

III. SCRATCHING OF FILMSLIDES

Examination of filmslides that have been used in reading projectors over a period of time has revealed considerable scratching, particularly on the emulsion side. Figure 4 shows a section of film that had been in use in a public library for a period of less than 2 years. This photograph was taken by reflected light to show the actual extent of damage. The scratching has not in this instance reached the stage where legibility is seriously impaired. However, it apparently brings

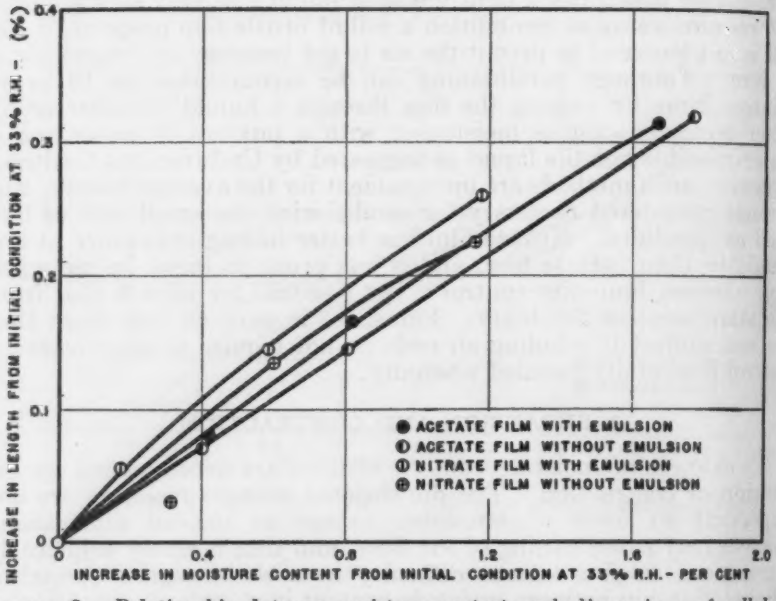

FIGURE 3.—*Relationship between moisture content and dimensions of cellulose acetate and cellulose nitrate motion-picture films.*

up a problem in connection with the care and use of filmslides. If the scratching cannot be avoided through improvements in the design of projectors and by keeping the films clean, it appears that the negative films of important records should be carefully preserved. It may be necessary to replace from time to time those positives that receive an excessive amount of use in projectors because of the accumulation of scratches. None of the commercial scratch-proofing treatments were tested for the purpose of determining their effectiveness in preventing scratching.

IV. CLEANING OF FILMS AND FILMSLIDES

It is important that film be kept clean, not only because extraneous material on the film affects legibility, but because dust particles cause scratching of the film when in use. The Bureau has found chemically

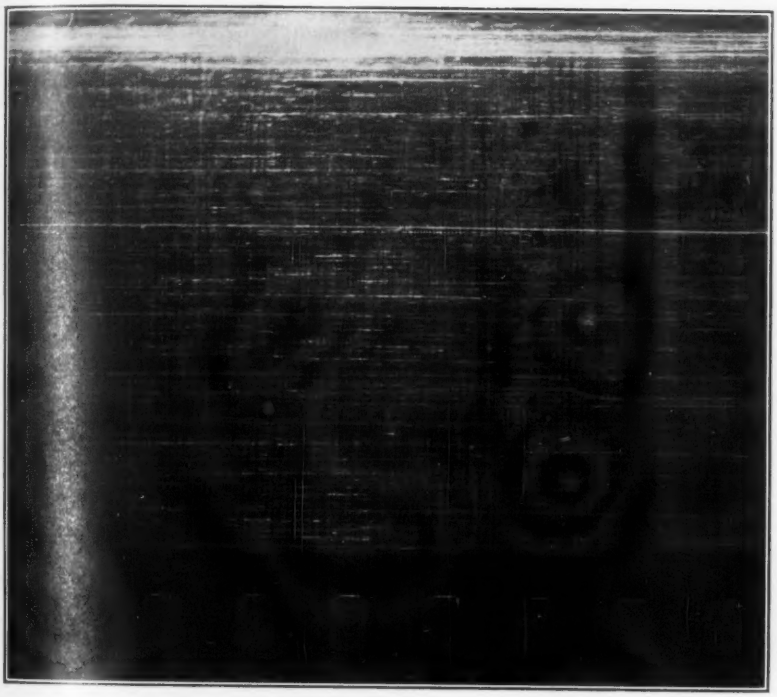

FIGURE 4.—*Scratches on cellulose acetate film resulting from normal use in projector.*

pure carbon tetrachloride to be quite satisfactory as a cleaning fluid. It is a good solvent for fats and oils, evaporates readily, is noncombustible, and does not have any measurable effect on the stability of the film. However, the fumes from this liquid are rather toxic and should not be inhaled. The use of this and other cleaning liquids is described by Crabtree and Carlton.[8] They recommend that the film be wiped gently with a silk plush moistened with the cleaning liquid. It is stated that cleaning machines suitable for roll films are available commercially, and that their use is preferable to hand cleaning. Film subject to intermittent use should be inspected at regular intervals for dust, finger marks, or traces of oil from the projectors that may make cleaning necessary to preserve the legibility and prevent scratching.

V. PROBLEMS IN THE STORAGE OF CELLULOSE NITRATE FILM

Nitrate motion-picture film presents special problems of storage and handling because of its highly combustible nature. It has a low ignition temperature combined with a high rate of combustion, and is capable of decomposition with little or no air supply, evolving poisonous, inflammable gases. Standards for the handling and storage have been established in the regulations of the National Board of Fire Underwriters.[9] However, storage from the standpoint of the preservation of valuable film requires not only the protection of the surroundings in the event of a fire within a storage vault but the proper isolation of films within the vault so that only the minimum amount of film will be destroyed in case of fire. Crabtree and Ives [10] found it possible to construct cabinets with metal-lined, insulated, individual film compartments that would prevent the complete burning of single rolls of film from igniting other film in the cabinet. Such cabinets are now available commercially, and their use inside safety vaults of suitable fireproof construction [11] [12] should afford adequate protection from fire. This system has been followed in the construction of the film-storage facilities at the National Archives.[13]

Film of the nitrate type is perishable because the cellulose nitrate base is unstable chemically. Deterioration is accelerated by increasing temperature or moisture, raising the pressure, or by contact with the products of decomposition. Hence, storage compartments and containers should be so vented as to prevent any accumulation of gases to raise the pressure as might result in sealed containers, or to injure the film by contact. Also from the standpoint of preservation, the lower the temperature and humidity the better. However, the advantages to be gained by storing at temperatures below about 50° F are probably more than offset by the added costs of air conditioning, and the tempering difficulties involved to prevent condensation when film is taken out of storage. Relative humidity above 50 percent is not recommended in any case. Even when stored under the most ideal conditions, nitrate film cannot be expected to last indefinitely, and valuable film should be inspected regularly for signs of

[8] Trans. Soc. Motion Picture Engrs. no. 30 (Aug. 1927).
[9] Regulations of the National Board of Fire Underwriters Governing the Production, Storage, and Handling of Nitrocellulose Motion-Picture Film. National Board of Fire Underwriters, New York, N. Y.
[10] J. Soc. Motion Picture Engrs. **15**, no. 3 (Sept. 1930).
[11] J. Soc. Motion Picture Engrs. **16**, no. 6 (June 1931).
[12] See foot note 9.
[13] J. Soc. Motion Picture Engrs. **26**, no. 6 (June 1936).

deterioration. Protective duplications should be made as soon as deterioration is evident, and it appears to be desirable to reproduce the negatives of permanent record value on the more stable acetate base before deterioration is evident.

VI. SUMMARY

The cellulose acetate film used as filmslides for records is hygroscopic. It adjusts its moisture content to conform to the humidity of the surrounding air, and changes in moisture content affect its properties.

The film is brittle under the conditions often encountered in rooms without air conditioning, making control of the moisture content essential. The conditions suggested for storage and use of film are those recommended for the preservation of books in libraries, namely, 50-percent relative humidity and 70 to 80° F. However, libraries without air conditioning can get satisfactory performance by storing the film slides in humidified cabinets or small rooms in which the relative humidity is not permitted to drop below 50 percent. Control of temperature is not considered essential, except that extreme variations should be avoided.

The emulsion side of film is easily scratched and despite care in handling, projecting, and cleaning to minimize abrasion, filmslides accumulate scratches. The positives in constant use may require occasional replacement; hence negative films of important records should be carefully preserved as a source of replacement.

Nitrate film is perishable and highly combustible. Storage of this type of film should be undertaken only in approved fireproof cabinets, and these should be within vaults of fireproof construction. Low temperature and low relative humidity are recommended to retard the deterioration of films in storage. Film containers for nitrate film should be vented to permit free escape of the products of decomposition (principally nitrous oxides) since their presence accelerates deterioration. It appears advisable to preserve pictures of permanent value by making negatives on acetate base, because of the perishable nature of nitrate film.

The authors are indebted to J. E. Gibson and M. Reiss for assistance in the work while assigned to the Bureau by the National Archives.

WASHINGTON, September 18, 1936.

U. S. DEPARTMENT OF COMMERCE NATIONAL BUREAU OF STANDARDS

RESEARCH PAPER RP943

Part of Journal of Research of the National Bureau of Standards, Volume 17, November 1936

HYDROCARBONS IN THE FRACTION OF A MIDCONTINENT PETROLEUM DISTILLING BETWEEN 115 AND 124° C[1]

By Robert T. Leslie[2]

ABSTRACT

The distillate from a midcontinent petroleum which boiled between 115 and 124° C was distilled and crystallized systematically in order to identify or detect, if possible, all the constituent hydrocarbons. Large quantities of paraffinic constituent were found in the distillate between 116 and 118.5° C. Mixed melting points and photomicrographs showed that this material was an additional quantity of the hydrocarbon which had been isolated in earlier work on the fraction. The physical properties of the most concentrated sample indicate that it was probably 2–methylheptane.

Smaller quantities of naphthenic constituents distilling between 119.2 and 119.8° C; 119.8 and 120.4° C; 120.4 and 120.8° C; and 122 and 124° C were crystallized repeatedly and the physical properties, cooling curves, and photomicrographs were studied. The photomicrographs of synthetic samples of *p*- and *m*-dimethylcyclohexanes and their mixtures were also studied. The first three fractions contained additional quantities of two naphthenic hydrocarbons which had been isolated before. They were characterized by a six-sided type of crystal, which was definitely neither *m*- nor *p*-dimethylcyclohexane, and a long prismatic type tending to develop fronds, which was probably *m*-dimethylcyclohexane. The fourth naphthenic fraction showed the characteristic crystal behavior of the predominant constituent but also showed the presence of a small quantity of paraffinic hydrocarbon. The combustion analysis also indicated the presence of about 8 percent of paraffinic constituent. Physical properties of all the fractions were determined.

It was estimated that the petroleum contained about 0.5 percent of 2–methylheptane, 0.2 percent of the cyclohexanes distilling between 119.2 and 120.8° C, and 0.04 percent of the cyclohexane boiling at 123.4° C.

CONTENTS

	Page
I. Introduction	761
II. Separation of the constituents by distillation and crystallization	762
III. Identification of the hydrocarbon isolated from the distillate boiling between 116 and 118.5° C	764
IV. Study of the constituents of the large-volume fraction distilling between 119.2 and 120.8° C	766
V. Tentative identification of the hydrocarbon isolated from the distillate boiling between 122 and 124° C	769
VI. Estimate of the relative quantities of the constituents	769

I. INTRODUCTION

Previous papers describe the separation of *n*–octane,[3] 2–methylheptane,[4] and a dimethylcyclohexane fraction [5] from the distillate of

[1] Financial assistance has been received from the research fund of the American Petroleum Institute. This work is part of Project 6, The Separation, Identification, and Determination of the Constituents of Petroleum. This paper was originally presented before the Pittsburgh meeting of the American Chemical Society.

[2] Research Associate at the National Bureau of Standards, representing the American Petroleum Institute.

[3] R. T. Leslie and S. T. Schicktanz, BS J. Research **6**, 377 (1931) RP282.

[4] R. T. Leslie, BS J. Research **10**, 609 (1933) RP552.

[5] R. T. Leslie, J. Research NBS **15**, 41 (1935) RP808.

a midcontinent petroleum boiling between 115 and 126° C. These hydrocarbons represent the three types of compounds of which the distillate is constituted, and the isolation of each required the development of new methods of attack. While the methods are still somewhat tedious and difficult, they have solved most of the problems which arise in the crystallization of the hydrocarbons probably present in this distillate. This paper describes the study of the considerable material remaining after the work described above. The material was subjected to exhaustive distillation and crystallization until practically all of it was reduced to large-volume fractions of which the major constituents could be identified.

II. SEPARATION OF THE CONSTITUENTS BY DISTILLATION AND CRYSTALLIZATION

The outline of the work is shown concisely in figure 1. Chart 1 of figure 1 shows the results of careful distillation following the removal of about 2 liters of octonaphthene from the distillate between 119 and 120° C.[6] The open circles and disks along the base line of this graph mark the approximate temperatures at which the known paraffinic and naphthenic compounds, respectively, are reported to boil.

Up to 119° C the low refractive indices indicated that the distillate was chiefly paraffinic. Cooling curves of the distillate in this range showed no arrests, and the material became glassy in appearance. Crystallization of the material which distilled between 116 and 118.5° C, by pouring a mixture of the oil with propane into liquid methane, resulted in the separation of a solid phase which yielded an oil with lower refractive index than that of the oil in the liquid phase. The distillate between 118.5 and 119.0° C gave only small amounts of solid phase in liquid methane.

Between 119 and 124° C the refractive indices of the fractions showed that they were highly naphthenic. The distillate which boiled at 119.8° gave a cooling curve with a slight arrest at −122°. Crystallization from methane of the distillate boiling between 119 and 124° C produced solid phases containing oil with higher index than that of the oil in the liquid phase. Above 124°, crystals with lower index than the liquid again resulted.

The two sections of distillate indicated by the cross-hatched areas were therefore crystallized separately, as shown by the diagram below chart 1. The areas in these diagrams are drawn on the same scale as the distillation charts and can be used for comparison of volumes. At this stage a total of about 9.5 liters of distillate in 200-ml lots was crystallized by mixing with propane and pouring into liquid methane.

The volumes of liquid and crystal fractions of the paraffinic distillate were in about the ratio of 2 to 3 and their refractive indices differed by 0.003. The crystal fraction was again crystallized as shown below chart 1 and was distilled carefully. The properties of the fractions from this distillate are shown in figure 2. The best fractions of the distillate were crystallized repeatedly until little improvement was observed in the shape of the cooling curve, and the properties of this final product are given in the table below chart 3 of figure 1.

[6] See footnote 5.

CHART 1 - DISTILLATION OF LIQUID FRACTION AFTER REMOVAL OF M - DIMETHYLCYCLOHEXANE

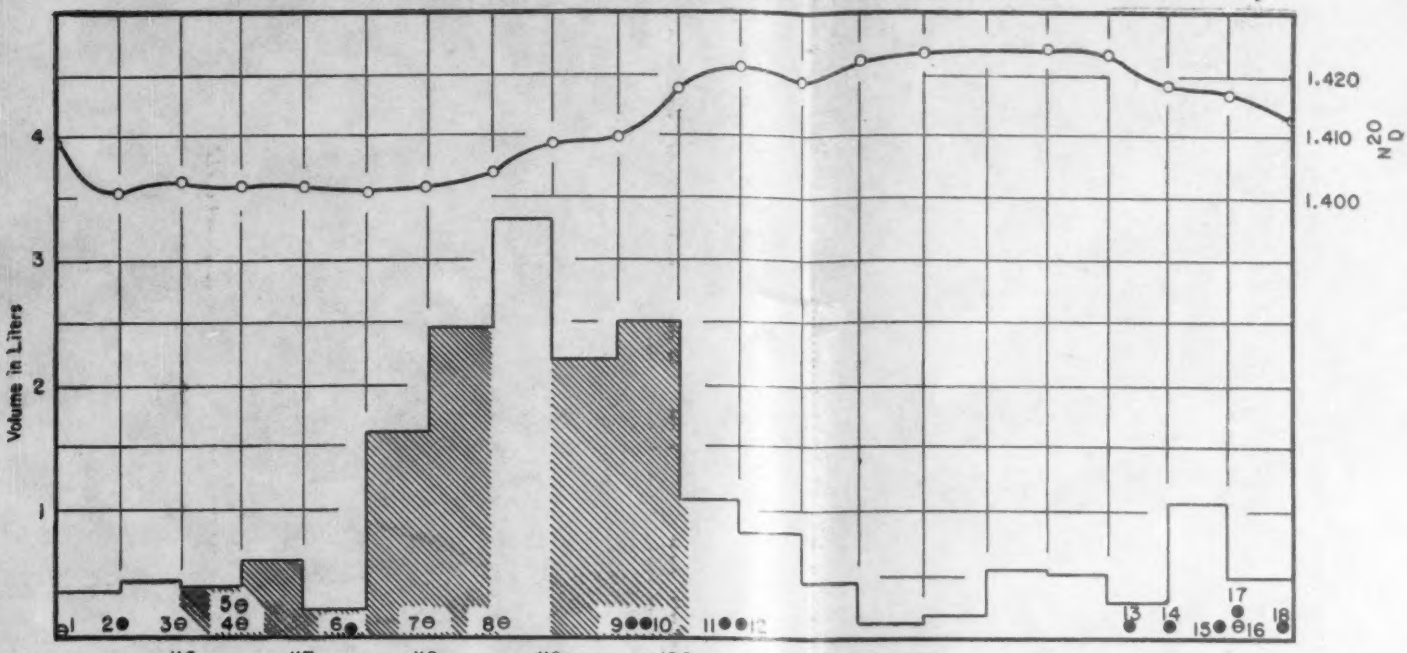

$R.I._D^{20}$ 1.399 - 1.403
Vol. 5000 ML
Chief Constituent Paraffin
Crystallized from liquid CH_4

1.403 | 1.407 | 3300 | Mixed

1.407 - 1.417 | 4500 | Naphthene Crystallized from CH_4

Distilled and Crystallized

1A 2A 3A 4A 5A 6A 7A

Product A
1300 ML

1.396
2000
117.3
-129.0

1.400
1900
116.9

1.397
2900

1.400
1800

1.416
2100
119.6
-114.5

1.410
1550
119.3

Liquid Fractions
7500 ML
Distilled

Distilled With Later Crystal Fractions

Chart 2

Chart 3

Hydrocarbons Reported in Literature

1	⊖	3 - Ethylhexane	[a]
2	●	1,1,3 - Trimethylcyclopentane	[b]
3	⊖	2 - Methyheptane	[b]
4	⊖	3,4 - Dimethylhexane	[c]
5	⊖	3 - Methylheptane	[d]
6	●	Cycloheptane	[e]
7	⊖	4 - Methylheptane	[c]
8	⊖	3 - Methyl - 3 - ethylpentane	[f]
9	●	trans - p - Dimethylcyclohexane	[g]
10	●	gem Dimethylcyclohexane	[g]
11	●	trans - m - Dimethylcyclohexane	[g]
12	●	1 - Methyl 3 - ethylcyclohexane	[h]
13	●	trans - o - Dimethylcyclohexane	[g]
14	●	1 - Mathyl 2 - ethylcyclopentane	[i]
15	●	1,1,3,3 - Tetramethyl 2 4 - dimethylcyclobutane	[b]
16	⊖	n - Octane	[j]
17	●	cis - p - Dimethylcyclohexane	[g]
18	●	cis - m - Dimethylcyclohexane	[g]

[a] International Critical Tables
[b] Beilsteins Erganzungswerk (1st Edition)
[c] Latham Clark, J. A. C. S. 33, 520 (1911)
[d] M. M. Tuot, Compt. Rend. 197, 1434 (1933)
[e] Beilsteins Handbuch (3rd Edition)
[f] Tatsi and Jurgens, Ber. 42, 2548 (1909)
[g] O. Miller, Bull. Soc. Belg. 44, 10, 513 (1935)
[h] N. D. Zelinsky, Ber. 35, 2679 (1902)
[i] Marshal and Perkin, Am. Soc. 51, 250 (1890)
[j] B. J. Mair, B S J. Res. 9, 457 Rp. 482 (1932)

CHART 2 - DISTILLATION OF LIQUID FRACTION

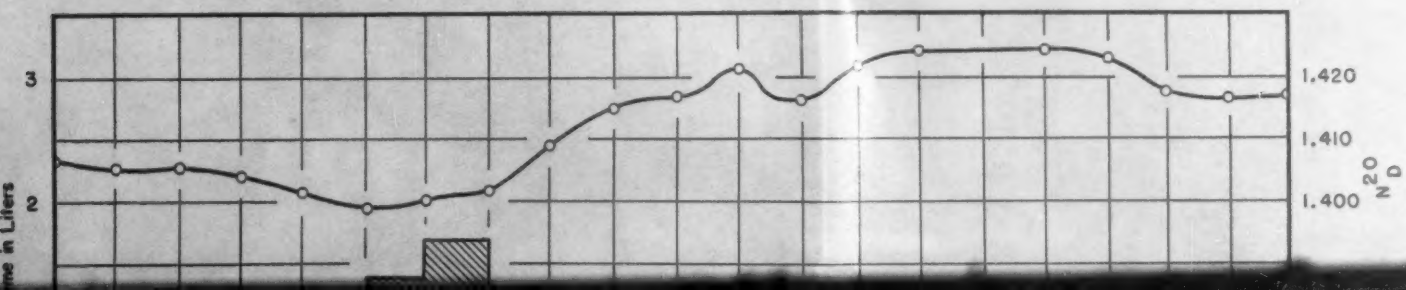

18 ● cis - m - Dimethylcyclohexane[9]

a International Critical Tables
b Beilsteins Ergenzungswerk (1st Edition)
c Latham Clark, J. A. C. S. 33, 520 (1911)
d M. M. Tuot, Compt. Rend. 197, 1434 (1933)
e Beilsteins Handbuch (3rd Edition)
f Total and Jurgens, Ber. 42, 2548 (1909)
g O. Miller, Bull. Soc. Belg. 44, 10, 513 (1935)
h N. D. Zelinsky, Ber. 35, 2679 (1902)
i Marshal and Perkin, Am. Soc. 51, 250 (1890)
j B. J. Mair, B S J. Res. 9, 457 Rp. 462 (1932)

Liquid Fractions
7500 ML
Distilled

Chart 2

Distilled
With Later
Crystal Fractions

Chart 3

CHART 2 - DISTILLATION OF LIQUID FRACTION

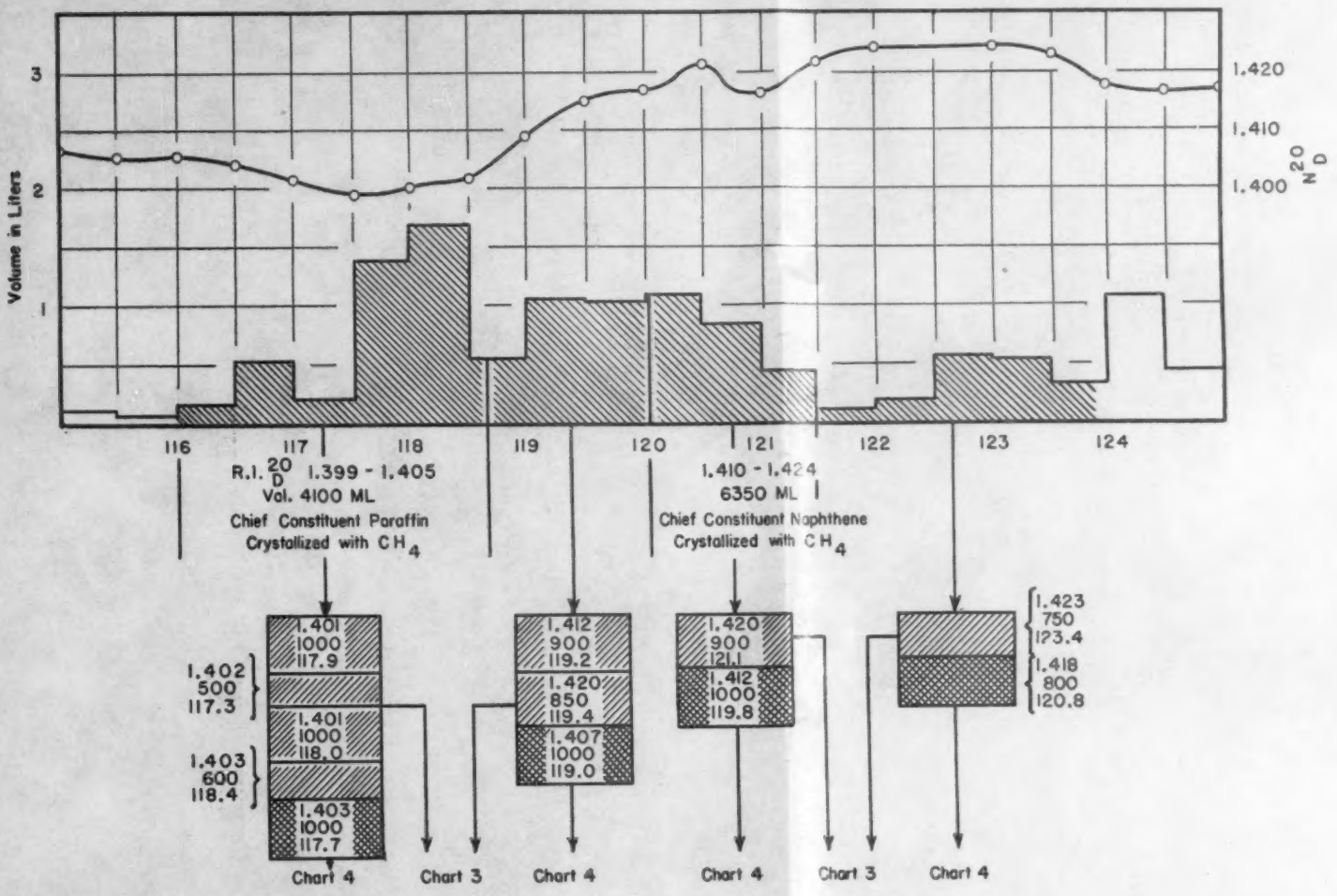

CHART 3 - DISTILLATION OF CRYSTAL FRACTIONS

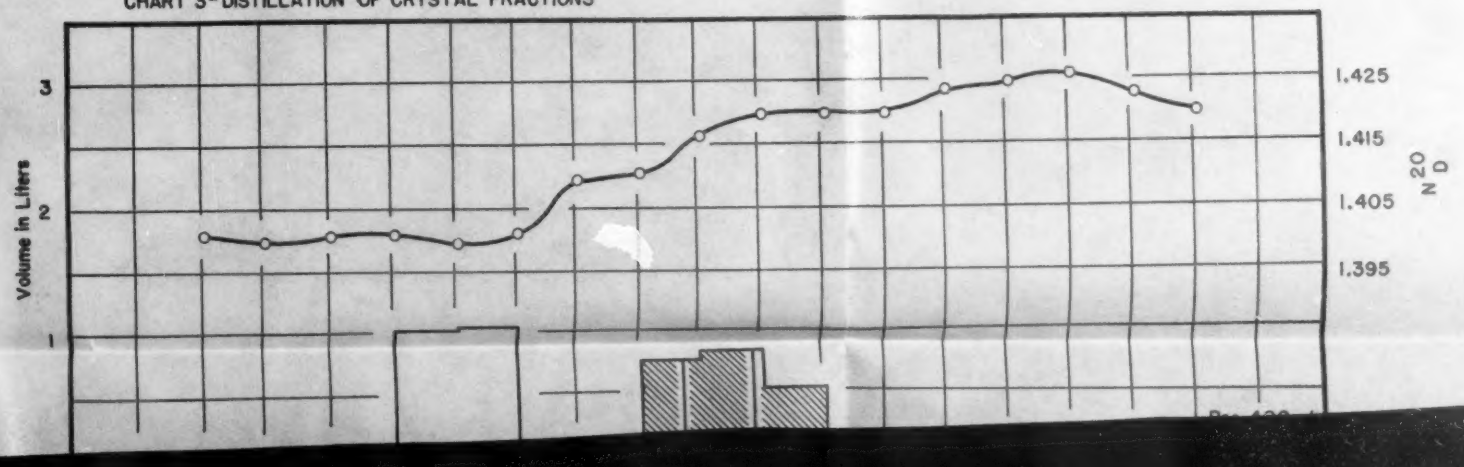

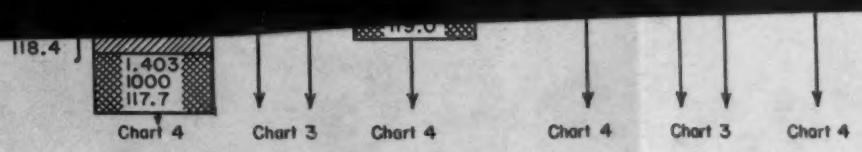

CHART 3 - DISTILLATION OF CRYSTAL FRACTIONS

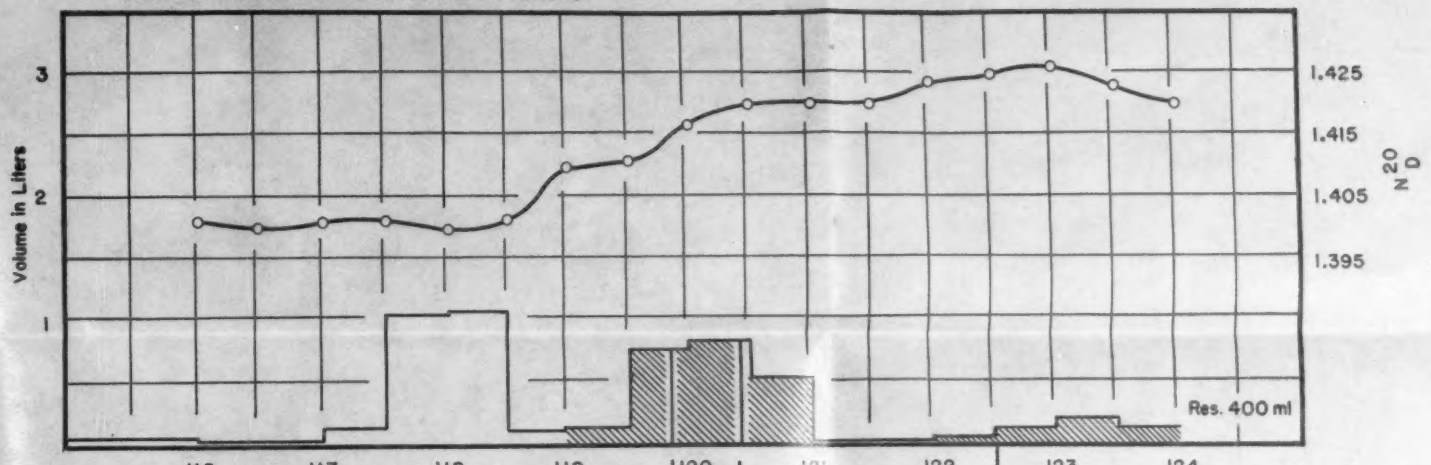

Divided into three lots based on distilling range

1.412 to 1.415	1.416 to 1.418	1.420 to 1.422	1.425 - 1.426
600	770	610	400
Crystallized with CH_4 and finally without solvent			Crystallized with CH_4 and finally without solvent

Legend

- Crystallizable distillate
- Crystal Fraction
- Liquid Fraction
- Uncrystallized distillate considered identified

All areas representing volumes are drawn to scale

Data in order

R.I $^{20}_{D}$
Vol. ml
B.P.°C
F.P.°C

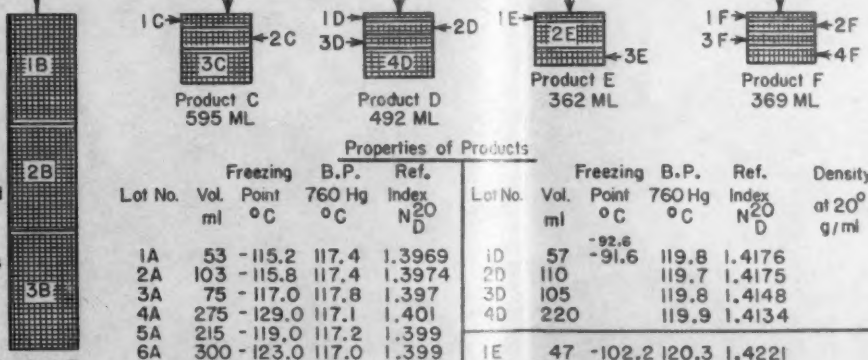

Properties of Products

Lot No.	Vol. ml	Freezing Point °C	B.P. 760 Hg °C	Ref. Index N^{20}_D	Density at 20° C g/ml
1A	53	-115.2	117.4	1.3969	
2A	103	-115.8	117.4	1.3974	
3A	75	-117.0	117.8	1.397	
4A	275	-129.0	117.1	1.401	
5A	215	-119.0	117.2	1.399	
6A	300	-123.0	117.0	1.399	
7A	285	-122.0	118.0	1.398	
1B	840		*117.6	1.3994	
2B	840		118.1	1.4008	
3B	960		118.6	1.4010	
1C	75	-95.6 -89.8	119.8	1.4176	
2C	190		119.5	1.4121	
3C	330		119.6	1.4121	
1D	57	-92.6 -91.6	119.8	1.4176	
2D	110		119.7	1.4175	
3D	105		119.8	1.4148	
4D	220		119.9	1.4134	
1E	47	-102.2	120.3	1.4221	
2E	205		120.7	1.4196	
3E	110		120.9	1.4186	
1F	60	-101.5	123.4	1.4238	0.76805
2F	70	-102.5	123.3	1.4231	
3F	92	-110.0	123.0	1.4234	
4F	147	-111.3	122.5	1.4212	

*Becomes vitreous

CHART 4 - DISTILLATION OF LIQUID FRACTIONS

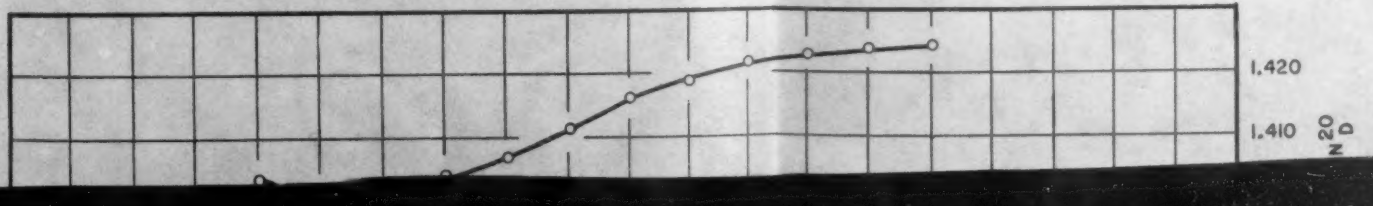

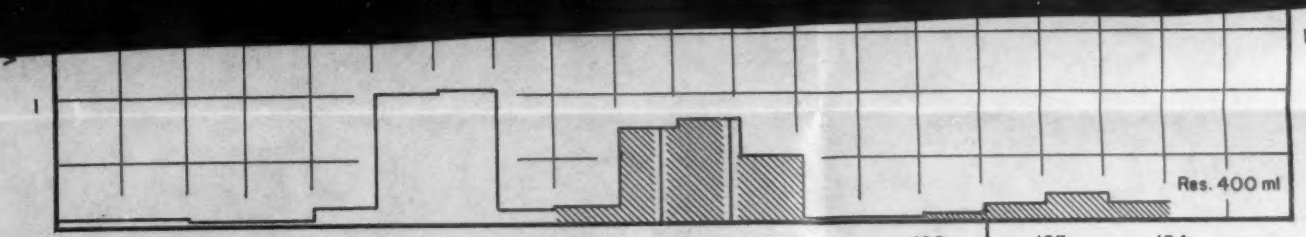

1.412 to 1.415 600 | 1.416 to 1.418 770 | 1.420 to 1.422 610

Crystallized with CH_4 and finally without solvent

1.425 - 1.426 400

Crystallized with CH_4 and finally without solvent

Divided into three lots based on distilling range

Legend

- Crystallizable distillate
- Crystal Fraction
- Liquid Fraction
- Uncrystallized distillate considered identified

All areas representing volumes are drawn to scale

Data in order

R.I n_D^{20}
Vol. ml
B.P. °C
F.P. °C

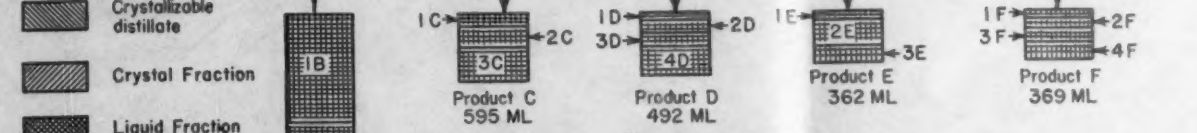

Properties of Products

Lot No.	Vol. ml	Freezing Point °C	B.P. 760 Hg °C	Ref. Index N_D^{20}	Density at 20° C g/ml
1A	53	-115.2	117.4	1.3969	
2A	103	-115.8	117.4	1.3974	
3A	75	-117.0	117.8	1.397	
4A	275	-129.0	117.1	1.401	
5A	215	-119.0	117.2	1.399	
6A	300	-123.0	117.0	1.399	
7A	285	-122.0	118.0	1.398	
1B	840		*117.6	1.3994	
2B	840		118.1	1.4008	
3B	960		118.6	1.4010	
1C	75	-95.6 -89.8	119.8	1.4176	
2C	190		119.5	1.4121	
3C	330		119.6	1.4121	
1D	57	-92.6 -91.6	119.8	1.4176	
2D	110		119.7	1.4175	
3D	105		119.8	1.4148	
4D	220		119.9	1.4134	
1E	47	-102.2	120.3	1.4221	
2E	205		120.7	1.4196	
3E	110		120.9	1.4186	
1F	60	-101.5	123.4	1.4238	0.76805
2F	70	-102.5	123.3	1.4231	
3F	92	-110.0	123.0	1.4234	
4F	147	-111.3	122.5	1.4212	

*Becomes vitreous

CHART 4 - DISTILLATION OF LIQUID FRACTIONS

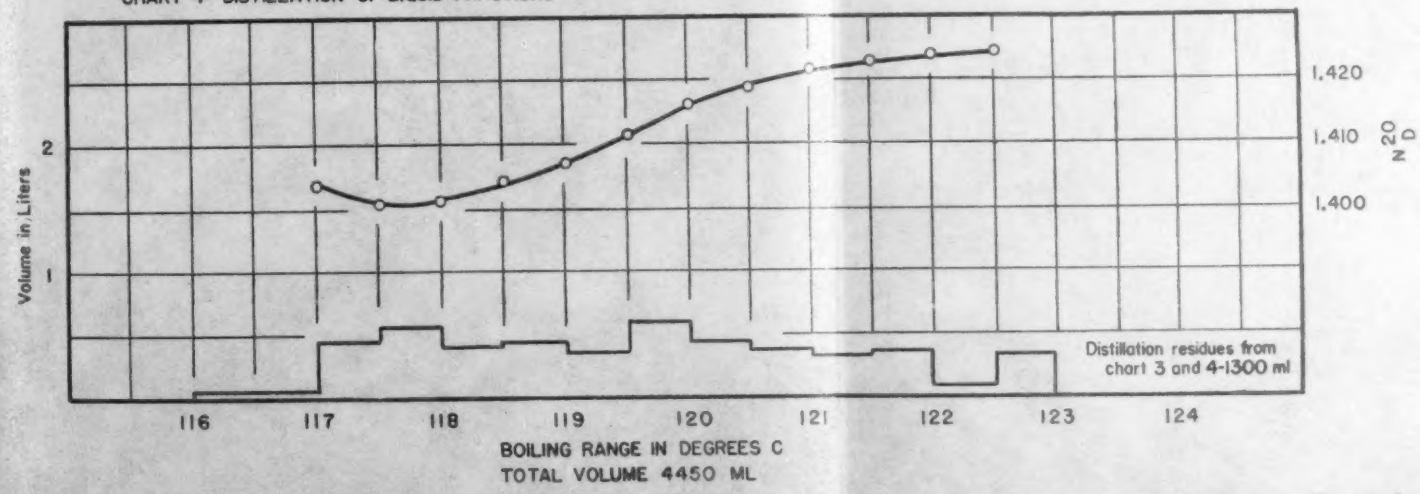

FIGURE 1.—*Flow-sheet of distillations and crystallizations performed in the isolation and detection of the constituent hydrocarbons of a petroleum distillate boiling between 115 and 124° C.*

Physical properties of the products (below chart 3). See legend and key to order and units in which properties are given.

99074—36 (Face p. 762)

UNIV. OF MICH.

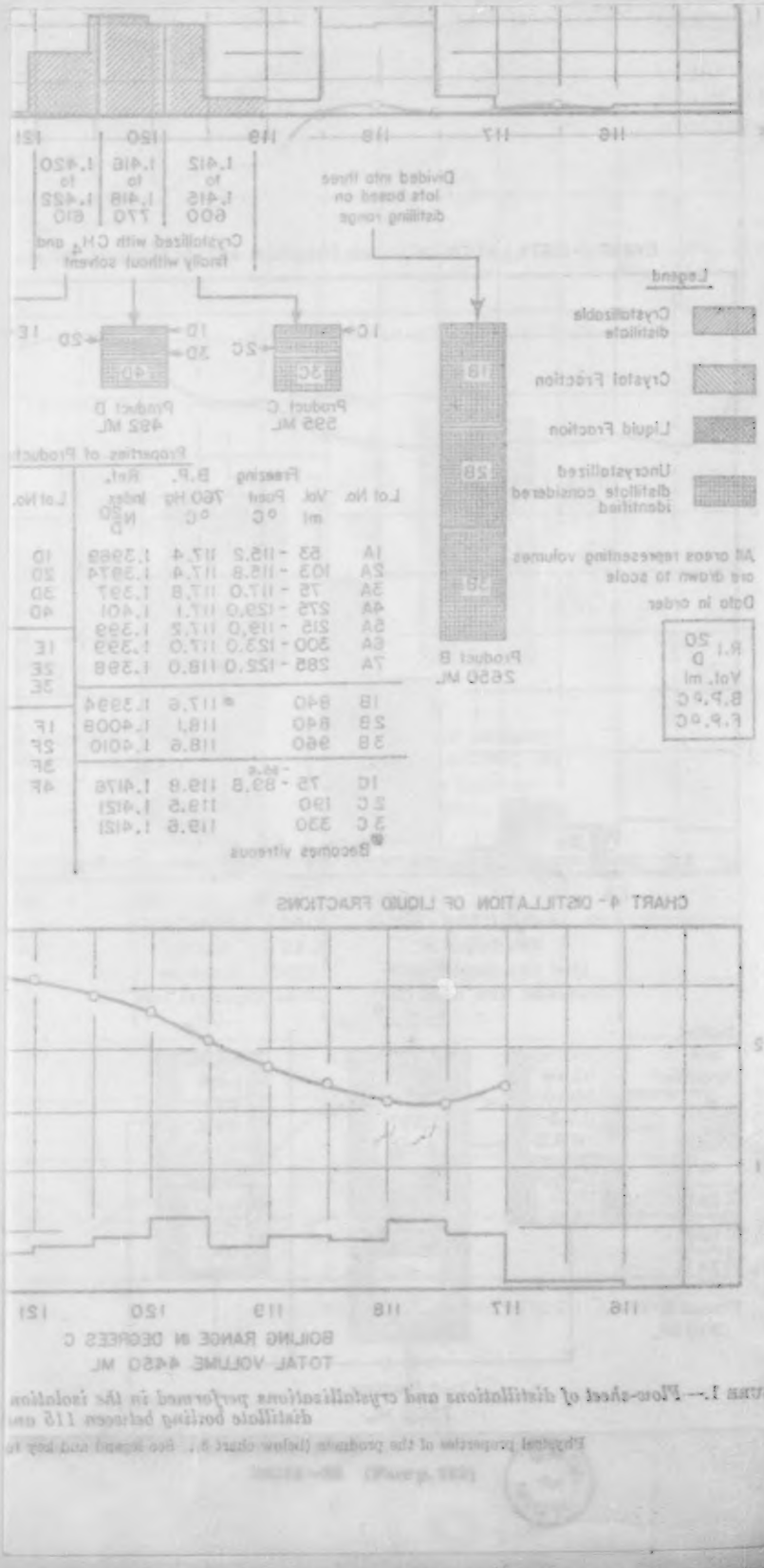

FIGURE 1.—Flow-sheet of distillations and crystallizations performed in the isolation
distillate boiling between 115 and

The ratio of the volumes of the liquid and crystal fractions of the naphthenic distillate was about 3 to 4 and the refractive indices differed by 0.006. The crystal fraction was distilled and combined with the distillate shown in chart 3.

All the liquid fractions, together with the part of the distillate of chart 1 which was not crystallized (118.5 to 119° C, and 120.2 and 124° C) were redistilled, and the results are shown by chart 2. This distillate was again divided into sections for crystallization. From the distillate between 116 and 118.6° C paraffinic crystals were again

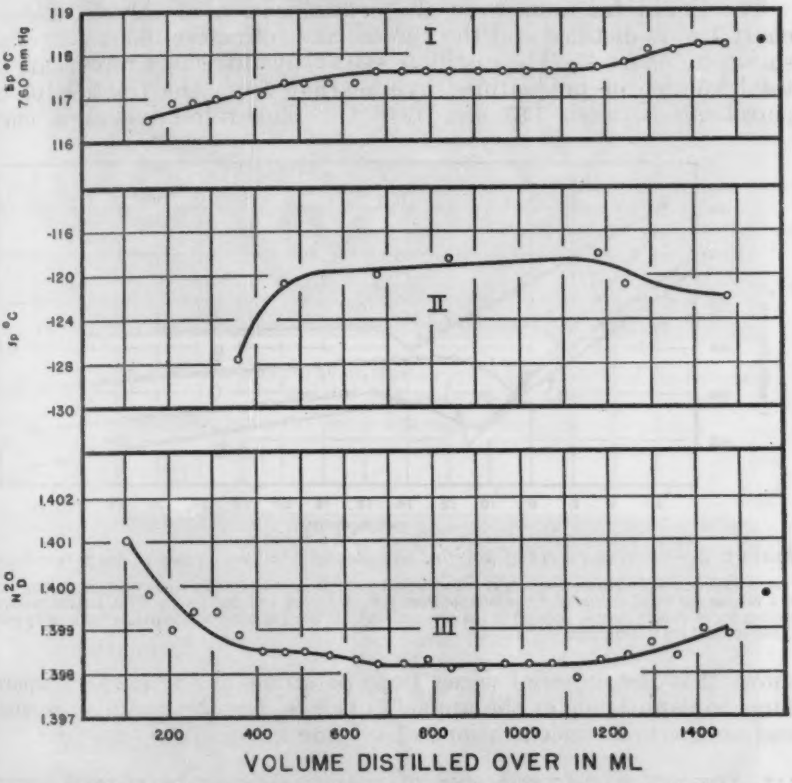

FIGURE 2.—*Properties of a fraction containing an isooctane crystallized from the petroleum after distillation, but before preparation of a final pure sample.*

Properties are plotted on the ordinates for each fraction of distillate against the total volume over on the abscissa.

obtained by freezing from solvents. The large volume distilling between 118.6 and 121.5° C was divided into two sections because it was suspected that there might be more than one naphthenic compound present in it. The section from 122.5 to 124° C definitely contained a naphthene not previously detected. The results of crystallizing the distillate from these sections are shown by the diagram below chart 2. About 10.5 liters of hydrocarbon was crystallized from methane in the second stage.

The crystal fractions from these crystallizations were distilled with the results shown by chart 3. The paraffinic crystal fraction again

concentrated between 117 and 118.5° C. This distillate was divided into three sections and was considered as identifiable without further treatment. The distillate between 119 and 121° C was divided into three parts, as shown by the cross-hatched areas, and crystallized repeatedly until the cooling curves of the best fractions did not improve rapidly with successive crystallizations. In the same way the distillate between 122.5 and 124° C was crystallized to obtain a fraction whose physical properties could be obtained for identification. The properties of all the products are given in the table below chart 3.

The liquid fractions from the crystallization of the distillate of chart 3 were distilled and the volume and refractive index curves are shown by chart 4. The distillate shown by this chart represents the total volume of unidentified hydrocarbon from the fraction of the petroleum between 115 and 124° C. The refractive-index curve

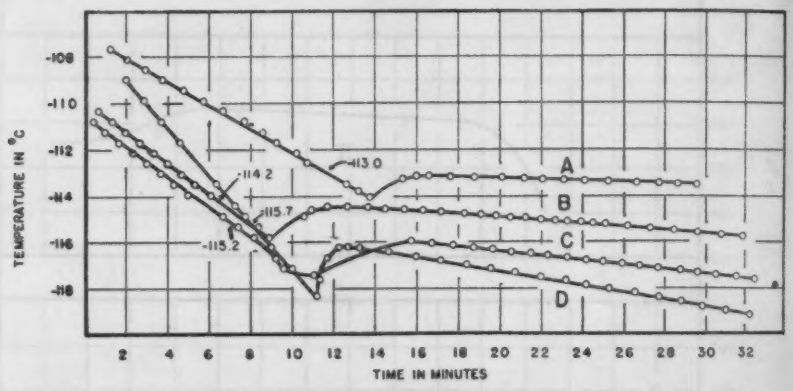

FIGURE 3.—*Cooling curves of purified samples of isooctanes isolated from petroleum.*

A, cooling curve of a purified sample of concentrated material isolated in a previous work; *B*, cooling curve of a mixture of equal volumes of the sample from previous work and the sample from present work; *C*, cooling curve of best sample isolated in the present work; *D*, cooling curve of sample represented by curve *C* before final crystallization.

shows that the material varies from paraffinic at the lower temperatures to naphthenic at the upper, as before, but the quantity is small and no marked concentrations of volume appear.

III. IDENTIFICATION OF THE HYDROCARBON ISOLATED FROM THE DISTILLATE BOILING BETWEEN 116 AND 118.5° C

The physical properties of the paraffin hydrocarbon (sample *1A*) are not greatly different from those of the hydrocarbon isolated in a previous work[7] and identified as 2–methylheptane. As in the previous work, none of the constants agree exactly with those of L. Clark,[8] but, in the absence of a sample of synthetic material with which to compare the properties, it has been assumed that the differences are due to differences in purity or to the methods of measuring the constants. This is not surprising when it is observed that the material isolated in this work has somewhat different constants from that

[7] R. T. Leslie, BS J. Research **10**, 609 (1933) RP552.
[8] J. Am. Chem. Soc. **31**, 107 (1909).

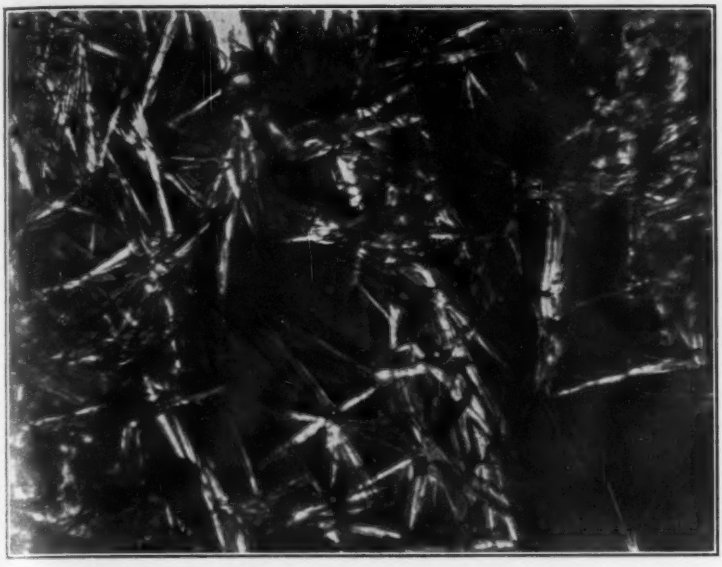

FIGURE 4.—*Photomicrograph of crystals from best sample of the isooctane isolated in present work.*

Crystallization induced by seeding with material precipitated from methane.

FIGURE 5.—*Photomicrograph of crystals of isooctane isolated in previous work.*

Crystallization induced as described in figure 4.

FIGURE 6.—*Crystals from a mixture of equal volumes of the hydrocarbons shown in figures 4 and 5.*

Note the similarity in the appearance of the crystals of all three samples.

previously obtained. To make certain that the differences were not due to the methods of observation, one of the less pure samples from the previous work was further concentrated, and its constants were found to be: boiling point 116.9° C (760 mm of Hg), refractive index, 1.3968^{20}_{D}, freezing point, −113.0° C. This boiling point is lower and the freezing point higher than those of sample *1A*. In figure 3 are shown the cooling curves of sample *1A*, of the purified sample from the previous work, and of a mixture of equal volumes of the two. Since the cooling curve of the mixture lies between the

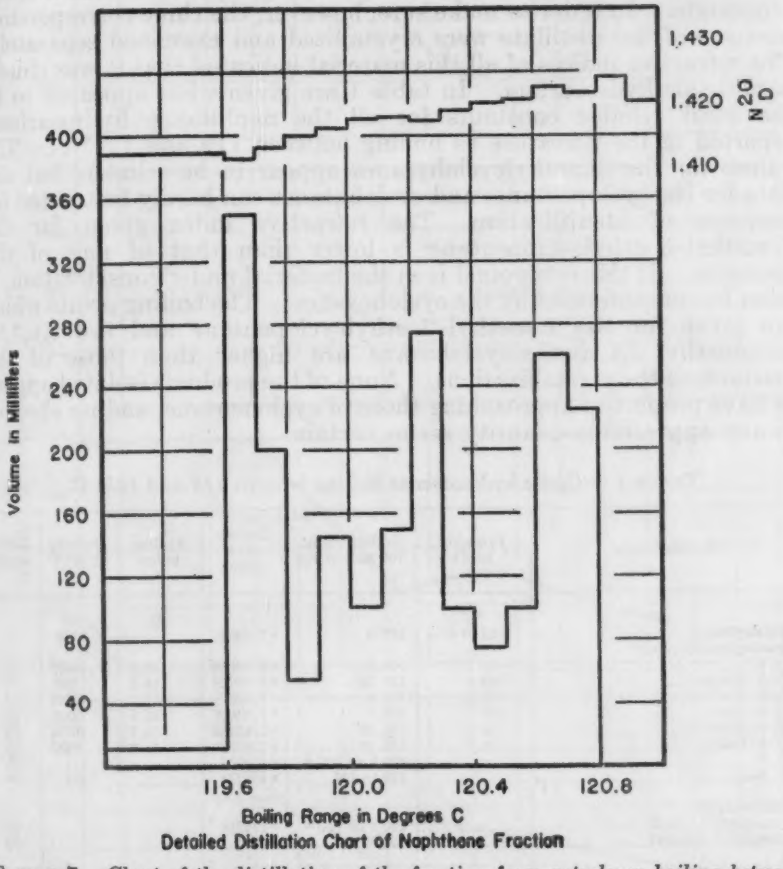

FIGURE 7.—*Chart of the distillation of the fraction from petroleum boiling between 119.2 and 120.8°* C.

These are the same data given in chart 3 of figure 1 but plotted at 0.1° C intervals instead of 0.5° C intervals.

other two it appears that the chief constituents of both samples are identical or that they form solid solutions.

Photomicrographs of the crystals from the three samples are shown in figures 4, 5, and 6. All three show needle-like crystals which are similar in appearance.[9]

[9] All photomicrographs in this paper were taken with an especially constructed microscope which will be described later. Magnification about 80×. Compare the photomicrographs of these hydrocarbons with those from paraffin waxes: C. C. Bachler and G. D. Graves, Ind. Eng. Chem. **19**, 718 (1927); S. W. Ferris, N. C. Cowles, Jr., and L. M. Henderson, Ind. Eng. Chem. **23**, 681 (1931); G. D. Graves, Ind. Eng. Chem. **23**, 702 (1931).

IV. STUDY OF THE CONSTITUENTS OF THE LARGE-VOLUME FRACTION DISTILLING BETWEEN 119.2 AND 120.8° C.

In figure 7 is shown a distillation chart of this fraction in which the volumes and refractive indices are plotted for 0.1° instead of 0.5° intervals as they are in chart 3 of figure 1. Three distinct concentrations of volume appear within the range when the data are plotted in this way. This may have been fortuitous, since it is doubtful whether the distillation was precise enough to produce such a sharp separation. In order to make sure, however, the three corresponding portions of the distillate were crystallized and examined separately. The refractive indices of all this material indicated that it was chiefly naphthenic hydrocarbon. In table 1 are given what appeared to be the most reliable constants for all the naphthenic hydrocarbons reported in the literature as boiling between 119 and 124° C. The values for the dimethylcyclohexanes appear to be reliable, but the data for the cyclopentanes and cyclobutanes can hardly be trusted for purposes of identification. The refractive index given for the 1–methyl–3–ethylcyclopentane is lower than that of any of the products. If this compound is in the material under consideration, it must be contaminated by the cyclohexanes. The boiling points which are given for the 1–methyl–2–ethylcyclopentane and the 1,1,3,3–tetramethyl–2,4–diethylcyclobutane are higher than those of the products of the crystallizations. None of the products isolated appear to have properties approaching those of cycloheptane, and its absence in any appreciable quantity seems certain.

TABLE 1.—*Cyclic hydrocarbons boiling between 118 and 125° C*

Hydrocarbon	Freezing point	Boiling point, 760 mm of Hg	Refractive index	Aniline point	Density at 20° C	References
	°C	°C		°C	g/ml	
Cycloheptane	−12 to −13	118.7[a]	[c] 1.44521		0.8108	[6]
Dimethylcyclohexanes:						
1, 1–	−34.1	119.8	[c] 1.42950	45.4	.78073	[1]
1, 2– (*trans*–)	−89.4	123.70	[c] 1.42768	48.3	.77601	[1]
1, 3– (*trans*–)	−79.4	120.4	[c] 1.42376	51.7	.76628	[1]
1, 3– (*cis*–)	−100	124.9	[c] 1.43099	46.3	.78348	[1]
1, 4– (*trans*–)	−37.2	119.63	[c] 1.42160	52.7	.76264	[1]
1, 4– (*cis*)	−91.6	124.59	[c] 1.43029	46.9	.78271	[1]
1, 3–		120.9 to 122.5	[b] 1.4253		.774	[2]
1, 4–		122 to 124	[b] 1.4271		.777	[2]
Cyclopentanes:						
1-methyl-3-ethyl		120.5 to 121.7[a]	[c] 1.4214			[2]
1-methyl-2-ethyl		124.7[a]				[4]
Cyclobutanes:						
1,1,3,3-tetramethyl 2,4-diethyl-cyclobutane.		124 to 125.7[a]				[5]

[1] O. Miller, Bul. soc. chim. Belg. **44**, 10, 513 (1935).
[2] F. K. Signaigo and P. L. Cramer, J. Am. Chem. Soc. **55**, 3326 (1933).
[3] N. D. Zelinsky, Ber. deut. chem. Ges. **35**, 2679 (1902).
[4] Marshal and Perkin, J. Chem. Soc. Trans. **57**, 250 (1890).
[5] Beilsteins Ergänzungsband **5**, 25 (Wedekind and Miller, Ber. deut. chem. Ges. **44**, 3236).
[6] Beilsteins Handbuch **5**, 29, 4th ed. (Willstatter, Kametaka, Ber. deut. chem. Ges. **41**, 1483).
[a] $n_{Hej}^{18.3}$; [b] n_{NaD}^{20}; [c] n_{NaD}^{18}.

The cooling curves of the samples from the three large fractions after repeated crystallization are shown by curves *1C*, *1D*, and *1E* of figure 8. Curves *1C* and *1D* show a peculiar double halt

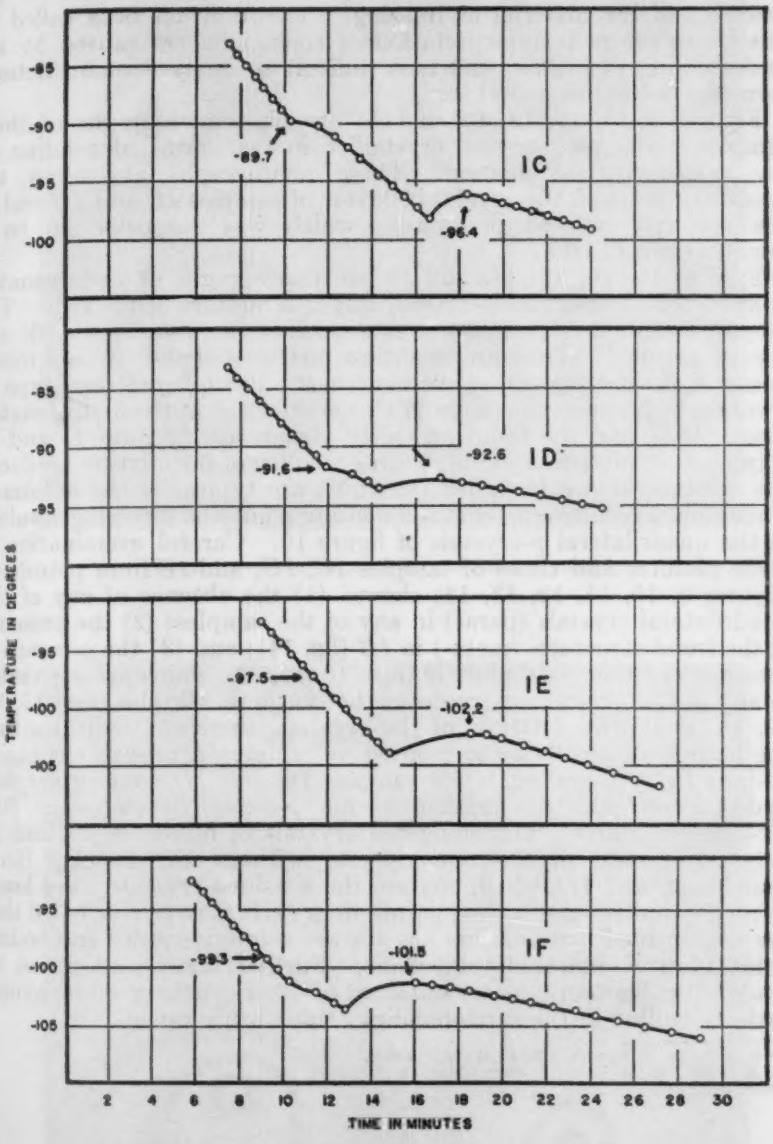

COOLING CURVES OF OCTONAPHTHENE FRACTIONS FROM PETROLEUM DISTILLING BETWEEN 119° AND 124°

FIGURE 8.—*Cooling curves of best samples isolated from distillate between 119.2 and 124° C*

1C, cooling curve of best sample from distillate between 119.2 and 119.8° C; *1D* best sample from distillate between 119.8 and 120.4° C; *1E*, best sample from distillate between 120.4 and 120.8° C; *1F*, best sample from distillate between 122 and 124° C.

similar to those in some of the curves obtained on a naphthene previously separated at about this temperature.[10] Curve *1E* does not exhibit this behavior. The double arrests may indicate eutectics, transitions in crystal forms, or metastable states due to the viscosity of the material at freezing. Attention has been called by Skau [11] to errors in interpretation of cooling curves caused by the undercooling of phases, and it is difficult to analyze such mixtures from the cooling curves alone.

Figures 9, 10, 11, 12, 13, and 14 are photomicrographs of these samples. The tendency to crystallize in two forms, depending on the treatment, is apparent. These photographs also show the similarity between the crystal behavior of samples *1C* and *1D* and of the material isolated previously, which was suspected to be a dimethylcyclohexane.

Figures 15, 16, 17, 18, and 19 are photographs of hydrogenated *m*-xylene, hydrogenated *p*-xylene, and of a mixture of the two. The preparation of these samples was described in connection with the previous work.[12] They are doubtless mixtures of the *cis*- and *trans*-forms of the corresponding cyclohexanes. The quadrilateral type of crystal which appears in figure 17 is characteristic of the hydrogenated *p*-compound and the frond or spiked structure of figures 15 and 16 is typical of the *m*-compound. Rapid cooling of the mixture produced the crystals, shown in figure 18, which are typical of the *m*-isomer, while slow warming almost to the melting point and recooling resulted in the quadrilateral *p*-crystals of figure 19. Careful examination of these pictures and those of samples *1C*, *1D*, and *1E* from petroleum (figures 9, 10, 11, 12, 13, 14) shows: (1) the absence of any of the quadrilateral crystals (para-) in any of the samples; (2) the presence of the frond structure (meta-) in *1E* (fig. 14); and (3) the presence of six-sided crystals in *1C* and *1D* (figs. 10, 11, 12), which are not visible in any of the photomicrographs of the synthetic samples (figs. 15, 16, 17, 18, and 19). Analysis of the crystals, therefore, indicates that the petroleum distillate represented by sample *1E* probably contains *m*-dimethylcyclohexane, while samples *1C* and *1D* contain a cyclic hydrocarbon, which is neither *m*- nor *p*-dimethylcyclohexane (the six-sided crystals). The elongated crystals of figures 9, 10, and 13 may be crystals of the *m*-compound without the fronds. Since samples *1C* and *1D*, which contain the six-sided crystals, have lower refractive indices and boiling points than *1E* it may be concluded that the unidentified hydrocarbon has a lower refractive index and boiling point than *m*-dimethylcyclohexane. Further identification can be made when photographs are obtained of other synthetic cyclic hydrocarbons boiling in the corresponding temperature range.

[10] R. T. Leslie, J. Research NBS 15, 41 (1935) RP808.
[11] E. L. Skau and B. Saxton, J. Phys. Chem. 37, 183 (1933).
[12] See footnote 10.

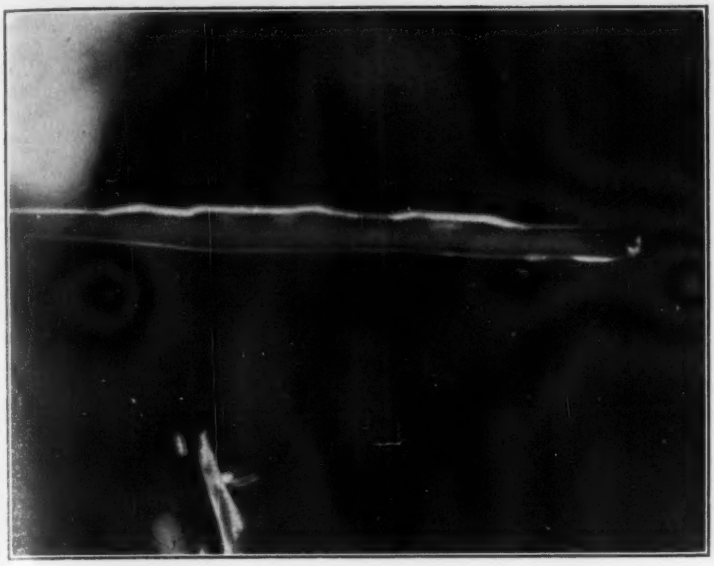

FIGURE 9.—*Long platelike crystal form of sample 1C.*

FIGURE 10.—*Crystals of sample 1C showing long plates with six-sided crystals attached.*

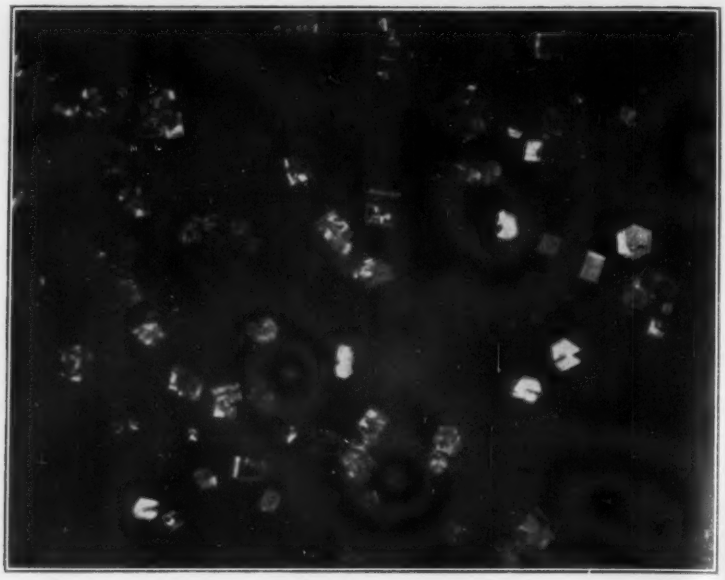

FIGURE 11.—*Crystals from sample 1C, showing only the six-sided forms.*

These were obtained by cooling the material below its initial freezing point until a dense matrix of crystals was visible, warming till almost all of the crystals melted, and recooling gradually.

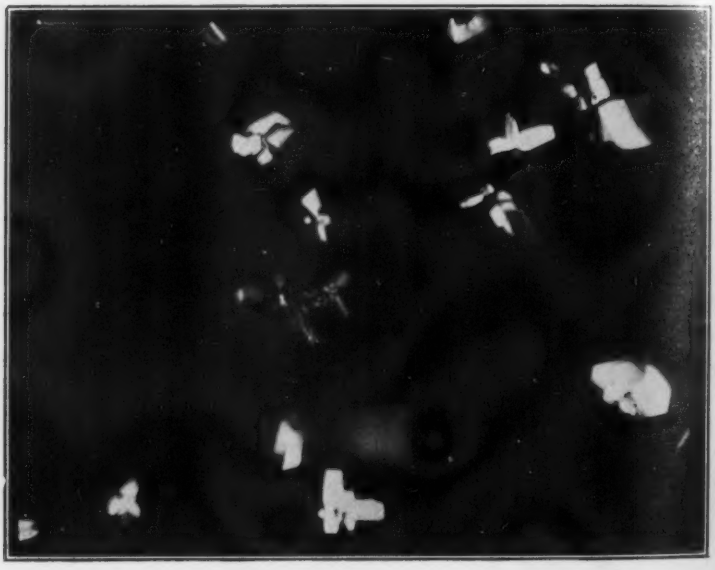

FIGURE 12.—*Crystals from sample 1D, showing six-sided types.*

These were obtained as described under figure 11.

FIGURE 13.—*Crystals from sample 1D, showing long platelike crystals.*
Compare with figure 10.

FIGURE 14.—*Crystals from sample 1E, showing long, platelike crystals with tendencies to grow fronds.*

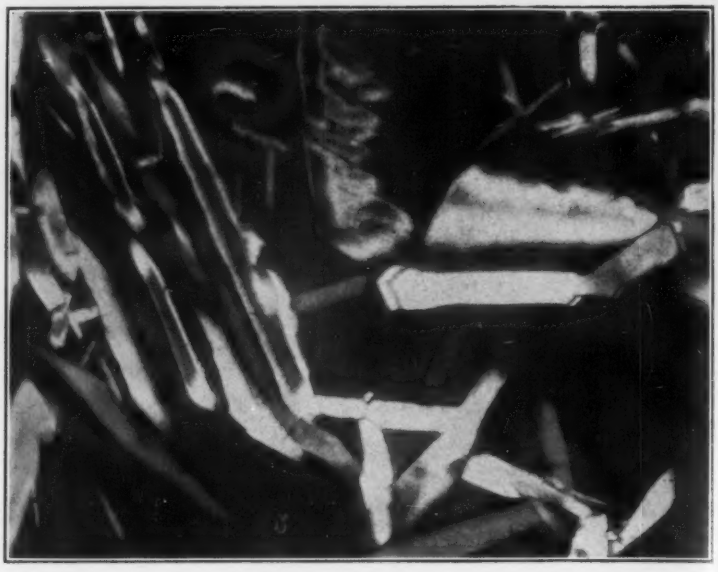

FIGURE 15.—*Crystals of hydrogenated m-xylene, showing long platelike crystals with tendencies to grow fronds.*

Compare with figure 14.

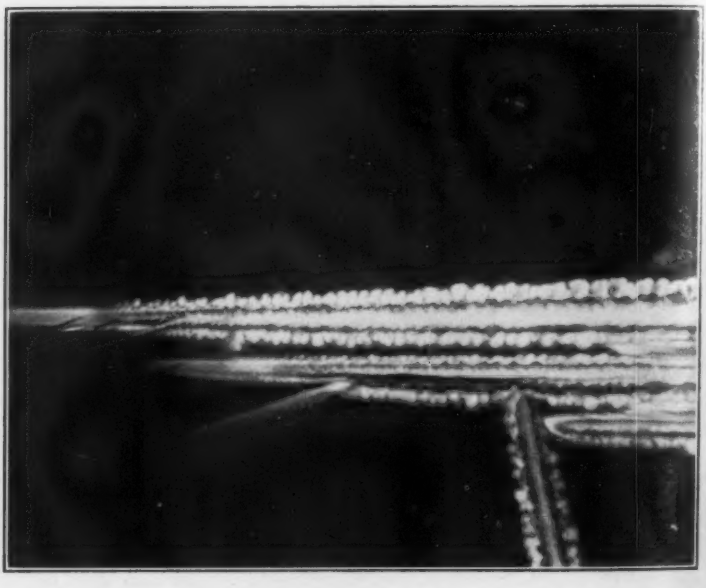

FIGURE 16.—*Another example of the frondlike growth characteristic of the hydrogenated m-xylene.*

Compare with figure 14.

FIGURE 17.—*Crystals from hydrogenated p-xylene, showing the characteristic quadrilateral type of crystal.*

Observe absence of such crystals in figures 9, 10, 11, 12, and 13.

FIGURE 18.—*Crystals formed in a mixture of equal volumes of the hydrogenated m- and p-xylene, showing fronds of the m-isomer.*

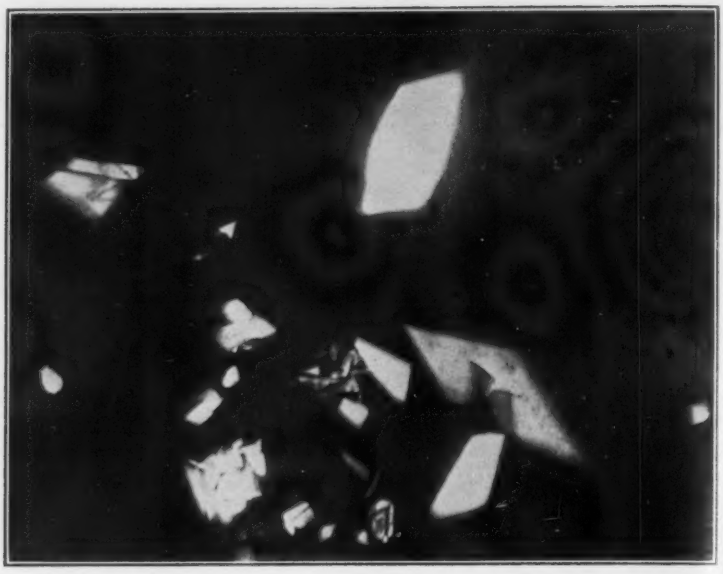

FIGURE 19.—*Crystals from same mixture as figure 18, but warmed almost to melting point and recooled slowly.*

Quadrilateral crystals of the *p*-isomer visible. Compare figures 18 and 19 with figures 9, 10, 11, 12, and 13. Difference in crystal behavior is to be noted.

FIGURE 20.—*Crystals from sample 1F, showing presence of needles which is probably a paraffinic constituent.*

This mat of crystals appears from the melt on undercooling.

FIGURE 21.—*Crystals from sample 1F, showing platelike crystals characteristic of the octonaphthene.*

These crystals were obtained by warming the mat shown in figure 20 almost to the melting point and recooling gradually.

UNIV. OF MICH.

V. TENTATIVE IDENTIFICATION OF THE HYDROCARBON ISOLATED FROM THE DISTILLATE BOILING BETWEEN 122 AND 124° C.

At the beginning of the work on the petroleum, the large volumes of *n*-octane masked the presence of any cyclic hydrocarbons in this boiling range,[13] and it is possible that quantities of cycloparaffins were contained in the residual paraffin distillate boiling above this temperature. The product as represented by sample *1F* was still contaminated with *n*- or iso-paraffin constituent, as shown by the prismatic needles which are visible in figure 20. The cooling curve shown by *1F* of figure 8 also suggests the presence of another constituent. Three combustion analyses gave an average value of 1.0108, with an average deviation of 0.0021, for the ratio of H_2O to CO_2. This indicates the presence of 8.6 ± 1.6 percent of paraffinic constituent. Careful warming of the crystals shown in figure 20 almost to the melting point and recooling developed the crystals shown by figure 21. These crystals are definitely angular plates with angles differing from those observed in samples *1C*, *1D*, and *1E*. The constants for the sample *1F* are given in the table below chart 3 of figure 1. The density was determined by the Division of Weights and Measures at the National Bureau of Standards and was estimated to be correct within 0.00005. The critical-solution temperature in aniline was found to be 52° C. Examination of table 1 shows that the material may be *trans-o*-dimethylcyclohexane containing enough paraffinic constituent to lower its refractive index and density.

VI. ESTIMATE OF THE RELATIVE QUANTITIES OF THE CONSTITUENTS

It must be emphasized that estimates of percentages in this work are only indications of the relative amounts of the constituents present. In all estimates made by the author the volumes, in liters, actually isolated have been doubled to compensate for losses and this quantity has been divided by 2,270 liters (the original volume of the crude petroleum from which the gasoline fraction was obtained). On this basis the estimated quantity of isooctane which boils at about 117° C should be increased from 0.15 percent (as given previously)[14] to 0.5 percent, the quantity of cyclohexanes from the distillate between 119.2 and 120.8° C should be increased from 0.15 percent[15] to 0.2 percent, and the quantity of cycloparaffin boiling at 123.4° can be placed at 0.04 percent.

The author acknowledges the assistance of W. W. Hewer in the crystallization and the photographic work, and for the determination of the critical solution temperatures in aniline.

WASHINGTON, August 12, 1936.

[13] R. T. Leslie and S. T. Schicktanz, BS J. Research **6**, 377 (1931) RP282.
[14] R. T. Leslie, BS J. Research **10**, 609 (1933) RP552.
[15] R. T. Leslie, BS J. Research **15**, 41 (1935) RP808.

U. S. Department of Commerce National Bureau of Standards

RESEARCH PAPER RP944

Part of Journal of Research of the National Bureau of Standards, Volume 17, November 1936

ESTIMATION OF CHROMATICITY DIFFERENCES AND NEAREST COLOR TEMPERATURE ON THE STANDARD 1931 ICI COLORIMETRIC COORDINATE SYSTEM

By Deane B. Judd

ABSTRACT

Estimation of chromaticity differences has been facilitated by the preparation of a standard mixture diagram showing by a group of ellipses the scale of perceptibility at the various parts of the diagram. The distances from the boundaries of the ellipses to their respective "centers" all correspond approximately to the same number (100) of "least perceptible differences."

The estimation of nearest color temperature has been facilitated by the preparation of a mixture diagram on which is shown a family of straight lines intersecting the Planckian locus; each straight line corresponds approximately to the locus of points representing stimuli of chromaticity more closely resembling that of the Planckian radiator at the intersection than that of any other Planckian radiator.

CONTENTS

	Page
I. Introduction	771
II. Estimation of chromaticity differences	773
III. Nearest color temperature	774

I. INTRODUCTION

Since the adoption, in 1931, by the International Commission on Illumination of a standard colorimetric coordinate system, by far the majority of fundamental colorimetric specifications have been expressed in that system.[1] A minor defect which is coming to be more keenly felt as the use of the system becomes more extended is the difficulty of interpreting differences in position on the standard mixture diagram in terms of degree and kind of chromaticity difference. The discovery of a projective transformation of the standard system whose Maxwell triangle yields nearly uniform chromaticity scales [2] is a step toward remedying this defect; on this triangle the length of any line is approximately proportional to the perceptibility of the chromaticity difference between the stimuli represented at the extremes of the line.

[1] D. B. Judd, *The 1931 ICI standard observer and coordinate system for colorimetry*, J. Opt. Soc. Am. **23**, 359 (1933).

[2] D. B. Judd, *A Maxwell triangle yielding uniform chromaticity scales*, J. Research NBS **14**, 41 (1935) RP756; also J. Opt. Soc. Am. **25**, 24 (1935).

The substitution of the uniform-chromaticity-scale (UCS) system for the ICI system immediately suggests itself, but there are several reasons why this should not be done at present. In the first place, although the UCS system was derived from and is a valid representation of about nine-tenths of the available data on sensibility to chromaticity differences, and although, furthermore, many divergent applications of it [3] have shown it to be a definite improvement in spacing over the ICI system, nevertheless the original data are neither sufficiently numerous nor sufficiently self-consistent to be considered definitely final. It is probable that further important improvements in spacing can be made. A second reason for adherence to the present standard ICI system is that the ICI system is more suited to the representation of photometric quantities; this may be seen from the fact that the ICI luminosity coefficients are 0, 1, 0, while the UCS luminosity coefficients are 0.08852, 0.11112, −0.09802. A third reason is that the applicability of data obtained by observing small apertures to observation of chromaticity differences between extended surface colors has not been demonstrated, nor have these data on small differences been shown to apply by simple addition to large chromaticity differences. The optimistic view that such applicability does not require demonstration has been fairly general, but extensive data which are being accumulated do not wholly justify this view. They indicate that the UCS triangle is applicable to small chromaticity differences between surface colors of large as well as small extent; furthermore, the application of the UCS triangle to large as well as small chromaticity differences between point sources (signal lights) fails to result in any discrepancies not explainable by aberrations of the lens system of the eye; but there are data which suggest that the UCS triangle is not applicable to large chromaticity differences between extended surfaces. For these three reasons no departure from the standard 1931 ICI system is proposed at this time.

Accordingly, then, for research purposes many determinations in the colorimetry section of the National Bureau of Standards are being recorded in duplicate, once in the ICI system and once in the UCS system; but there are also many determintions which are expressed in the ICI system alone. For such determinations some of the advantages of the UCS system may be obtained if there is available a graphical representation of the relative scales of the two systems. The present paper serves to give two such representations; one of them shows how the scale of perceptibility varies over the ICI mixture diagram on the assumption that the UCS system gives accurately uniform chromaticity scales as it was intended to do, the other shows, on the same assumption, isotemperature lines to aid in the estimation of nearest color temperature for near-Planckian colors.[4]

[3] See, for example, D. B. Judd, *A method for determining the whiteness of paper*, Paper Trade J. **100**, no. 21 (1935) TS40; also Tech. Assn. Pap. [18] 392 (1935); and D. B. Judd, *A method for determining whiteness of paper, II*, Tech. Assn. Pap., [19] 359 (1935).

[4] For these terms and concepts, see R. Davis, *A correlated color temperature for illuminants*, BS J. Research **7**, 659 (1931) RP365.

II. ESTIMATION OF CHROMATICITY DIFFERENCES

The equilateral Maxwell triangle of the ICI system, and all three of the mixture diagrams obtained by plotting in rectangular coordinates one of the ICI trilinear coordinates (x,y,z) against another, fail to array color stimuli in such a way that equal chromaticity differences are indicated by lines of equal length. It is therefore impossible to give any single reliable perceptibility scale of chromaticity which will apply to the whole diagram as a scale of miles applies to a map.

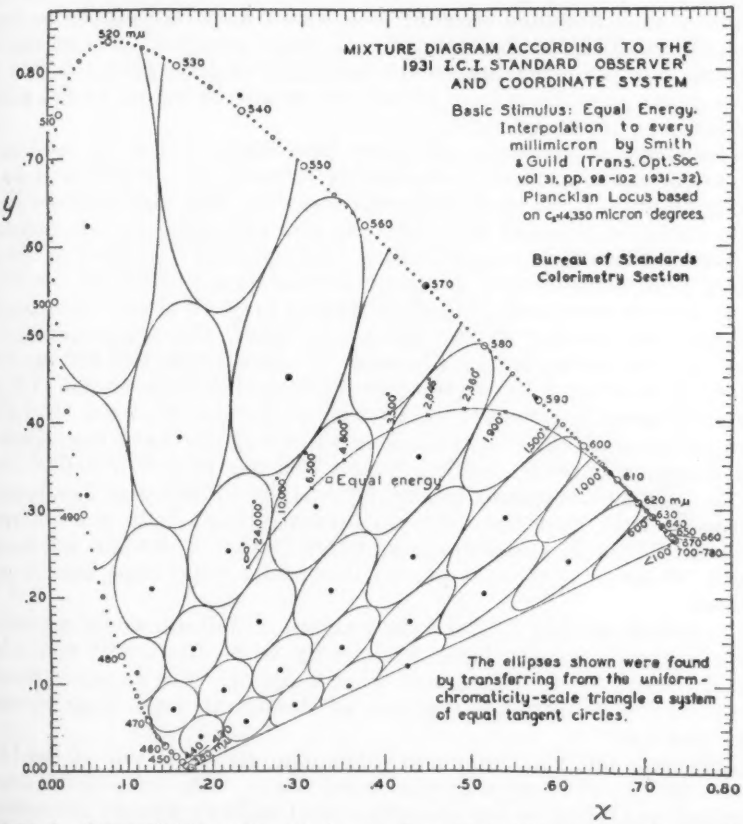

FIGURE 1.—*Perceptibility scales for the standard 1931 ICI colorimetric coordinate system*

The distances from points on the boundary of each ellipse to the indicated point within it all correspond approximately to 100 times the chromaticity difference just perceptible with certainty under moderately good observing conditions.

Instead of a single perceptibility scale there is required for a given direction on the mixture diagram a different scale for each different portion of the diagram, and for each point a different scale is, in general, required for each direction. In an effort to provide such a complete set of approximate perceptibility scales for the ICI mixture diagram a group of thirty tangent circles on the UCS system have been transferred to the (x,y)-plot of the ICI system where they appear as tangent ellipses of various sizes, eccentricities, and orientations; see figure 1. The distances from points on the boundaries of

these ellipses to the point within them representing the transformed centers of the original circles give the desired scales of perceptibility; one one-hundredth of each such distance refers to a chromaticity difference just perceptible with certainty under moderately good experimental conditions (careful monocular observation of a 6° circular field divided along a diameter yielding retinal illuminations between 200 and 1,000 photons).

The indicated maximum variation in the scales of perceptibility is about 14 to 1; the distance from point to boundary along the major axis of the largest ellipse ($x=0.23$, $y=0.77$) is about 0.25, while the smallest such distance parallel to a minor axis (see ellipse inclosing $x=0.43$, $y=0.12$) is about 0.018. In most practical uses of the ICI system, however, the maximum variation is only about 5 to 1 because green samples whose colors are so saturated as to fall within the largest ellipses are rare.

The following example will show how figure 1 may be used as an aid in the estimation of chromaticity differences. Suppose it be required to know how much the dominant wave length of a yellow signal light could be changed from 580 mμ and still keep the chromaticity difference no more perceptible than that between the signal at 580 mμ and a bare incandescent lamp at a color temperature of 2,360° K. Since signals produced by yellow glasses may be closely matched by one part or another of the spectrum, itself, the spectrum may be used for this estimation. The scale in the direction of 580 mμ from 2,360° K is about 0.13 per 100 "least perceptible differences" (LPDs); the scale along the spectrum near 580 mμ is about 0.04 per 100 LPDs. The distance on the diagram along the spectrum locus equivalent to the distance between 2,360° K and 580 mμ is: 0.075 (0.04/0.13)= 0.023. This corresponds to slightly less than 3 mμ near 580, hence it would be said that the diagram indicates that both the difference between 2,360° K and 580 mμ and that between 580 and 583 mμ are about 60 times that least perceptible under good experimental conditions.

It is worth noting that a yellow signal of 580 mμ would resemble a bare vacuum-tungsten lamp sufficiently to be frequently confusible; this accounts for the nonuse of such a signal. For example, railway signal yellow is a reddish yellow of dominant wave length greater than 588 mμ.[5]

This example also serves to emphasize that the size of the LPD varies widely with experimental conditions. The unfavorable conditions often arising in the observation of railway signals (momentary viewing of point source at a retinal illumination of less than 100 photons with no comparison light) require perhaps 50 to 100 times as large chromaticity differences for discrimination as are required under good laboratory conditions.

III. NEAREST COLOR TEMPERATURE

An important practical application of the UCS system is its use in finding from any series of colors the one most resembling any neighboring color of the same brilliance. In this system the method, of course, is to draw the shortest line from the locus of the series to the

[5] Association of American Railroads, Signal Section Specification 69-35, Signal glasses (exclusive of hand lantern globes). Manual of Signal Section, AAR, part 136 (1935).

point representing the neighboring color. This is the geometric equivalent of the method of observation on which many plans of color grading are based. The characteristic of these plans is that they pay attention to chromaticity differences along a series of color standards, and in the usual case that no member of the series gives a perfect chromaticity match, the nearest match is set and the residual difference neglected. In this way a problem which, strictly, is two-dimensional finds a one-dimensional solution that is close enough to be of practical use.

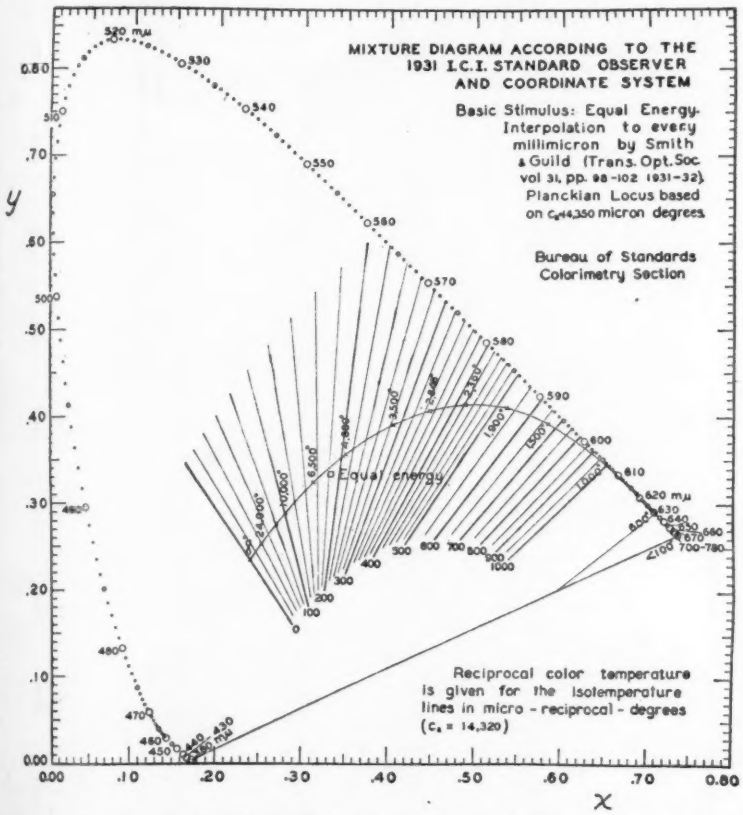
MIXTURE DIAGRAM ACCORDING TO THE 1931 I.C.I. STANDARD OBSERVER AND COORDINATE SYSTEM
Basic Stimulus: Equal Energy. Interpolation to every millimicron by Smith & Guild (Trans. Opt. Soc. vol 31, pp. 98-102 1931-32). Planckian Locus based on c_2=14,350 micron degrees
Bureau of Standards Colorimetry Section
Equal energy
Reciprocal color temperature is given for the isotemperature lines in micro - reciprocal - degrees (c_2 = 14,320)
y
x
520 mμ
700-780
620 mμ
430 mμ
0.00
.10
.20
.30
.40
.50
.60
.70
0.80

FIGURE 2.—*Iso-temperature lines shown on the standard 1931 ICI colorimetric co ordinate system.*

Color stimuli specified on an iso-temperature line give closer chromaticity matches with the indicated Planckian color than with Planckian colors at neighboring color temperatures.

In finding nearest color from the series the UCS system may be used directly. The locus of the series is plotted together with the point representing the neighboring chromaticity, and the shortest line through the point to the locus, usually the normal, gives the nearest chromaticity of the series. It is also possible to carry out the operation once for all by drawing on the UCS triangle a number of normals to the locus of the series completely covering at sufficiently small intervals the areas of the triangle near the locus. These normals can

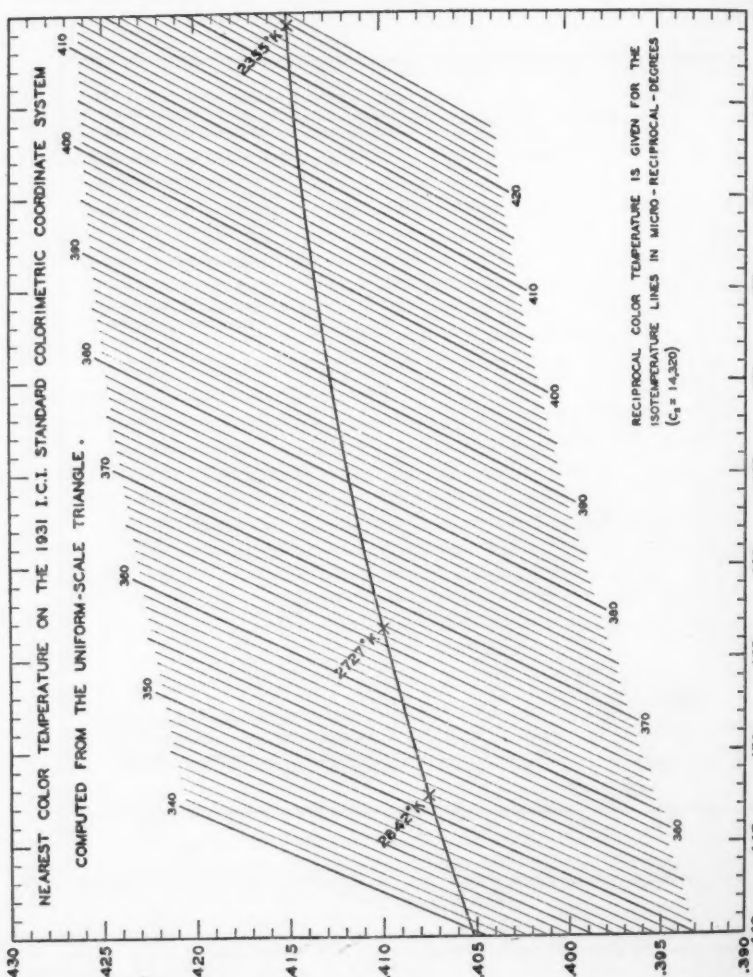
NEAREST COLOR TEMPERATURE ON THE 1931 I.C.I. STANDARD COLORIMETRIC COORDINATE SYSTEM
COMPUTED FROM THE UNIFORM-SCALE TRIANGLE.
RECIPROCAL COLOR TEMPERATURE IS GIVEN FOR THE ISOTEMPERATURE LINES IN MICRO-RECIPROCAL-DEGREES (C_2 = 14,320)
2135°K
2727°K
2962°K
y
x

FIGURE 3.—*Iso-temperature lines shown for a small section of figure 2.*

This region includes the most-used portion of the color-temperature scale for incandescent lamps.

then be transformed to any other desired system and the determination of nearest chromaticity carried on entirely outside the UCS system. This has been done by McNicholas in the estimation of nearest chromaticity of vegetable oils on both the wave-length scale and on the scale composed of combinations of Lovibond 35-yellow with various Lovibond red glasses.[6] Figure 2 shows a similar series of normals to the Planckian locus transferred to the standard 1931 ICI system.[7] By means of these transferred

TABLE 1.—*Trilinear coordinates of Planckian stimuli and reciprocal of slopes of the iso-temperature lines as a function of reciprocal color temperature*

$1/\theta$ $C_2=14{,}320$ μrd	Trilinear coordinates of Planckian locus		Reciprocal of the slopes of the isotemperature lines
	x	y	
0	0.2399	0.2342	−0.672
20	.2458	.2429	−.611
40	.2526	.2524	−.536
60	.2605	.2629	−.450
80	.2693	.2743	−.359
100	.2794	.2869	−.266
120	.2909	.3003	−.175
140	.3037	.3141	−.089
160	.3171	.3272	−.012
180	.3306	.3396	+.057
200	.3445	.3512	+.120
220	.3583	.3619	+.175
240	.3723	.3717	+.227
260	.3865	.3805	+.275
280	.4006	.3883	+.319
300	.4142	.3950	+.361
320	.4273	.4006	+.400
340	.4403	.4052	+.437
360	.4526	.4089	+.472
380	.4646	.4117	+.505
400	.4760	.4136	+.535
420	.4868	.4148	+.563
440	.4973	.4153	+.590
460	.5072	.4152	+.615
480	.5167	.4146	+.639
500	.5256	.4136	+.661
550	.5460	.4093	+.713
600	.5638	.4033	+.762
650	.5797	.3962	+.808
700	.5941	.3886	+.849
800	.6183	.3731	+.923
900	.6370	.3587	+.983
1000	.6521	.3451	+1.036

normals (iso-temperature lines) nearest color temperature estimated

[6] H. J. McNicholas, Color and spectral transmittance of vegetable oils, J. Research NBS 15, 99 (1935) RP815; also Oil & Soap 12, 167 (1935); see his figure 8.

[7] Figure 2 is a reproduction of a figure previously used (see footnote 1, p. 771). Since that time a new color-temperature scale has been adopted (see footnote 9, p. 778) and coincidentally the value of C_2 used was changed from 14 350 to 14 320 micron degrees to conform with the International Temperature Scale. This change in C_2 makes only 0.2-percent change in the temperature (or reciprocal temperature) and is too small to be shown in figure 2. For this reason the old diagram has been used. In figure 3, however, the change (about 0.8 μrd) could be easily seen.

In table 2, the values of color temperature listed were taken from Davis' paper in which the older value of 14 350 was used for C_2.

according to the UCS system may be approximately read from specifications in the ICI system. Figure 3 shows a small section of figure 2 to an enlarged scale with one normal drawn in for each microreciprocal-degree (μrd); as pointed out by Priest,[8] who proposed the use of reciprocal color temperature, "a difference of one micro-reciprocal-degree is fairly representative of the doubtfully perceptible difference in chromaticity under the most favorable conditions of observation." The large drawing from which this reproduction was made has been used in connection with a check of the present color-temperature scale[9] with blue filters whose use resulted in near-Planckian colors. The original drawing was found to reproduce estimates of nearest color temperature found directly from the UCS system with a maximum error less than 0.1 μrd. It will be noted that the normals extend only over the region immediately in the neighborhood of the Planckian locus. The experimental setting of nearest color temperature when a considerable chromaticity difference exists between the illuminant in question and the Planckian radiator at any temperature becomes increasingly difficult and ambiguous as the chromaticity difference is increased. It is doubtful whether the solution given by the UCS system is valid much further than the normals have been extended on figure 3; and figure 2, which shows them extended considerably further, may be criticized because it seems to make the false implication that a definite, unambiguous nearest color temperature can be found experimentally for illuminants having colors very notably non-Planckian.

TABLE 2.—*Comparison of conjunctive wave length referring to nearest color temperature via the UCS system with that referring to Davis' correlated color temperature*

θ C_2=14,350°K	$1/\theta$ C_2=14,320μrd	Conjunctive wave length, λ_j, in mμ	
		Nearest color temperature via UCS system	Davis correlated color temperature
1,803	555.8	588.4	586.5
2,011	498.3	585.6	584.2
2,532	395.8	580.2	579.5
3,053	328.2	575.4	575.5
3,585	279.5	570.9	572.9
4,116	243.5	567.2	570.2
4,663	214.9	563.0	568.8
5,222	191.9	559.1	567.0
5,781	173.3	555.5	565.8
6,359	157.6	549.8	564.8
6,945	144.3	546.8	564.0
7,549	132.7	542.0	563.2
8,181	122.5	537.7	562.6
8,826	113.5	533.5	562.1
9,483	105.7	530.0	561.4
10,187	98.4	526.2	561.0
10,876	92.1	524.5	561.2
11,587	86.5	521.7	561.0
13,161	76.1	517.0	560.3
14,817	67.6	514.4	560.3

[8] I. G. Priest, *A proposed scale for use in specifying the chromaticity of incandescent illuminants and various phases of daylight*, J. Opt. Soc. Am. **23**, 41 (1933).

[9] H. T. Wensel, D. B. Judd, and Wm. F. Roeser, *Establishment of a scale of color temperature*, BS J. Research **12**, 527 (1934) RP677.

To facilitate the construction of large-scale plots for accurate work such as figure 3 there have been included in table 1 the trilinear coordinates of the Planckian locus on the ICI system for the reciprocal color temperatures represented by the transformed normals on figure 2, and the reciprocals of the slopes of these transformed normals. The reciprocals of the slopes are given instead of the slopes, themselves, for convenience because, as may be seen from figure 2, the slope becomes infinite in the neighborhood of 160 μrd, but is nowhere zero. Interpolation between the values given in table 1 will yield points on the Planckian locus and also the slopes of the corresponding iso-temperature lines.

Table 2 shows a comparison of conjunctive wave length, λ_j, referring to correlated color temperature computed by Davis' empirical method, with that referring to nearest color temperature from the UCS system. The former were taken from Davis' table 6,[10] the latter were found by extending the iso-temperature lines on the original large-scale plot of figure 2 until they cut the spectrum locus. It may be noted that the agreement is good down to 250 μrd (up to 4,000° K) but is rather poor at lower reciprocal color temperatures where validity of the UCS system is best established.[11]

WASHINGTON, August 28, 1936.

[10] BS. J. Research **7**, 659 (1931) RP365.
[11] J. Research NBS **14**, 41 (1935) RP756; J. Opt. Soc. Am. **25**, 24 (1935).

U. S. DEPARTMENT OF COMMERCE NATIONAL BUREAU OF STANDARDS

RESEARCH PAPER RP945

Part of Journal of Research of the National Bureau of Standards, Volume 17, November 1936

SOIL-CORROSION STUDIES, 1934. RATES OF LOSS OF WEIGHT AND PENETRATION OF NONFERROUS MATERIALS

By Kirk H. Logan

ABSTRACT

The soil-corrosion investigation, which was started in 1922, had its origin in the need for information concerning the effects of soils on iron and steel. Specimens of protective coatings and of nonferrous metals were added from time to time, mostly at the request of manufacturers or others who were interested in the behavior of certain materials when exposed to certain soils. A systematic study of the corrosion of nonferrous materials underground was not begun until 1932, and in the latest tests the specimens represent only copper and copper alloys. The number of nonferrous specimens exposed to soils has grown to approximately 9,000, of which about 2,500 have not been removed.

Differences in dimensions of the specimens buried prior to 1932, insufficient numbers of specimens of each material, and the introduction of too many factors that may affect corrosion have resulted in complications of the data to such an extent that in many cases positive decisions as to the rates of corrosion or the effects of possible influences on corrosion cannot be made. Nevertheless, although the dispersion of the data is large, certain tendencies are sufficiently well defined to be of practical importance. The results of the experiments should be of value also as indicators of the direction which more systematic investigations should take.

This report summarizes the effects of a large variety of soils on many nonferrous metals and alloys. Data on the corrosion of iron subjected to the same conditions are also given. In general, the nonferrous materials, with the possible exception of aluminum and its alloys, in certain soils corrode less than the ferrous materials under similar soil conditions, but none of the materials tested was free from corrosion in all soils. It appears, therefore, that in the choice of materials soil conditions should be given consideration. Unfortunately, few people have made systematic studies of soils from the standpoint of corrosion and not many can predict from the chemical or physical analysis of soils their effect on metals exposed to them.

The proper selection of materials for use underground requires special knowledge of soils, metals, electrochemistry, and economics.

CONTENTS

	Page
I. Introduction	782
II. Properties of soils at test sites	782
III. Corrosion of nonferrous metals and alloys	788
1. Corrosion of lead	788
2. Corrosion of copper and alloys of copper	793
3. Corrosion of aluminum and zinc	796
IV. Effect of interconnecting different metals	800
V. Deterioration of nonmetallic pipe	803
VI. Summary	803

I. INTRODUCTION

The original plans for the soil-corrosion investigation, which was started in 1922, dealt primarily with ferrous pipes, although the corrosion of cable sheath was given some consideration. When it appeared that ferrous materials corroded rather rapidly under some soil conditions, it seemed desirable to obtain data on nonferrous materials which might also be used underground.

Specimens of nonferrous materials were therefore added from time to time when ferrous specimens were removed. This paper concerns itself with these nonferrous materials. Like the reports on the ferrous materials, this is a progress report, and for a complete understanding of it the reader should refer to some of the earlier reports. The most important of these is Bureau Technologic Paper 368,[1] which described the soils in the original test, gives the analyses of some of the materials, and records the results of the examination of the first nonferrous specimens that were removed after an exposure of approximately 2 years. Research Paper 95 [2] contains data on the corrosion of lead cable sheath, and Research Papers 359 and 638 [3] contain corrosion data on a considerable variety of nonferrous materials.

II. PROPERTIES OF SOILS AT TEST SITES

Table 1 gives the names of the soils corresponding to the soil numbers, together with the locations of test site and the local organization cooperating in the test. Table 2 gives the properties of the soils. The test sites were selected as representative of typical soil conditions, and do not necessarily represent the prevailing soil conditions in the city near which the test was conducted. It should be remembered that within the boundaries of a city of moderate size there are usually several widely different soils.

TABLE 1.—*Identification of soils*

Soil	Soil type	Location	Cooperating organization
1	Allis silt loam	Cleveland, Ohio	East Ohio Gas Co.
2	Bell clay	Dallas, Tex	Dallas Gas Co.
3	Cecil clay loam	Atlanta, Ga	Dept. of Pub. Works.
4	Chester loam	Jenkintown, Pa	Philadelphia Elec. Co.
5	Dublin clay adobe	Oakland, Calif	East Bay Municipal Utility District.
6	Everett gravelly sandy loam.	Seattle, Wash	Dept. of Pub. Works.
7	Silt loam	Cincinnati, Ohio	Union Gas and Electric Co.
8	Fargo clay loam	Fargo, N. Dak	Union Light, Heat and Power Co.
9	Genesee silt loam	Sidney, Ohio	Tide Water Pipe Line Co., Ltd.
10	Glouchester sandy loam	Middleboro, Mass	Town of Middleboro.
11	Hagerstown loam	Baltimore, Md	Dept. of Pub. Works.
12	Hanford fine sandy loam	Los Angeles, Calif	Southern Calif. Gas Co.
13	Hanford very fine sandy loam.	Bakersfield, Calif	San Joaquin Light and Power Corp.
14	Hemstead silt loam	St. Paul, Minn	Northern States Power Co.
15	Houston black clay	San Antonio, Tex	San Antonio Public Service Co.

[1] K. H. Logan, S. P. Ewing, and C. D. Yeomans, *Bureau of Standards soil-corrosion studies: I. Soils, materials, and results of early observations.* Tech. Pap. BS **22**, 447 (1928) T368, 50c.

[2] K. H. Logan, *Soil-corrosion studies 1927–28.* BSJ Research **3**, 275 (1928) RP95, 10c.

[3] K. H. Logan, *Soil-corrosion studies; Nonferrous metals and alloys, metallic coatings, and specially prepared ferrous pipes removed in 1930,* BS J Research **7**, 585, (1931) RP359, 10c.

K. H. Logan and R. H. Taylor, *Soil-corrosion studies 1932. Rates of loss of weight and pitting of ferrous and nonferrous specimens removed in 1932 and metallic protective coatings,* BS J Research **12**, 12, (1934) RP638, 5c.

TABLE 1.—*Identification of soils*—Continued

Soil	Soil type	Location	Cooperating organization
16	Kalmia fine sandy loam	Mobile, Ala	City of Mobile.
17	Keyport loam	Alexandria, Va	Alexandria Water Co.
18	Knox silt loam	Omaha, Neb	Omaha and Council Bluffs Electrolysis Committee.
19	Lindley silt loam	Des Moines, Iowa	Des Moines Gas Co.
20	Mahoning silt loam	Cleveland, Ohio	Dept. of Pub. Utilities.
21	Memphis silt loam	Memphis, Tenn	Board of Water Commissioners.
22	Merced silt loam	Buttonwillow, Calif	San Joaquin Light and Power Corp.
24	Merrimac gravelly sandy loam.	Norwood, Mass	Boston Consolidated Gas Co.
25	Miami clay loam	Milwaukee, Wis	Dept. of Pub. Works.
26	Miami silt loam	Springfield, Ohio	City of Springfield.
27	Miller clay	Bunkie, La	Standard Pipe Line Co.
28	Montezuma clay adobe	San Diego, Calif	San Diego Consolidated Gas and Electric Co.
29	Muck	New Orleans, La	Sewerage and Water Board.
30	Muscatine silt loam	Davenport, Iowa	United Light and Power Engineering and Construction Co.
31	Norfolk sand	Jacksonville, Fla	City Commission of Jacksonville.
32	Ontario loam	Rochester, N. Y	Dept. of Pub. Works.
33	Peat	Milwaukee, Wis	Milwaukee Gas Light Co.
34	Penn silt loam	Norristown, Pa	Philadelphia Elec. Co.
35	Ramona loam	Los Angeles, Calif	Los Angeles Gas and Elec. Co.
36	Ruston sandy loam	Meridian, Miss	Peoples Water and Gas Co.
37	St. Johns fine sand	Jacksonville, Fla	Jacksonville Gas Co.
38	Sassafras gravelly sandy loam.	Camden, N. J	Camden Water Dept.
39	Sassafras silt loam	Wilmington, Del	Delaware Power and Light Co.
40	Sharkey clay	New Orleans, La	New Orleans Pub. Serv. Co.
41	Summit silt loam	Kansas City, Mo	Kansas City Gas Co.
42	Susquehanna clay	Meridian, Miss	City of Meridian.
43	Tidal marsh	Elizabeth, N. J	Standard Oil Development Co.
44	Wabash silt loam	Omaha, Neb	Omaha and Council Bluffs Electrolysis Committee.
45	Unidentified alkali soil	Casper, Wyo	Stanolind Oil and Gas Co.
46	Unidentified sandy loam	Denver, Colo	Public Service Co. of Colo.
47	Unidentified silt loam	Salt Lake City, Utah	Mountain Fuel Supply Co.
51	Acadia clay	Spindletop, Tex	Sinclair Prairie Pipe Line Co. of Tex.
53	Cecil clay loam	Atlanta, Ga	Dept. of Pub. Works.
54	Fairmount silt loam	Cincinnati, Ohio	Union Gas and Elec. Co.
55	Hagerstown loam	Baltimore, Md	Bureau of Water Supply.
56	Lake Charles clay	El Vista, Tex	Gulf Pipe Line Co.
57	Merced clay adobe	Tranquillity, Calif	Standard Oil Co. of Calif.
58	Muck	New Orleans, La	Sewerage and Water Board.
59	Peat	Kalamazoo, Mich	Dept of Pub. Utilities.
60	do	Plymouth, Ohio	Ohio Fuel Gas Co.
61	Sharkey clay	New Orleans, La	New Orleans Pub. Service Co.
62	Susquehanna clay	Meridian, Miss	City of Meridian.
63	Tidal marsh	Charleston, S. C	Commissioners of Pub. Works.
64	Unidentified alkali soil	Cholame Flats, Calif	Shell Oil Co.
65	do	Wilmington, Calif	Shell Oil Co.
66	Mohave sandy loam	Phoenix, Ariz	City Water Dept.
67	Cinders	Milwaukee, Wis	Milwaukee Gas Light Co.

TABLE 2.—*Properties of soils* [a] *in the National Bureau of Standards soil-corrosion investigation*

(mg-eq = milligram equivalent)

A = Alkaline.
C = Not determined.
G = Good; *F* = Fair; *P* = Poor; *VP* = Very poor.

Soil [b]	Soil type	Mean temperature [c]	Annual precipitation [c]	Internal drainage of test site	Moisture equivalent	pH	Total acidity mg-eq per 100 g of soil	Resistivity at 60° F	Composition of water extract mg-eq per 100 g of soil						
									Na+K as Na	Ca	Mg	CO_3	HCO_3	Cl	SO_4
		°F			%			ohm-cm							
51	Acadia clay	69.	49.	P	47.1	6.2	13.2	190	10.27	15.55	5.03	0.00	0.56	5.75	22.00
52	Alkali knoll	69.	47.	P	54.8	8.8	A	234	4.20	.33	.18	.52	1.36	1.33	1.26
1	Allis silt loam	49.2	33.8	P	28.6	7.0	11.4	1,215	.72	.25	.43	.00	.09	.09	.83
2	Bell clay	65.5	36.2	P	37.6	7.3	3.5	684	.28	1.09	.13	.00	1.18	.04	.18
101	Billings silt loam	52.0	8.8	F	30.0	7.3	A	261	5.21	19.24	1.43	.00	.66	1.56	22.48
102	do	52.0	8.8	F	20.4	7.3	A	103	22.63	16.56	3.85	.00	.56	4.67	36.82
103	do	52.0	8.8	F	30.6	7.3	A	81	22.01	13.32	2.00	.00	.18	11.09	25.70
104	Cecil clay	60.2	46.1	G	34.1	4.6	11.0	8,500							
3	Cecil clay loam	61.2	48.3	G	29.1	5.2	11.5	30,000							
53	do	61.2	48.3	G	33.7	4.6	9.6	17,794							
105	do	64.2	44.5	G	34.2	4.8	12.9	28,000							
106	do	60.	46.	G	38.8	4.8	12.8	25,000							
107	Cecil fine sandy loam	60.1	46.3	G	29.6	4.8	11.8	54,400							
108	Cecil gravelly loam	61.2	48.3	G	34.3	4.9	11.2	44,400							
4	Chester loam	54.	40.	F	22.2	5.6	7.6	6,670							
57	Cinders	46.1	30.1	VP	11.1	8.0	A	455	.77	3.03	.53	.00	.55	.08	2.89
5	Dublin clay adobe	56.4	23.4	P	28.8	7.0	6.5	1,346	.93	.48	.10	.00	.69	.03	.25
6	Everett gravelly sandy loam	51.0	34.0	G	12.2	5.9	12.8	45,100							
54	Fairmount silt loam	53.2	38.6	P	26.1	7.0	3.5	886	.59	10.10	.59	.00	.70	.08	9.05
8	Fargo clay loam	39.	21.	P	37.0	7.6	A	350	1.42	1.72	2.55	.00	.71	.01	4.43
109	Fresno fine sandy loam	63.	9.	P	18.6	8.4	A	497	2.62	.07	.10	.31	.59	1.56	.48
110	do	63.	9.	P	18.4	10.2	A	531	3.53	.07	.12	1.49	1.07	.79	.25
111	do	63.	9.	P	22.1	7.3	A	51	41.55	16.21	.44	.00	.58	34.58	23.41
9	Genesee silt loam	51.2	39.0	P	24.8	6.8	7.2	2,820							
10	Gloucester sandy loam	50.	41.	F	13.0	6.6	3.6	7,460							
11	Hagerstown loam	55.4	42.6	G	32.0	5.3	10.8	11,000							
55	do	55.4	42.6	G	32.0	5.8	10.9	5,213							
13	Hanford fine sandy loam	62.4	15.2	F	12.4	7.1	2.5	3,190	.39	.50	.16	.00	.40	.00	.14
12	Hanford very fine sandy loam	64.6	5.6	F	21.7	9.5	A	280	6.23	.09	.13	.00	1.12	1.64	3.76
14	Hempstead silt loam	44.2	27.2	F	17.2	6.2	5.6	3,320							
15	Houston black clay	68.9	27.2	F	51.4	7.5	5.0	486	2.13	.88					
112	Imperial clay	71.	2.	F	30.2	7.4	A	149	22.15	14.09	1.29	.00	2.00	.13	.73
113	do	71.	2.	F	34.6	7.4	A	102	9.56	.84	.51	.00	.36	10.04	25.98
16	Kalmia fine sandy loam	67.3	61.6	F	22.2	4.4	11.8	8,290					.63	6.26	4.05
17	Keyport loam	61.6													

16	Houston black clay	68.9	27.2	F	51.4	7.6	5.0	489	2.18	.55	.20	.00	2.00	.13	.73
112	Imperial clay	71.	2.	F	30.2	7.4	A	140	22.18	14.09	1.29	.09	.36	10.94	25.98
113	do	67.3	61.6	F	34.6	7.4	A	102	9.56	.84	.51	.00	.63	6.26	4.06
16	Kalmia fine sandy loam	55.	42.	P	22.2	4.4	11.8	8,290							
17	Keyport loam				30.8	4.5	19.1	5,980							
18	Knox silt loam	50.6	27.8	G	28.4	7.3	1.4	1,410	.27	.63	.20	.00	.94	.00	.25
56	Lake Charles clay	69.	49.	P	28.7	7.1	4.5	406	3.12	.69	.47	.00	.80	1.59	3.04
114	do	69.	49.	P	35.8	7.1	C	320	2.65	.68	.26	.00	.77	1.84	.93
19	Lindley silt loam	49.5	32.0	G	28.4	4.6	10.9	1,970	.38	.32	.41	.00	.16	.03	.46
20	Mahoning silt loam	49.2	33.8	P	22.4	7.5	1.5	2,870	.25	.48	.20	.00	.51	.00	.15
21	Marshall silt loam	54.4	37.1	F	31.2	6.2	9.5	2,370							
22	Memphis silt loam	61.6	47.7	G	28.4	4.9	9.7	5,150							
115	do	65.6	51.9	G	25.7	6.9	4.7	3,450							
116	Merced clay	63.4	8.1	F	39.7	9.2	A	320	9.30	.33	.18	4.60	2.10	1.17	1.57
57	Merced clay adobe	63.	8.	P	40.9	7.7	A	128	23.40	13.50	4.51	.00	.34	1.15	37.50
117	Merced clay loam adobe	63.	8.	P	51.8	8.5	A	106	36.19	14.66	.83	.00	1.55	2.89	46.53
23	Merced silt loam	65.	6.	P	24.7	9.4	A	278	8.38	.38	.22	.02	1.87	1.12	5.57
24	Merrimac gravelly sandy loam	50	41	G	13.0	4.5	12.6	11,400							
25	Miami clay loam	46.1	30.1	F	25.8	7.2	4.7	1,780	.23	.70	.41	.00	1.01	.03	.10
26	Miami silt loam	53	37	G	16.4	7.3	2.6	2,980	.27	.50	.31	.00	.70	.03	.12
27	Miller clay	67	56	P	42.6	6.6	3.7	570	.53	1.86	1.12	.00	2.00	.08	1.54
66	Mohave sandy loam	69.7	7.8	G	16.5	8.7	A	232	6.55	.51	.18	.00	.73	2.77	2.97
28	Montezuma clay adobe	61.0	10.3	P	24.6	6.8	C	408	1.50	.06	.18	.00	.12	.99	.89
29	Muck	69.3	57.4	VP	34.5	4.2	28.1	1,270	2.15	1.92	1.55	.00	.00	1.69	2.30
58	do	69.3	57.4	VP	57.8	4.0	79.3	712	2.03	2.23	1.29	.00	.00	.47	2.54
30	Muscatine silt loam	49.9	32.1	P	29.4	7.0	2.6	1,300	.32	.65	.40	.00	.71	.09	.24
118	Niland gravelly sand	71	2	F	6.1	7.3	A	273	4.30	1.03	.64	.00	.20	5.01	.86
31	Norfolk sand	69.3	47.4	G	2.8	4.7	1.8	20,500							
120	do	67.7	57.9	G	4.4	5.7	1.3	34,400							
121	do	71.8	49.4	G	3.0	4.8	1.2	16,400							
119	Norfolk sandy loam	64.2	44.5	G	24.1	4.7	9.7	10,800							
32	Ontario loam	47.6	32.8	G	17.8	7.3	0.5	5,700	.23	.70	.12	.00	.73	.01	.42
122	Panoche clay loam	63	6.4	F	30.0	7.4	A	552	2.32	.05	.26	.00	.70	.07	1.40
33	Peat	46.1	30.1	VP	72.8	6.8	36.0	800	1.52	7.30	4.06	.00	C	2.27	2.13
59	do	49	31	VP	43.6	5.5	33.3	1,659	1.03	3.08	2.70	.00	.00	3.47	1.04
60	do	49	37	VP	43.4	2.6	297.4	218	2.91	10.95	2.86	.00	.00	.00	56.70
34	Penn silt loam	54	40	F	23.4	6.7	7.0	4,900							
35	Ramona loam	62.4	15.2	G	18.0	7.3	5.7	2,060	.68	.68	.49	.00	1.10	.06	.35
36	Ruston sandy loam	64.0	53.0	G	13.8	4.5	4.6	11,200							
37	St. Johns fine sand	69.3	47.4	P	7.0	3.8	15.3	11,200							

[Illegible]

[a] Measurements and determinations by I. A. Denison and R. B. Hobbs.
[b] For locations of soils see table 1.
[c] Data furnished by U. S. Weather Bureau. Values with no figures to the right of the decimal point are for some nearby city.

TABLE 2.—*Properties of soil in the National Bureau of Standards soil-corrosion investigation*—Continued

Soil	Soil type	Mean temperature	Annual precipitation	Internal drainage of test site	Moisture equivalent	pH	Total acidity mg-eq per 100 g of soil	Resistivity at 60° F	Composition of water extract mg-eq per 100 g of soil						
									Na+K as Na	Ca	Mg	CO_3	HCO_3	Cl	SO_4
		°F			%			ohm-cm							
38	Sassafras gravelly sandy loam	54	40	G	3.0	4.5	1.7	38,600							
39	Sassafras silt loam	54	40	P	24.2	5.6	6.6	7,440							
40	Sharkey clay	69.3	57.4	P	33.0	6.0	9.4	970	.56	.58	.44	.00	.93	.07	.28
61	do	69.3	57.4	P	30.8	5.9	8.6	943	.73	.68	.33	.00	.71	.10	.91
41	Summit silt loam	54.4	37.1	F	33.1	5.5	11.0	1,320	.30	.54	.36	.00	.78	.04	.46
42	Susquehanna clay	64.0	53.0	P	34.8	4.7	28.2	13,700							
62	do	64.0	53.0	P	34.6	4.1	24.2	6,922							
123	do	65.8	43.4	P	37.6	4.1	21.9	6,840							
124	Susquehanna silt loam	66.0	42.7	P	36.0	4.4	28.1	1,160							
125	Susquehanna fine sandy loam	65.8	43.4	P	37.2	3.9	28.3	5,770							
43	Tidal marsh	52	43	VP	55.4	3.1	36.8	60	45.10	5.17	9.45	.00	.00	43.30	37.00
63	do	66.0	45.2	VP	46.7	2.9	100.2	84	33.60	6.85	4.00	.00	.00	12.70	36.60
44	Wabash silt loam	50.6	27.8	G	31.2	5.8	8.8	1,000	1.05	1.08	.66	.00	1.97	.82	.41
	UNIDENTIFIED SOILS														
45	Alkali soil	47.2	15.3	P	14.8	7.4	A	263	8.15	3.70	.70	.00	.24	.18	11.98
46	Sandy loam	50.0	14.1	G	7.6	7.0	C	1,500							
7	Silt loam [4]	53.2	38.6	P	34.3	4.4	29.8	2,120							
47	do	51.6	16.1	P	25.7	7.6	3.0	1,770	.67	.72	.39	.00	.88	.06	.48
64	Alkali soil	58	16	VP	41.1	8.3	A	62	28.10	2.29	.76	.00	.89	28.80	.26
65	do	62.4	15.2	F	26.4	7.2	A	148	7.65	12.40	2.20	.00	1.30	6.05	16.90

[4] Previously classified erroneously as Fairmount silt loam.

The selection of the sites for soil-corrosion tests was governed by the desire to secure soils representative of the soil types to which extensive pipe lines were exposed.

As is indicated by the names of the soil types, the textures of the soils range from coarse sands to very heavy clays. The range in texture is also indicated by the moisture-equivalent values.

The temperatures given in column 3 of table 2 are the average annual atmospheric temperatures of cities near which the specimens were buried, and show in a very general way one of the conditions which affect corrosion.

The mean annual precipitation shown in column 4 has a bearing on corrosion, but the effect of precipitation is modified by its distribution throughout the year, by surface and subsurface drainage, and by the capacity of the soil to hold moisture. The character of the subsurface drainage is indicated in column 5. The moisture equivalent given in column 6 is a measure of the capacity of the soil to retain moisture and is the percentage of moisture (in terms of the dry weight of the soil) which is retained by a soil sample when subjected to a centrifugal force of 1,000 times gravity.

The moisture-equivalent values range from 2.8 percent for Norfolk sand to 72.8 percent for the peat soil at Milwaukee.

The acidity or alkalinity of the soil solution is indicated by the pH values, which range from 2.6 for the peat soil at Plymouth, Ohio, to 10.2 for the Fresno fine sandy loam at Kerman, Calif.

Some soils have a greater capacity to maintain their acidity than others. This is shown by the total acidity of the soil, expressed in milligram equivalents of hydrogen per 100 grams of soil. The greatest total acidity value, 297.4, was found for the peat at Plymouth, Ohio. The pH value for this soil was 2.6, while a tidal marsh with a pH value almost as low, 3.1, showed a total acidity about one-eighth as large. It will be noted also from the values of total acidity that soils which are more alkaline than the conventional neutral point, pH 7, often contain hydrogen ions.

The resistivity of the soil indicates capacity to conduct the electric currents which flow in the course of the corrosion process. It also indicates the amount of salts in the soil solution. This soil property is so important that in certain localities it is a fairly satisfactory indicator of the corrosivity [4] of the soil with respect to ferrous materials.

Table 2 shows that the resistivities of soils in the soil-corrosion investigation range from 54,400 ohm-cm for the Cecil fine sandy loam to 51 ohm-cm for the Fresno fine sandy loam (*111*). These values are for saturated soils at 60° F. In the more-arid regions the soils are at times nearly dry and the values for their resistivities in the field are considerably greater than those given in the table. The physical properties of some of these soils and their relations to the corrosion of iron are described in RP696.[5]

Water extracts of soils were prepared as follows: A suspension of soil and water in the ratio 1:5 was shaken mechanically at intervals for a total of 24 hours during a period of 72 hours. The compositions of the water extracts, as shown in table 2, are important because of

[4] R. R. Sheppard. *Pipe line currents and soilre sistivity as indicators of local corrosive soil areas.* BS J. Research 6, 683 (1931) RP289.

[5] I. A. Denison and R. B. Hobbs. *Corrosion of ferrous metals in acid soils.* J. Research NBS 13, 125 (1934) RP696, 5c.

the effect of the salts in solution on the resistivity of the soil and because of their influence of the character of the corrosion products, which may form protective deposits.

Since underground corrosion has been found to depend largely on soil conditions, an examination of table 2 will make clear that averages of corrosion data from different soils are of little practical value in the estimation of what is to be expected in any one locality.

Those interested in the classification of soils and their distribution will find part III of the Atlas of American Agriculture[6] helpful. The paper does not discuss corrosion.

Table 3 shows the nonferrous materials reported in this paper, their symbols, dimensions, and actual or nominal compositions. In all cases except the lead the analyses were furnished by the manufacturer supplying the material. Such analyses are quite satisfactory for the study of underground corrosion since the precision with which rates of corrosion can be determined is not usually sufficient to show the effects of small changes in the composition of the materials tested.

III. CORROSION OF NONFERROUS METALS AND ALLOYS

1. CORROSION OF LEAD

Lead is used underground principally to provide a flexible connection between water mains and services, as water service pipe, and as a sheath for power and telephone cables. Power and telephone cables are usually drawn into ducts and therefore not exposed directly to soil action, although ducts may contain silt. Occasionally lead-covered cables are laid in direct contact with the soil, although this is not generally considered the best practice, partly because of the danger of damage when the soil is disturbed.

Four varieties of lead specimens appear in the soil-corrosion investigation, as shown in table 3. Table 4 shows the rates of corrosion for the cable sheath materials. For the rates of corrosion comparison of wrought iron and steel buried approximately 12 years in the same soils are included. Each rate for the lead is based on a single specimen. Most of the antimonial lead specimens were of approximately twice the area of those of commercial lead. The maximum rates of penetration of the former as recorded in the table represent the average of the two deepest pits on separate halves of the specimen. In the earlier reports the recorded maximum rate of penetration regardless of the dimensions of the specimen, is based upon the average of the deepest pit on each side of the specimen.

It is of interest to note that in certain soils which are very corrosive with respect to iron, such as Hanford very fine sandy loam, Merced silt loam, and other alkali soils, lead corrodes but slowly. Table 4 shows that in 32 out of 35 cases the antimonial lead specimens *A* lost weight more rapidly than those of commercially pure lead, *H*, also the rate of penetration was greater in 20 instances. Similar indications of the greater corrodibility of the antimonial lead specimens were observed on previous examinations of these materials. It will be noted, however, that the variation in the rates of corrosion in different soils is much greater than the differences between the two materials.

[6] C. F. Marbut. *Soils of the United States.* Part III of the Atlas of American Agriculture, July 1935, Government Printing Office, $5.00.

TABLE 3.—*Form, dimensions, and chemical composition of materials*

LEAD ALLOYS [a]

Symbol	Material	Form	Dimensions [b]	Chemical composition (in percent)					
				Cu	Zn	Sn	Pb	Ni	Other elements
			Inches						
NN	Hearth refined lead.	Cast	6×2×.25	0.002			99.99		0.004 Bi.
N	Chemical lead	do	6×2×.25	.57			99.93		0.009 Ag.
H	Commercial lead	Sheet	22×3.5×.11	.013			99.95		0.037 Bi.
A	Antimonial lead	do	22×8.5×.12	.062			99.12		0.82 Sb.

COPPER ALLOYS

E	Copper	Pipe	17×1.1×.108	99.97					
C	do	do	12×1.7×.145	99.9					
M	do	do	12×.9×.06	99.93					
A	do	do	13×1.7×.144	99.94					0.018 P.
P	do	do	12×.9×.06	99.94					0.015 P.
M [c]	do	do	12×1.5×.062						
H	do	Sheet	6×2×.05	99+					
S	Brass	Cast	Irregular	91.86	7.72	0.08	0.34		
t	do	do	do	87.06	5.31	5.86	1.77		
l	do	do	do	85.48	6.20	3.52	4.80		
F	do	Pipe	12×1.7×.143	85.18	14.80				0.01 Fe.
H	do	do	17×1.1×.108	84.99	14.97		.01		0.03 Fe.
i	do	Cast	Irregular	74.94	20.12	1.43	2.57		0.94 Fe.
H	do	Pipe	12×1.7×.143	71.28	27.39	1.30	.01		0.02 Fe.
Bl	do	Sheet	6×2×.05	70	30				
K	do	Pipe	12×1.7×.08	67.08	31.07		.84		Trace of Fe.
J	do	do	13×1.7×.145	66.50	33.06		.42		0.02 Fe.
B	do	do	12×.8×.103	60	40				
Bt	do	Nipple	2×.8×.106	60	40				
L	do	Pipe	12×1.7×.08	60.06	39.58		.36		Trace of Fe.
Ms	do	Ell	2×.7×.16	59.00	38.50		2.50		
A	do	Rod	12×.4	47.00	40.50		2.50	10	
E	Bronze	Pipe	12×1.7×.141	97.15		1.80			0.01 Fe. 1.04 Si.
L	Bronze	Plate	6×2×.25	90		10			
N [d]	Cu-Si alloy	Pipe	12×1.7×.145	98.11		.14		0.01	0.11 Fe. .18 Mn. 1.49 Si.
D	do	do	12×1.7×.143	95.46				.08	.21 Fe. 1.06 Mn. 3.19 Si.
G	Cu-Ni alloy	do	12×1.7×.145	74.45	4.99			20.04	0.52 Mn.
N	Cu-Al alloy	Rod	12×.4	87.00					3.5 Fe, 9.5 Al.
Zl	Zinc	Sheet	6×2×.06		99.5				
Zl	do	Plate	6×2×.25		99.5				
P	do	Sheet	6×2×.06	(e)	(e)	(e)	(e)	(e)	(e)

ALUMINUM ALLOYS

				Cu	Fe	Si	Mn	Al	
Cl	Aluminum	Sheet	6×2×.06	0.09	0.33	0.3	0.03	99.25	
Cl	Al-Mn	do	6×2×.06	.16	.51	.44	1.12	97.75	0.02 Zn.
Cl	Duralumin	do	6×2×.06	4.10	.30	.23	.62	94.23	0.52 Mg.

[a] Analysis by J. A. Scherrer, National Bureau of Standards.
[b] Dimensions of plates and sheets given as (length)×(width)×(thickness); dimensions of pipes as (length)×(outside diameter)×(wall thickness); dimensions of rods as (length)×(diameter).
[c] These specimens have streamlined caps and couplings soldered in place.
[d] Some of these specimens have brazed joints.
[e] Standard composition.

TABLE 4.—*Rates of loss of weight and maximum penetration lead cable sheath exposed 10 to 12 years*

Soil [a]	Cable sheath rates of loss (oz/ft²/yr)		Rates of penetration (mils/yr)		Ferrous pipe	
	A [b]	H [c]	A [b]	H [c]	Rates of loss (oz/ft²/yr)	Rates of penetration (mils/yr)
1	0.345	0.173	8.1	9.4	0.79	7.5
2 [d]	.095	.067	2.0	2.1	.51	4.7
3 [d]	.062	.059	.8	1.8	.37	5.6
4	.149	.177	5.3	4.3	.57	8.2
5 [d]	.185	.135	11.8	4.0	.57	3.5
6 [d]	.035	.025	1.0	1.1	.10	1.7
10	.074	.088	1.7	1.3	.40	3.8
11	.040	.034	1.9	1.3	.17	6.2
14	.181	.049	5.2	2.0	.39	8.2
15 [d]	.051	.036	1.4	2.5	.68	5.1
17	.037	.028	2.9	1.7	.80	3.5
18	.042	.016	1.6	1.3	.24	3.8
19	.113	.040	2.8	1.3	.29	5.5
20	.304	.268	6.6	4.4	.52	5.2
22	.155	.085	2.5	1.6	.64	5.6
24	.021	.015	1.3	1.6	.12	2.2
25	.045	.028	3.0	2.4	.28	3.9
26	.041	.018	1.8	2.5	.32	3.5
27 [d]	.095	.067	3.3	2.7	.66	4.9
28	.221	.069	4.0	1.0	1.70	16.4
29 [d]	.353	.343	1.4	1.1	1.50	11.4
30	.201	.126	5.7	4.4	.47	4.8
31 [d]	.026	.022	1.3	.7	.24	2.8
33	.050	.028	1.0	1.5	.30	5.2
34	.260	.067	7.6	9.2	.38	3.7
35 [d]	.019	.017	2.1	3.4	.16	1.9
36 [d]	.046	.032	1.2	1.4	.23	4.0
38	.032	.025	1.0	2.1	.20	2.4
39	.148	.099	3.5	3.0	.47	5.8
41	.049	.039	1.6	1.6	.51	6.9
43	.043	.019	1.9	1.2	1.31	7.8
44	.070	.038	1.7	1.1	.30	5.8
45	.038	.021	1.2	2.0	.85	7.7
46	.081	.015	2.8	1.2	.38	6.2
47	.130	.122	4.8	9.1	.25	2.2

[a] See table 1 for names of soils.
[b] Antimonial lead.
[c] Commercial lead.
[d] The antimonial lead specimens in these soils were 4.25 inches wide and the rate of penetration is based on the depth of the one deepest pit.

In most of the soils the rate of corrosion of the lead specimens is much lower than that of the corresponding ferrous specimens. In Allis silt loam (*1*), Dublin clay adobe (*5*), Mahoning silt loam (*20*), Muscatine silt loam (*30*), Penn silt loam (*34*), Ramona loam (*35*) and in the unidentified silt loam at Salt Lake City (*47*), the averages of the rates of penetration for the lead specimens are greater than for the corresponding ferrous specimens. These soils are not severely corrosive with respect to ferrous materials. Their chief common characteristic is their low content of sulfates, as will be seen in table 2. It will also be seen from comparing tables 2 and 4 that the lead did not corrode severely in soils high in sulfates.

The data in table 4 should be used with considerable caution for several reasons. Two specimens of the same material in the same soil may not corrode at the same rate. This is illustrated in table 5 where it will be noted that in some instances one specimen corroded

50 percent more rapidly than another specimen of the same material under nominally the same soil condition. This illustrates a soil-corrosion phenomenon which is common to all outdoor soil-corrosion

TABLE 5.—*Dispersion of rates of corrosion of lead*

SOIL 22.—12-YEARS' EXPOSURE

Material	Loss of weight	Maximum penetration
	oz/ft²/yr	mils/yr
A197	0.168	3.2
A198	.129	2.3
H197	.087	1.4
H198	.082	2.0

SOIL 29.—10-YEARS' EXPOSURE

A52	0.446	1.4
A55	.259	1.4
H52	.443	1.3
H55	.242	1.0

tests in which the soils are not in some way modified to secure unusually uniform soil conditions. The data as here presented do not reveal the effect of shape or area on the depth of penetration as has been shown in Research Paper 883.[7] Likewise changes in the rate of corrosion are not indicated.

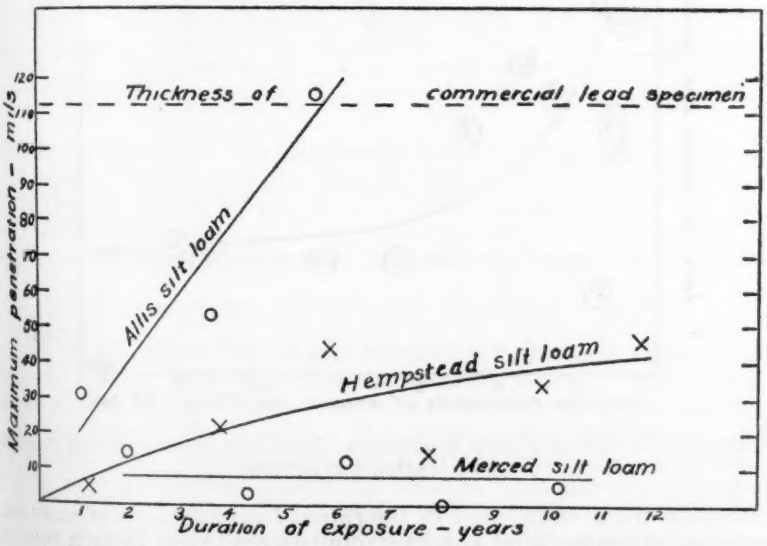

FIGURE 1.—*Pit depth-time graphs for lead sheaths in three soils.*

The influence of duration of exposure on the depth of the pits on lead is illustrated in figure 1. The pit depths are the averages of the

[7] K. H. Logan. *Soil-corrosion studies 1934. Rates of loss of weight and penetration of ferrous specimens.* J. Research NBS **16**, 431 (1936) RP883.

two deepest pits, one on each side on each of two specimens, one of commercial lead and the other of antimonial lead. It is noted that in Merced silt loam, a soil high in sulfates, the pits increased in depth very little, if at all, as the period of exposure was prolonged. Apparently, a very effective coating, probably of lead sulfate, was formed. In Hempstead silt loam the penetration continued but at a decreasing rate; while in Allis silt loam the penetration was approximately proportional to the duration of exposure up to 6 years, at which time the specimens were punctured.

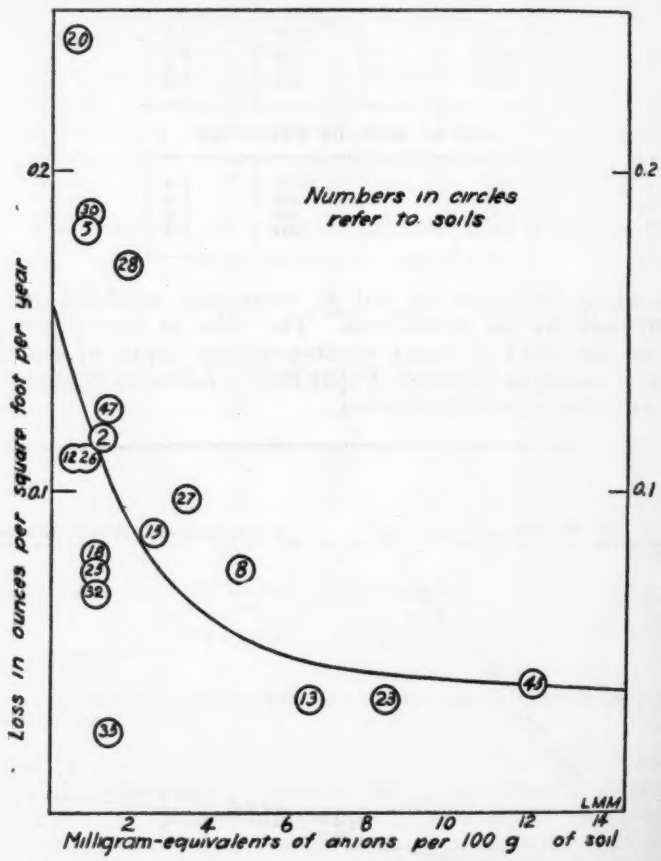

FIGURE 2.—*Correlation of rates of corrosion of lead with concentration of chlorides, bicarbonates, and sulfates.*

Because of the wide range in the rates of corrosion, an attempt was made to determine what soil characteristics resulted in high rates of corrosion of lead. This has not been altogether successful because of insufficient data and the large number of different factors involved in each soil condition. Figure 2 shows the relation between the concentration of chlorides, bicarbonates, and sulfates in some of the soils to the averages of the rates of loss of weight for periods of exposure varying between 2 and 12 years. The addition of the available data for other soils would not materially affect the shape of the curve,

although it would be extended. Sulfates predominated in these soils. Although the curve shows in a general way that the salts tended to reduce the corrosion of lead, it should not be used for determining the loss of lead because the rates used are average rates, whereas, as was shown in figure 1, the change in the rate of corrosion with time is different for different soils.

In general, soils containing large quantities of organic material and soils which are poorly drained, appear to be corrosive to lead, but exceptions to this statement may be found. For example, the tidal marsh is not severely corrosive, probably because of the presence of sulfates. The muck soil at New Orleans was the most corrosive with respect to loss of weight but caused no serious pitting. It should be evident from these statements that the corrosiveness of a soil with respect to lead cannot be predicted from any one soil characteristic. Specimens of chemical lead and hearth-refined lead were exposed to five soils only. Table 6 gives the data on these specimens for four periods of exposure.

TABLE 6.—*Effect of impurities on rates of loss of weight of lead*

[Rates in ounces per square foot per year]

Soil[1]	1 to 2 years' exposure				6-years' exposure				8-years' exposure				10-years' exposure			
	A[2]	*H*	*N*	*NN*	*A*	*H*	*N*	*NN*	*A*	*H*	*N*	*NN*	*A*	*H*	*N*	*NN*
18	0.02	0.03	0.14	0.03	-----	-----	0.05	0.01	-----	-----	0.12	0.04	-----	-----	0.04	0.01
19	.62	.51	.64	.34	0.32	0.38	.38	.24	-----	-----	.51	.31	0.35	0.34	.51	.28
33	.26	.49	.34	.19	.11	.10	.19	.11	0.08	0.07	.12	.08	-----	-----	.18	.07
35	.06	.07	.06	.03	.04	.02	.05	.06	.06	.03	.08	.05	.04	.03	.08	.06
45	-----	-----	.05	.02	.05	.04	.08	.03	.04	.03	.10	.04	.05	.04	.09	.02

[1] See table 1 for names of soils.
[2] See table 3 for names of materials.

The table shows that the antimonial lead lost weight at higher rates in 74 percent of the tests and that the refined lead lost weight more slowly than the chemical lead in 95 percent of the tests. These data confirm the experiences of other investigators who found that impurities or alloying elements tend to accelerate the corrosion of lead.

2. CORROSION OF COPPER AND ALLOYS OF COPPER

Brass in the form of cocks and valves has been used underground for many years. More recently copper and brass have been used for service pipe and, in some instances, for small distribution mains.

The copper-rich alloys used in this investigation are listed in table 3. Table 7 gives the corrosion data obtained from the specimens in 42 soils. As a rule two specimens of each material were removed from each location, but in a few cases one or more of the specimens were not found. Usually the loss of weight of these two specimens did not differ greatly, but in some cases one showed a loss 50 percent greater than the other.

These averages suggest that the rod *A*, which is an alloy of copper, zinc, lead, and nickel, is less resistant to soil action than the alloy of copper, aluminum, and iron.

The copper-zinc-lead-nickel alloy (*A*) was most susceptible to attack. The forged brass alloy (*Me*) corroded more rapidly than the alloy *M*. Both were relatively susceptible to attack.

TABLE 7—*Corrosion of copper-rich alloys* [1] *exposed 8 years*

M=Shallow metal attack, roughening of the surface but no definite pitting.
P=Definite pitting, no pits greater than 6 mils.
U=Unaffected by corrosion.
S=Severe uniform corrosion, impossible to measure penetration because of even destruction of surface.
D=Selective corrosion such as dezincification over large areas.
d=Selective corrosion in spots.
Z=Destroyed by dezincification.

Soil [2]	Average rate of loss of weight (oz/ft²/yr)						Condition of surface and pit depth [3]				
	Copper pipe		Brass		Cu-Zn-Ni rod *A*	Cu-Al-Fe rod *N*	Copper pipe		Brass pipe *B*	Cu-Zn-Ni rod *A*	Cu-Al-Fe rod *N*
	M	*P*	Pipe *B*	Ell *Me*			*M*	*P*			
1	0.060	0.063	0.007	0.185	0.157	0.057	1.5	*P*	*M, D*	*P*	*M, D*
2	.073	.016	.080	.228	.131	.046	*P*	*P*	*P, D*	*P*	*M, d*
3	.027	.029	.074	.109	.156	.063	*P*	*P*	1.2, *d*	1.2	*D*
4	.019	.019	.144	-------	.176	.070	1.3	*M*	*P, D*	1.3	*D*
5	.068	.087	.054	.525	.141	.061	*M*	*M*	*M, D*	*P*	*D*
6	.055	.025	.039	.033	.070	.0025	*M*	*M*	*M, d*	*P*	*U*
7	.039	.052	.171	-------	.307	.044	*P*	*P*	*P, D*	1.2	*M, D*
8	.024	.019	.018	.319	.136	.026	1.5	1.3	*M, d*	1.5	1.9, *d*
9	.041	.041	.105	.112	.116	.0082	*P*	*P*	*P, D*	*P*	*M*
10	.100	.103	.182	.198	.231	.036	*P*	*P*	1.3, *D*	1.0	*D*
12	.312	.278	.222	-------	.199	.090	1.5	*S*	*P, D*	*M*	*P, d*
13	.023	.031	.101	.024	.012	.028	*P*	*P*	*M, D*	*M*	*M, d*
14	.040	.025	.044	.089	.096	.017	*P*	.9	*P, d*	1.9	*M, d*
15	.013	.016	.030	-------	.045	.026	*M*	*M*	*D*	*d*	*d*
16	.057	.058	.170	.166	.234	.093	3.3	1.9	1.3, *D*	.9	*d*
17	.037	.040	.059	.257	.108	.049	*M*	*M*	*M, d*	*P*	*D*
18	.0076	.0077	.021	.070	.044	.013	*U*	*M*	*M, d*	1.3	*U*
19	.039	.040	.122	.067	.165	.027	1.1	*P*	*P, D*	1.3	*M, d*
20	.042	.039	.044	.193	.138	.044	1.5	1.2	*P, d*	*P*	*D*
22	.068	.070	.195	.283	.277	.075	1.9	1.0	1.1, *D*	*P*	*M, D*
23	.118	.135	.752	1.853	.288	.169	1.9	1.3	*Z*	*U*	*D*
24	.017	.019	.022	.045	.040	.021	*M*	*M*	*U*	*P*	*D*
25	.012	.011	.051	.142	.126	.043	*P*	*U*	*P, D*	*P*	*D*
26	.010	.011	.048	.101	.103	.026	*U*	*M*	*M, D*	*P*	1.9, *d*
27	.019	.031	.050	-------	.121	.032	*P*	*M*	*M, D*	*P*	*D*
28	.084	.079	.080	-------	.163	.107	*P*	*P*	*M, D*	*P*	*M, D*
29	.123	.116	.275	-------	.257	.082	*P*	*P*	*P, D*	1.9	*M, d*
31	.021	.025	.045	.082	.070	.039	*M*	*P*	*M, d*	*P*	1.0
32	.049	.018	.089	.152	.129	.016	*U*	*M*	1.0, *D*	1.3	*d*
33	.137	.117	.175	.218	.208	.040	.9	1.0	*P, D*	1.3	*M, d*
34	.016	.022	.057	.080	.177	.021	*M*	*P*	*M, D*	*P*	*d*
35	.017	.016	.020	.422	.063	.039	*M*	*P*	*D*	1.0	*D*
36	.023	.024	.056	.049	.113	.022	*P*	*P*	1.3, *d*	1.3	*M, d*
37	.169	.162	.152	.274	.175	.060	1.8	1.3	*P, D*	*P*	*M, d*
38	.025	.043	.028	.037	.034	.019	*M*	*P*	*M, d*	*P*	*U*
40	.125	.168	.349	.330	.385	.092	2.3	4.1	1.8, *D*	1.9	*d*
41	.036	.040	.083	.083	.155	.020	*P*	*M*	.9, *D*	*P*	*d*
42	.047	.049	.095	.089	.154	.057	*P*	1.1	*P, D*	1.9	*P, D*
43	.635	.555	.026	.022	.007	.022	*S*	*S*	*M, d*	*U*	2.3
44	.079	.061	.175	-------	.248	.026	*P*	*P*	1.3, *D*	2.4	*P, d*
45	.033	.030	.016	.214	.081	.030	1.0	1.0	*d*	1.0	*D*
47	.052	.0053	.0031	.027	.0046	.0038	*U*	*U*	*D*	*M*	*D*

[1] See table 3 for identification of materials.
[2] See table 2 for names of soils.
[3] The letters indicate the condition of the worse of 2 specimens. The figures are rates of maximum penetration, in mils per year.

It is necessary to point out here the fact that brasses high in zinc sometimes undergo selective corrosion known as dezincification in which there is little or no pitting and a loss of strength and service life greater than is indicated by the loss of weight. Extreme cases of dezincification are shown in figure 3. In most cases the specimens high in zinc were not pitted and no attempt was made to determine

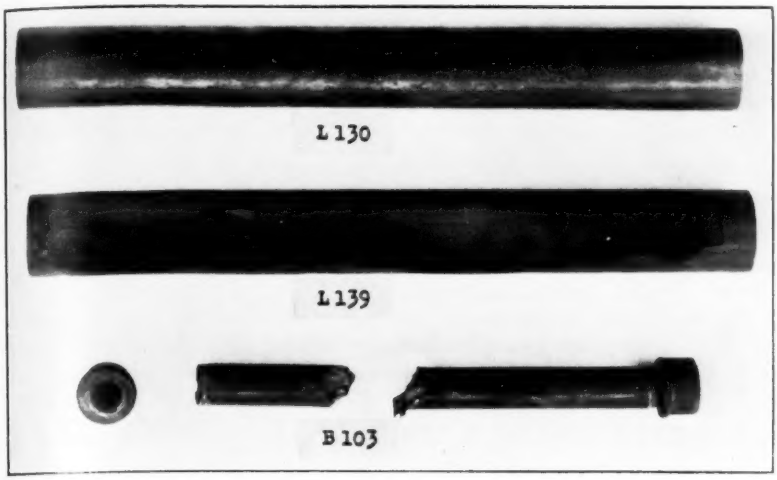

FIGURE 3.—*Dezincification of Muntz metal.*

L130, Exposed for 2 years to an alkali soil; *L139*, exposed 2 years to cinders; *B103*, exposed 10 years to Merced silt loam, an alkali soil.

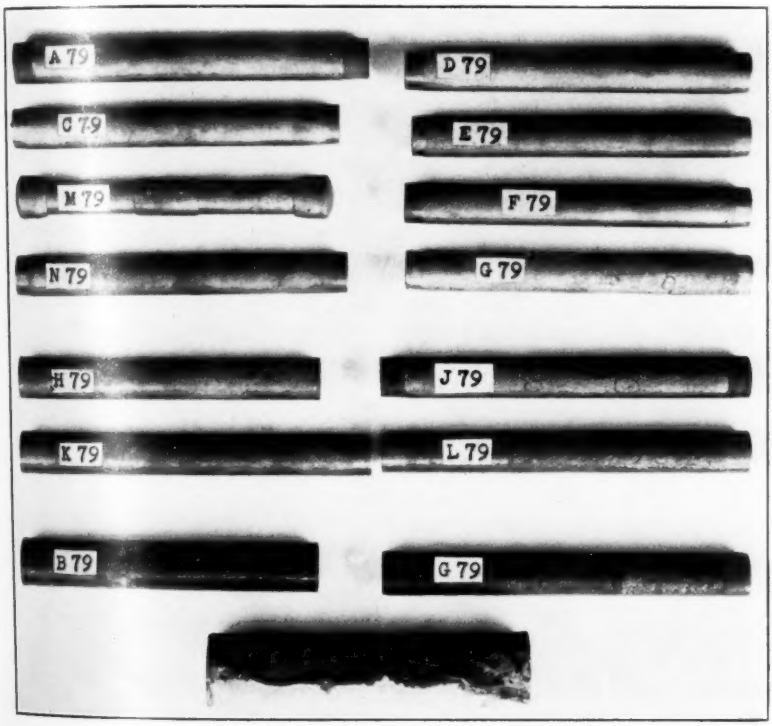

FIGURE 4.—*Nonferrous specimens from a peat soil.*

See table 3 for identification of the nonferrous materials. At the bottom of the figure specimen *B79* is wrought iron, *G79* is cast iron, and the unnumbered specimen is a cement-asbestos pipe. The lengths of the specimens are from 10 to 14 inches.

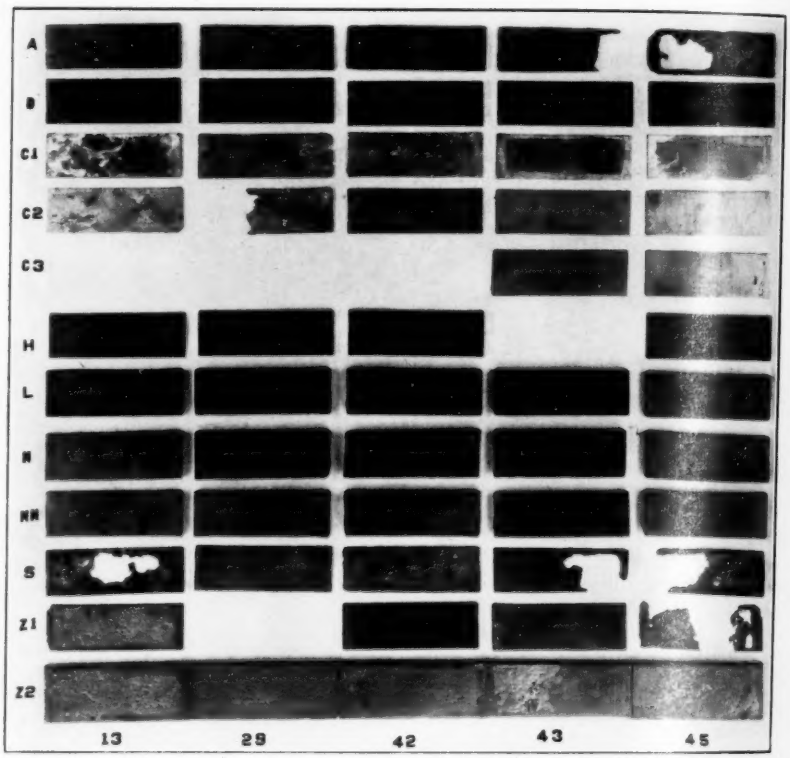

FIGURE 5.—*Condition of miscellaneous specimens.*

Conditions of miscellaneous specimens exposed to five soils for approximately 10 years. *A*, Open-hearth iron; *B*, brass; *C1*, aluminum; *C2*, Al–Mn alloy; *C3*, duralumin; *H*, copper; *L*, bronze; *N*, chemical lead; *NN*, refined lead; *S*, copper bearing steel; *Z1*, rolled zinc; *Z2*, cast zinc. The soils are as follows: 13, Hanford very fine sandy loam; 29, muck; 42, Susquehanna clay; 43, tidal marsh; 45, unidentified soil containing sulfates.

the depth of the dezincification. The worse of the two specimens at each locality is indicated in table 7, but in most cases the specimens of the same material did not differ greatly.

Six widely different soils were chosen from the original test sites for tests of materials which were not available in sufficient quantities to permit their burial at all test sites. Five of these soils are severely corrosive with respect to iron. Table 8 shows the rates of loss of weight for all the copper-alloy specimens removed from these soils. The figures are based on the losses of weight of two specimens. It will be noted that the rates of corrosion of all of the copper alloys are low except in soil 43, a tidal marsh high in sulfides. In this soil copper lost more weight than the copper alloys, but the high-zinc alloys showed some local dezincification. The differences in rates of corrosion of similar materials in the same soil are probably accidental. Such differences are characteristic of soil-corrosion data from the field.

Prior to 1932 such nonferrous specimens as were buried were tested at the request of some manufacturer or organization for a special purpose. Comparison of materials is difficult because of differences in exposed areas, durations of exposures and other accidental influences. Because of these difficulties and the evident need for information on the usefulness of nonferrous materials underground, a new test of corrosion-resistant materials was begun in 1932. Two samples of each nonferrous material were removed from each of 14 of the new test sites in 1934. The appearance of the nonferrous specimens from the peat soil is shown in figure 4. At the bottom of the figure are shown a wrought iron specimen, *B79*, a cast-iron specimen, *G79*, and a specimen of a cement-asbestos pipe. The specimens are approximately 12 inches long.

TABLE 8.—*Rates of loss of weight of copper alloys* [1] *in 6 soils*

[In ounces per square foot per year]

Soil [2]	Copper				Brass						
	Pipe			Sheet *H*	Pipe *H*	Sheet *B* [1]	Pipe *B*	Ell *Me*	Rod *A*	Bronze sheet *L*	Cu-Al rod *N*
	E	*M*	*P*								
13	0.052	0.023	0.031	0.015	0.022	0.077	0.101	0.024	0.012	0.015	0.028
24	------	.017	.019	------	------	------	.022	.045	.040	------	.021
39	.040	.123	.116	.116	.061	.153	.275	------	.257	.131	.082
43	.080	.047	.049	.044	.105	.051	.095	.089	.154	.046	.057
43	.562	.635	.555	------	.070	.010	.026	.022	.007	.460	.022
45	.028	.033	.030	.015	.020	.074	.016	.214	.081	.049	.030

[1] See table 3 for analyses of materials.
[2] See table 1 for names of soils.

The average rates of loss of weight of the nonferrous specimens are given in table 9 and the conditions of the specimens are shown in table 10. In cases where specimens subjected to similar conditions differed, the worse condition was recorded.

Because rates of corrosion frequently change with time, and because not many specimens have been examined, definite conclusions should not be drawn from these tables. In general, tables 9 and 10 confirm the data in tables 7 and 8. It should be remembered that cinders from other sources may differ considerably from those used at site 67.

Since data on the corrosion of copper appear in several tables discussion of the effects of soils on this material has been withheld until all of these tables have been presented. From these tables it will be seen that copper corrodes most rapidly in soils containing sulfides. The scale which is formed under these conditions does not appear to have much protective value. Copper corrodes rapidly also in some cinders, perhaps because they also contained sulfides. This should be kept in mind when light-weight pipe is used in city streets containing cinder fills.

In most soils, however, the rate of corrosion of copper and its alloys is much lower than that for ferrous materials, as will be seen by comparing the data in tables 7, 8, 9, and 10 with the last two columns of table 4. It is interesting to note in tables 7, 8, 9, and 10 that in the tidal marshes (soils *43* and *63*), the Muntz metal pipe appears definitely superior to the copper pipe.

TABLE 9.—*Rates* [1] *of loss of weight of nonferrous specimens exposed approximately 2 years*

Soil [2]	Tough pitch Cu *C*	Deoxidized copper [3] *A*	Red brass *F*	Admiralty metal *H*	Two and one leaded brass *K*	Brass—66% Cu; 33% Zn *J*	Muntz metal *L*	Bronze—97% Cu; 1% Si; 1.8% Sn *E*	Alloy—98% Cu; 1.5% Si *N*	Alloy—95% Cu; 3% Si *D*	Alloy—75% Cu; 20% Ni, 5% Zn *G*
51	0.21	0.20	0.17	0.16	0.085	0.17	0.35	0.26	0.18	0.23	0.14
53	.062	.061	.060	.070	.13	.052	.097	.12	.097	.090	.059
55	.072	.075	.068	.079	.11	.094	.10	.16	.076	.080	.061
56	.059	.051	.054	.040	.080	.042	.072	.12	.075	.050	.033
57	.0036	.0062	.0054	.0061	.041	.041	.24	.031	.012	.012	.0099
58	.066	.082	.061	.096	.13	.11	.10	.094	.054	.056	.074
60	.71	.76	.76	.59	.59	.89	.90	.84	.68	.69	.72
61	.10	.062	.12	.18	.12	.12	.17	.20	.14	.14	.13
62	.080	.079	.077	.11	.15	.12	.17	.17	.11	.13	.091
63	.64	.55	.27	.12	.23	.021	.069	.57	.80	.61	.32
64	.35	.74	.17	.13	.12	.30	2.11	.41	.72	.35	.041
65	.26	.90	.27	.16	.072	.72	1.27	.25	.58	.58	.089
66	.055	.15	.092	.12	.13	.18	.33	.20	.10	.11	.11
67	1.56	1.97	1.66	2.75	3.39	8.20	(4)	1.61	2.74	2.09	1.03

[1] Average for two specimens in ounces per square foot per year.
[2] See table 1 for names of soils.
[3] See table 3 for analyses of materials.
[4] Destroyed.

Sufficient data are not available for plotting the relation of the period of exposure to the corrosion for individual soils. A comparison of the average rates of loss of weight for the materials listed in table 7 with corresponding data for 4-year-old specimens indicates little or no change in the rates of corrosion. This may indicate that the corrosion-resisting properties of copper are due to low electrochemical potential rather than to the formation of protective films, or that such films as are formed reach their maximum effectiveness very soon after the material is exposed to soil.

3. CORROSION OF ALUMINUM AND ZINC

Data on specimens of aluminum and zinc removed in 1934 are shown in table 11, together with those for other specimens of the same dimensions and periods of exposure. The appearance of these specimens is shown in figure 5. (Specimens *C1*, *C2*, and *C3*.) The blank spaces represent lost specimens. In the case of the aluminum

TABLE 10.—*Surface condition* [1] *and rate of penetration of nonferrous specimens exposed approximately 2 years*

M=Shallow metal attack, roughening of surface but no definite pitting.
P=Definite pitting but no pits greater than 6 mils.
U=Apparently unaffected by corrosion.
S=Severe uniform corrosion; impossible to measure penetration because of uniform destruction of surface.
D=Selective corrosion over large areas, i. e., several square inches per square foot.
d=Selective corrosion in small spots.
Z=Destroyed by dezincification.

Soil [2]	Tough pitch copper *C*	Deoxidized copper [3] *A*	Red brass *F*	Admiralty metal *H*	Two and one leaded brass *K*	Brass—66% Cu; 33% Zn *J*	Muntz metal *L*	Bronze—97% Cu; 1% Si; 1.8% Sn *E*	Alloy—98% Cu; 1.5% Si *N*	Alloy—95% Cu; 3% Si *D*	Alloy—75% Cu; 20% Ni; 5% Zn *G*
51	*M*	*M*	*M*	*M, d*	*M, D*	*M, D*	*M, d*	*P*	*M*	*M*	*d, M*
53	*M*	*P*	4.1	6.1, *d*	*M, d*	5.1, *d*	*P, d*	6.6	*P*	*P*	*P, d*
55	*P* [4]	*P*	6.3	11.6	*M, d*	5.8	5.3, *d*	7.4	*P*	5.8	4.3, *d*
56	*M*	*M*	*M* [3]	*M, d*	*M, d*	*M, d*	*d*	6.5	*P*	*M*	*M, d*
57	*M*	*U*	4.2	*P, d*	*M*	*M, d*	*M, d*	12.6	*M*	*M*	*d*
58	*P*	*M*	*M*	*P, d*	*M, d*	*M, d*	*P, d*	6.0	*M*	*M*	7.0
60	*P*	5.2, *S*	7.8	5.2	*P, d*	9.4	7.8, *d*	14.1	6.8	*P*	8.3
61	*P*	*P*	*P*	8.4, *d*	*P, d*	10.5, *d*	*P, d*	*P*	*P*	*M*	*P, d*
62	*P*	4.1	5.2	8.8	*P, d*	*P, d*	*P, d*	9.9	*P*	4.7	*P, d*
63	4.3	*M*	*P*	*M*	*M*	*P*	*M*	13.4	*P*	*P*	*P*
64	5.8	*S*	12.0	13.1, *d*	*M*	*P, d*	*P, D*	11.0	5.8	13.1	*P*
65	*P*	*S*	5.2	18.3	*M, d*	*M, d*	*M, D*	12.0	4.2	*P*	*P*
66	*P*	6.3	*P*	*M, d*	*M, d*	*M, d*	*P, d* [3]	6.3	9.4	*P*	*M, d*
67	17.3	21.8	14.9	25.7	29.2	*Z*	*Z*	21.2	23.2	17.3	12.4

[1] Condition or rate of maximum penetration on worse of 2 specimens; figures are in mils per year.
[2] See table 1 for names of soils.
[3] One specimen only.

alloys the loss was due in most cases to the almost complete destruction of the specimens. Table 11 is comparable with similar tables in earlier reports.[8]

TABLE 11.—*Rates of loss of weight and penetration of miscellaneous metals and alloys buried approximately 10 years*

P=Definite pitting, no pits greater than 6 mils.
S=Severe surface corrosion, impossible to measure penetration because of even destruction of surface.
M=Shallow metal attack, roughening of surface but no definite pitting.
D=Dezincification over large areas.
d=Dezincification in spots.
f=Failure of 1 or more holes.

Material [5]	Soil *13* [6]		Soil *29*		Soil *42*		Soil *43*		Soil *45*	
	Loss [7]	Pits [8]	Loss	Pits	Loss	Pits	Loss	Pits	Loss	Pits
NN, refined lead	0.010	1.1	0.28	1.4	0.068	*P*	0.062	0.9	0.020	1.1
N, chemical lead	.037	1.7	.51	1.3	.18	2.5	.076	1.2	.088	1.8
H, copper	.015	*M*	.12	*S*	.044	*P*	------	------	.015	*P*
B, brass	.077	*M, D*	.15	*P*	.051	*M, D*	.010	*M, d*	.010	*M, D*
L, bronze	.015	1.1	.13	5.5	.046	*M*	.46	1.1	.049	3.1
Zf, sheet zinc	.35	4.0	.46	3.9	.085	1.7	.23	3.3	*f*	*f*
Zg, cast zinc	.34	7.0	.53	5.5	.078	1.8	.22	6.8	.94	9.8
P, sheet zinc	.19	5.2	.38	*f*	.11	2.0	.45	3.7	*f*	*f*
Cl, aluminum	.009	2.1	*f*	*f*	.035	*f*	.016	*P*	.047	*f*
Ck, Al-Mn-alloy	.038	*f*	.096	*f*	.020	1.4	.021	1.3	.031	1.9
Ck, Duralumin	------	------	------	------	.14	*f*	.014	*M*	*f*	*f*
A, open-hearth iron	.98	*f*	.58	6.2	.56	7.0	*f*	*f*	*f*	*f*
S, steel+0.2% Cu	*f*	*f*	.69	*f*	.54	5.9	*f*	*f*	*f*	*f*

[6] See table 1 for names of soils.
[5] See table 3 for names and analyses of materials.
[7] Loss is given in ounces per square foot per year.
[8] Rate of maximum penetration in mils per year.

[8] See table 20, Tech. Pap. T368; table 8, Research Pap. RP359; and table 12, Research Pap. RP368 References to these papers have been made in earlier parts of this report.

Figure 6 shows the relation of the average maximum penetration to the duration of exposure of zinc specimens to five soils. Each point is based on the average of the deepest pits on each of two specimens. In two of these soils the rates of penetration appear to increase with the period of exposure.

Table 11, as well as similar tables previously published,[9] shows that the purer zinc (hearth refined) corrodes less rapidly than the zinc which contains more impurities.

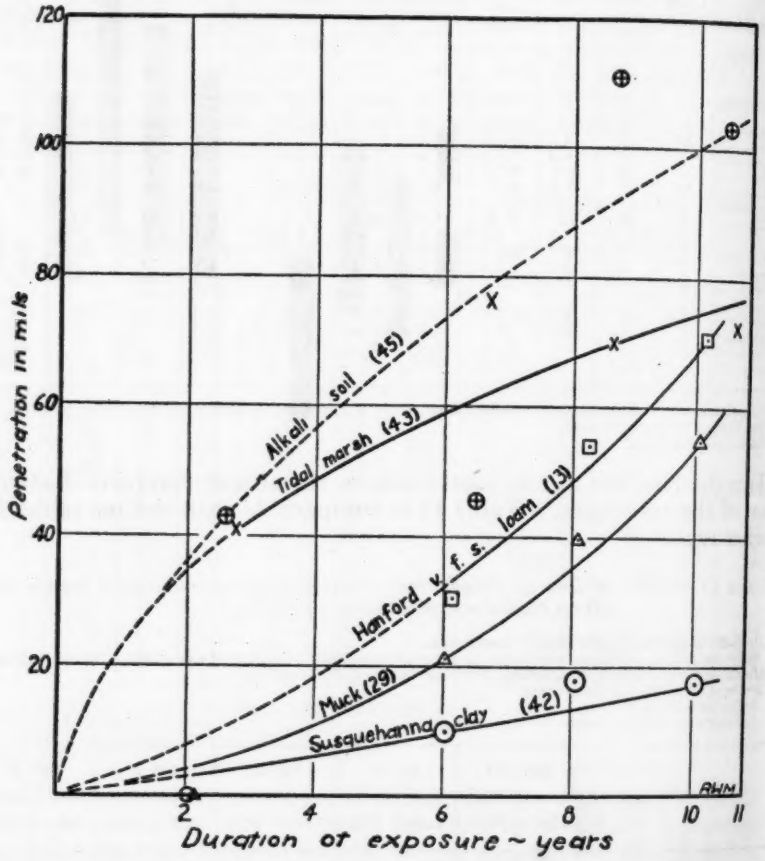

FIGURE 6.—*Relation of the maximum penetration of zinc to the duration of exposure.*

Under some circumstances the corrosion of the aluminum and aluminum-manganese alloy occurs mostly beneath the surface of the metal which is raised to form blisters beneath which a white powder is found.

It was not practicable to remove all of this powder without destroying some of the uncorroded metal and for this reason the losses of weight for the above mentioned materials as given in table 11 are inaccurate. They show, however, in a general way at least, the relative corrosiveness of the soils with respect to these materials. Since, as

[9] p. 544 Tech. Paper BS T368; p. 594, Research Paper RP359; p. 138, Research Paper RP638.

has been shown, soils differ greatly in many ways, general conclusions as to the usefulness of thin aluminum sheet underground should not be drawn. The data indicate that the effect of the soil on the aluminum alloy should be investigated before the material is used underground.

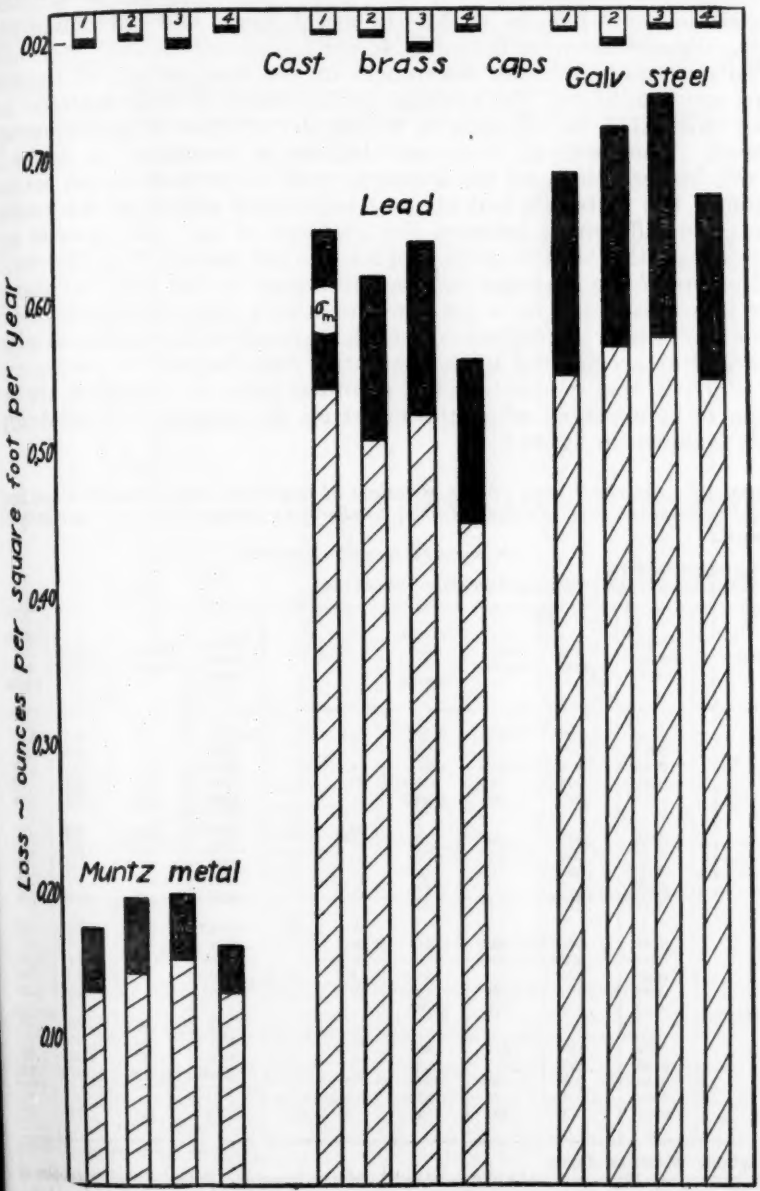

FIGURE 7.—*Average rates of corrosion of cast-brass fittings and attached nipples in 15 soils.*

At the top of the figure are shown the average rates of corrosion of four cast-copper alloys in the form of caps. Below are the rates of corrosion of the nipples attached to each variety of cast cap. See table 3 for analyses of materials. The solid ends of the column show the standard errors, σ_m, of the averages.

IV. EFFECT OF INTERCONNECTING DIFFERENT METALS

Several experiments have been undertaken to determine the effect of placing two metals in contact under several soil conditions. The earliest of these in the National Bureau of Standards soil-corrosion investigation consisted of four varieties of cast-brass alloys each connected to short lengths of Muntz metal, lead, and galvanized-iron pipe. Specimens were buried in 45 soils.

To determine whether differences in the composition of the cast caps are significant, the average performance of each material has been calculated for all soils in which all varieties of specimens appeared. The result of these calculations is presented in figure 7. It will be seen that, on the average, small differences in the composition of the materials had at most only small effects on the results. Thus the differences between the averages of the specimens in any group, e.g., the Muntz metal nipples, are not greater than the standard errors of the averages and therefore may be the result of chance. For this reason the data for the four alloys have been averaged in table 12. Since the corrosion of each material in this table was either retarded or accelerated by its potential with respect to the material to which it was connected, the recorded rates of corrosion are not those to be expected when the materials are exposed independently. This is shown in figure 8.

TABLE 12.—*Average*[1] *rates of loss of weight of cast brass caps, and of brass, lead, and galvanized-steel nipples attached to the caps exposed for approximately 10 years.*

[In ounces per square foot per year]

f=Specimen destroyed.
(1)=Threads of nipple stripped and data could be not used.

Soil [a]	Cast-brass caps	Brass nipples	Lead nipples	Galvanized steel nipples	Soil [a]	Cast-brass caps	Brass nipples	Lead nipples	Galvanized steel nipples
1	0.0159	0.624	1.808	2.317	26	0.0117	[b] 0.092[2]	0.321	0.221
2	.0083	.073	(1)	.230	27	.0036[11]	.117	.385[1]	.293
3	.0144	.053	.416[2]	.311	29	.0259[10]	.561[3]	(1)	1.924
4	[b] .0184[2]	.268[3]	.487[2]	.651[3]	30	.0065	.066	.284	.410
5	.0137[11]	.317[2]	.943	1.368[5]	31	.0044	.025	.422	.296
6	.0081	.026	.154	.121	32	.0062[11]	.111	.263[3]	.240
7	.0134[8]	.033[3]	.352[1]	.604	33	.0558	.319[3]	.288	.592[6]
8	.0065[14]	.093[3]	.143[3]	.477[5]	35	.0046	.0034	.041	.132
9	.0261	.192	.549	.424	36	.0089[11]	.049	.414	.224
10	.0171[14]	.210[5]	.536[5]	.672	37	.0214[11]	.165	.430[2]	.740
11	.0132	.071	.693[3]	.346	38	.0054[10]	.023	.218	.202
13	.0041	.079[3]	.356	.766	40	.0196	.256	.493	.671
14	.0038	.033	.565	.258	41	.0084[9]	.099	.597	.244
15	.0030	.050	.328	.425	42	.0087[10]	.101[3]	.782	.654
17	.0350	.246	.738	1.103	43	.1467[7]	.017[2]	.032[2]	1.580[4]
19	.0234	.136	.517	.354	44	.0142	.039	.286	.353
20	.0196	.153	.617	.538	45	.0291	.154	.135	*f*
22	.0142	.203	.691	.907	46	.0072	.046	.140	.603
24	.0061	.014	.101	.078	47	.0105[11]	.019[2]	.093	.443
25	.0094	.075	.429	.185	Average for all soils	.0172	.134	.434	.580

[a] See table 1 for names of soils.
[b] From most soils 12 cast caps and 4 nipples of each kind were removed. Superscript gives number when other than normal.

Figure 8 shows that rate of loss of weight of the cast-brass caps was about half that for copper pipe in the same soils. This may have been the result of cathodic protection or because the cast alloys were more resistant to corrosion. The latter conclusion is suggested by the relative rates of corrosion of the castings, since those containing the least copper corroded the least.

The value for the Muntz metal nipples was about 50 percent higher than for pipes of the same material, while that for the galvanized

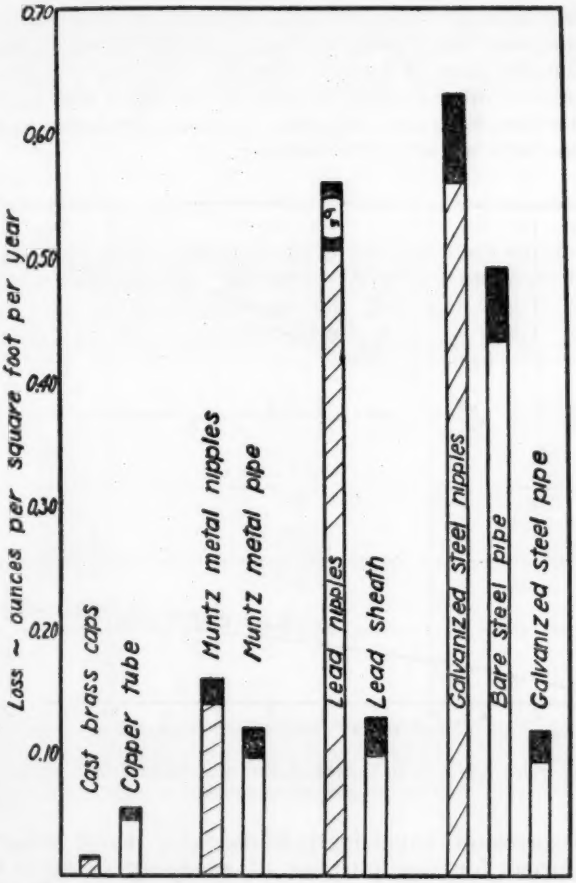

FIGURE 8.—*Effect of interconnecting different metals.*

The cross-hatched columns show the average rates of corrosion of the materials affected by galvanic action. The solid ends of the columns show the standard errors (σ_m) of the averages.

nipples was six times that for galvanized pipe in the same soils. The values for the galvanized nipples were about 25 percent greater than for unprotected steel pipe. Facts to be considered in this connection are that there was no zinc on about one-half inch of the nipples where they were threaded and probably the coating on the nipples was not as heavy as on the pipes.

A surprising result shown in figure 8 is that the lead nipples lost weight almost as rapidly as those of galvanized steel. Of course a partial explanation of this fact is that the density of the lead is nearly

50 percent greater than that of the other metals. This explanation, however, scarcely seems adequate since in service lead connected to brass cocks has a reputation for lasting much longer than galvanized steel under similar conditions. It seems probable that if the nipples had been longer and larger with respect to the cast caps the results of the test would have been somewhat different.

The most striking difference was between the rates of loss of the lead nipples and the corresponding rates for the lead cable sheath. The average rate of loss for the nipples was about five times that for the cable sheath. The relation between the two when exposed to Hempstead silt loam is shown in figure 9. There seems to be a tendency for the rate of corrosion of the nipples to decrease. The rate of corrosion of the cable sheath in the same soil appears to be constant, perhaps because sufficient corrosion products had not been deposited to form an effective coating.

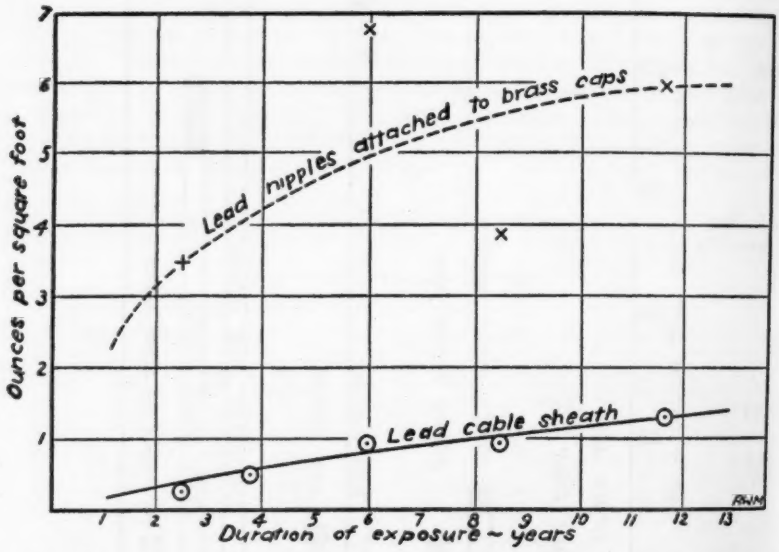

FIG. 9.—*Comparison of losses of weight of lead nipples and cable sheath for different periods of exposure.*

The soil-corrosion investigation contains three other sets of materials buried for the purpose of studying galvanic corrosion. The forms of these specimens are shown in figure 10. The unlabeled specimen consists of two strips of cast iron united by a brazed joint. The pipe from which the sections were cut was cast in a mold in which portland cement was used to prevent the metal from sticking to the sand. The pipe manufacturer who prepared the specimens left the cement on them because this is the way the joint would be used in practice. For the same reason no care was taken to remove the flux used in making the joint. The uneven distribution of the corrosion may therefore be accounted for in several ways. However, after 8 years' exposure to a corrosive soil there was no serious corrosion at the joint.

Specimens of copper pipe joined by copper stream-line soldered fittings (*M1*, fig. 10) and specimens of a copper-silicon alloy pipe

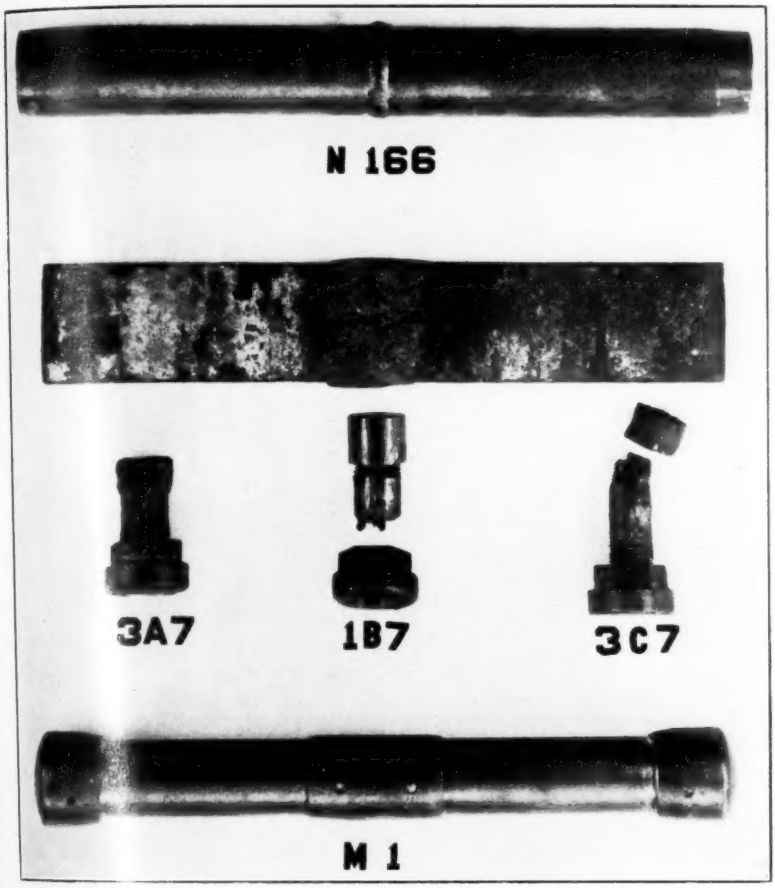

FIGURE 10.—*Types of specimens used in studying the effect of joining dissimilar metals.*

N, Copper-silicon alloy exposed to peat soil for 2 years; unnumbered, brazed joint on cast iron exposed 8 years; *3A7*, *1B7*, *3C7*, cast brass caps attached to lead, Muntz metal, and galvanized steel, respectively, and exposed for 10 years to Allis silt loam; *M1*, soldered joints on copper pipe exposed 2 years in a tidal marsh.

with bronze welds at the middle of the specimens (*N166*, fig. 10) showed no definite evidence of corrosion which could be attributed to galvanic action after 2 years' exposure. The brass caps and attached nipples shown also in figure 10 are from a soil which is severely corrosive. They show the form of the specimens reported on in figures 8 and 9, and in table 12.

V. DETERIORATION OF NONMETALLIC PIPE

In addition to the large variety of specimens of metallic pipe and sheet, the soil-corrosion investigation includes two varieties of nonmetallic pipe developed for the transportation of water. These specimens buried while the materials were being developed do not represent the materials now marketed by those who furnished them. In both cases the manufacturers believe that their more recent products have overcome the weaknesses shown by the specimens.

The oldest nonmetallic specimens in the test were of wood fiber, coated inside and out with a bituminous substance which cracked and lost its plasticity in some soils. The fiber absorbed sufficient moisture to cause some of the specimens to increase in length about 5 percent. No tests of strength of the materials have been made. The coating had such a low melting point that it softened and became sticky when the specimens were exposed to the sun at the warmer test sites. The results of the test suggest that the pipe material itself should be more nearly moisture-proof since it has been demonstrated that moisture penetrates most thin bituminous coatings. It has also been shown that it is very difficult to secure and maintain a perfectly continuous bituminous coating on a pipe line because of the nature of bitumens.

The other material is composed of 85 percent of portland cement with the addition of 15 percent of asbestos fiber. The specimens of this material were exposed for approximately 2 years to 15 soils severely corrosive with respect to ferrous materials. As the specimens absorbed moisture, loss of weight determinations were not made. The specimens showed no pitting and it seemed best therefore to determine their condition by inspection.

The following comments were made by a representative of the manufacturer: "Inspection of specimens of asbestos cement pipe has shown surface corrosion on those samples which were in contact with acid soils and cinders. Also, some surface disintegration has been noted on those specimens in contact with soils containing soluble sulphates."

The test specimens were not representative of the grade sold as pressure pipe; therefore, the results may not be representative of what could be expected in the case of the more dense structure of pipe intended for pressure service. Until the specimens have been exposed for longer periods a detailed report on the condition of each specimen would add little to the above quotation.

VI. SUMMARY

The data on the nonferrous specimens were insufficient to justify positive conclusions as to the rates of corrosion of the materials under any specific soil condition. However, the following conclusions are suggested by the data.

1. No metal or alloy has been found superior to all others for all soil conditions, but for each condition some suitable material is available.

2. With but few exceptions the rates of loss of weight and penetration were less for the nonferrous specimens than for the ferrous specimens subjected to the same soil conditions.

3. Lead in contact with some soils became badly pitted within a few years. Until the causes of this pitting are better understood, cable sheaths should be placed in direct contact only with soils known to be noncorrosive.

4. The differences in the rates of corrosion of different varieties of lead were small but the purest lead corroded the least. Antimonial lead appeared to corrode at a slightly higher rate than the commercial lead cable sheaths.

5. The rate of corrosion of lead gradually decreased in some soils but appeared to be maintained in certain soils such as tidal marshes.

6. The presence of chlorides, bicarbonates, and particularly sulfates, in soils favors the formation of films or deposits which retard corrosion of lead.

7. Copper and alloys high in copper corroded slowly in most soils. The highest rates of corrosion of copper occurred in soils containing sulfides.

8. The rates of corrosion of all copper alloys were higher in cinders than in any type of soil tested.

9. The corrosion of copper and high-copper alloys was more nearly uniform over the surface than was the corrosion of ferrous materials in most soils.

10. Muntz metal dezincified in a considerable number of soils and probably should not be exposed to severe soil conditions.

11. The rates of corrosion of copper and brass appeared to change less with time than did the corresponding rates for ferrous materials.

12. Zinc corroded rather rapidly in a few soils. In some soils the loss of weight of zinc was nearly proportional to the duration of the exposure. In such soils effective protective films were not formed. The protection which a zinc coating affords under such soil conditions is the result of cathodic protection at the expense of the zinc or due to the corrosion resistance of the zinc-iron alloy layers.

13. Aluminum and some of its alloys corroded rapidly under most of the soil conditions to which they were exposed.

14. The interconnection of dissimilar metals exposed to soil resulted in the partial protection of one of them and in more rapid corrosion of the other. Sometimes, however, the formation of corrosion products of one of the materials prevented continued corrosion.

The cleaning, weighing, and measuring of the specimens was done mostly by R. B. Hobbs, L. M. Martin, and I. Bohrer, on whose skill and care the reliability of the data largely depends. The last two made and checked most of the computations and assisted in the preparation of the tables and drawings. Dr. I. A. Denison and Mr. Martin made many valuable suggestions as to the interpretation of the data.

WASHINGTON, August 13, 1936.

○